DESIGN AND SYNTHESIS OF ACHIRAL AND CHIRAL BENZODIAZEPINES AND IMIDAZODIAZEPINES TO MODULATE THE ACTIVITY OF GABAA RECEPTORS FOR THE TREATMENT OF CANCER, CNS DISORDERS AND PAIN

by

Farjana Rashid

A Dissertation Submitted in

Partial Fulfillment of the

Requirements for the Degree of

Doctor of Philosophy

in Chemistry

at

The University of Wisconsin-Milwaukee

August 2021

ABSTRACT

DESIGN AND SYNTHESIS OF ACHIRAL AND CHIRAL BENZODIAZEPINES AND IMIDAZODIAZEPINES TO MODULATE THE ACTIVITY OF GABAA RECEPTORS FOR THE TREATMENT OF CANCER, CNS DISORDERS AND PAIN

by

Farjana Rashid

The University of Wisconsin-Milwaukee, 2021
Under the Supervision of Professor James M. Cook

A series of α2/3-subtype selective $GABA_A$ receptor agonist imidazodiazepines (IBZs) were synthesized and investigated. The lead compound (KRM-II-81) exhibited anxiolytic, antinociceptive and anticonvulsant effects, displayed promising α2/3 GABAergic subtype selectivity in HEK cells and noteworthy anxiolytic activity and no sedation nor ataxia using a rotarod assay in mice (80mg/Kg) or rats (300 mg/Kg).Based on the "privileged imidazodiazepine (IMZD) structures" derived from the unified pharmacophore model of Milwaukee, the design, synthesis and biological activities of more than 30 novel 2' Cl achiral $GABA_AR$ α2/α3 subtype selective imidazodiazepines (IMDZs) related to KRM-II-81 achiral ligand Hz-166 are described. Several compounds from the α2/3 subtype selective group are anxiolytic, antidepressant, and are targeted toward the treatment of major pain, epilepsy disorders. In regard to the design of new 2'Choloro benzodiazepine analog, an improved large-scale synthesis of (2-amino-5-bromophenyl) (2-chlorophenyl) (4)was performed which is very expensive in market (1800 USD/ 500g). A novel synthetic route with minimal cost for large quantity production of the (4) was described here. After several attempt and optimization, the yield of 2 amino 5 bromo 2'Cl benzophenone was increased from 35-44%. No column

chromatography was needed to purify the large-scale product. This new developed route to synthesize of (2-amino-5-bromophenyl) (2-chlorophenyl can be applied to synthesize another benzophenone with different substituents.

FR-II-60 and more than 30 analogs were designed, synthesized, and evaluated where (4) was used as a starting material. The goal of this research is to design new analogs with improved metabolic stability that also retain the desired biological properties with little or no side effects for the treatment of CNS disorders, pain. The α2/3 selective achiral oxazole, FR-II-60 looks very good in rodent models for the treatment of epilepsy and pain. It exhibited anti-depressant and anxiolytic activities in mice. It shows sightly sedation using a rotarod assay in mice (40, 80mg/Kg) due to the presence of halogen (Cl) at 2' position in its structure. No cytotoxicity observed in HEK293 cell in lower concentration (up to 300 uM). Behavioral observations in female rhesus monkeys after the administration of FR-II-60 (3mg/kg, iv) did not show any deep sedation. Further study of this compound is presently taking place. According to the data and ongoing research FR-II-60 looks very promising ligand to treat conditions such as chronic pain and epilepsy.

After evaluation of a series of novel IMDZs that were α5 subtype selective for the treatment of asthma, one compound MIDD0301 (originally named GL-II-93) was found to be orally active and as an inhalant in rodent asthma models. Ligand MYM-FR-II-88 and FR-III-45 was as active as GL-II-93 in the airway smooth muscle (ASM) relaxation assay. FR-III-45 does not induce any immunotoxicity in animal models as well as no sedation nor ataxia using a rotarod assay in mice up to dose 40 mg/Kg. This research is still ongoing and several ligands, especially the α5 subtype selective acid, described herein have been shown to relax precontracted human and guinea pig airway smooth muscle and could deliver a novel treatment for asthma patients.

The medulloblastoma is known as a Pediatric brain cancer, It's subtype, subgroup 3 also has a high expression of the. *GABRA5*. The α 5 selective ligand QH-II-066 and KRM-II-08 positive allosteric modulators showed very high potency in cell viability by decreasing the expression of HOXA5 which is a homeobox transcription factor that controls p53 expression. To understand the role of α5-$GABA_AR$ in group 3 cell viability, 763 primary medulloblastoma patient tumor has been studied. Two ligands FR-I-44 and FR-I-43 have also been screened in a particular cell line D283 and did not show appreciable potency compared to KRM-II-080. Although these ligands did not show any cytotoxicity in HEK293 cell, it might show some potency in other cancer cell lines- an area of research that is currently ongoing.

TO

Arya, my little princess.

TABLE OF CONTENTS

LIST OF FIGURES

LIST OF TABLES

LIST OF SCHEMES

LIST OF ABBREVIATIONS

ACh	acetylcholine
AHR	airway hyperresponsiveness
AP-4	4-aminopyridine
ASM	airway smooth muscle
BALF	bronchoalveolar lavage fluid
BBB	blood-brain-barrier
BQL	below the quantification limit
BZD	benzodiazepine
BzR	benzodiazepine receptor
CFA	complete Freund’s adjuvant
CDAP	chlordiazepoxide
CINP	chemotherapy-induced neuropathic pain
CMC	carboxymethyl cellulose
CNS	central nervous system
COPD	chronic obstructive pulmonary disease
CRS	chronic restraint stress
DI	diazepam-insensitive
DLM	dog liver microsomes
DNP-KLH	dinitrophenyl hapten-keyhole limpet hemocyanin
DS	diazepam-sensitive
ETSP	Epilepsy Therapy Screening Program
FDA	Food and Drug Administration

FST	forced swim test
GABA	gamma-aminobutyric acid
$GABA_AR$	gamma-aminobutyric acid type A receptors
$GABA_BR$	gamma-aminobutyric acid type B receptors
GINA	Global Initiative for Asthma
hERG	human ether-à-go-go-related Gene
HEK	human embryonic kidney cells
HDM	house dust mite
HLM	human liver microsomes
HPLC	high-performance liquid chromatography
ICSS	intracranial self-stimulation
IMDZ	imidazodiazepine
IgG	immunoglobulin G
IP	intraperitoneal
IV	intravenously
KA	kainic acid
KOR	kappa opioid receptors
LABA	long-acting β_2 agonist
LR	Lawesson's reagent
LTG	lamotrigine
MAM	methylazoxymethanol acetate
MCh	methacholine
MDD	major depressive disorder

MED	minimal effective dose
MES	maximal electroshock
MLM	mouse liver microsomes
MOE	Molecular Operating Environment
MPE	maximum possible effect
MRM	multiple reaction monitoring
MTD	minimal toxic dose
mTLE	mesial temporal lobe epilepsy
MW	molecular weight
NAM	negative allosteric modulator
NIMH	National Institute of Mental Health
NO	nitric oxide
NMDA	*N*-methyl-D-aspartate
Ova s/c	ovalbumin sensitized challenged
PAM	positive allosteric modulator
PBR	peripheral benzodiazepine receptor
PCLS	precision-cut lung slice
PCP	phencyclidine
PDSP	Psychoactive Drug Screening Program
PEG	polyethylene glycol
PFC	mouse prefrontal cortex
PI	protective indices
PK	pharmacokinetics

PPI	prepulse inhibition
PTZ	pentylenetetrazole
PWT	paw withdrawal threshold
PO	oral administration
RLM	rat liver microsomes
SABA	short-acting β_2 agonist
SAR	structure-activity relationship
scMET	subcutaneous metrazole
SE	severe epilepsy
SEM	standard error of the mean
SLA	spontaneous locomotor activity
SNL	sciatic nerve ligation
SSRI	selective serotonin reuptake inhibitors
sRaw	specific airway resistance
SST	somatostatin
TLC	thin-layer chromatography
TLE	temporal lobe epilepsy
TPE	time of peak effect
TSPO	translocator protein
UCMS	unpredictable chronic mild stress

ACKNOWLEDGMENTS

First of all, I would like to express my sincerest gratitude to my PhD supervisor Professor James M. Cook for teaching me, mentoring and guiding me through the entire journey. I am thankful to him for his patience and understanding, his affection and care, and his guidance in both my academic and personal matters. I was fortunate to have his mentorship in all my research projects. Moreover, I am thankful for his support and guidance in my future career plan.

I would like to thank all the members of my doctoral thesis committee, Dr. Alexander E. Arnold, Dr. Alan W Schwabacher, Dr. Arsenio A Pacheco and Dr. Xiaohua Peng for the helpful suggestions and help with both my coursework and research during my time at UWM.

I am thankful to my collaborators, and I consider myself fortunate to be a part of such a great hardworking team. I have learned a lot in the process of working with them and this has helped me become a better researcher. I am particularly grateful to Dr. Miroslav Savić (University of Belgrade, Serbia), Dr. Jeff Witkin (Eli Lilly and Company, USA), Dr. Donna M. Platt (Mississippi Medical School, USA Dr. Soma Sengupta (Emory University, USA), Dr. Charles W. Emala (Columbia University, USA) Dr. John Chan. A special thanks to Dr. Leggy A. Arnold and Dr. Stafford (UW-Milwaukee, USA).

I am thankful to all the members of the Cook group, both past and present. It has been a life-changing experience being a part of this amazing group. I am thankful to the former members of the group Dr. Toufiqur Rahman, Dr. Rajwana Jahan, Dr. Guanguan Li, Dr. V. V. N. Phani Babu Tiruveedhula, and Dr. Daniel Knutson. I am also thankful to the current members of the group. Especially, I thank Md Yeunus Mian for his suggestions, discussions, and insightful ideas which really helped me in my research. I would like to thank Dishary Sharmin and Sepideh Rezvanian for their excellent support. I would like to thank Kamal Prasad Pandey and Prithu Mondal for

helping me in my research as well as with solvent duties, changing the heavy argon tank during my pregnancy made my life so much easier in the lab. A special thanks to Dr. Lalit Kumar Golani for teaching me the molecular modeling. I would like to thank each and everyone in this great lab group for the endless support they've provided over the years and particularly the last few months leading up to my defense presentation. I will always remember our Saturday meetings, working late hours in the lab. I am also thankful to my friend Vilasini Rajaratnam for helping me learning HPLC and HRMS.

I would like to acknowledge the financial and academic support of the Department of Chemistry at UW-Milwaukee, the UW-Milwaukee Graduate School, and the National Institutes of Health (NIH). I am grateful to Dr. Frank H Holger for his valuable help for NMR, and Mr. Neal Korfhage for the design and fabrication of very specialized glassware. I greatly appreciate Dr. Anna Benko for her outstanding expertise and support during the last couple of years for help with mass spectroscopy. I would also like to thank Dr. Shama Mirza for her help in the analysis of mass spectra. I would also like to thank Mr. Kevin Blackburn, Ms. Elise D. Nicks, Ms. Wendy Grober, Ms. Shelley Hagen, Ms. Mary Eckert, and Ms. Goldie Gibbs for being there for me whenever I needed help.

At last, but not the least, I'd like to thank my family for always being there for me. Without my family members I would not be where I am today. I want to thank my father Md Mamunur Rashid and my late mother Sayeeda Akhter for giving birth to me and teaching me to dream big. Their endless love, support and trust enabled me to pursue a PhD degree. I am thankful to my sister Farhana Rashid, brother Saifur Rashid, sister-in-law Nilufa Nipu and nephew Tazwar Rashid for their love and encouragement.

I am grateful to my beloved husband Dr. Anik Iqbal who is always there for me and makes

my life so beautiful. A special thanks to my beautiful daughter Arya Iqbal who was born during my amazing PhD journey. She has sacrificed a lot for her mom's degree. When I was working late at lab, she was staying awake at home missing me. Just her presence in my life has fueled my research work; gave me the much-needed motivation and encouragement to keep going.

I also want to thank my father-in-law Sarker Javed Iqbal, mother-in-law Syeda Shirin Sultana and brother-in-law Sarker Asif Iqbal for always encouraging me and believing in me.

Chapter 1. Introduction

The gamma-aminobutyric acid (γ-aminobutyric acid), or GABA, is an amino acid that naturally occurs in the human body. This amino acid works as a neurotransmitter in the human brain. GABA is considered an "inhibitory neurotransmitter" because it inhibits, or blocks certain signals to the Central Nervous System (CNS) and decreases the overall neuronal activity.[1] When GABA attaches to a protein ion channel in the brain (GABA receptor), it produces a calming effect. There are two main classes of GABA receptors: $GABA_A$ receptors ($GABA_AR$) and $GABA_B$ receptors ($GABA_BR$). The latter is not discussed in this thesis. Another formerly used class, the $GABA_A$-rho receptors ($GABA_CR$) are now considered members of the $GABA_ARs$, as their rho (ρ) subunits are related to $GABA_ARs$.[2] The $GABA_ARs$ can be found in the chloride channels of integral membrane proteins knows as ligand-gated ion channels (LGICs). The LGICs enable fast synaptic transmission in the order of milliseconds (0.001 s) in the nervous system as well as somatic neuromuscular junction; therefore are considered fast-acting transmembranes.[3] When activated, $GABA_AR$ causes a suppression of neuronal transmission by hyperpolarizing the electrochemical gradient in the chlorine channel.[4] In contrast, the $GABA_BRs$ are slow-acting receptors that work in potassium and calcium channels.[5] The available literature has long suggested that the neurological disorders such as schizophrenia, anxiety disorder, epilepsy, neuropathic pain disorders, clinical depression, etc. are all connected to the $GABA_ARs$ in the central nervous system.[6-10]

Numerous researchers have reported the potential relationship between the $GABA_AR$ and the CNS diseases, where they attribute its pharmacological benefits to the abundance of a specific combination of $GABA_AR$ subunits.[11] Of a total of nineteen subunit isoforms that are found in the

human body (α1-6, β1-3, γ1-3, δ, ε, π, θ, ρ1-3)[12], $GABA_AR$s host a combination of the α, β and γ2 subunits (α1-6β1-3γ2) in a stoichiometric ratio of 2:2:1.[2] This is the requirement for a completely effective allosteric function by benzodiazepines at the α-γ2 interface.

The immunocytochemistry studies of rodents have determined that the central nervous system of such animals contain different distributions of $GABA_AR$ assemblies.[13] The $GABA_AR$ subunits are highly abundant throughout the rodents' brains both as synaptic and extrasynaptic receptors.[14] Of all the $GABA_A$ receptors in rat brain, 60% consist of α1β2γ2 whereas some of the other subunits are found in lower percentages. Among these, α2 and α3 are present at about 20-30% and α5 at about 5%.[14-17] Furthermore, there is also evidence of the presence of $GABA_A$ receptors in the other bodily tissues such as the sinoatrial node of the heart, intestines, lungs, stomach, etc.[1]

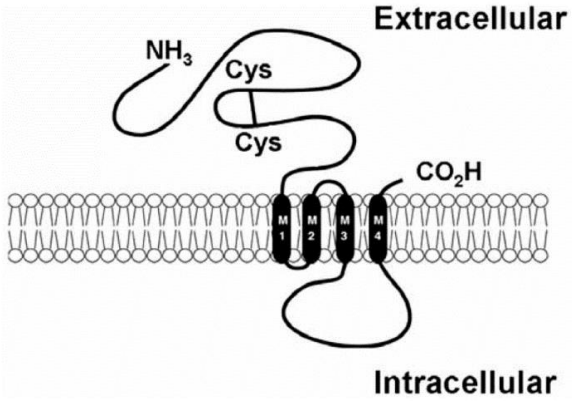

Figure 1. A suggested GABAAR subunit topology. The beginning of the extracellular domain with the N-terminal end, and the M1-M4 are regions within the membrane. (Modified from the Figure in Burt, et al. [18] and Clayton, et al.[19])

A $GABA_AR$ subunit has a molecular mass of about 50 kD with a receptor structure characterized by high homology. As shown in **Figure 1. A suggested GABAAR subunit topology. The beginning of the extracellular domain with the N-terminal end, and the M1-M4 are regions within the membrane. (Modified from the Figure in Burt, et al. [18] and**

Clayton, et al.[19]), there are four transmembrane domains (M1-M4) in the lipid bilayer of the neuron of each receptor subunit. The $GABA_AR$s have their N- and C- terminals situated outside the cell membrane, including possible glycosylation sites. Also, there is a Cys-loop enabled by a disulfide bond at the N- terminal end. Beneath the membrane, there exists a large intracellular region between M3 and M4. The intracellular region is mainly responsible for regulating $GABA_AR$ at phosphorylation sites. A hetero- or homo- pentameric chloride channel is formed by five monomeric $GABA_AR$ subunits arranged in the shape of a ring.[18-20] (**Figure 2**)

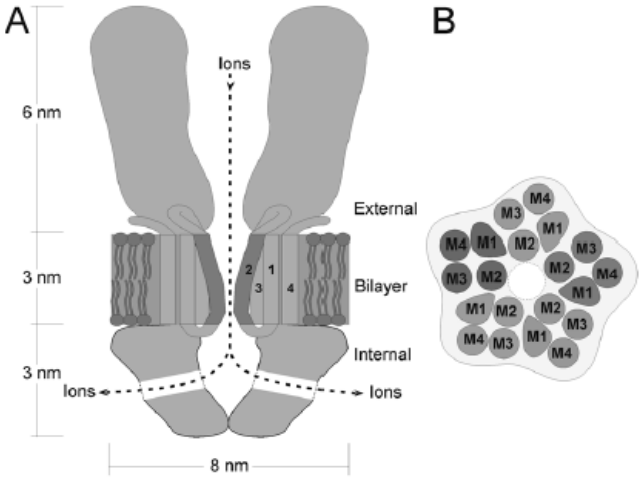

Figure 2. A depiction of the ligand-gated chlorine ion channel $GABA_AR$. (A) shows the longitudinal vision and (B) the cross-sectional vision. The M1-M4 transmembrane domains labeled accordingly. The M2 domain mostly exists in the pore lining within the lipid bilayer membrane. (Modified from the Figure in Keramidas et al.[20], and Clayton et al.[19])

It is quite well known and reported across the literature that $GABA_AR$s feature a number of binding sites for psychoactive compounds such as benzodiazepines, anesthetics, barbiturates, neurosteroids, ethanol, etc. at the synapse and synaptic ion channels.[1, 2, 11, 15, 19] Illustrated in the **Figure 3** is the clockwise arrangement of the αβαβγ subunits in the extracellular region. This view clearly illustrates the binding sites of $GABA_AR$. While benzodiazepines bind at the $\gamma^-\alpha^+$ interface, the GABA binds at the two $\alpha^-\beta^+$ interfaces.[1, 2, 8, 19] Another interface of interest is that of $\beta^-\alpha^+$ which was recently reported as the binding site for the subtype-selective CGS 9895 PQ site.[19, 21, 22]

Moreover, this receptor has been found to be α6-selective.[23-25] Additionally, barbiturates and ethanol can also bind in the intra-channel region to enhance the response as well as open up the pores directly which in turn exposes the patient to the possibility of addiction and death.[1, 2, 15-18, 26, 27]

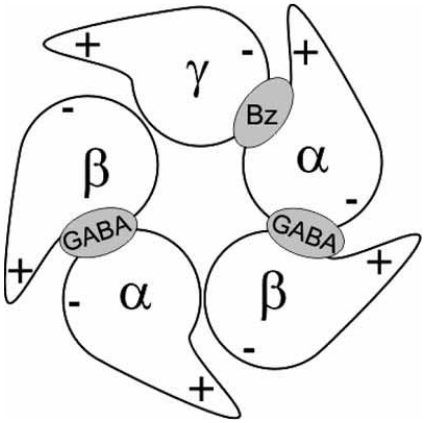

Figure 3. The schematic arrangement in the α1β3γ2 $GABA_AR$ subtypes as viewed from the synaptic cleft. The GABA and BZD binding sites are located at the interfaces of $\beta^+\alpha^-$ subunits and $\alpha^+\gamma^-$ subunits respectively. The + represents the loop C of each subunit. (Modified from the Figure in Clayton, et al.[19] and Ernst, et al.[28])

1.1. Benzodiazepines (BZDs)

Benzodiazepines (BZDs) are a general class of drugs that are prescribed by doctors for treatment of a variety of different conditions. In the United States, the Food and Drug Administration (FDA) has approved benzodiazepines for the treatment of insomnia, anxiety disorders (generalized and social), seizure disorders (e.g. epilepsy) and panic disorder. It has been prescribed for such conditions for over 50 years in this country.[29, 30] Other uses of the drug includes sleep disorders, bipolar disorders, managing alcohol withdrawal, etc.[31]

BZDs were first discovered by Leo Sternbach in 1955. Perhaps the most well-known, widely used and commercially successful BZD drug is diazepam or Valium which was marketed as back as 1963.[29] The immense commercial success of diazepam can be attributed to the drug's

potency, low toxicity,[32] fast and efficient penetration of the blood-brain barrier, negligible drug-drug interaction within the liver, fast absorption of the drug in the gastrointestinal tract and efficient distribution within the brain, etc.[33-36]Some common BZD structures illustrated in **Figure 4**, all of which have some common features: a core of a benzene ring attached to a diazepine ring which in turn is attached to a pendant C ring.[37]

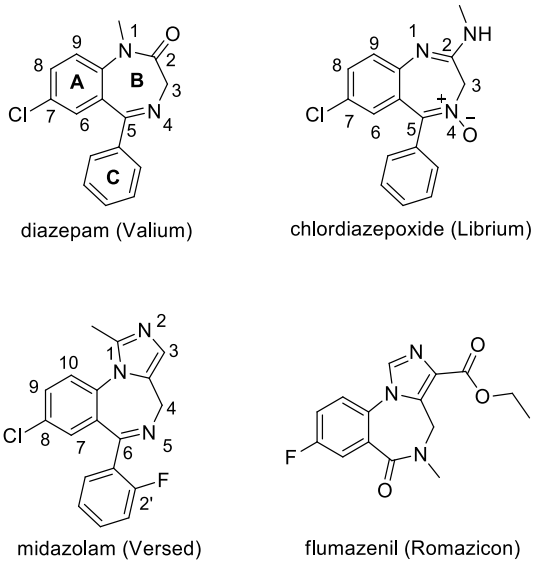

Figure 4. The structures of several well-known BZDs: diazepam, chlordiazepoxide, imidazodiazepine (IMDZ) midazolam and flumazenil. The atoms are labeled for both BZDs and IMDZs. All four of them can bind at the DS sites, but only flumazenil can also bind to the DI sites.

Generally, the benzodiazepines including the ones shown in **Figure 4** as well as alprazolam have very high, non-selective affinity for $GABA_AR$ at the BzR binding site at the $\gamma^-\alpha^+$ interface.[1, 2, 8, 19] Thus, the pharmacological properties of the BZDs are dependent mostly upon the α and γ subunits rather than the β subunits.[38] The existing evidence suggests that the BZDs interact most prominantly with the $\alpha_{1\text{-}3,5}\beta_{2/3}\gamma_2$ subtypes of the $GABA_ARs$ and less effectively with the $\gamma_{1,3}$ subtypes.[39] The two other subtypes α_4 and α_6 are not very sensitive to BZDs.[40] The α_4 and α_6 subtypes do not bind with diazepam (1,4- benzodiazepine) and midazolam (imidazodiazepine),[41,

[42] but readily bind with dugs like flumazenil.[12] This is because of the absence of the pendent phenyl C ring in the flumazenil structure (**Figure 4**) and the above are called diazepam insensitive sites(DI).

A BZD is incapable of modulating $GABA_AR$ by itself, without the presence of GABA.[43] Rather, the affinily of GABA to $GABA_AR$ is enhanced by the binding of the BZD to the $GABA_AR$ ion channel, resulting in the hyperpolarization of the neuronal membrane electric potential.[44] This is how BZDs are capable of lowering the neuronal firing frequency, which is the desired outcome that results in numerous pharmalocological effects including anticonvulsive effects, ataxic, anxiolytic effects but also ataxic, sedative and amnesic effects. These properties have earned as the BZDs the preferrable drug for variuos CNS disorders (e.g. GAD, SAD, PTSD, status epilepticus, panic disorders, etc). On the other hand, BZDs also have undesirable effects on the human body, some of which can be attributed to the simulteneous non-selective binding and efficacy at other $GABA_ARs$.[2, 29] The common adverse effects of BZDs are well reported in the literature, which includes sedation, amnesia, ataxia, addiction, dependence, fatigue, withdrawals, muscle-relaxation and building up of tolerances to the anticonvulsant and antinociceptive effects.[45-47] Therefore, the current stage of BZD drugs have left much room for research and improvements. It is desired to design better drugs for CNS disorders with similar or better pharmacological effects to BZDs but with little to no side effects.

1.2 Modulation of BZDs on the Pharmacological Effects of GABAAR

Over the years, strong evidence has been found confirming that the pharmacological effects of the GABAARs are dependent upon the modulation of receptor subtypes, principally the αx subunits. The pharmacological effects associated with each subunit have been determined by receptor binding, pharmacological methods, and a molecular genetic procedure by introducing a

point mutation into the respective α subunits. This remarkable work was accomplished by Mohler, Sieghart, McKernan, Sigel, Seeburg, Squires, and Haefely. This process takes place via replacing the histidine amino acid by an arginine amino acid in the subunit: (α1His101Arg,48 α2His101Arg, α3His126Arg,49 and α5His105Arg50). The subject animals that were found with the above mutations were administered diazepam and the behavioral response was recorded. Any changes to the response compared to the untreated animals were attributed to the mutated subunits.48-50 These results have been summarized in

Table 1**.**

Subtype	Associated Effect
α1	Axiolytic,sedation, anterograde amnesia, ataxia, some anticonvulsant action, addiction, dependence, as well as involved in the development of tolerance, and muscle relaxation
α2	**Anxiolytic**, **anticonvulsant action**, **antihyperalgesic effects**
α3	Some **anxiolytic action**, **some antinociceptive effects,** anticonvulsant action at higher doses, some muscle relaxation at higher doses
α4	Diazepam-insensitive (DI) site, important in lung disorders in the periphery
α5	Cognition, learning, temporal and spatial memory (maybe memory component of anxiety); schizophrenia, depression and in the peripheral-asthma
α6	Diazepam-insensitive (DI) site, important in Tic disorders, Tourette's syndrome, migraine, trigerminal orafacial pain and perhaps schizophrenia

Table 1. The CNS effects at $GABA_A$ α_{1-6} receptor subunits.[19, 48-60] Presented at the Mona Symposium (2014), University of the West Indies.[61] Earlier reported, in part, by Mckernan et al. (ACNP). Pharmacology indicated in red was discovered by pharmacologists in collaboration with the Milwaukee group. Presented by J. Cook at the BBC meeting, San Antonio, March 2018.

The α1 subunits with $GABA_AR$s are associated with the mediation of a number of conditions (e.g. anxiolytic, sedative effects, ataxia, anterograde amnesia, development of tolerance, dependence, addiction, anticonvulsant actions, muscle relaxation etc.).[48, 62] On the other

hand, the α2 subunit of $GABA_AR$s are mainly anxiolytic, antinociceptive and anticonvulsant effects,[49, 53] as well as occasional muscle relaxation and hypnotic effects. The triple-point mutation study and the work of Zeilhofer, Cook et al. have already confirmed that the antihyperalgesic effects of the $GABA_AR$ take place mainly in the spinal cord.[51, 57] The α3 subunits containing $GABA_AR$s are responsible for possible anxiolytic, anticonvulsant, antinociception and muscle relaxation effects.[49, 53-55] The α5 subunits containing $GABA_AR$s play a role in cognition such as memory, spatial learning and possibly in a memory component of anxiety.[50, 56] The α4 and α6 subunits containing $GABA_AR$s do not exhibit any appreciable ataxic or sedative CNS effects, which is due to the lack of a large binding pocket for the pendant C ring of the BZDs.[41, 42] Recently, is has been shown that the α4 and α5 subunit containing $GABA_AR$s are expressed in the peripheral nervous system (PNS) of the lungs as well, which opens up the possibility of treating asthma with IMBZDs.[58, 59, 63]Savic et al. have just reported that GABA(A) BZR are located in blood vassels. Moreover, Knutson et al. reported that the α6 Bz/GABAergic subtypes are associated with diseases such as migraine, trigeminal pain, tic diseases (e.g. Tourette's syndrome), OCD and possibly schizophrenia.[23-25]

The influx of the chloride ions into membrane ion channels is also capable of causing the pharmacological effects due to the $GABA_AR$s enabled by the allosteric modulation of the GABA in the central nervous system. On the chloride channel, a BZD binds to the $GABA_AR$ BZD allosteric site locking increasing the orthosteric binding of GABA to the chloride channel and holding the ion channel open longer. After the $GABA_AR$ is bound to GABA, it changes its conformation causing the frequency and duration of opening of the chloride channel to increase and the membrane potential to decrease. (**Figure 5**) This process further reduces the neuronal transmission- causing the pharmacological effects in the CNS. Although BzR ligands in the

absence of GABA are incapable of acting on the chloride channels, they can still modulate the influx of the chloride ions and the opening frequencies of other allosteric complex modulators in the presence of GABA.[64-66] There are mainly three types of BZDs that are capable of interacting with $GABA_A$/BzR. The first, the agonist or the positive allosteric modulators (PAMs) enhance the activity of GABA as well as increases the chloride ion influx. This type of BZDs do not bind at the GABA binding site. The second, the inverse-agonist or the negative allosteric modulators (NAMs), reduce both the activity of GABA and the chloride ion influx. This causes the depolarization of the membrane and also the increase in the neuronal firing frequency. These BZDs readily bind at the GABA binding sites. The third kind are the compounds termed the antagonists[2] which do not modify the functions of the GABA and yield no pharmacological effects. The antagonists are capable of blocking both PAMs and NAMs from binding at the BzR site, Since they have high binding affinity but no allosteric modulation.[19] On the other hand, antagonists such as flumazenil, βCCt, 3PBC, etc. are used to reverse BZD overdose and other responses caused by BZD.[67] These drugs have the ability to occupy BzR sites and prevent the other BZDs from binding.

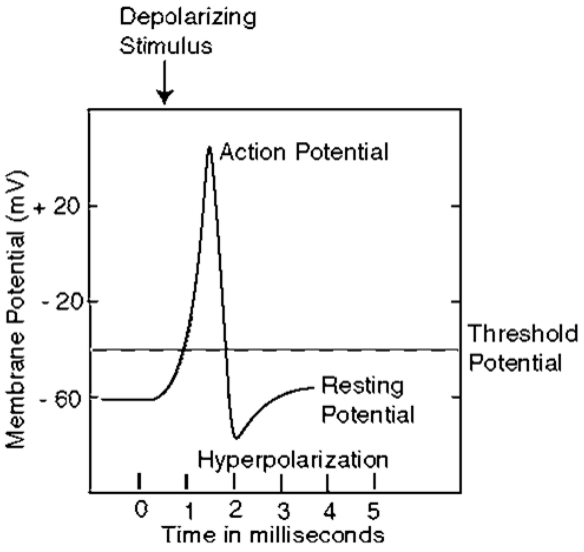

Figure 5. The changes in membrane potential during the "depolarization stimulus" initiating a nerve signal, plotted as a function of time. A hyperpolarized state is characterized by a

potential considerably above the threshold. (Modified from the Figure in the Ph.D. thesis of Terry Clayton[68])

In order to make progress towards better ligand design for the treatment of various CNS disorders, it is important to understand the pharmacological effects from $GABA_AR$s. The BZD allosteric modulation and the multiplicity of $GABA_AR$ subtypes is central to this concept. As an example, α1-subtype selective antagonists are able to reverse effects induced by BZDs such as ataxia, hypnosis, amnesia, sedation, respiratory depression, etc. whereas α1-subtype selective agonists can induce these effects. The ligands that are α2/3/5 or α2/3-subtype selective agonists or partial agonists with α1-subtype antagonist effects (inverse agonists) or no effects at all and have been found able to treat convulsions, anxiety disorders, diabetic neuropathy, inflammatory pain, neuropathic pain and in animal models and they have very little sedative effects, if at all. Moreover, α-5 subtype selective invers agonists are able to help with learning and memory deficiencies especially if it binds only to the α-5 subtype. Proper understanding of these features are very valuable in developing a spectrum of pharmacological effects.

1.3. Molecular Modeling – Pharmacophore Model

Although the development of newer and more improved BZDs is much desired, one of the biggest barriers to that goal in recent years has been the crystallization of the transmembrane protein $GABA_AR$, and more critically the $\alpha_{1\text{-}6}\beta_{1\text{-}3}\gamma_2$ GABA subtypes. The conventional methods for investigating the effects of BZDs and develop new drugs have been the fragment-based molecular modeling and the structure-activity relationship (SAR) studies, until recently. In 2019, the structure of the α1β3γ2 ion channel was determined via electron microscopy which permits much better understanding of BZD binding and pharmacology.

The Unified Pharmacophore/Receptor Model, that has been developed in Milwaukee, WI over the course of a few decades, is based on *in vitro* binding affinities of the 50 rigid ligand at BzR subtypes. Over the years, the studies included over 150 different agonists, antagonists and inverse agonists.[19, 52, 60, 69] Approximate binding pockets were generated by overlaying subtype selective ligands for $\alpha_{1\text{-}6}\beta_{2/3}\gamma 2$ $GABA_ARs$ on planar template ligands within the BZD binding site. The ligands were studied from fifteen classes of structural families (e.g. BZDs,[70] triazolopyrimidines,[71] β-carbolines,[72-74]pyridodiindoles,[75, 76] pyrazoloquinolines[77] and imidazopyridines[78]). A 2-D representation of the pharmacophore model has been illustrated in **Figure 6**. The four important descriptors (H_1 (Y210), H_2 (H102), A_2 (T142) and L_1) are used as anchor points. Here, H_1 and H_2 are the donor sites of the two hydrogen bonds; A_2 is the acceptor site of one hydrogen bond and L_1 is the lipophilic pocket. In the other lipophilic regions (L_2, L_3, and L_{Di}), the ligand-protein interactions are mediated by van der Waals interactions and p – π , π – π stackings are responsible for the effect on the ion channel. The proposed negative steric repulsive regions (S_1, S_2, and S_3) represent the proteins.[19, 52]

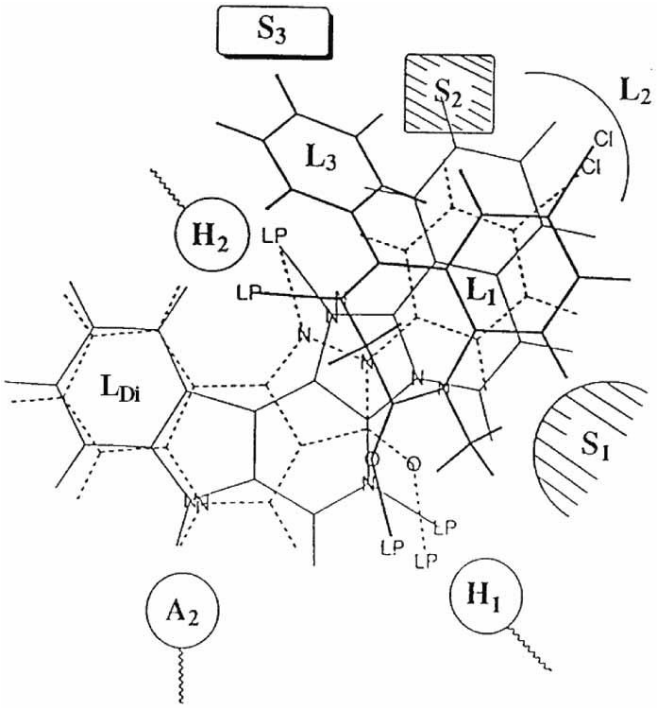

Figure 6. The locations of the descriptors and areas of the Milwaukee-Unified Pharmacophore/Receptor Model for BZD at $GABA_AR$ BzR. Here, pyrazolo[3,4-c]quinolin-3-one (CGS-9896) is shown as a dotted line, diazadiindole is as a thin line, and diazepam as a thick line aligned within the unified pharmacophore/receptor model for the BzR. H_1 and H_2 are the hydrogen bond donor sites within the BzR. A_2 is a hydrogen bond acceptor site that might be relevant in potent inverse agonist activity in vivo. L_1, L_2, L_3, and L_{Di} denote the four lipophilic regions and S_1, S_2, and S_3 denote the regions of negative steric repulsion. LP stands for the lone pair of electrons on the nitrogen (N) or oxygen (O) atoms of the ligands. (Modified from the Figure in Clayton et al.[19])

The BzR was studied via ligand docking using the pharmacophore model. The main results of this study are shown in **Figure 7**. These results have been instrumental in the ongoing ligand design and ligand modification.[19] It was found that in the region L_2 there is a small difference between the induced volumes of the subtypes α1 and α2. It was also determined from the included volumes of α2 and α3 that the corresponding binding pockets containing $GABA_AR$ subtypes are very similar in size, lipophilicity and shape. The induced volume of the α4 subtype was generally smaller than that of the α6, and this difference was more prominent in the L_2 and L_{Di} regions. Moreover, the L_3 liphophilic pocket is negligible in the α4 and α6 BZR, which is consistent with

the fact that they are both DI sites do not have the binding pocket required for the pendant phenyl rings in the common BZDs and IMDZs. The α5 subtypes have the largest L_2 region, which is an important observation for α5 selectivity with reduced binding at α1 subtypes. An example of that is the switch from a Cl atom (diazepam) to an ethinyl group (QH-II-066) at the C(7) position which increases the α5/α1 ratio by nearly a factor of 9 (from 1.27 to 11.22) as shown in **Figure 8**.[52, 79] This breakthrough has led to QH-II-066, a potential treatment for cancer. Moreover, it was recently reported that the development of tolerance to the antinociceptive effects of BZDs are caused by the coupling of α1 and α5 subtypes.[80] For this reason, it is beneficial to attempt to limit the binding affinities and efficacy at both of these subtypes, which has guided in the synthesis of several antinociceptive compounds that did not exhibit the development of tolerance to its effects.[61, 81, 82] This is a groundbreaking achievement, for the treatment of status epilepticus in humans; the conventional BZDs develop tolerance after just about three days but KRM-II-81(2) and HZ-I-66(1) do not in animal models.

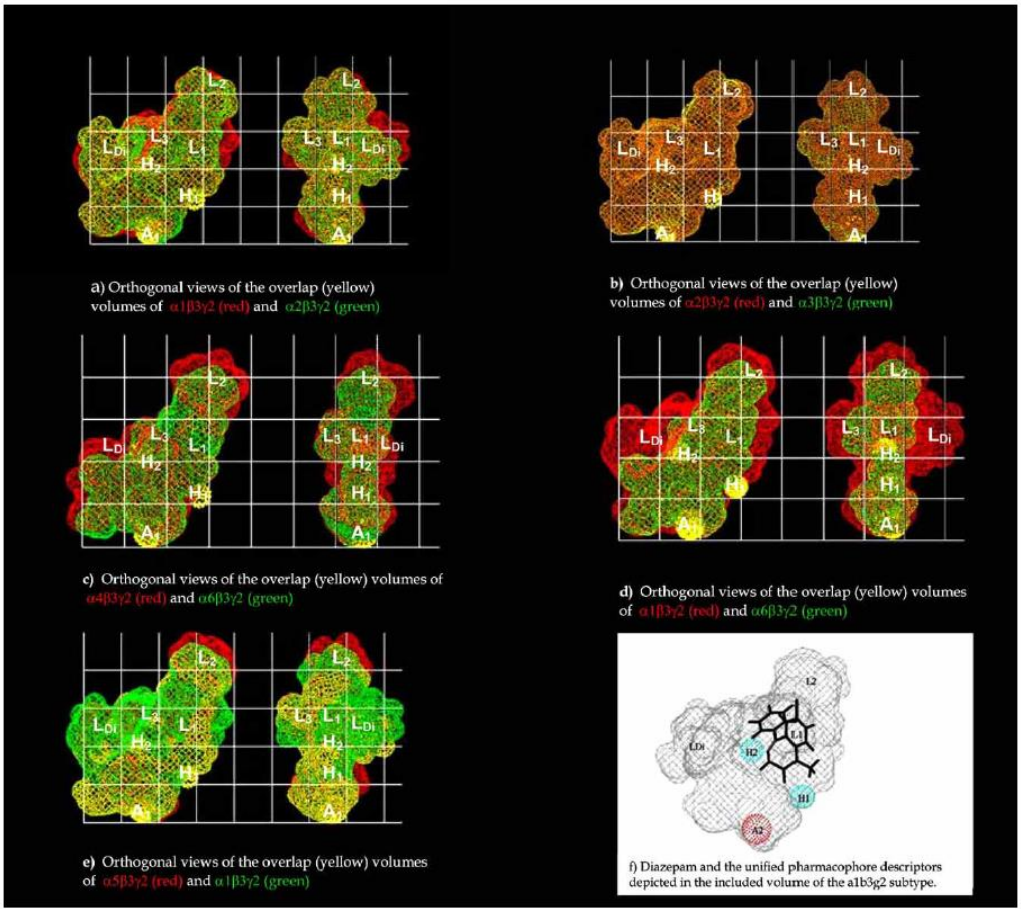

Figure 7. These images depict the overlaps between the induced volumes derived from receptor subtype selective ligands: a) α1 and α2; b) α2 and α3; c) α4 and α6; d) α1 and α6; e) α1 and α5; f) diazepam and the descriptors of the unified pharmacophore model in the included volume of the α1 subtype. The yellow color indicates an overlap has occurred, and each grid is 4 Å in side measures.[60]

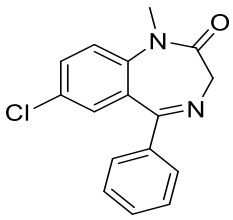

diazepam

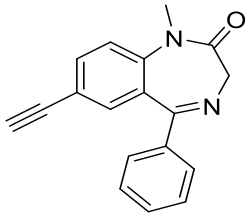

QH-II-066

Bz/GABA$_A$ receptor binding data (K_i = nM)

	α1	α2	α3	α5	α1/α5	
diazepam	14	20	15	11	1.27	**Change in Selectivity 8.83**
QH-II-066	76.3	42.1	47.4	6.8	11.22	

Figure 8. Bz/GABA$_A$R in vitro binding data of diazepam and QH-II-066. (Modified from the Figure in the Ph. D. thesis of M. Poe and T. Clayton) [52, 79]

There have been some recent developments that are important for this research. Several updated pharmacophore models and homology models have been proposed over the years.[60] A new lipophilic region (L_4) have been reported at the C(4) position in two chiral methyl enantiomers of the IMDZ class, namely, from SH-053-2'F-*R*-CH_3 (α5 subtype-selective) and its enantiomer SH-053-2'F-*S*-CH_3 (α2/3/5 subtype-selective); as shown in **Figure 9**. The region L_4 was only located in α5, and not in α2 or α3 subtypes. The volumes of both enantiomers (R and S) indicate that the binding pocket is adequate for them. But the R-isomer did not fit in the either of the α2 and α3 binding pockets. This resulted in zero efficacy in the case of the R-isomer at the α2 and α3 subtypes. The findings of the pharmacophore receptor model agreed with the efficacy data from the above which was a non-sedating anxiolytic in rhesus monkeys. While the R-isomer was not anxiolytic. (fischer 2000) α2/3/5 subtype-selective ligand.[60]

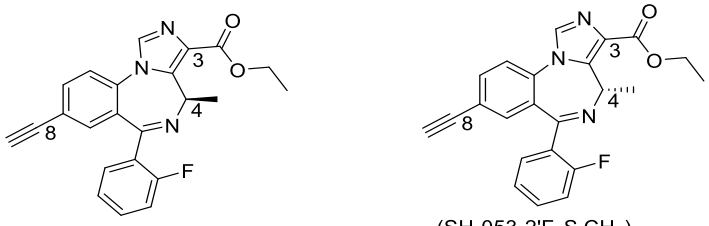

Figure 9. The structures of enantiotopic chiral imidazodiazepine (IMDZ) ligands 1 and 2.

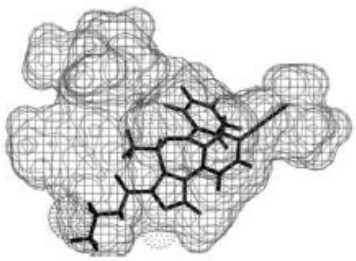

SH-053-2′F-S-CH_3 **2** fits the pharmacophore in the included volume of the alpha 2 subtype

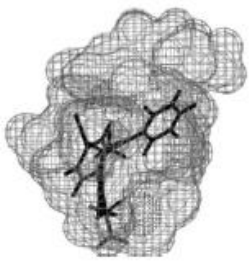

The left image of figure rotated 90°. It can be clearly seen that **2** fits within the included volume

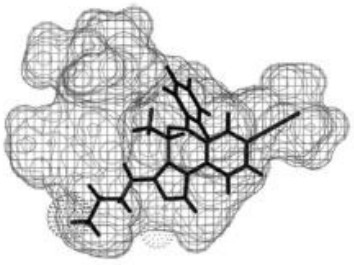

SH-053-2′F-R-CH_3 **1** does not fit the pharmacophore in the included volume of the alpha 2 subtype

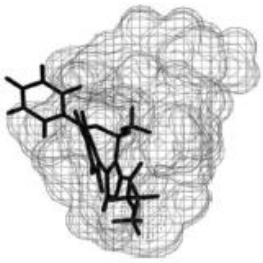

The left image of figure rotated 90°. It can be clearly seen that the conformation of **1** is such that the pendant 6-phenyl sticks outside the included volume

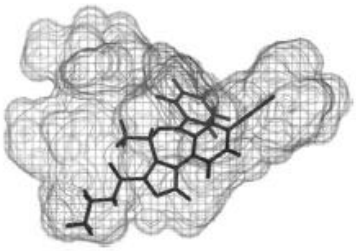

SH-053-2′F-S-CH_3 **2** fits the pharmacophore in the included volume of the alpha 5 subtype

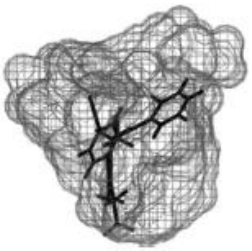

The left image of figure rotated 90°. It can be clearly seen that **2** fits within the included volume

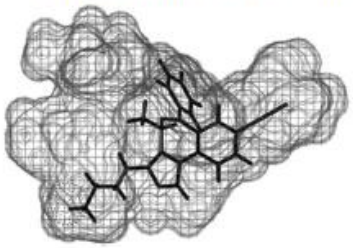

SH-053-2′F-R-CH_3 **1** fits the pharmacophore in the included volume of the alpha 5 subtype

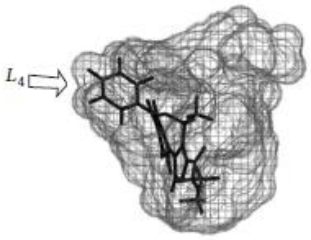

The left image of figure rotated 90°. It can be clearly seen that **1** fits within the included volume

Figure 10. The ligand occupation of SH-053-2'F-R-CH_3 (31) and SH-053-2'F-S-CH_3 (32) in the pharmacophore/receptor models of α2 and α5 subunits. (Modified and reproduced from that reported by Clayton et al.)[60]

Chapter 2: Achiral α2/3 Imidazodiazepines for the Treatment of Epilepsy and Pain

2.1. Lead Compound

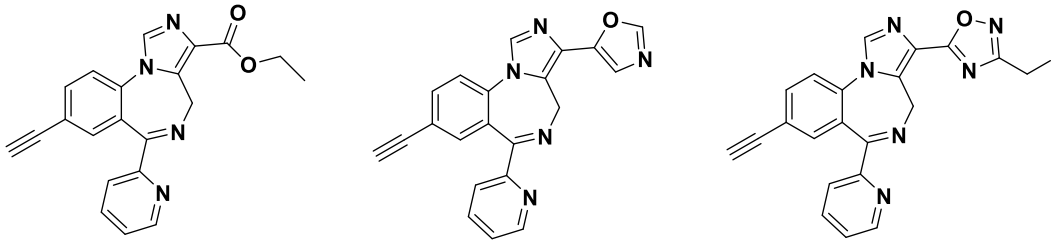

Figure 11. The lead compound for pain, epilepsy and seizure

HZ-166 (**1**) was an α2/3 subtype selective GABAkine(PAM) which showed no sedation nor motor impairment compared to diazepam[82]. **HZ-166 (1**) exhibited its efficacy in different animal models of anxiolytic activity of a drug[83] and anticonvulsant action of compounds.[84] In addition, it is active against Pain models of rodents.[85] **HZ-166** is stable in human liver microsomes (HMLs), but it is not as stable in mouse liver microsomes due to its metabolically liable ester function , Hydrolysis to the carboxylic acid and decrease the BBB penetration and bioavailability. To increase the stability in mouse liver different types of bioisosteres have been synthesized and **KRM-II-81 (2)** is one of them which is an oxazole bioisostere of an ester function. It is sterically close to the non-sedating microsomes GABAKine, MP-III-024(C-3 methyl ester)

KRM-II-81(2) was synthesized by reducing the ester function of **HZ-166(1)** with $LiAlH_4$ to an alcohol and this was followed by the oxidation with manganese dioxide to convert the alcohol into an aldehyde. This was further treated with TosMIC and K_2CO_3 to provide the final oxazole with 28% yield.[86] To increase the yield and also minimize the steps a new route was addressed to

convert the ester directly to aldehyde using diisobutyl-*tert*-butoxyaluminum hydride (PDBBA), which was subsequently treated with TosMIC and K_2CO_3 to generate the final product **KRM-II-81(2)** in 71% yield.[87] In addition, the improved large scale GLP -focused to **HZ-166(1)** was reported with an overall yield of 27.6%.[88]

2.2. Pharmacology

In electrophysical systems, the ability of **KRM-II-81(2)** on amplification of GABA signaling was studied. In recombinant receptors which consist of alpX/beta3/gamma2 receptors were administrated with GABA and the expansion effect on the induced current due to GABA combined with **KRM-II-81(2)** was measured. According to the electrophysiological recording of **KRM-II-81(2)**, it demonstrated that it was a α2/3 $GABA_AR$ subtype-selective ligand due to its higher potency at 100 nM with a very low potentiation at α1 or α5 containing $GABA_ARs$. In comparison to **KRM-II-81(2)**, diazepam showed more potentiation α1- and α5-containing GABAARs. In comparison to **KRM-II-81(2)**, PF-06372865 (a-2/3/5- selective) ligand was 9000 times more effective at α1 and 11 times more effective at α5. The coupling of these two subtypes increases the possibility of the development of tolerance to the antihyperalgesic and anticonvulsant side effects.[80]

In radio ligand binding studies, the IC_{50} value for **KRM-II-81(2)** was more than 10 mM for NMDA, AMPA, kainite, h5HT receptors (1a-f, 2a-c, and 5-HT7), hACHE, hADRa (1a, 1b, 1d, 2a, 2b, 2c), hADRb (1 and 2), hADORA3, hD1, hD2S, hDAT, hH1, hM2, hM3 which illustrated that it did not bind to other off target receptor proteins. Moreover, as **KRM-II-81(2)** did not bind to the hERG ion channel this greatly decreased the likely effectof a the heart QT problems. **KRM-II-81(2)** exhibited weak activity at the norepinephrine transport (NET). At a **KRM-II-81(2)**

concentration of 1 μM, more than 50% radioligand can be replaced. In addition, **KRM-II-81(2)** did not inhibit CYP 3A4, CYP2D6, and CYP2C9 enzyme.[86]

2.3. Pharmacokinetics

In a cytotoxicity assay in HEK293T cells, **KRM-II-81(2)** showed good liver microsomal stability and the value of the LD_{50} is greater than 100 mM.[86] After intraperitoneal and oral dosing in rat, **KRM-II-81(2)** showed excellent bioavailability. In comparison with HZ-166 (1), the concentration of **KRM-II-81(2)** in the rat plasma sample was 3910 nM wheres, the concentration of HZ-166 (1)was less than 12.2 nM.[86] In addition, the concentration of **KRM-II-81 (2)** after oral dosing in mouse was tested for 0.25-12h and found the highest concentration of the drug (600 nM) after 1h dosing.

2.4. Antiepileptic activity.

The antiepileptic activities of the lead compounds are discussed in this section.

Acute Seizure Models:

In the 6 Hz 44 mA seizure model in mice (i.p.), maximal electroshock seizure (MES) model, in rats (i.p.), and subcutaneous metrazol (pentylenetetrazole) seizure model (s.c. MET) in rats (p.o.); which are known as a“first-pass” animal acute seizure models to identify the anticonvulsant activity of ligand has been applied and KRM-II-81 was anticonvulsant in all three.

The 6 Hz kindled seizure model is found to be very useful as an early identification screening for potential anticonvulsant drugs that can reduce the seizure which caused by a long-duration, low frequency (6 Hz) stimulation, where sometimes different screening methods are not able to identify. Mice were pretreated p.o. with **KRM-II-81** (**2**), and after 2 hours the mice were challenged with 6 Hz stimulation for 3 seconds through corneal electrodes at 44 mA intensity and

the observation for seizure activity was recorded. Ligand(**2**) was anticonvulsant for the motor impariment and possible toxicity , another group of mice were treated with **KRM-II-81(2)** and observed at 4 hours after dosing. **KRM-II-81(2)** was not abe to protect the mice (n=8) that were challenged to 6Hz stimulation at the dose of 10 mg/kg. Mice, which were orally admistrated with **KRM-II-81(2)** provided protection for 3 out of 8 at the dose of 25 mg/kg. After 2 hours of oral dosing full protection was achieved at the dose of 50 mg/kg. No motor impariment, as well as toxicity or loss of righting response was observed at the dose of 50 mg/kg. At the oral dosing of 100 mg/kg mild tremors were observed in the mice and with the oral dosing of 200 mg/kg severe tremor was observed in 3 out of 8 mice. They lost their ability of righting reflex at the dose of 150 mg/kg and most noable is at the dose of 120 mg/kg. However, there were 3 metabolities in mice,which are believed to be the reason of this effect. Because these metabolities in rats were very low and at 300 mg/Kg (p.o) and there was no sedation on the rotarod nor loss of righting reflex. Moreover, in monkeys there were none of the metabolities and there was no sedation at 10 mg/Kg and no observed toxicity.

Dose	**Number protected/number tested**	
10	0/8	
25	3/8	
50	**7/8**	
Dose	**Number with observed motor effects**	**Observation**
50	**0/8**	
100	3/8	tremor
150	5/8	tremor, unable to grasp
200	8/8	more severe tremor, loss of righting

Table 2. A summary results of the 6 Hz seizure model and the motor effects study of KRM-II-81 (2) p.o. (Originally reported by Witkin, et al[89])

The maximal electroshock is one of the standard assays for initial screening for potential antiepileptic drugs in vivo animal models.[90] The 1,3-oxazole KRM-II-81 (2) along with diazepam, Hz-166 (1) were assessed in the MES test.[89] For the following procedure male CD-1 mice (n=10)

were selected. The pre-test adminstration(i.p) was done 30 minutes prior to testing and one of the foloowing drugs was used ; vehicle (1% CMC), diazepam (1, 3 or 6 mg/kg), ester **1** (3, 10 or 30 mg/kg) or oxazole (3, 10 or 30 mg/kg). The animals were subjected to 10 uA electroshock for 0.2 seconds which induced the tonic-clonic seizures in their hindlimb. The protection of animal from tonic and/or clonic seizures at the hindlimb defines the effectiveness of the drug. At the dose of 3mg/kg diazepam (DZP) was able to decrease MES-induced convulsions. At the dose of 3 mg/kg KRM-II-81(2) was slightly effective and at the dose of 10 mg/kg it was able to exhibit more anticonvulsant activity and the dose of 30 mg/kg it was able to protect the animals fully from tonic and clonic seizures where HZ-166 (1) was not able to show any effectivenss up to 30 mg/kg dose.

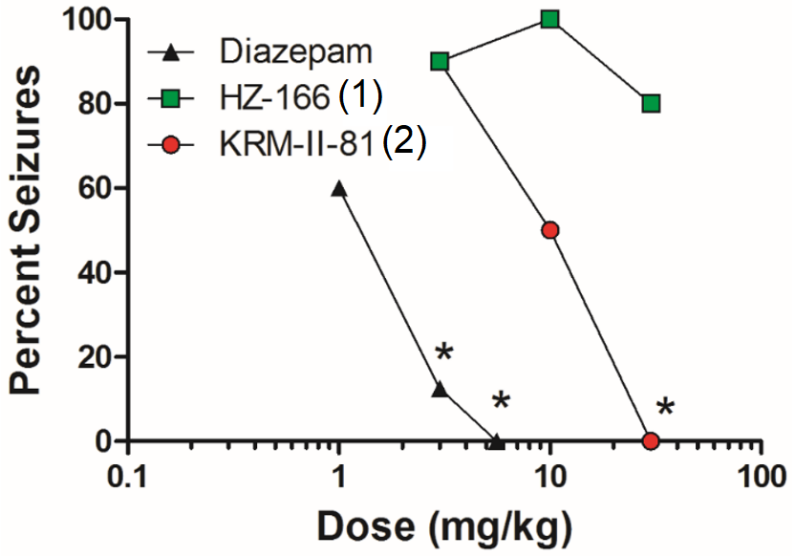

Figure 12. Seizure percentage vs dosage of Diazepam, HZ-166 (1) and KRM-II-81 (2) in the MES assay for the evaluation of their anticonvulsant activities. Male CD-1 mice (n = 10) were administrated i.p. 30 min before testing with either vehicle (1% CMC), diazepam (1, 3 or 6 mg/kg), KRM-II-81 (3, 10 or 30 mg/kg) or HZ-166 (3, 10 or 30 mg/kg). Analyzed using ANOVA (Dunnett's test versus vehicle: * P < 0.05). (Adopted from Figure in Witkin, Cook et al) [89]

A commonly used antagonist of $GABA_AR$s is pentylenetetrazole (PTZ), which is used to effect convulsion activities in animal models of seizure and epilepsy. The 1,3-oxazole **KRM-II-**

81 (**2**) diazepam (DZP) and **Hz-166** (**1**)[89] were assessed in the PTZ-induced seizure test. At first DZP (3 or 10 mg/kg), **1** (30 mg/kg) or **2** (10, 30 or 60 mg/kg) was given to the animals and they were then allowed to recover for 30 mins. Then PTZ (35 mg/kg) was administrated in order to induce seizures. The seizure activity on the rat were recorded. At the dose of 3mg/kg, diazepam was able to reduce PTZ induced seizures and the was able to achieve the full protection at the dose of 10 mg/Kg.The etheyl ester HZ-166 (1) was able to reduce some PTZ induced convulsion at the dose of 30 mg/kg. The 1,3-oxazole (**2)**exhibited some effectiveness at the dose of 10 mg/kg and gave full protection from PTZ-induced convulsions at the dose of 30 and 60 mg/kg. According to this assay, Diazepam is 10X more active than **KRM-II-81(2)** in order to provide protection to the animal from PTZ induced seizures. The data achieved from this assay was found to be consistant with the MES-induced assay. Before the PTZ induced assay, the animals were checked for potential motor impairmemts during 1 and 2 hours by doing inverted screen assay. For the inverted screen assay, rats were dosed with the drug and were scored for 1 min after 25 mins of dosing. Diazepam was found to have a minimal toxic dose (MTD) of 10 mg/kg with sedation/ataxia. For comparison, the MTD for 2 was reported to be 150 mg/kg (see more details in the ETSP report in Appendix V) with no ataxia and sedation was reported up to doses up to 250 mg/kg. The protective index (PI) had been calculated according to the following formula: (PI) = $F(MTD_{inverted\ screen}/MED_{PTZ\ convulsions})$. The PI values for diazepam and **KRM-II-81**(**2)** were 1 and 5 respectively. Thus **2** was found to have a wider safe therapeutic range than diazepam. Furthermore, at NINDS, ETSP; KRM-II-81(2) was given up to rats and no sedation nor ataxia or loss of righting response

was observed.

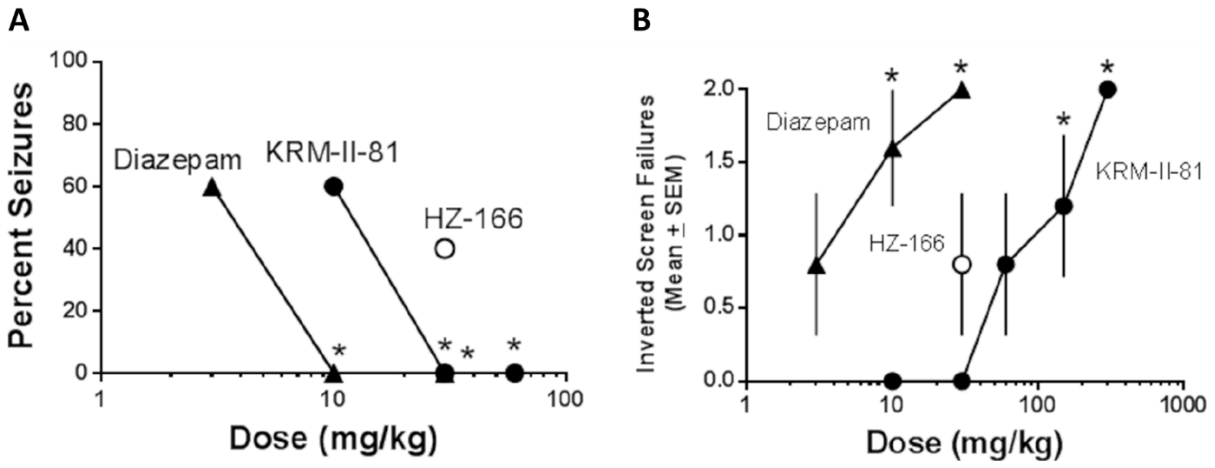

Figure 13. Seizure percentages in pentylenetetrazole (PTZ)-induced seizures (35 mg/kg, s.c.) (A) and mean inverted screen failures (B) with different doses of diazepam, Hz-166 (1), KRM-II-81 (2). Significant probability was analyzed by Fisher's Exact Probability test (*: p<0.05). For the motor score, n = 5 (diazepam, 3 mg/kg) or 8 (all other data) rats, 0=climbed over to the top of the screen, 1= hanging on to screen, 2= fell off. Data were analyzed by ANOVA followed by Dunnett's test with * p<0.05. PTZ alone produced convulsions in 96 ± 4%. The baseline motor scores were 0.12 ± 0.8. (Adopted from Figure in Witkin et al.) [89]

A seizure threshold assay was performed to determine the threshold limits on the decrease of seizure threshold for the drugs (**KRM-II-81(2)**, **HZ-166 (1)** and diazepam). The rats were divided into two groups (with and without drug pretreatment). For both groups PTZ was administrated i.v. to induce convulsions and the threshold doses were recorded. It was found that the appropriate necessary PTZ dosage (administrated as bolus) to induce seizures was 35 mg/kg, while the threshold was 37.1 ± 1.9 mg/kg. These results have been outlined in **Figure 14**. The results imply that all the three drugs raised the requirment of PTZ dosage for inducing seizures. While 1 mg/kg Diazepam was able to increase the required dosage to 49 mg/kg, 60 mg/kg of ethyl ester Hz-166 (1) did not increase the required dosages. A dose of 10 mg/kg of 1,3 oxazole KRM-II-81(2) required 71 mg/kg of PTZ to induce convulsions. Furthermore, 60 mg/kg of KRM-II-

81(2) increased the dosage requirement to 108 mg/kg. In contrast, the anticonvulsant drug Valproic acid, at 300 mg/kg, only increases PTZ dosage requirement to 81 mg/kg. While diazepam was clearly the most potent, KRM-II-81 (2)was found to have a much wider range of dosage effect.

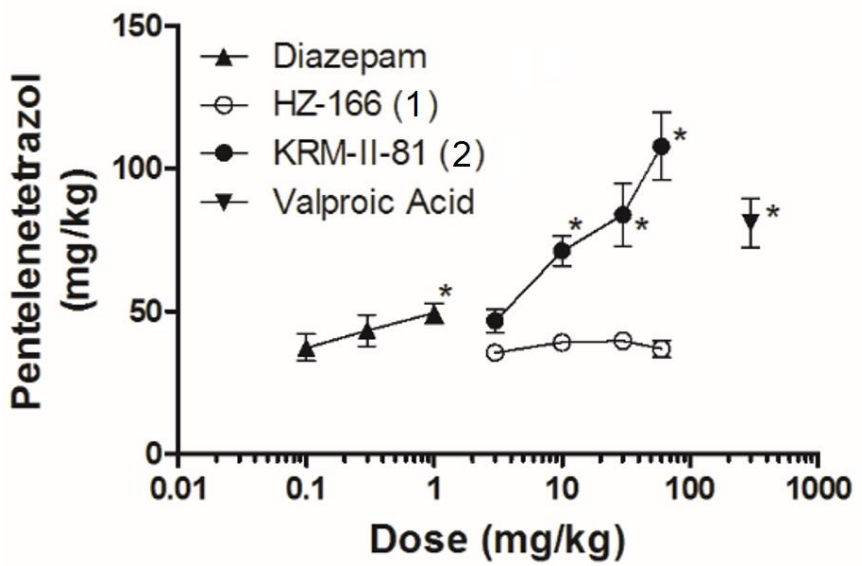

Figure 14. The determination of the threshold of Hz-166 (1), KRM-II-81 (2), and diazepam (DZP) against PTZ-induced seizures. Subjects were dosed with diazepam, KRM-II-81, HZ-166 or valproic acid 30 minutes prior to an i.v. infusion of PTZ until convulsions occurred in subjets, n = 8. Analyzed using ANOVA (Dunnett's test: * P < 0.05). (Modified from Figure in Witkin, et al) [89]

The protective index (PI) was calculated following the method described above. A PI value >1 represents a separation between anticonvulsant and side-effect doses. PI=1 means there is no difference between the doses and PI<1 indicates the dosage to induce a toxic effect is smaller than the dosage required for the desired effect. As illustrated in **Table 2**, **KRM-II-81(2)** exhibited a much broader safety margin between the dose producing the desired effect and that inducing side effects**. KRM-II-81(2)** exhibited a strong and wide anticonvulsant profile against seizures in animals induced by both PTZ and electrical stimulus.

Assay	KRM-II-81	Diazepam
Electroshock	15	3.3
PTZ Clonus	5	**1**
PTZ Threshold	15	10
After-Discharge Threshold	15	**1**
After-Discharge Duration	15	**<1**
Seizure Severity	15	**1**

[a]PI values were calculated as the minimal effective dose producing motor impairment /minimal effective doses producing efficacy. Values for HZ-166 could not be calculated for any measure due to lack of efficacy. Values of ≤1 are highlighted in bold.

Table 3. PTZ-induced seizure data.

Chronic Seizure Model

The anticonvulsant effects of KRM-II-81 were further analyzed using the following chronic seizure models: the lamotrigine (LTG) resistant amygdala-kindled seizure model in rats (i.p.), the corneal kindled seizure model in mice (p.o.), model of mesial temporal lobe epilepsy (mTLE) induced by the focal chemoconvulsant injection in mice (p.o.), and the chronic post-SE (KA) spontaneously seizing in rats: Stage 1 (i.p.). Since the acute seizure models indicated the possibilty of an anticonvulsant ligand **KRM-II-81(2)**, this ligand was furtehr investigated in the chronic seizure models. Large scale synthesis of **KRM-II-81(2)** and **MP-II-080 (3)** was executed prior to this process, as it was essential.

One of the fastest and lower-cost screening processs for potential anticonvulsant ligands at ETSP is the corneal kindled mouse model. This method involves either electrical shock or epileptogenic drug stimuli. The results obtained in this study was further confirmed by the pharmacological profiles of drugs tested in humans for partial epilepsy. In the corneaal kindled mouse model, stage 5 seizures were induced in CF-1 mice by subjeting them to kindled electrical

stimulations (3 mA, 60 Hz) for a duration of 3 s on 12 h intervals. The stimulation process was continued for 10-14 days. The testing period was considered to start 5-7 days after the last day of stimulation. A group of 8 mice were administrated **(2)** p.o. with increasing doses of **KRM-II-81 (2)** (1, 3, 8, 5, 15, 25, 30 mg/kg). The time of peak effect (TPE) was measured after 2 h. **KRM-II-81(2)** was confirmed to possess moderate anticonvulsant effects at doses as low as 3 mg/kg, whereas considerable effects were obtained at doses over 8 mg/kg. The full protection was achieved at the dose of 15 mg/kg. It should be noted that **KRM-II-81(2)** was not found to exhibit any toxicity in doses lower than 50 mg/kg and 120 mg/kg in mice and rats respectively.

Dose (mg/kg)	Time (hrs)	N / F	C	Individual Seizure Scores	Average Seizure Scores	Toxicity N / F
1	2	0 / 8		5,5,5,5,5,5,5,5	5	
3	2	2 / 8		5,5,5,5,0,5,5,0	3.75	
8	2	6 / 8		1,0,0,4,0,0,0,5	1.25	
15	2	8 / 8		0,0,0,0,0,0,0,0	0	
25	2	8 / 8		0,0,0,0,0,0,0,0	0	
30	2	8 / 8		0,0,0,0,0,0,0,0	0	
N: number of animals protected or toxic.			F : total number of animals tested.		C : Comment code.	

Table 4. The effect of KRM-II-81 in a corneal kindled mouse model

The lamotrigine (LTG)-resistant amygdala-kindled rat model is used both for investigating drug-effectiveness against symptomatic seizures as well as comparison of multiple drugs for effectiveness against resistant epilepsy. A state of resistant epilepsy was achieved in the animals by making them LTG-resistant. A daily administration of lamotrigine (5 mg/kg) causes a resistance to Na+ channel blockers during the kindling acquisition state. The effectiveness of **KRM-II-81(2)** in the cases of resistent epilepsy was tested by administering the LTG-resistant mice with doses of 1, 5, 10, 20 and 40 mg/kg of the drug. The time of peak effect (TPE) in this case was determined

to be 1 h. The doses of 5 and 10 mg/kg of **KRM-II-81(2)** were moderately successful at protecting the animals, whereas 50% protection was achieved at a dosage of 20 mg/kg. At an even higher level of 40 mg/kg, signification protection was achieved where 75% of the animals were protected 1 hr post-administration of KRM-II-81(2) (outlined in **Figure 15**). A 40 mg/kg dosage of KRM-II-81(2) not only lowered the siezure score by nearly 60%, it also cut the duration of seizure by half (**Figure 15 B & C**).

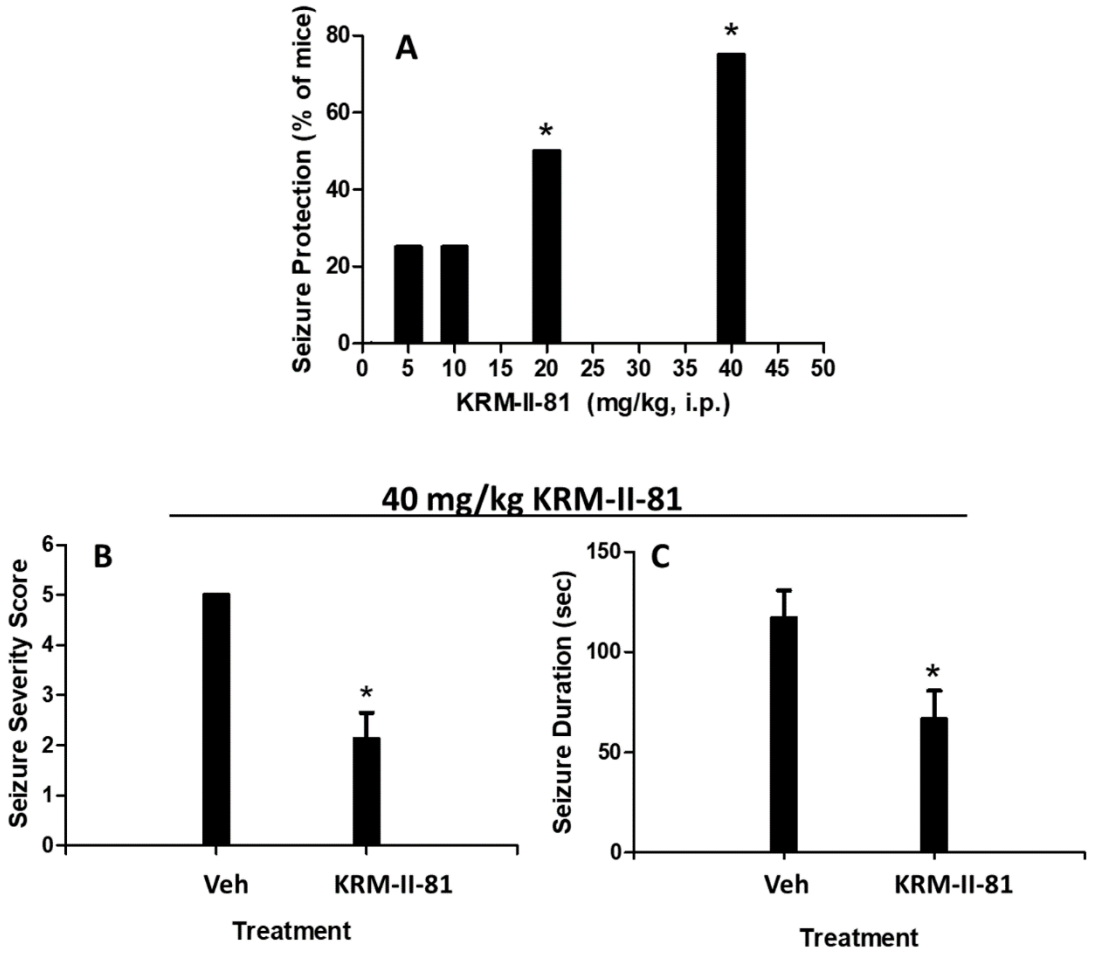

Figure 15. The seizure protection percentage at the doses of 1, 5, 10, 20, and 40 mg/kg (A), seizure severity at 40 mg/kg as compared to vehicle (B) and seizure duration at 40 mg/kg as compared to vehicle (C) of lamotrigine (LTG)-resistant amygdala-kindled rats administered with KRM-II-81 (2). The average seizure scores ± S.E.M.and afterdischarge duration is noted, as are the number of animals protected from seizure (defined as a Racine score < 3) over the number of animals tested.

The MTLE mouse model includes many features of Temporal Lobe Epilepsy (TLE) in humans. One of the major causes of refractory epilepsy is Mesial Temporal Lobe Epilepsy (MTLE), originating from the hippocampus of the affected patient's brain. For this test, a non-convulsive Severe Epilepsy (SE) was induced in a subject mouse by the administration by injection i.v. of the neurotoxin Kainic Acid (KA) (1 mmol in 100 mL of vehicle) as an epileptogenic agent. This induced severe epilepsy in the animal that can last for hours. An electrode was implanted into the left part of the hippocampus of male rats in order to measure Paroxysmal Hippocampal Discharges (HPD). After 4 weeks of KA administrations, the mice reached a stage of recurrent seizures (30-60 times per hour, each lasting 15-20 s). A group of MTLE mice (n = 5) were injected i.v. with KRM-II-81 (15 or 30 mg/kg) and EEG recordings were raken 20 min prior and 90 min post-administration of the drug. The HPD signals were recorded each time for a 20-min interval starting 10 min before the PTE. **KRM-II-81(2)** was able to reduce the rate of epilepsy to 31.3% at a dosage of 15 mg/kg and to 8.7% at 30 mg/kg (Table 5). This data confirms the potential of the drug as a possible cure for refractory epilepsies in humans.

Dose and TPE	Recording Period	Mouse 1	Mouse 2	Mouse 3	Mouse 4	Mean	SEM
15 mg/kg	Baseline	11	18	23	15	16.75	2.53
peak	120 min	2	5	9	6	5.50	1.44
120 min	% peak effect	18.18	27.78	39.13	40.00	31.27	5.18

Table 5. The effect of KRM-II-81 (2) at 15 mg/kg on in MTLE mice model.

Dose and TPE	Recording Period	Mouse 1	Mouse 2	Mouse 3	Mouse 4	Mouse 5	Mean	SEM
30 mg/kg	Baseline	13	20	12	18	8	14.20	2.15
	110 - 130 min	5	1	0	0	0	1.20	0.97
Peak 120 min	% peak effect	38.46	5.00	0.00	0.00	0.00	8.69	7.51

Table 6. The effect of KRM-II-81 (2) at 30 mg/kg on in MTLE mice model.

Status Epilepticus (SE) is a type of severe epilepsy, where either repeated seizures happen without an interval of full recovery or continuous seizures occurs for longer than 30 min. In the SE-induced spontaneous recurrent seizure model, rats were administered i.p. with Kainic Acid (7.5 mg/kg) on an hourly basis for up to 4 h to induce SE in the animals. At the end of the 4 h period, all animals achieved stage 5 seizures. The treatment was continued for 10 weeks. Then each animal was implanted with a wireless telemeter into the peritoneal space under its skin. This implant was used for EEG monitoring and only the rats with the highest seizure burden scores were selected for the study (n = 24). During the first week of the study, the baseline seizure rate was determined. The rats were then divided into a vehicle and a drug-treated group (n = 12 each). On the week 2, the subject animals were administered with **KRM-II-81(2)** (20 mg/kg) for a period of 5 days. On week 3, the rats were given only vehicle treatment for washout. The cross-over paradigm was used to account for any possible design variations. A group of rats (n = 6) were administered with vehicle only, whereas another group of rats (n = 6) were administered first with the vehicle and then with **KRM-II-81 (2)**. The animals were monitored post-treatment and a list of detected events was produced. The results indicated that **KRM-II-81(2)** considerably improved the condition of KA-induced SE in the rats that were treated with the drug either on week 2 or week 3. A 75% drop in daily seizure burden score was observed in the test group. 50% of the drug-treated rats were protected from SE whereas the baseline and the vehicle did not exhibit any changes. The generalized seizures were found to be recurrent in the control group during the vehicle treatment period. These results have been outlined in **Figure 16**.

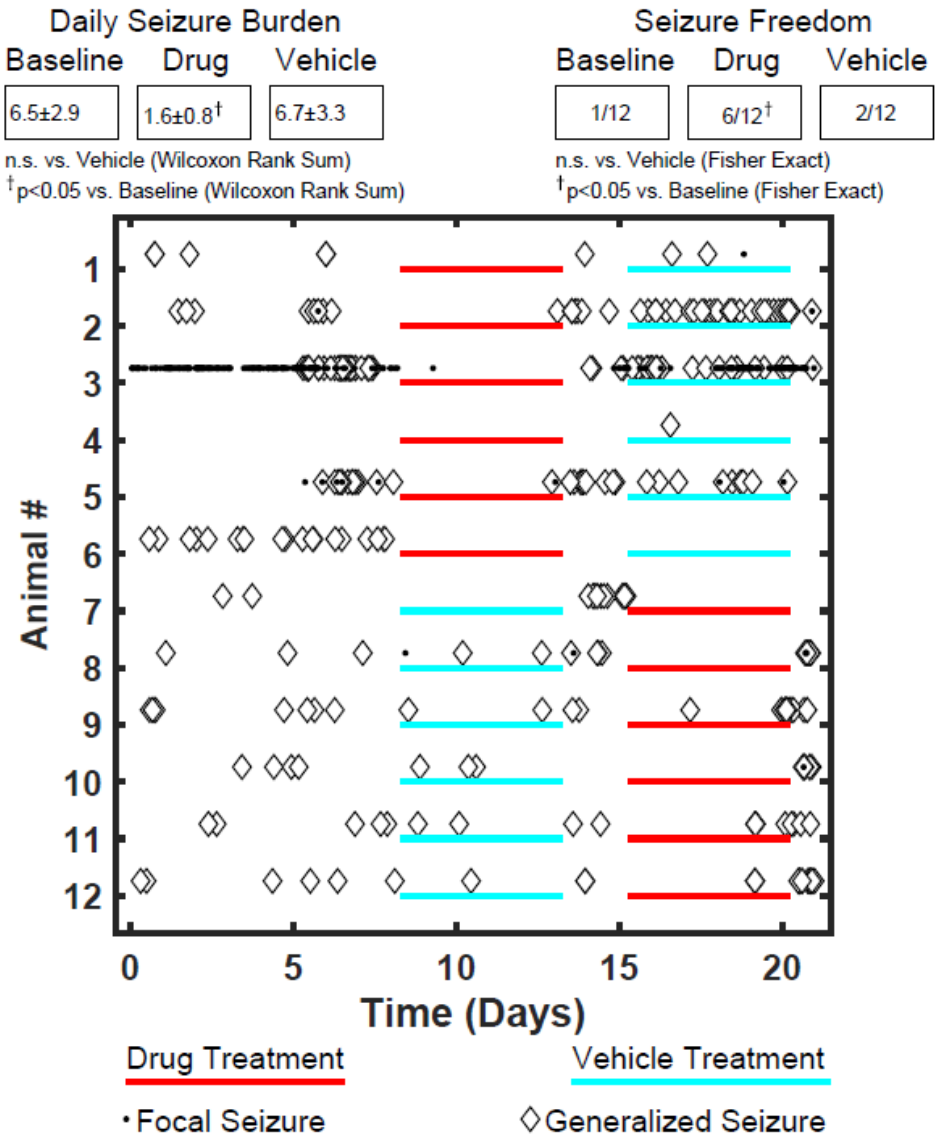

Figure 16. The effect of KRM-II-81 (2) in the spontaneous recurrent seizures caused by SE in rat models. At week 1, a baseline seizure rate is determined. A group of rats (n = 12) were enrolled in Stage 1 chronic monitoring and then split into two treatment groups (n = 6/group). On week 2, one group of rats was given 20 mg/kg of KRM-II-81 (2) for 5 days, (Monday-Friday). At the end of the treatment period, rats were monitored throughout week 3 with only vehicle treatment. On the other hand, the second group (n = 6) received vehicle first, followed by the treatment of 2. Each data represents a seizure event. * p<0.05 as compared to the vehicle group. (Unpublished data)

Combination therapy

Adult male Sprague-Dawley rats (Envigo, Indianapolis, IN, USA) weighing 200-250 g were used for these studies. The animals were kept in 12/12 h light/dark cycles. The access to food and water were only restricted during the experimental sessions. A group of 8 rats were selected for each session. The inflammatory pain was induced by inoculating the anesthetized rats with Complete Freund's Adjuvant (CFA) (0.1 mL), injected into the right hind foot pad. On the other hand, neuropathic pain was induced by the Chronic Constriction Injury (CCI) procedure. Upon anesthetizing the rats, the sciatic nerves were exposed and four ligatures (4-0 chromic gut; Roboz Surgical Instrucment Co. Inc., Rockville, MD) were placed on each rat about 1 mm apart around the sciatic nerve.

Mechanical hyperalgesia was determined using von Frey filaments (1.4 g – 26 g; North Coast Medical, Mogran Hill, CA) two days post-inoculation and 7 days post-surgery respectively. These subject animals were placed in elevated chambers with mesh floors. The filaments (starting with 1.4 g in ascending order) were applied to the medial plantar of the hind paw for approximately 2 s until buckling occurred. The mechanical threshold is defined as the lowest force that cause the animal to withdraw the hind paw. The time course study was conducted upon administering a single injection of either one of the compounds (**KRM-II-81 (2)**, NS16085 or the vehicle) and assessments made every 15 min for a duration of 4 h. For cumulative dosing procedures, measurements were made every 20 min and each dosage was administered immediately after measurement.

The food maintained operant responding experiments were carried out in commercially available chambers inside a sound-reducing, ventilated enclosures.[91] Two groups of rats (n=8)

were trained to press a lever for food. The chamber contained one active and another inactive lever. There were six experimental cycles, and each cycle started with a 15-min inactive period during which the chamber was dark, followed by a 5-min response period under light during which pressing the active lever would dispense food. The drugs were administered in combination at the beginning of each inactive period. The response period ended either after 5 min or after dispensing 5 food pellets- whichever came first. The light was turned off at the end of each cycle.

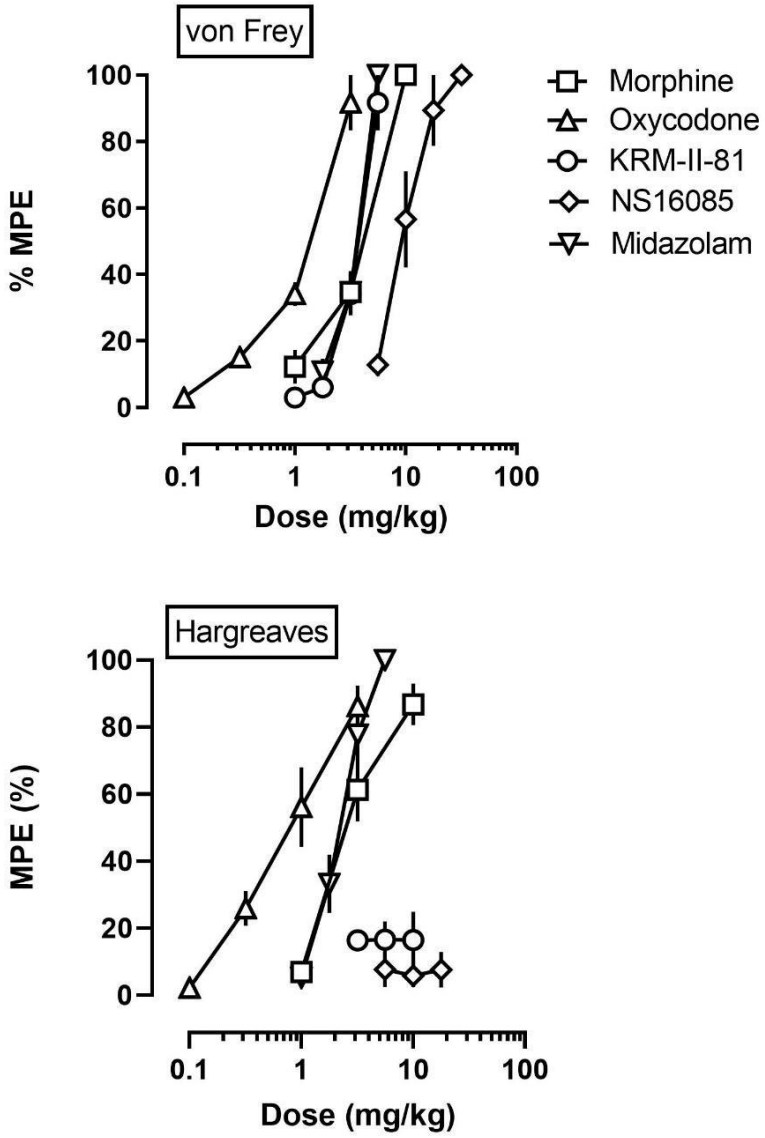

Figure 17. The effects of oxycodone, morphine, and $GABA_A$ receptor positive allosteric modulators on CFA-treated rats (shown as percentage in von Frey (top) and Hargreaves (bottom) assay.

Treatment	von Frey	Hargreaves
Morphine	3.17 (2.59, 3.89)	2.99 (2.45, 3.65)
Midazolam	3.05 (2.96, 3.73)	2.66 (1.95, 2.67)
KRM-II-81	3.84 (3.13, 4.72)	> 10
NS16085	9.63 (7.39, 12.5)	> 17.8
Oxycodone	1.13 (0.90, 1.43)	0.91 (0.56, 1.47)

Oxycodone/Midazolam		
1:3	1.96 (1.34, 2.87)	1.08 (0.41, 2.90)
1:1	1.03 (0.83, 1.30)	0.68 (0.35, 1.34)
3:1	0.76 (0.58, 1.00)	0.52 (0.37, 0.73)
Oxycodone/KRM-II-81		
1:3	3.29 (2.77, 3.91)	3.55 (1.98, 6.36)
1:1	1.76 (1.32, 2.32)	2.80 (1.54, 5.09)
3:1	0.93 (0.68, 1.27)	0.67 (0.32, 1.40)
Oxycodone/NS16085		
1:3	6.36 (4.02, 10.1)	11.0 (7.07, 17.2)
1:1	4.60 (2.91, 7.29)	3.34 (1.99, 5.62)
3:1	2.32 (1.81, 2.96)	1.16 (0.57, 2.37)
Morphine/Midazolam		
1:3	1.84 (1.35, 2.51)	1.93 (1.28, 2.91)
1:1	1.79 (1.29, 2.48)	0.86 (0.69, 1.07)
3:1	0.67 (0.47, 0.96)	0.27 (0.14, 0.52)
Morphine/KRM-II-81		
1:3	1.88 (1.50, 2.36)	1.23 (0.83, 1.83)
1:1	1.44 (1.25, 1.65)	0.87 (0.51, 1.50)
3:1	0.83 (0.72, 0.95)	0. 56 (0.42, 0.74)
Morphine/NS16085		
1:3	5.37 (4.26, 6.76)	3.98 (3.19, 4.96)
1:1	4.07 (3.06, 5.40)	2.46 (1.95, 3.10)
3:1	2.60 (2.05, 3.30)	1.88 (1.33, 2.65)

Table 7. ED50 values (95% CL) for different individual and combination drugs in the von Frey (center column) and Hargreaves' test (right column). For drug combinations, only the ED50 values of the GABAA PAMs are shown.

The mean Paw Withdrawal Threshold (PWT) under control conditions for the von Frey test was 23.4 g. The PWT value after the CFA administration was 4.67 g. Significant reduction of PWT was observed after the administration of **KRM-II-81(2)** and NS16085. The potent dosage for these two drugs were found to be 3.2-5.6 mg/kg and 10-32 mg/kg, respectively. The $GABA_A$ receptor PAMs mildazolam, **KRM-II-81(2)** and NS16085 all produced significant mechanical

analgesia. These drugs are also promising in combination therapy with opioids such as oxycodone and morphine.

2.5. Behavioral effects of subtype-selective $GABA_A$ PAMs

For this study, adult male Sprague-Dawley rats (Envigo, Indianapolis, IN, USA) weighing 200-250 g were used. The animals were maintained and prepared for experiments. The inflammatory pain was induced and mechanical hyperalgesia was measured. The animals were administered a single injection of one of the three drugs: **KRM-II-81(2)**, NS16085 and midazolam at the beginning of each test session and then placed in the test chamber.

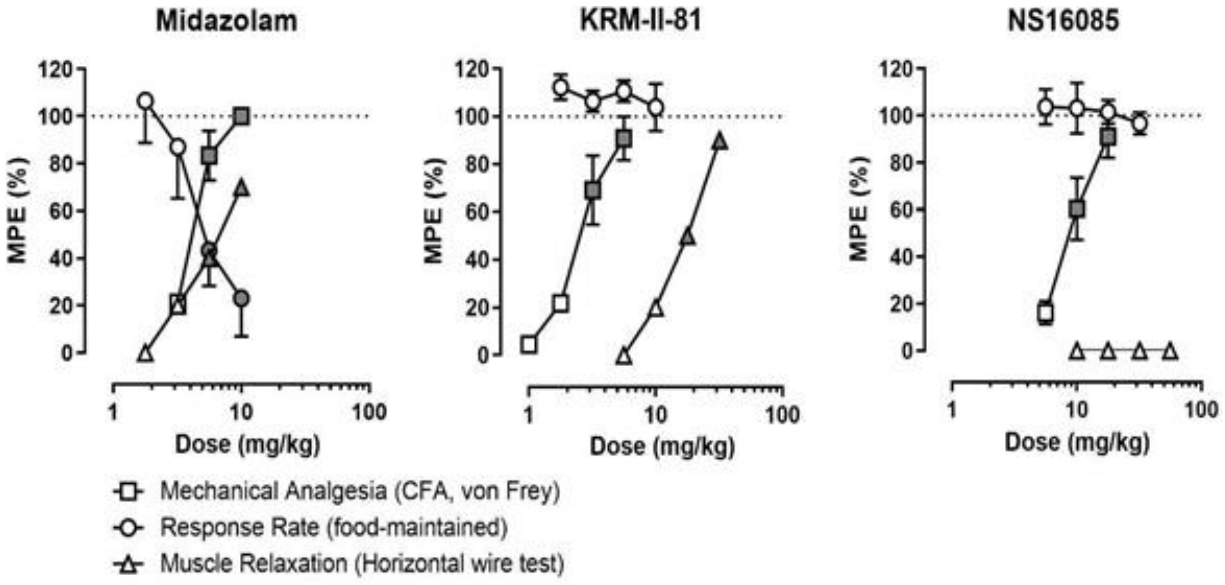

Figure 18. The effects of GABAA PAMs on CFA-induced mechanical nociception, muscle relaxant activity and control responding rate. The filled-in symbols (gray) indicate that effects are significantly different from vehicle treatment condition ($p < 0.05$).

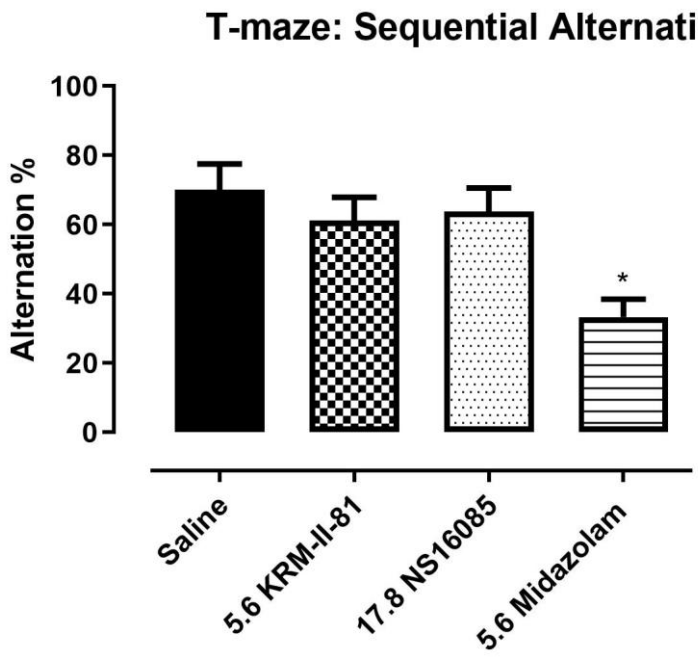

Figure 19. The effects of $GABA_A$ PAMs on the working memory in rats as percentage of alternation for different drugs. Asterisks indicate scores which are significantly different from the saline-treated group ($p < 0.05$).

Place escape/avoidance paradigm

The affective-emotional component of pain was analyzed on the basis of the place escape/avoidance paradigm.[92, 93] The animals were placed in an inverted cage that was painted half white and half black. The 60 g von Frey filament was applied to the hind paws of the rats every 15 s over the course of 30 min. When the rat was on the black side of the cage, the filament was applied on the inflamed paw and when it was on the white side, the filament was applied on the non-inflamed paw. The percentage of time spent on the white half of the cell was used to determine the escape/avoidance learning. This was a blind experiment, where the experimenter was unaware whether the vehicle or one of the drugs had been administered to the animal.

Horizontal wire test

A horizontal wire (galvanized, 16 gauge 1/16" diameter) was strung across the cage. A group of 10 rats were lifted by the tail and allowed to grasp the wire, following the previously established procedure.[94] If the animal was unable to complete the task within 3 s, it was recorded. The cumulative dosage procedure was followed in this study. Measurements were made every 20 min and the next dosage of drug was administered immediately after measurement. This was also a blind test where the experimenter was unaware of the drug and dosage.

T-maze spontaneous alternation task

A Plexiglass T-maze was constructed and painted with a grey color for this experiment. The maze was 30 cm tall, with the start arm and goal arm having the measurements of 50 cm x 16 cm and 50 cm x 10 cm, respectively. Guillotine doors were positioned at the midpoint of each arm to prevent the animal from escaping after a choice was made. Four groups of rats (n=10 each) were selected and each group treated with one of the following: **KRM-II-81 (2)**, NS16085, midazolam and saline. The treatments were administered 20 minutes before the first trial. A total of seven trials were carried out. At the beginning of each trial, the animal was placed in the start arm and allowed 2 min to choose either the right or left goal arm. Once its whole body had entered its chosen goal arm, the guillotine door was quietly slid down to prevent the animal from escaping. After keeping the animal confined for 30 s, it was removed and placed back in the home cage for another 30 s. This process was repeated until all 7 trials were done. This was a blind experiment where the experimenter was unaware of the drugs administered. In the placed escape/avoidance study, a dosage of 1.0 – 3.2 mg/kg of **KRM-II-81(2)** was found to significantly reduce the behavior

25 – 40 min after administration of the drug. In the horizontal wire test, the **KRM-II-81(2)** produced a dose-dependent impairment of the grasping reflex and increased myorelaxant activity at dosage 17.8 and 32 mg/kg. In the T-maze test, the mean alternation percentage was reduced from 70% to 61% in case of **KRM-II-81(2)** which was deemed to be statistically insignificant. In general, **KRM-II-81(2)** and NS16085 both displayed a favorable side-effect profile in comparison with midazolam. Both drugs were able to selectively produce analgesic effects. These data strongly suggest that **KRM-II-81(2)** and NS16085 are able to produce analgesia without causing the undesired pharmacological effects associated with benzodiazepines.

2.6. Discriminative Stimulus Effects

The subject animals were chosen and prepared following the same method as described in the section 2.5. Behavioral effects of subtype-selective GABAA PAMs For the drug discrimination studies, two-lever operant chambers were placed inside sound-attenuating and ventilated enclosures following previously published procedures.[95-97] Two groups of animals were trained to discriminate saline from midazolam or **KRM-II-81(2)** (3.2 mg/kg, injected i.p.). This is a multiple-cycle training procedure described in the previous literature.[97, 98] Each cycle started with a 15-min timeout period where the chamber was kept dark. After that, light was turned on and a 5-min response period was started during which a cue light above each lever was illuminated. Ten consecutive correct responses would result in food delivery. Each lever was predetermined to either resulting into an injection of the saline or the drug (midazolam or KRM-II-81). The response period ended after 5 min or the delivery of 10 food pellets.

The training session started at single-cycles. The animals were trained by first administering either of the drugs or their respective vehicles. These sessions were conducted on a

daily basis and alternated between drug and saline every two days. When an animal would achieve 90% or better accuracy of responses, it was promoted to multi-cycle training. During the multi-cycle trainings, each day would either consist of two vehicle/drug training sessions or one to three vehicle-only sessions. There were also training cycles with five consecutive vehicle training days. This training protocol was to ensure that there was minimal lever-bias in the animals.

The test sessions were similar to the training sessions and lasted up to five cycles. During the test sessions, 10 consecutive responses on either lever delivered food pellets. The animals were administered either the vehicle or the drugs before the first cycle of teach test session. The drugs were prepared and administered i.p. While rats achieved reliable dose-discrimination with midazolam, only 40-80% of the response was produced with KRM-II-81. Upon a series of over 115 training sessions, reliable drug discrimination response was not achieved with KRM-II-81. This is an important finding because the ability of drug discrimination indicates the potential of abuse of a certain drug. **KRM-II-81 (2)** does not substitute for midazolam which indicates it will not create dependence addiction like benzodiazepines.

2.7. Chemistry of deutarated analog of KRM-II-81

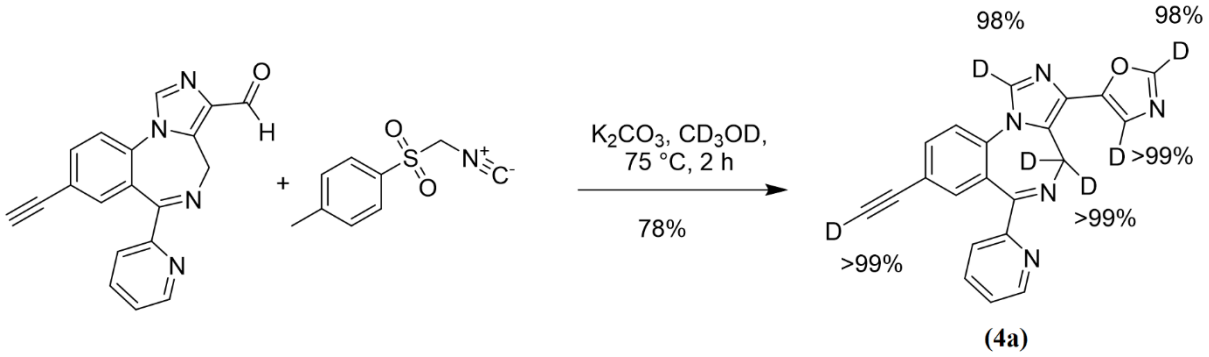

Scheme 1. Synthesis of D5 KRM-II-81

The synthesis of the deuterated analog of KRM-Ii-81, D_5-KRM-II-81 followed the same procedure as KRM-II-81 except dry CD_3OD was used here for deuterium source. The toluenesulfonylmethyl isocyanide, K_2CO_3 and the aldehyde were dissolved in CD_3OD instead of methanol and run for 2 h. For full conversion mass spectroscopy and NMR were employed over time to ensure deuterium atoms had replaced the corresponding hydrogen atom.. From D6 KRM-II-81 to D5 KRM-II-81, the deuterium on C8 position was exchanged with proton by using methanol which was the proton source. In this case the amount of methanol is very important.

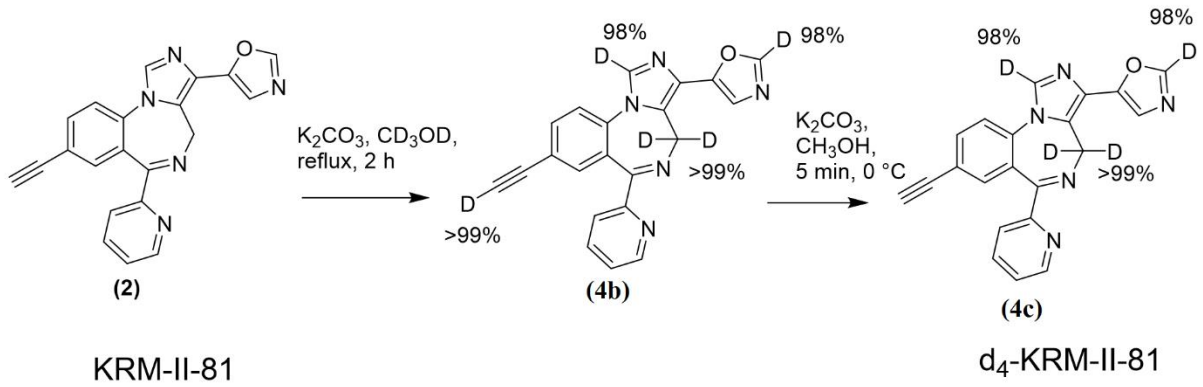

Scheme 2. Synthesis of d4-KRM-II-81.

In case of d4 KRM-II-81, KRM-II-81 was stirred with base K_2CO3 dissolved in dry CD_3OD. It was heated to reflux for 2 h. Again, to exchange the C (8) deuterium with a proton methanol was added quantitative amount and heated for 30 minutes as shown above.

In previous several studies it was found that introduction of a chlorine molecule into one or more certain positions of a molecule can improve the biological activity. For SAR, different analog with 2'Cl of lead compound KRM-II-81 had synthesized. Most of them are noncytotoxic and less sedative in rotarod assay. The 2'Cl non chiral analog of KRM-II-81 has discussed in this section.

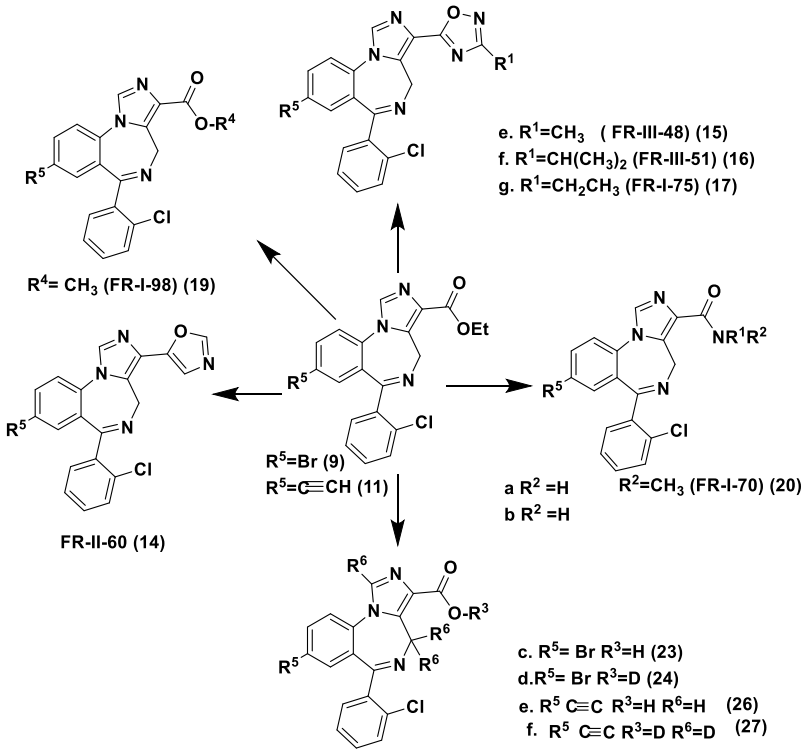

Figure 20. Analogs and bioisosteres of the lead compound

2.8. Molecular Docking

Recently, several cryo-EM independent studies have provided crucial insights into the structure the heteropentameric $GABA_A$ Rs ion channels.[99-102] These structures not only yielded unprecedented insights into the overall architecture of heteropentameric $GABA_A$ Rs but also into the protein interactions of diverse ligands including the agonist GABA and positive allosteric modulators (PAM) BZDs (diazepam and alprazolam).[103] The $GABA_A$ receptor-signaling mechanism is described by a "lock and pull" mechanism. The binding of GABA at the $\beta3^+/\alpha1^-$ interface leads to the movement of loop-C, which initiates a concerted global anti-clockwise motion in the extra cellular domain (ECD). The BZDs facilitate this motion by binding at the $\alpha1^+/\gamma2^-$ ECD interface.[103] Examination of cryo-ER structures of the $\alpha1\beta3\gamma2L$ $GABA_A$ R (6HUP

and 6HUO) clearly illustrates what is believed to be the active conformations of diazepam (DZP) and alprazolam (ALP). These cryo-ER structures reveal three of the most important interactions which are important for BZDs to function as a PAM, i) bifurcated hydrogen bonding with α1Ser205, ii) halogen bonding with the backbone of α1His102, note that flunitrazepam and clonazepam have nitro group at C7 which are highly likely involved in a hydrogen bond with the histidine side chain and the compensating halogen bond interactions with diazepam and, iii) pi-pi stacking with α1Tyr210 and α1Phe100 showed in **Figure 21 and Figure 22**. In the case of diazepam the α subunit is indispensable because diazepam have other binding site but in our research we are only interested in at the BZPs binding site.[104] DZP and ALP interact with the α1His102 *via* halogen bonding with the backbone carbonyl as shown in **Figure 21 and Figure 22**. The distance between the chlorine atom and carbonyl oxygen of α1His102 was 3.8 Å in the DZP bound cryo-ER structure (6HUP) and 2.9 Å in the case of ALP (6HUO). The σ-hole angle is 165-167° in both cyro-ER structures. The bifurcated hydrogen bond formed by ALP with α1Ser205 is shorter than that configured with bound DZP. The shorter halogen bond and bifurcated hydrogen bond interaction are consistent with the more potent affinity of ALP toward α1 as compared to DZP.

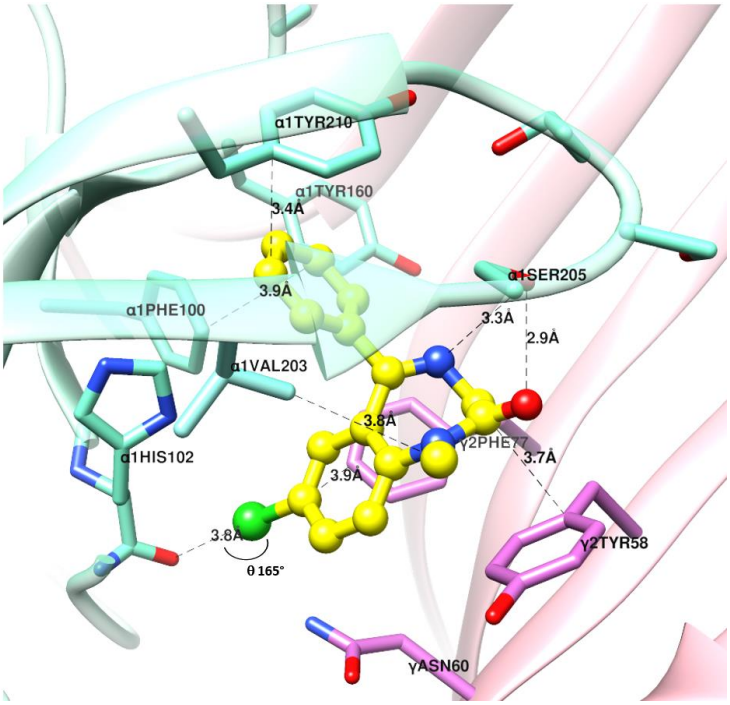

Figure 21. Diazepam (yellow) in a complex with α1 (aquamriane) and γ2 (orchid) subunits of α1β3γ2L $GABA_A$ receptor 6HUP. Dashed lines indicate π–π interactions, hydrogen bonds and halogen bond.[100]

The active confirmation of BZDs is unique at the $\alpha^+\gamma^-$ interface of $GABA_A$ R and enable the ligands to function as PAMs. The movement of the loop-C at the $\alpha^+\gamma^-$ interface during $GABA_A$ channel opening is facilitated by BZD binding in this unique conformation. The unique active confirmation of BZDs is further evident from two cryo-ER structures (6HUP and 6HUO), both structures of which have similar active confirmations of DZP and ALP (**Figure 22** and **Figure 23**).[103] Flumazenil is a competitive antagonist of BZDs and it is used as an antidote in the treatment of benzodiazepine overdose.[105] Examination of the cryo-ER structure of flumazenil (6D6U) with the $GABA_A$ R illustrates that flumazenil binds at the $\alpha^+\gamma^-$ interface in a different conformation as compared to DZP or ALP (**Figure 22** and **Figure 23**).[102] Examination of the cryo-ER structure (6D6U) also indicates that flumazenil does not form the two key interactions of the bifurcated hydrogen bond and the halogen bond interaction with the protein. The lack of these two

interactions is responsible for the inability of flumazenil to facilitate the loop-C movement at the $\alpha^{+}\gamma^{-}$ interface of the $GABA_A$ R. Therefore, flumazenil acts as a competitive antagonist at this site (**Figure 23**) where it overlaps with only part of the structure of the BZDs.

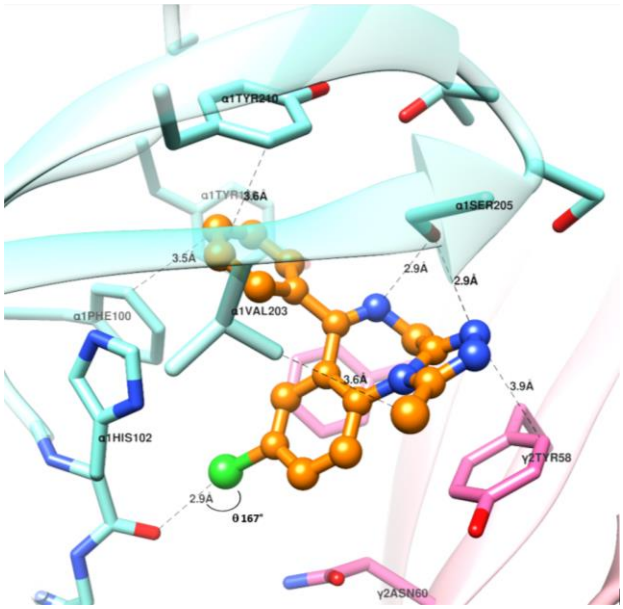

Figure 22. Alprazolam (orange) in the complex with α1 (aquamriane) and γ2 (orchid) subunits of α1β3γ2L $GABA_A$ receptor 6HUO. Dashed lines indicate π–π interactions, hydrogen bonds and a halogen bond.

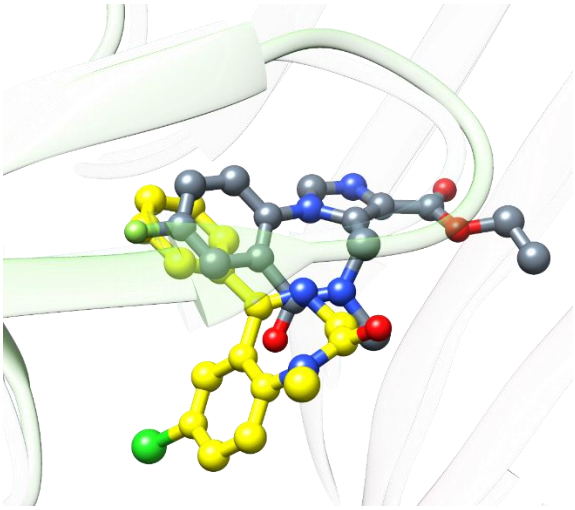

Figure 23. Overlap of diazepam (yellow) and flumazenil (grey) in complex with α1 (aquamriane) and γ2 (orchid) subunits of α1β3γ2L $GABA_A$ receptor 6HUP and 6D6U.

The sequence alignment of α1-6 subunits indicates that in the α4 and α6 peptides the α1His102 is replaced with an arginine residue, the larger side chain of which sterically clashes with ALP and DZP. This explains why classical BZDs such as DZP and ALP do not act on $GABA_A$ R subtypes containing α4 or α6 subunits. In addition, the pocket L3 is smaller. The His102 is conserved in α1-3 and α5 subunits. The amino acid residues involved in the interaction with the pendant phenyl ring of DZP and ALP are conserved in α1-3 and α5 subunits. Examination of the loop-C region of the α subunits show subtle differences in amino acid residues inside the BZDs binding site. The Ser205 residue in the α1 subunit is replaced in the α5 subunits with Thr205. Moreover, the Val203 residue in the α1 subunit is replaced with an Ile203 in α2-3 and α5 subunits. These subtle differences in amino acids provides unique 3-dimensional shapes of BZD R binding pockets.

The cryo-ER structure of the α1β3γ2L $GABA_A$ Rs (6HUP and 6HUO) has been used with the help of Dr. Golani to interrogate the differences in the molecular interactions.[103] The role of the halogen atom at C7 in the DZP ring can be explained by this and also the molecular interactions of the 2'-substituent on the pendent phenyl ring of DZP can be investigated by this docking.

Here structural docking studies were conducted to identify the unique structural features of **KRM-II-81(2)** that might be responsible for reduced sedative effects. **KRM-II-81(2)** with poor interaction with α1-associated GABAARs is described, **KRM-II-81(2).**[86] KRM-II-81 was docked in the ALP (alprazolam) bound CryoER structure (6HUO). Overlay of the bound ALP conformation and the best pose of **KRM-II-81(2)** showed that the pendant ring of both compounds bound similarly; however, the imidazodiazepine ring and triazole/imidazole rings bound in a different conformation.[106] The chlorine atom at the C8 position in alprazolam formed a halogen

bond with the carbonyl oxygen of the α1His102 amino acid backbone. In contrast, the acetylene in place of the chlorine atom at C8 of **KRM-II-81 (2)** did not interact with this α1His102. Docking scores of alprazolam and **KRM-II-81 (2)** were -10.8 kcal/mol and -9.4 kcal/mol, respectively demonstrating that alprazolam binds more strongly to the α1β3γ2L $GABA_A$ receptor as compared to **KRM-II-81(2)**

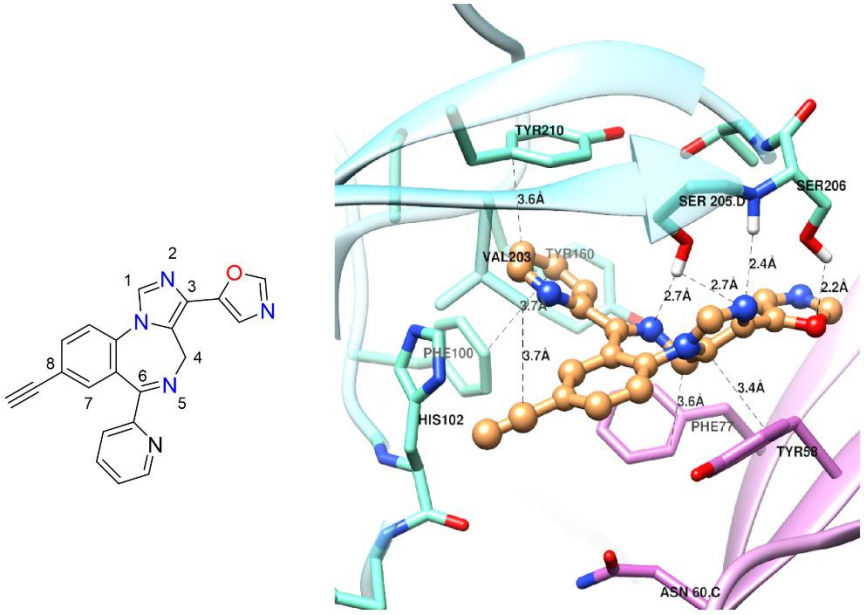

Figure 24. Binding of KRM-II-81 at the $\alpha^{+}\gamma^{-}$ interface of the $GABA_A$ receptor. Docked KRM-II-81 (sandy brown) in complex with the α1β3γ2L $GABA_A$ receptor

FR-II-60 (14) was also docked with ALP (alprazolam) bound CryoER structure (6HUO) (**Figure 26**). **FR-II-60 (14)** does not interact with the α1His102 *via* a halogen bond with the backbone carbonyl KRM-**II-81(2)**. In **FR-II-60 (14)**, the acetelene group forms a hydrogen bond instead of a halogen bond with Val203, in addition the three centered bifurcated hydrogen bond is formed between the N atom of seven membered ring, the nitrogen of the imidazole top ring and the oxazole ring with the SER205 which value is 2.1A. The bifurcated hydrogen bond formed by **FR-II-60 (14)** (2.1 A) with α1Ser205 is shorter than that configured with bound **KRM-II-81(2)**

(2.7A). The shorter halogen bond and bifurcated hydrogen bond interaction should make **FR-II-60 (14)** more potent the α1β3γ2 sites as compared to KRM-II-81. The docking score of **FR-II-60 (14)** and **KRM-II-81(2)** is -10.8 kcal/mol and -9.4 kcal/mol respectively. Due to the halogen atom at 2' position of **FR-II-60 (14)**, it forms one more halogen bond with the Val203. The analysis of **FR-II-60 (14)** on the rotarod is very important to test the alignment of the molecule, because indication from this model suggest **FR-II-60(14)** will be more sedating than **KRM-II-81(2).**

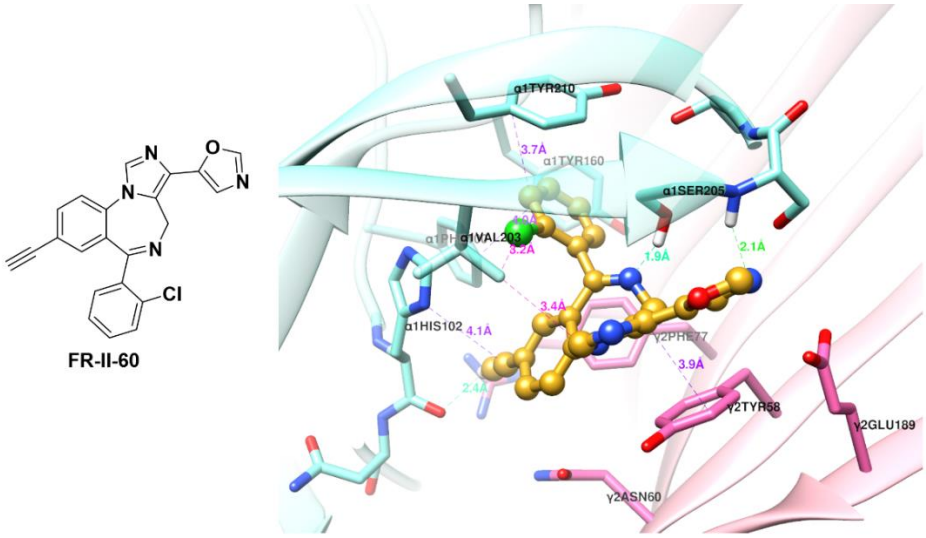

Figure 25. Binding of FR-II-60 at the $\alpha^{+}\gamma^{-}$ interface of the $GABA_A$ receptor. Docked KRM-II-81 (sandy brown) in complex with the α1β3γ2L $GABA_A$ receptor

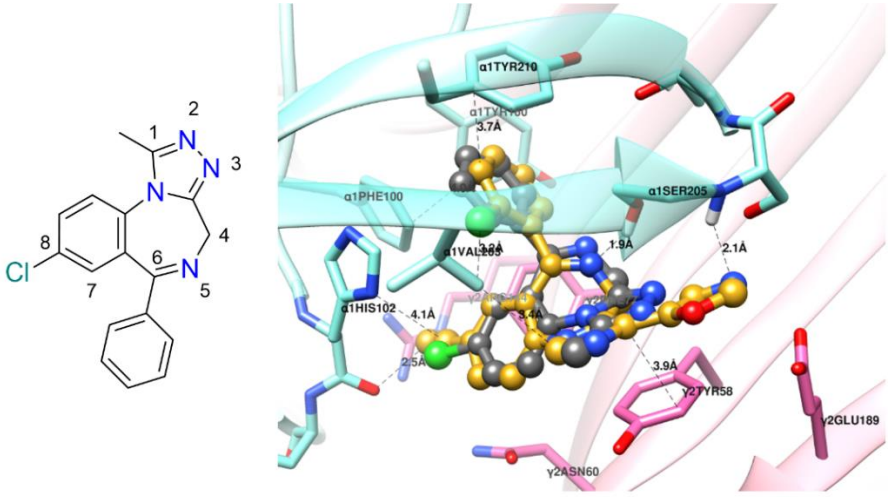

Figure 26. Overlap of FR-II-60 (yellow) and Alprazolam (grey) in complex with α1 (aquamriane) and γ2 (orchid) subunits of α1β3γ2L $GABA_A$ receptor 6HUO. Dashed lines indicate π–π interactions, hydrogen bonds and halogen bond.

2.9. Chemistry of FR-II-60

To synthesize FR-II-60 and other analogs of 2'Cl amino benzophenone, the starting 2`amino benzophenone was synthesized first. Many kinds of routes have been tried to make this starting material. At first the lithium halogen exchange reaction was attempted in the presence of n-BuLi and this was followed by addition of 4-Br amino benzoic acid. After several attempts with different kinds of optimization (temperature, solvent, time), this route was developed. The other route, Friedel-craft benzoylation was found. The proposed Friedel–Crafts benzoylation of 4-aminobenzophenone using different kinds of Lewis acids is a method which consists of three steps (i) the first step is to protect the amino group in order to stop N-acylation, (ii) the second step requires the Friedel–Crafts benzoylation reaction, (iii) and the third step is the deprotection of the amide in acidic solution. Different types of Lewis acids were used but only $ZnCl_2$ was able to provide the desired final 2'Chloro benzophenone. Under this Lewis acid contains a Fries-type rearrangement was attempted under the same conditions. But that reaction did not work and this confirmed that $ZnCl_2$ with heat effected the Friedel–Crafts acylation.

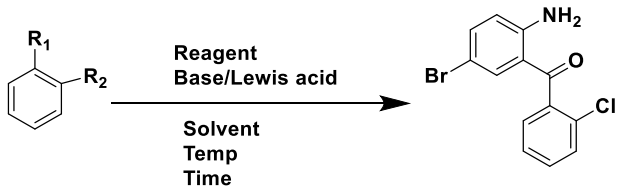

Scheme 3. Reaction Scheme for (2-amino-5-bromophenyl)(2-chlorophenyl)methanone

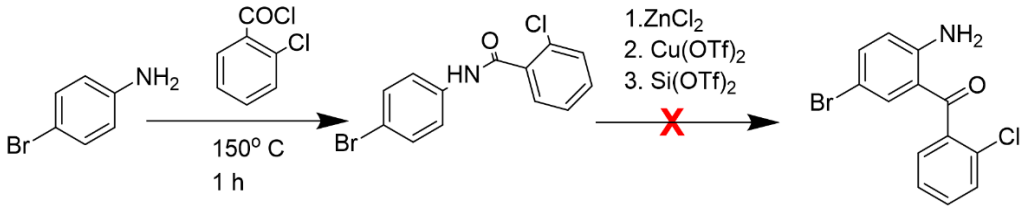

Scheme 4. The failed attempt of synthesis of (2-amino-5-bromophenyl)(2-chlorophenyl)methanone

Entry	R1	R2	Reagent	Lewis Acid	Base	Solvent	Temp (0 C)	Time	% yield
1.	Br	Cl	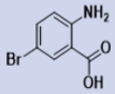	–	n-BuLi	THF	70	24 hr	–
2.	I	Cl	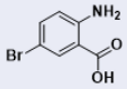	–	n-BuLi	THF	70	24 hr	–
3.	COCl	Cl	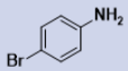	Silver Triflate	–	neat	120-230	42hr	–
4.	COCl	Cl	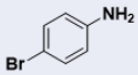	Cu(II) triflate	–	neat	120-230	42hr	–
5.	COCl	Cl	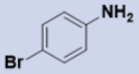	ZnCl2	–	neat	120-230	42hr	41%

Table 8. Optimization of large scale synthesis of (2-amino-5-bromophenyl)(2-chlorophenyl)methanone

A mixture of 4-bromoaniline and 2-chlorobenzoyl chloride was charged in a 3L round bottom flask and the mixture was heated to and kept at 150°C for an hour under an argon atmosphere. The temperature was gradually increased to 220-230°C and kept for 6-7 h for complete evolution of HCl. After cooling to 120°C, water was added dropwise, and the mixture was stirred and heated to reflux for 30 minutes. The hot water layer was decanted, and this procedure was repeated three times to remove white $Zn(OH)_2$. The resulting gummy mass was finally dissolved in a mixture of 30.0 mL of H_2O, 90.0 mL of CH_3COOH and 210.0 mL of concentrated H_2SO_4 and refluxed for 24 hours to deprotect the amine. Although the yield was very poor due to the steric hindrance of the ortho chloro group accompanied by the electron withdrawal bromine atom the Lewis acid–base adduct formed between the aniline with $ZnCl_2$, the best yield

was 44%. This reaction was scaled up to 200 grams and run 6 times to provide the expensive 2'Chloro benzophenone.

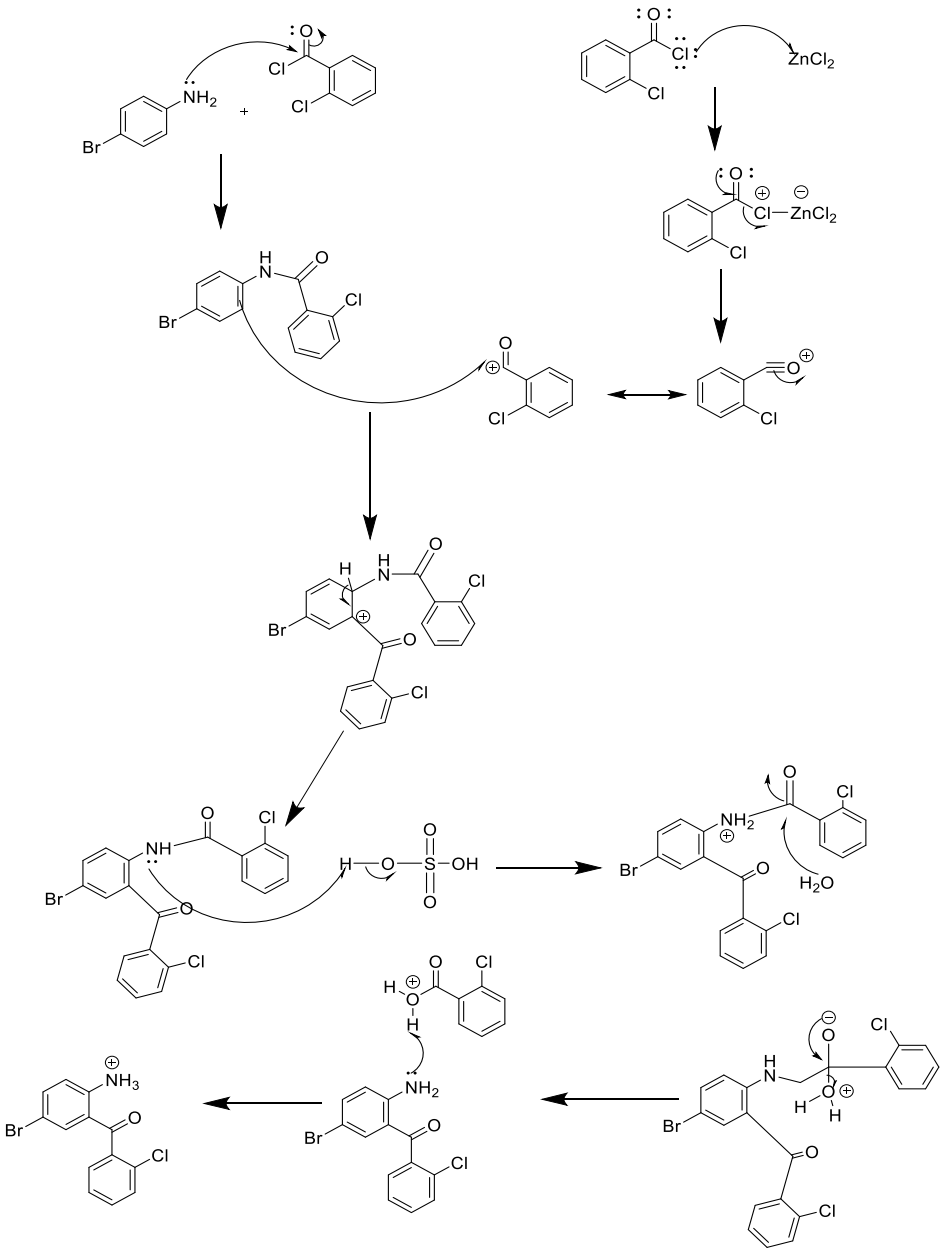

Figure 27. Proposed mechanism for 2'Cl benzophenone

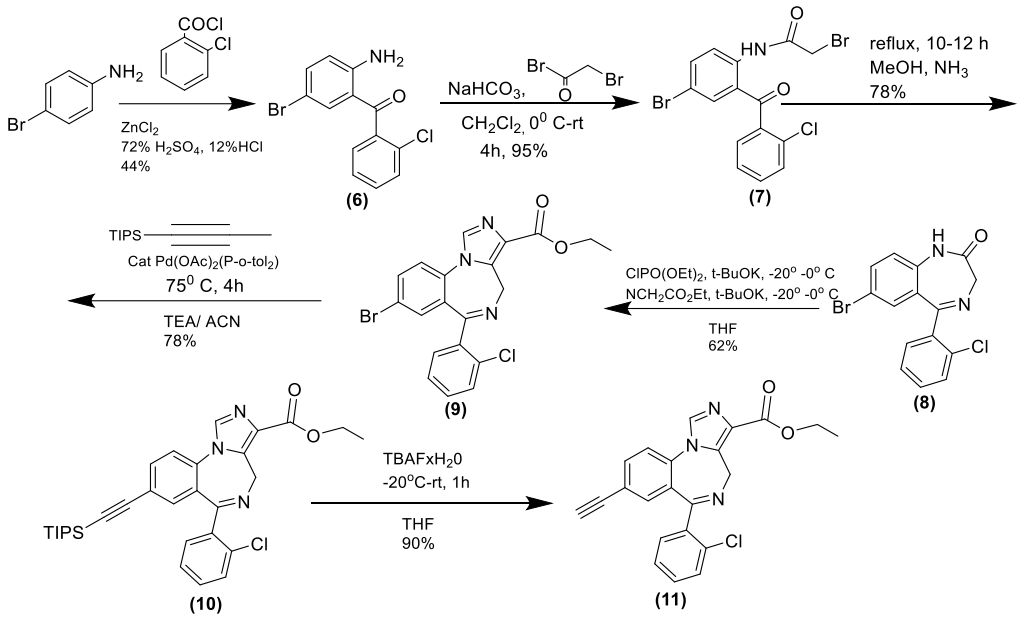

Scheme 5. The total Synthesis of ethyl acetelene ester of 2'Cl benzophenone (6)

To acylate the 2'chloro benzophenone **(6)** in the presence of sodium bicarbonate, bromoacetyl bromide was employed. The acylated intermediate **(7)** was isolated and without any column chromatography it was purified by washing the solid with 10% ethyl acetate and hexane mixture. To make the cyclized amide the acylated intermediate **(7)** was dissolved in methanol and this was followed by adding a saturated solution of NH_3 in meyhanol to produce a β-amino amide intermediate which further cyclized to form the amide **(8)**. There are two problems associated with this route; the first of which was the imidate by product which formed due to the use of excess saturated ammonia and the prolonged time of reaction was on big scale. This is the reason for less yield upon the scale up chemistry. This imidate by product was isolated and the structure confirmed by Dr. Danial Knutson. The second problem was purification, column chromatography is needed to purify **(8)** at this stage. Consequently a new method was developed by Dr. Knutson based on the work of by Blažević and Kajfež[107] and further refined by Cepanec,[108] where hexamethylenetetramine-(HMTM) was used instead of a saturated solution of ammonia. This Delépine reaction, which is used to make primary amines from alkyl halides using HMTM

followed by acidic hydrolysis of the quaternary ammonium salt was established by the French chemist Stéphane Marcel Delépine.[109]

In this new approach, by using HMTM this furnished the quaternary ammonium via a nucleophilic substitution reaction which subsequently was hydrolyzed to produce the β-amino amide intermediate. This intermidiate further condensed with the carbonyl function of the benzophenone and yield the 2' Cl-benzodiazepine **(8)**. In this reaction solvent plays very important role to increase the yield. It was noticed that using primary alcohol (methanol and ethanol) increase the tendency to have β-alkoxy amide as by product. To avoid this by product IPA (isopropyl alcohol) was used as a solvent. This reaction was finished in 4 hours. After cooling to the room temperature, the IPA was concentrated under reduced pressure. The off-white solid was precipitated and was filtered off. In the remaining IPA filtrate, water was added dropwise and product which was dissolved in the IPA started precipitated. The next batch of precipitate was again filtered off. The yield of this reaction was 95% and no column chromatography was needed.

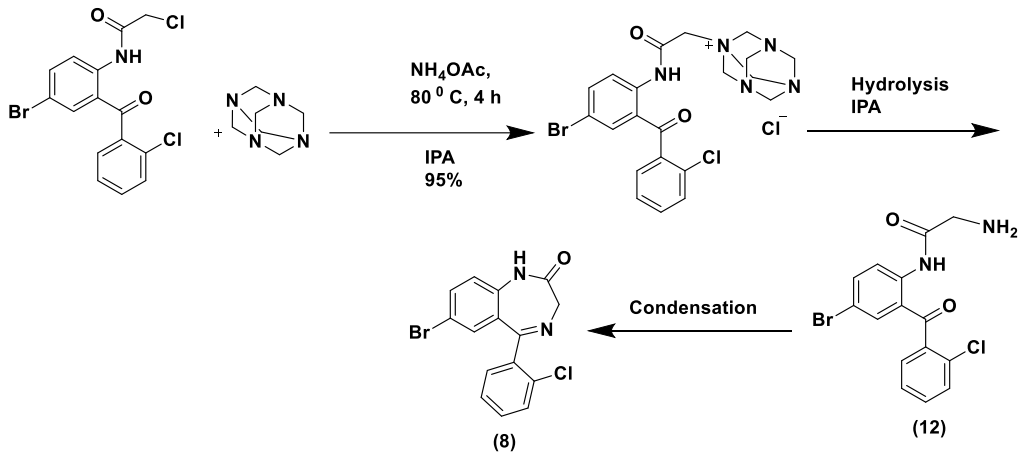

Scheme 6. Hexamethylenetetramine-Based Cyclization Reaction

The next step involved the installment of imidazole ring to the benzodiazepine ring. In well studied conventional process potassium t-butoxide was used as a base to deprotonate the amide of the benzodiazepine that can underwent a nucleophilic addition reaction with diethylchlorophosphate to form an iminophosphate. This was followed by a nucleophilic addition with the enolate of ethyl isocyanoacetate yielded the desired imidazodiazepine. The purification of the product was done by column chromatography. Moreover, the reagent was added to the reaction mixture by cooling it to -78^{o} C and again running for few hours at room temperature. This process was developed in the 2'N imidazodiazepine series which was also applied to the 2'Cl benzodiazepine and monitored by TLC.[88] The temperature and addition of the reagent plays a very important role in this reaction. The formation of the iminophosphate ion required -20^{o} C to form and the nucleophilic addition of the enolate of ethylisocyanate requires needs -30-35^{o} C, so the temperature was tried to keep -20 to 15^{o} C the entire time until the last reagent was added. Also, the isocyanate reagent including the potassium t-butoxide (in a mixture with THF) was added dropwise to the reaction mixture to control the rate of reaction. In the modified procedure, the homogenous solution of THF and benzodiazepine under argon pressure was cooled to -20^{o} C, after which the mixture of potassium t-butoxide and dry THF was added to the reaction mixture dropwise. The reaction was stirred for 1 h while the temperature was maintained -20^{o} to -15^{o} C. Then the diethylchlorophosphate (1.4 eq) was added to the reaction mixture dropwise and the reaction stirred for 2 more hours at -20^{o} to -15^{o} C. After checking the TLC when no starting material was left, which indicated the formation of the iminophosphate intermediate was complete, the ethyl isocyanoacetate was added dropwise and right after that a mixture of potassium t-butoxide and dry THF was added dropwise to the reaction mixture. The second portion of potassium t-butoxide helps to form the enolate, to add the iminophosphate intermediate. After

addition of all the reagent, the reaction mixture was allowed to stir for 12 h in room temperature. When the reaction was complete, the reaction was quenched with 5% sodium bicarbonate solution, which was followed by extraction by DCM. After washing with the brine, all the organic layer combined and concentrated under reduced pressure to obtain a brownish colored slurry and this was washed with t-butyl methyl ether (tBME) to remove all the phosphate related byproducts. In this modified method no column chromatography was needed and the reaction yield increased from 56% to 65%. This process was scaled up to 90 g and run for 5 times.

To convert the aryl bromide to the silyl protected acetylene, the copper free Sonogashira coupling reaction was performed. In the previous method TMS-acetylene (1.5 eq) and bis(triphenylphosphine) palladium (II) diacetate (Pd(OAc)2(PPh3)2) was employed as the catalyst, as well as a large excess of triethylamine was used. The reaction time was 15 hours, moreover the catalyst was too much sensitive to air. A small amount of oxygen can poison the catalyst and to avoid the problem a very careful de- gassing protocol was required. Sometimes to complete the reaction excess TMS-acetylene was needed and added with fresh catalyst but this could react with the 2'Cl as well and form a byproduct. Moreover, the purification was very difficult if there was any starting aryl bromide left because the final product protected silyl acetylene has very close Rf values.

Since the catalyst was very sensitive to oxygen, a different catalyst which is less sensitive to oxidation was needed. The previous catalyst was poisoned very easily due to the oxidation of the triphenylphosphine and the triphenylphosphine oxide was difficult to remove. Consequently, a different ligand tri-ortho-tolylphosphine [$(P(o\text{-}tolyl)_3$] was used with the catalyst which has a larger cone (194^0) than triphenylphosphine (145^o). Since this catalyst is less sensitive to air, there is no need to de-gas the system. In addition, the TIPS-acetylene reagent (1.2 eq) was used instead

of the TMS-acetylene (1.5 eq) to easy separation from starting bromide compound. The Rf of the TIPS protected product is not close to the starting aryl bromide consequently, it is easy to remove the sedating bromide. In this modified process the reaction time reduced from 15 hour to 4 hour. The silica pad was used to remove the undissolved, used catalyst after reaction. The filtrate was extracted with dicholoromethane and sodium bicarbonate to eliminate triethylammonium bromide. All the organic layers combined and concentrated. This was followed by a flash chromatography to remove baseline impurities. This modified method increased the yield 72 to 78%. This Process scaled up to 60 g and repeated 5 times.

The next step was to remove the TIPS group by using tetrabutylammonium fluoride which is a source of F^-. The homogenous mixture of the TIPS acetylene and THF was cooled to -20^o C as the deprotection began at -20-15^o C, then TBAF·xH2O (1.0M in THF) was added dropwise to the reaction mixture. The process was completed after 1 hour and was confirmed by the TLC (Silica gel). After quenching the reaction with water, ethyl acetate was added to the reaction mixture to make a biphasic solution. All the organic layers were combined and reduced under pressure. The crude residue was purified by flash column chromatography which was able to remove the TBA-OH and TIPS-F side products. This reaction was scaled up to 50 g and repeated 5 times. The best yield of this reaction 90%.

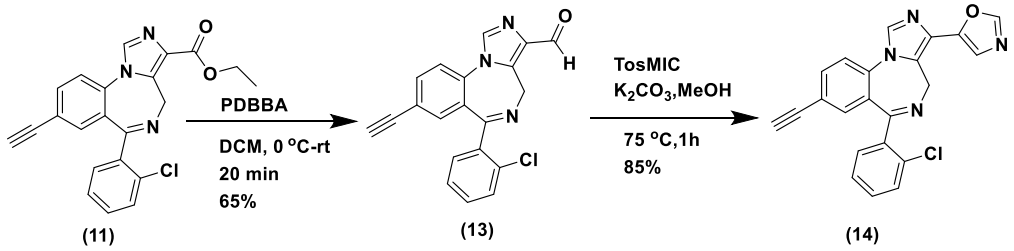

Scheme 7. Synthesis of FR-II-60

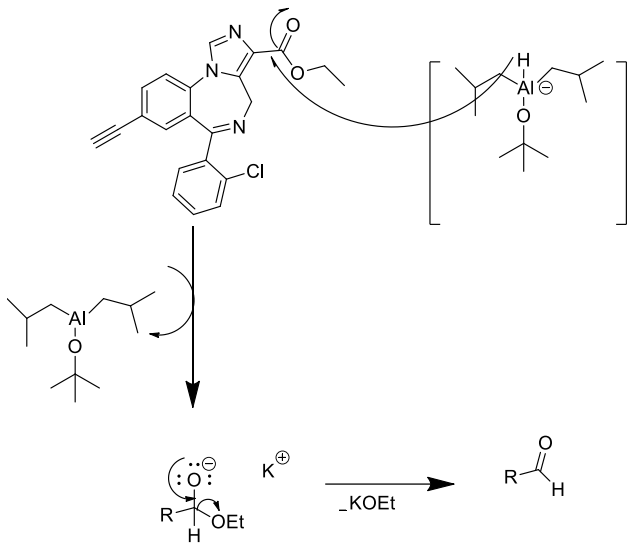

Figure 28. Proposed mechanism for ester to aldehyde

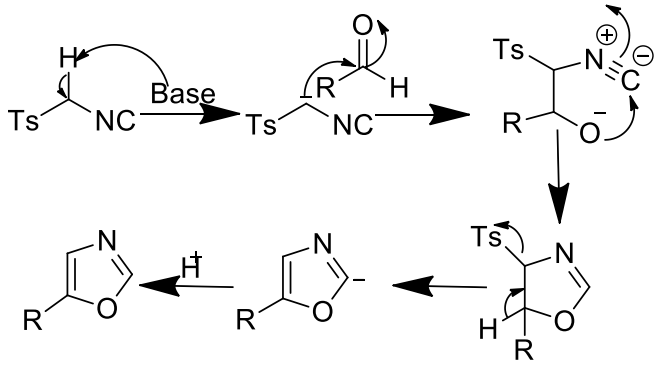

Figure 29. Proposed mechanism for aldehyde to oxazole

1,3 oxazole is one of the exclusive bioisosteres which has a an electron density diagram similar to an ester functional group. In the past different kinds of 1,2,4-oxadiazoles have shown very good therapeutic profiles and important clinical value. In this research it was found that **KRM-II-81(2)** which is a 1,3 oxazole of a 2'N imidazodiazepine demonstrated very good anticonvulsant activity as well as anxiolytic properties with good bioavailability. It was anticonvulsant in different animal assay and antinociceptive in 8 assays. However, the 1,3 oxazole in 2'Cl series never had been reported before.

In order to synthesize the 2'Cl 1,3 oxazole, the first step is to convert the ester function to aldehyde, and which is the most challenging step. In the case of choosing a reducing agent for the diazepine moiety is very difficult because the[N(5)-C(6)] imine bond undergoes reduction very also the aldehyde can be reduced to the alchol very easily. Diisobutylaluminium hydride (DIBAL) which is very well known reducing agent and widely emplyed to convert an ester to aldehyde in the case of 2' F series of IMDZ it worked very well and the aldehyde with a reported yield of 75-80%. However, it did not work well in case of 2'N series of IMDZ. In 2'Cl series, **FR-I-59(11)** was treated with DIBAL at -78^{o} C but the yield was very poor and also most of the ester remained. The purification was also very hard since the elution time of ester and aldehyde on the comlumn was very close. To solve this problem a new reducing agent was employed by Li et. al.[87] Potassium diisobutyl-*t*-butoxy aluminum hydride (PDBBA)[110] was used to convert 2' N IMDZ ester to aldehyde and the desired reported yield was very good. However, the reaction time was very short. The same reducing agent was used in 2'Cl series and monitored by TLC in every two minutes. In this new method, the PDBBA was freshly made before the reaction. In dry THF potassium t-butoxide was added and cooled to 0^{o} C then the same equvalents of DIBAL in hexane was added dropwise and this was allowed to stir at 0^{o} C to room temparature for 2 hour. As PDBBA had three bulky groups, the steric hinderence prevented reduction of the imine bond. In this case only one hydride was available.Consequently, the reaction could more easily be controlled. This retarded reduction also of the aldehyde to the alchol.

The freshly made PDBBA was poured into the homogenous mixture of DCM and **FR-I-59 (11)** at 0^{o} C and monitored by taking TLC at each minutes. However in 5 minutes the reaction was expected to be complete, as it was reported in 2'N series, but in the case of 2'Cl the reaction is not complete. In 5 minutes, some ester remained unconverted and some aldehyde had reduced

to the alchol. So the equivalance of PDBBA had to be optimized. In the 2'N series the PDBBA was employed 1.5 eq. The amount of PDBBA was reduced in the 2' Cl series to 1.2 eq used and again observed. But this time there is less amount of alchol but again some ester remained unconverted. Even when the PDBBA was reduced to 1 eq and monitored by TLC and this time more ester remained. The second changes that was done to monitor the temparature at 0^{o} C in the flask when PDBBA was added.

In drug discovery, some of the problem with metabolism had been solved by replacing the ester fuction with its bioisosteres.[111-115] The 1,2,4- oxadiazoles containing compounds had been reported to to have broad radius of pharmaceutical and biological uses containing anti-inflammatory and analgesic activities.[116] The ligand MP-III-080 (3) which is a 1,2,4-oxadiazole subtituted with a 2' N function with 2'N is a very potent compound and proved to be a anticonvulsant, anxiolytic and antinociceptive activities in different kinds of animal models. FR-I-75**(16)** is a analoge of **MP-III-080 (3)** which is also showed α2, α3 selectivity might be a promising back up ligand.

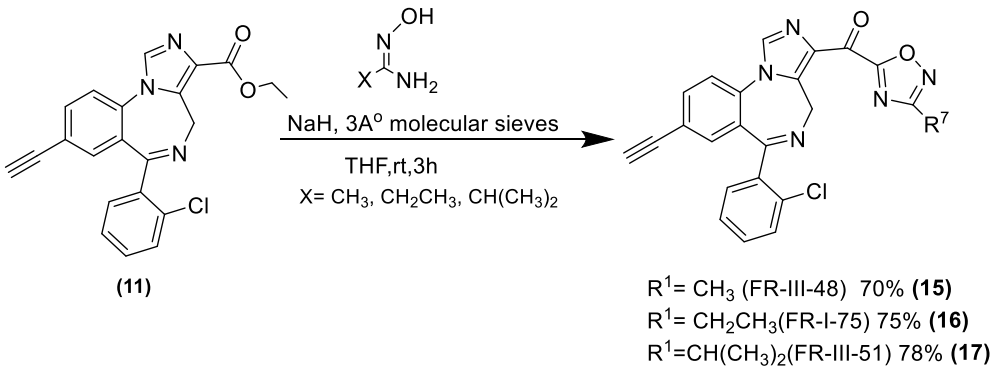

Scheme 8. Synthesis of oxadiazole

To synthesize the 1,2,4-oxadiazole, with 3 Å molecular sieves the corresponding oxime was treated with 1 equivalent of sodium hydride and stirred, the ethyl ester was added after 30 minutes and this was allowed to run in room temperature for 2 h. As mentioned earlier in case of FR-II-60, the imine [N(5)-C(6)] double bond can easily undergo reduction so the equivalents of sodium hydride and the temperature is very important in this case. An excess of sodium hydride can reduce the imine bond which can cause the formation of a byproduct.[117] The first step of synthesis the 1,2,4-oxidiazole was formation of an amidoxime anion, which initiate the acylation with ester and produce a *O*-acylamidoxime and this was followed by a thermal cyclizataion to afford 1,24-oxadiazole. However high temparature can cause a low yield. So the conventional route of refluxing was avoided and this reaction was performed at room temparature.

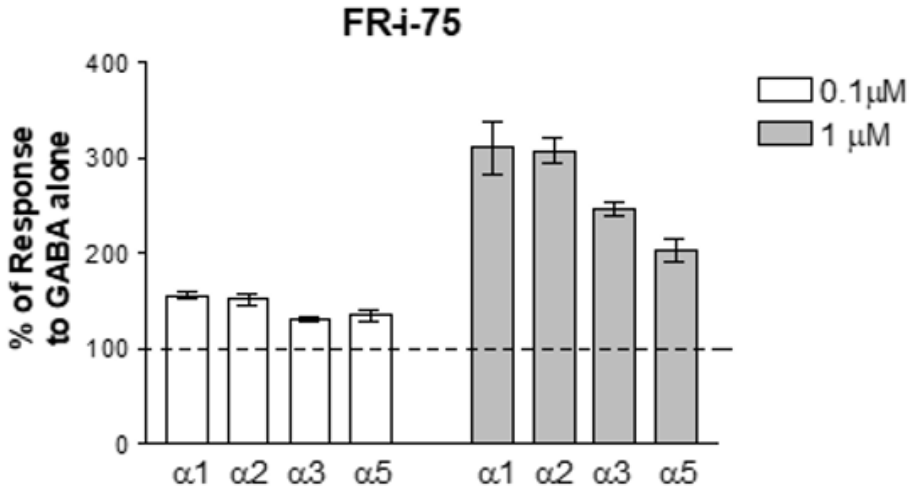

Figure 30. Efficacy data of FR-I-75 with EC_3 GABA Concentration

Efficacy data at 100 nM, EC3 GABA of FR-I-75 **(16)** is illustrated in **Figure 30** is According to the data FR-I-75 is α1, α2,3 subtype selective with potent efficacy. Although in rotarod assay there was no sedation at 10,30,60 min at the dose of 40mg/kg. FR-I-75**(16)** resulted

almost no efficacy in 100 nm, in HEK cells. It shows α1 and α2 selectivity at 1µM. However, at 100 nM (0.1 µM) it exhibits very poor efficacy at α1, α2 and α3. FR-I-75 does not show any cytotoxicity in HEK293 cell. (IC50 value reported 375.6 nM)

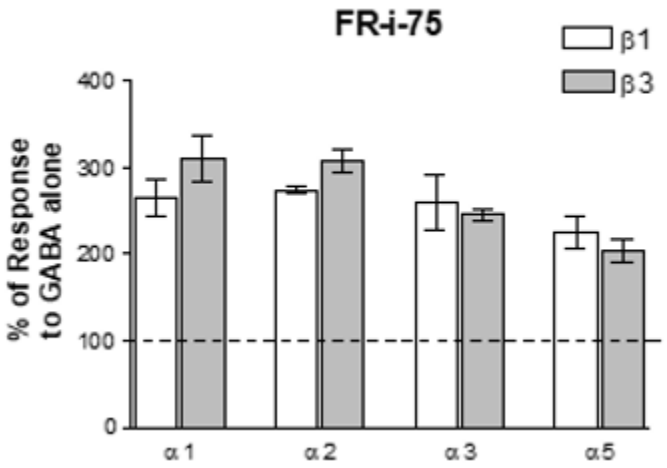

Figure 31. Efficacy data of FR-I-75 at β1 (EC_3 GABA)

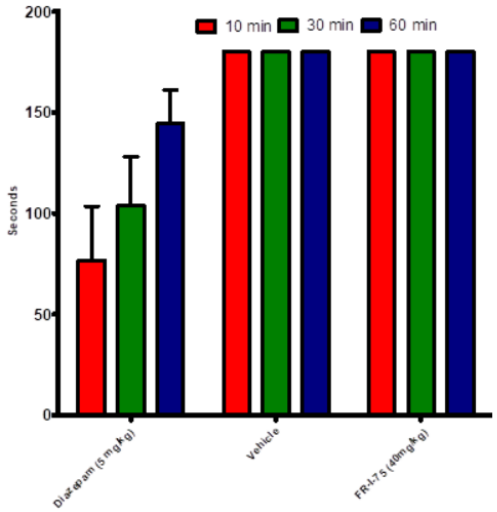

Figure 32. Rotarod assay in female CFW ice of FR-I-75

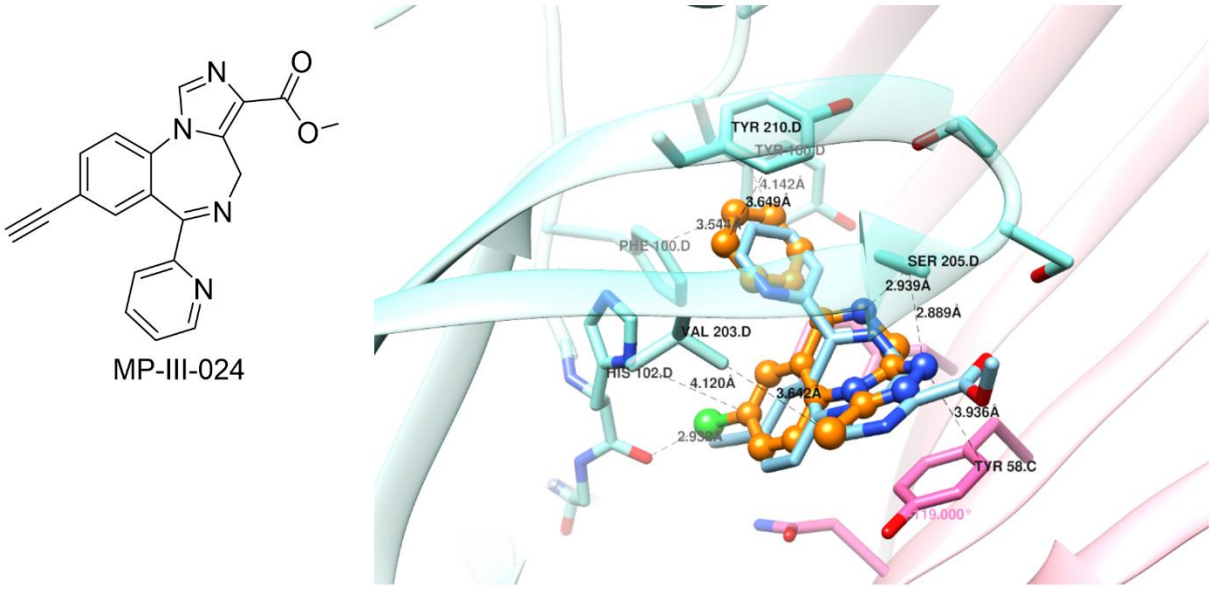

Figure 33. Cyro Er Structure of MP-III-024

Another promising α2, α3 subtype selective ligand is MP-III-024 (2' N analog) which has better metabolic stability than the ethyl ester HZ-166 **(1)** in rodents. The ethyl ester may undergo omega minus one oxidation in the liver, wheres the methyl ester can not.MP-III-024 had shows both anxiolytic , antinociceptive activity in different types of animal models. To make the analoge of MP-III-024 in 2'Cl series, the ethyl ester of 2'Cl was dissolved in dry methanol and then stirred with sodium methoxide under reflux for 0.5 hour.

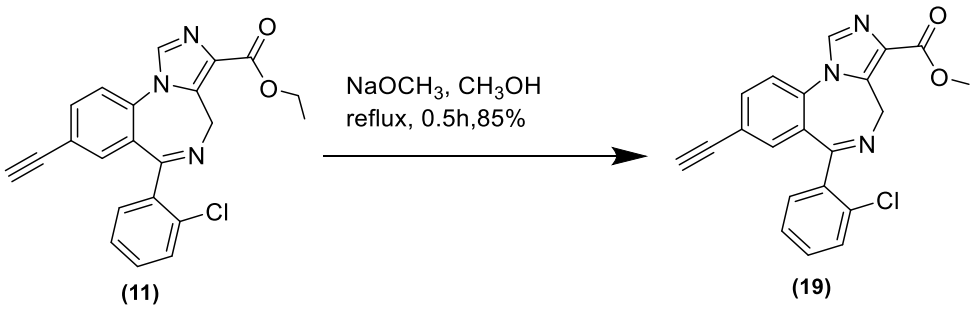

Scheme 9. Synthesis of methyl ester

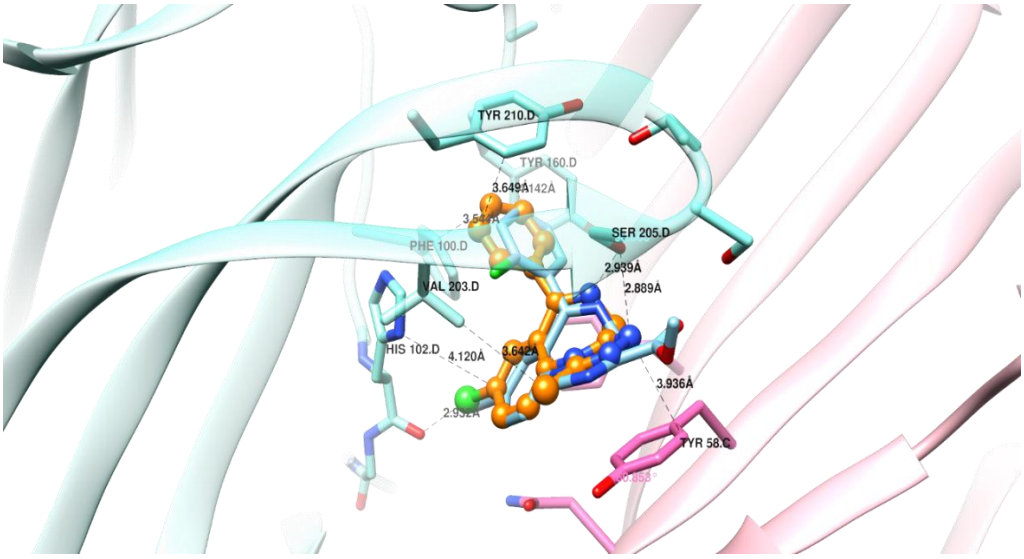

Figure 34. Modeling of FR-I-98 at the $\alpha^{+}\gamma^{-}$ interface of $GABA_A$ receptor of the cyro er structure.

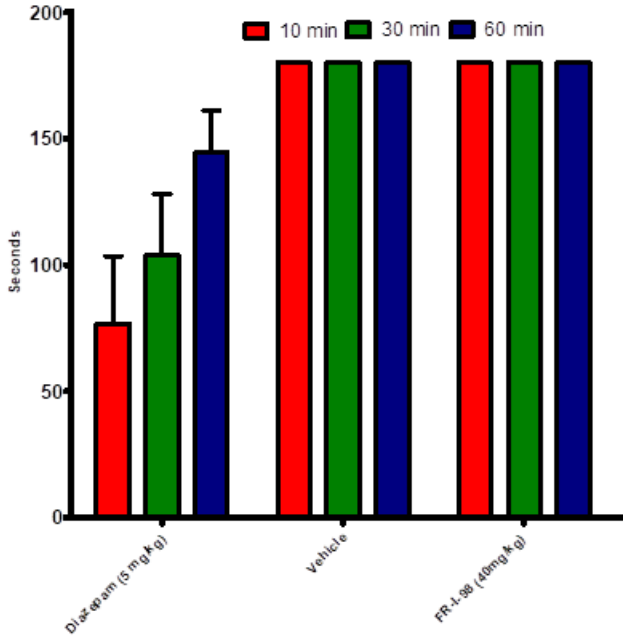

Figure 35. Rotaraod assay of FR-I-98

According to the Cyro ER structure of FR-I-98 **(19)**, It shows the same the binding activity of alpha 1 like MP-III-024. FR-I-98 (19) does not interact with α1His102 *via* halogen bonding with the backbone carbonyl as does MP-III-024. In FR-I-98 **(19)**, the acetelene group forms a

hydrogen with Val203 and that is why it is different from MP-III-04, the three centered bifurcated hydrogen bond form between the N atom of the seven membered ring, the imidazole top ring and the oxazole ring with the SER205 which value is 2.93A. The bifurcated hydrogen bond formed by FR-I-98(19) (2.9 A) with α1Ser205 is same as configured with bound MP-III-024 (2.9A). The shorter halogen bond and bifurcated hydrogen bond interaction might make FR-I-98 less potent affinity toward α1 as MP-III-024. FR-I-98 **(19)** at this point looks like a potential back up agent of MP-III-024 (antinociceptive) but in depth bioanalysis now required.

2.10. Biology of FR-II-60

FR-II-60 was screened in the 6 Hz kindled seizure model to verify their abilty to reduce the seizures induced by low frequency (6 Hz) stimulation employed for a long time. The male CD-1 mice (n=4) were given 6 Hz stimulation for 3 seconds with the corneal elctrode at 44mA, 2 hours after the dosing (i.p) of FR-II-60 (14).To observe the prospective motor impariment and probable toxicity another group of mice were given a high dose of FR-II-60 (14) (30, 100, 300 mg) After half an hour dosing of 30 mg/kg,FR-II-60 (14) was able to protect 3 out of 4 mice and the full protection was observed at the dose of 300 mg/kg at 2 hour.

In case of KRM-II-81 (2) after 30 mg/kg it was able to protect 1 out of 4 mice and the full protection was observed at the dose of 300 mg/kg after half an hour.

Time(Hours)		0.25		0.5		2.0	
Test	Dose (mg/kg)	N / F	Comment Code	N / F	Comment Code	N / F	Comment Code
6HZ	30 100 300			3 / 4 3 / 4 3 / 4		1 / 4 3 / 4 4 / 4	
MES	30 100 300			2 / 4 4 / 4 4 / 4		1 / 4 4 / 4 4 / 4	
Rotarod	30 100 300			4 / 8 6 / 8 8 / 8		0 / 8 5 / 8 7 / 8	
72 hour mortality	30 100 300	0 / 16 0 / 16 0 / 16					

Table 9. Effect of FR-II-60 (12) in the 6 Hz kindled seizure model

In maximal electroshock (MES) assay FR-II-60 (14) showed good potency as an antiepileptic agent as illustrated, 30 minutes prior to testing the male CD-1 mice (n = 4) were given (i.p.) vehicle (1% CMC), FR-II-60 (14) (30,100,300 mg/kg). Then the mice were given 10 uA electroshock during the test to induce the clonic and tonic seizure for 0.2 seconds. The observation was recorded. The reduction of the clonic and tonic seizures at the hindlimb caused by the elctroshock indicates the protection of the animal. FR-II-60 (14) was able to reduce the MES-induced convulsions at the dose of 30 mg/kg. the full protection was observed at the dose of 100 mg/kg.

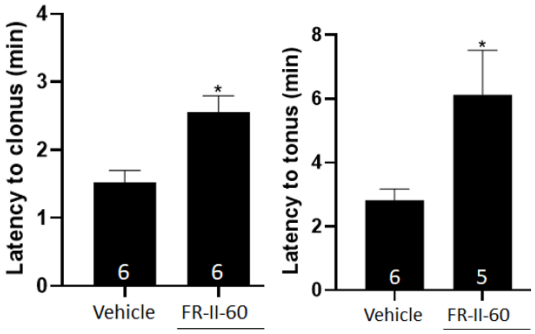

Figure 36. Longer duration of action of FR-II-60 against PTZ-induced seizures in C57BL/6 mice

FR-II-60 (14) was evaluted in the PTZ (pentylenetetrazole) -induced seizure test. PTZ was given to the C57BL/6 male mice at a dose of 75 mg/kg after sixty minutes of oral dosing with DZP (3 or 10 mg/kg), **FR-II-60 (12)** (10 mg/kg). Mice were observed for sixty minutes after PTZ administration for clonic and tonic seizures and death. At the dose of 10 mg/kg **FR-II-60 (14)** significantly increased the latency to produce clonic and tonic seizures produced by PTZ. There was a trend for **(14)** to protect against PTZ-induced lethality (3/6 mice with vehicle treatment died, whereas 0/6 **FR-II-60 (14**) treated mice died. No mice died (n=4) after 60-, 120-, 240- and 480-minutes observation. **KRM-II-81(2)** was able to reduce the clonic and tonic seizure induced by PTZ at the dose of 30 mg/kg.

No Motor Impairment in the Rotarod Study:

FR-II-60 (14) was asssesd in the rotarod(oral) assay for a longer test period with higher doses in order to verify the dose of toxicity as well as ataxic and sedative effect. **FR-II-60 (14)** showed a very little sedative at the dose of 40 mg/kg but at the higher dose it did not showed any sedativeness. No tremor or death was reported even at the very high dose (120 mg/kg) which was confirmed by the data of ETSP/NINDS . However, at the dose of 100 mg/kg and 300 mg/kg 8 out of 8 mice were sedated.

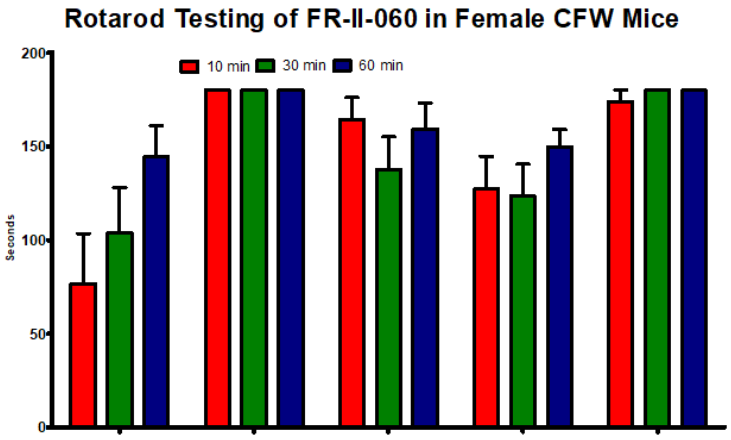

Figure 37. Rotarod assay of FR-II-60 in female CFW mice

Cytotoxicity of FR-II-60 (14):

ThFR-II-60 is not very toxic as the lC50 is high (275). This means that it does not show much toxicity until higher concentrations, 300 uM in this case.

Behavioral observations of FR-II-60:

Three adult rhesus monkeys have implanted iv catheters. Twice a week a FR-II-60 the tested drug (0.1-3 mg/kg) was injected via iv and an observer (blinded to the drug administered) scores behavior for 5 minutes at predetermined intervals (5, 10, 20-, 40-, 80,160- and 320-min post drug infusion). Max score per behavior was 20.

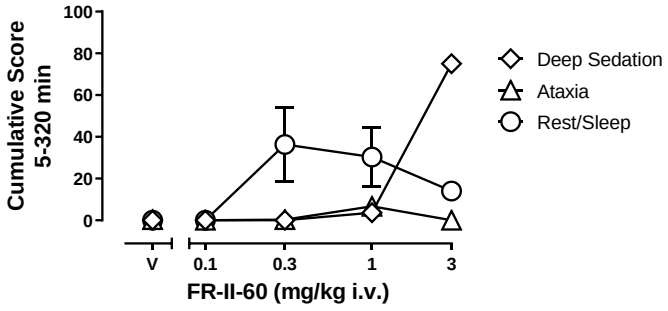

Figure 38. Behavioral observations in female rhesus monkeys after administration of FR-II-60 (0.1-3mg/kg, iv)

Three adult rhesus monkeys were implanted with i.v catheters. Twice a week **FR-II-60 (14)** (0.1-3 mg/kg) was injected via i. and an observer (blinded to the drug administrated) scored the behavior for 5 minutes at predetermined intervals (5,10,20,40,80,160 and 320 min post drug infusion). The maximum score per behavior was 20.

For the time course graph, the averages of all monkeys were employed (Mean ± SEM) at that time point are graphed. Here the assay emphasized on sedative measures (ataxia, sleep/rest posture and deep sedation) and one added a species-specific behavior that is relatively frequent (forage).

For the cumulative graph, all observation scores across the 320 min are summed up and then the average of the monkeys (Mean ± SEM) are graphed. According to this study, only one monkey at the dose of 3 mg/kg showed some sedation.

2.11. Metabolic Study of FR-II-60 (14)

According to the PK study the concentration of FR-II-60 (14) in brain is much less than KRM-Ii-81 (2). It decreased with time and the highest concentration was found after 4 hour which was 143.80 ng/ml. The concentration of the compound (14) in plasma and kidney sample also found very less than KRM-II-81 (14). It is possible that the more lipophilic FR-II-60 (14) was metabolized much faster in the liver than the more polar (2'N) KRM-II-81 (2) leading to less accumulation in tissues.

KIDNEY	Mean (nmol/kg)	SEM
FR-II-60 15 min	191.11	27.36
FR-II-60 30 min	165.08	44.43
FR-II-60 1 h	110.20	13.43
FR-II-60 2 h	431.42	67.89
FR-II-60 4 h	113.16	11.02
FR-II-60 8 h	576.57	9.18
FR-II-60 24 h	569.30	400.01

KIDNEY	Mean	SEM
Cmax (ng/ml)	322.52	98.65
tmax (h)	13.33	5.33
AUC0_24 (ng*h/ml)	4424.84	1177.88
AUC0-∞ (ng*h/ml)	5575.96	2245.95
t1/2 (h)	4.94	1.52
β (1/h)	0.15	0.05

Table 10. Metabolic stability of FR-II-60 (14) in kidney

PLASMA	Mean (nmol/L)	SEM
FR-II-60 15 min	7.17	0.18
FR-II-60 30 min	10.50	1.66
FR-II-60 1 h	18.14	5.19
FR-II-60 2 h	9.47	1.14
FR-II-60 4 h	10.12	1.11
FR-II-60 8 h	217.46	114.77
FR-II-60 24 h	127.65	32.83

PLASMA	Mean	SEM
Cmax (ng/ml)	124.86	47.55
tmax (h)	9.00	7.51
AUC0_24 (ng*h/ml)	1153.73	489.79
AUC0-∞ (ng*h/ml)	1183.04	478.76
t1/2 (h)	2.07	1.11
β (1/h)	0.58	0.25

Table 11. Metabolic stability of FR-II-60 (14) in plasma

BRAIN	Mean (nmol/kg)	SEM
FR-II-60 15 min	26.09	0.55
FR-II-60 30 min	28.19	4.69
FR-II-60 1 h	27.60	1.88
FR-II-60 2 h	40.11	5.51
FR-II-60 4 h	143.80	112.18
FR-II-60 8 h	30.45	4.15
FR-II-60 24 h	28.26	3.07

BRAIN	Mean	SEM
Cmax (ng/ml)	58.55	41.58
tmax (h)	4.67	1.76
AUC0_24 (ng*h/ml)	407.87	112.44
AUC0-∞ (ng*h/ml)	548.37	165.89
t1/2 (h)	6.89	0.20
β (1/h)	0.10	0.00

Table 12. Metabolic stability of FR-II-60 (14) in brain

2.12. PDSP data of FR-II-60 (14)

PDSP code	Receptor	Inhibition 1	Inhibition 2	Inhibition 3	Inhibition 4	Mean %	Secondary
58187	5-HT1A	35.27	28.53	20.97	21.96	26.68	
58187	5-HT1B	25.21	0.72	6.85	9.33	10.53	
58187	5-HT1D	36.58	18.55	5.97	25.26	21.59	
58187	5-HT1E	6.7	-13.71	-3.65	8.14	-0.63	
58187	5-HT2A	47.3	31.59	33.44	34.21	36.64	
58187	5-HT2B	20.19	-2.03	-6.3	-8.65	0.8	
58187	5-HT2C	10.4	12.19	-9.05	-11.14	0.6	
58187	5-HT4	9.07	1.9	46.7	24.3	20.49	
58187	5-HT5A	43.49	7.71	-6.03	-13.29	7.97	
58187	5-HT6	29.4	2.82	-5.84	-17.64	2.19	
58187	5-HT7A	23.93	15.31	4.43	-11.96	7.93	
58187	Alpha1A	18.98	3.98	5.98	-5.83	5.78	
58187	Alpha1B	20.24	3.49	-13.27	-9.25	0.3	
58187	Alpha1D	18.1	21.27	19.34	25.28	21	
58187	Alpha2A	30.14	17.38	3.8	1.86	13.3	
58187	Alpha2B	24.94	18.81	13.8	16.5	18.51	
58187	Beta1	14.84	11.53	6.98	57.25	22.65	
58187	Beta2	1.98	3.9	11.07	-3.35	3.4	
58187	Beta3	42.38	15.44	26.79	41.04	31.41	
58187	D1	19.89	-9.98	11.18	52.79	18.47	
58187	D2	-10.33	1.54	-16.27	-21.02	-11.52	
58187	D3	-1.7	-2.73	11.29	-13.04	-1.55	
58187	D4	-5.66	10.1	5.51	4.98	3.73	
58187	D5	-2.63	0.95	11.45	29.31	9.77	
58187	DAT	14.14	-12.55	-5.25	-23.79	-6.86	
58187	DOR	22.54	15.11	8.78	22.91	17.34	
58187	GABAA	28.92	15.4	-1.88	-8.64	8.45	
58187	H1	-1.75	-2.32	-15.38	-8.75	-7.05	
58187	H2	10.37	11.52	27.65	0.84	12.6	
58187	H3	34.32	23.66	17.82	31.02	26.71	
58187	H4	-16.25	-22.9	-6.66	2.93	-10.72	
58187	KOR	68.89	48.82	52.64	43.4	53.44	Secondary
58187	M1	11.57	1.98	3.86	11.76	7.29	

58187	M2	34.76	5.13	1.63	-6.07	8.86	
58187	M3	-0.63	12.03	14.38	-5.09	5.17	
58187	M4	25.23	-5.55	-12.21	1.01	2.12	
58187	M5	18.87	-9.43	-18.9	-25.65	-8.78	
58187	MOR	7.34	15.42	14.34	11.48	12.15	
58187	NET	12.86	-11.38	-8.39	-35.03	-10.49	
58187	PBR	47.44	33.47	27.04	33.16	35.28	
58187	SERT	6.32	-5.1	-28.66	-18.94	-11.6	
58187	Sigma 1	27.43	-11.4	7.01	12	8.76	
58187	Sigma 2	66.2	59.33	46.58	69.92	60.51	Secondary
58187	NTS1	-7.97	-17.15	-18.07	-5.22	-12.1	
58187	Alpha2Beta2	-3.2	-3.91	-4.73	-4.97	-4.2	
58187	Alpha2Beta4	1.5	0.75	-8.57	-8.68	-3.75	
58187	Alpha3Beta2	4.08	-4.13	-2.94	-9.23	-3.06	
58187	Alpha3Beta4	20.47	10.67	12.22	13.41	14.19	
58187	Alpha4Beta2	0.62	2.08	1.63	-5.98	-0.41	
58187	Alpha4Beta2 (Rat Brain)	-8.59	24.31	3.23	-1.04	4.48	
58187	Alpha4Beta4	13.71	20.8	8.25	11.53	13.57	
58187	Alpha7	27.69	14.67	14.4	0.48	14.31	
58187	NET	-8.85	-10.39	-10.29	-25.89	-13.86	
58187	PBR	50.13	46.9	21.69	41.53	40.06	
58187	SERT	-11.09	16.57	21.75	-9.6	4.41	
58187	GABAA	5.67	9.55	-14.26	-27.54	-6.65	

Table 13. PDSP data of FR-II-60

2.13. Efficacy data of FR-II-60 (14)

According to the selectivity data from **Figure 39** (A) at 0.1 μM in HEK cell it shows very poor efficacy at α1, α2, α3 and α5. However, at higher concentration 1μM it exhibits more potent selectivity at α1 as well as α2, α3. And from **Figure 39** (B) α with β3 and γ2L subunits, it is clear from the data that poor efficacy at the β3 ion channels at 1 μM is about the same at β1

ion channel. Whereas, in the non-sedating KRM-II-81(2) even at 0.1 μM shows difference in efficacy at β1 versus the more potent β3 ion channels.

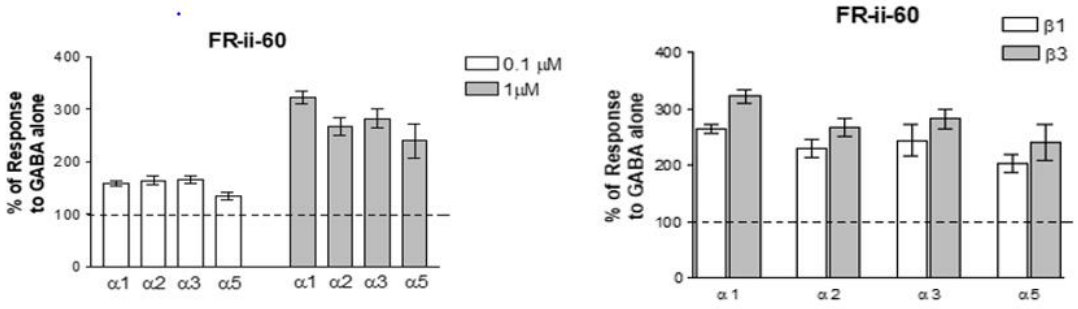

Figure 39. Efficacy data of FR-II-60(14) (A) Efficacy data of FR-I-75 at β1 (EC_3 GABA) . B) Whole-cell voltage clamp recordings from transiently transfected HEK-293T cells. α indicated is co-transfected with β1 and γ2L GABA concentration is EC_{3-5}

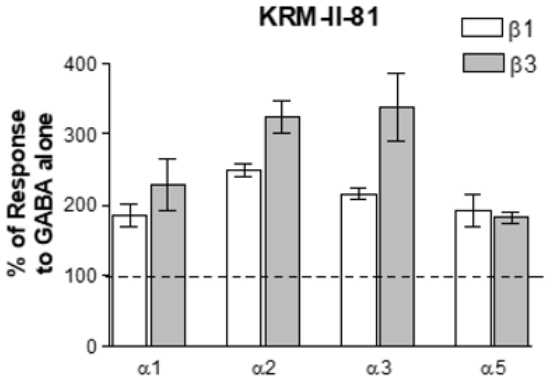

Figure 40. Efficacy data of KRM-II-81(2). Whole-cell voltage clamp recordings from transiently transfected HEK-293T cells. α indicated is co-transfected with β1 and γ2L GABA concentration is EC_{3-5}

2.14. Conclusion

For over 70 years, GABAkines have been important and highly used medicines with diazepam being on the list of Essential Medicines of the World Health Organization. A search for the perfect GABAkine has been ongoing for this period of time: therapeutic efficacy with reduced side-effect burden (sedation, motor-impairment, respiratory depression, tolerance, and dependence) has been the primary goal of this search. To date, multiple a-subtype selective GABAkines have not fully succeeded either because the sought-after efficacy/side-effect margin was not attained or, in the case of ocinaplon, because of unanticipated liver toxicity.

Several new GABAkines are currently in development including three neuroactive steroids, and two a2/3-prefereing KRM-II-81(2). The neuroactive steroids are in clinical development for depression and intractable epilepsy. KRM-II-81(2) is the newest GABAkine to enter development and is currently in the late preclinical phase. Preclinical pharmacological studies of KRM-II-81(2) have demonstrated its efficacy in animal models of anxiety, depression, acute and chronic pain, epilepsy, and traumatic brain injury. The preclinical data highlight the possibility of developing provocative new drugs in areas of clinical need, which might also provide insight into the neural substrates of these disease states.

FR-II-60 (14) is a good analog of KRM-II-81(2). It shows good activity in acute seizure model with no mortality. It is not sedative as well as not toxic until high dose. The PK study is needed to recheck its metabolic stability. Further, extensive investigation necessary. FR-II-60 (14) might serve as a backup compound to KRM-II-81 (2). However, FR-I-75 (16) at this point looks promising as a backup compound for MP-III-080. FR-I-98 (19) also looks very promising and could be a very good back up compound for MP-III-024.

2.15. Experimental

(2-amino-5-bromophenyl)(2-chlorophenyl)methanone: (FR-I-11) (6)

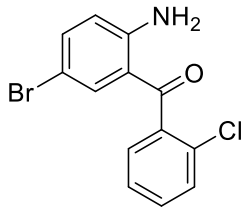

A mixture of 4-bromoaniline (100g, 581.3 mmol) and 2-chlorobenzoyl chloride (203.16g, 1162.6 mmol) was charged to a 3L round bottom flask and the mixture was heated to 150^{o}C and kept at 150^{o}C for an hour under an argon atmosphere. The mixture was then heated to 180-220°C and anhydrous zinc chloride (95.06 g, 697.56 mmol) was added in one portion. The temperature was gradually increased to 220-230°C and kept for 6-7 h until complete evolution of HCl(g) was observed. After cooling to 120°C, water was added dropwise carefully, and the mixture was stirred and heated to reflux for 30 minutes. The hot water layer was decanted, and this procedure was repeated three times to remove white $Zn(OH)_2$. The resulting gummy mass was finally dissolved in a mixture of 30.0 mL of H_2O, 90.0 mL of CH_3COOH and 210.0 mL of concentrated H_2SO_4 and refluxed for 24 hours to deprotect the amine. Once the reaction was completed, the mixture was cooled to room temperature and poured into a 5L Erlenmeyer flask containing ice-water. The reaction product was extracted with dichloromethane (3x500 mL), which separated the product from the acid-soluble 4-bromoaniline. The organic layer was then washed with an aq. $NaHCO_3$ (2x300mL) to remove the benzoic acid and then aq. 10% sodium chloride solution (2x400mL).

The organic layer was dried with magnesium sulfate and concentrated under reduced pressure. The gummy mass was then purified by a flash column chromatography (300g silica gel, EtOAc (5): hexane(95)) and the solvents were evaporated under reduced pressure. The residue was dried in vacuum(30^{o}C) for 4 h to afford a yellow solid (79.4g,44%). **1H NMR** (500 MHz, CDCl3) δ 7.50 – 7.47 (m, 1H), 7.44 (td, J = 7.7, 1.4 Hz, 1H), 7.37 (ddd, 2H), 7.32 (dd, J = 7.5, 1.2 Hz, 1H), 7.28 (d, J = 2.1 Hz, 1H), 6.64 (d, J = 8.8 Hz, 1H), 6.52 (s, 2H). **13C NMR** (126 MHz, CDCl3) δ 196.36 (s), 150.27 (s), 138.97 (s), 137.90 (s), 136.19 (s), 130.81 (s), 130.73 (s), 130.10 (s), 128.44 (s), 126.84 (s), 118.94 (s), 118.63 (s), 106.70 (s).**HRMS** (ESI/IT-TOF) m/z: $[M + H]^{+}$ Calcd for C13H9BrClNO 309.9629; found 309.9604.

2-bromo-N-(4-bromo-2-(2-chlorobenzoyl)phenyl)acetamide (FR-I-15)(7)

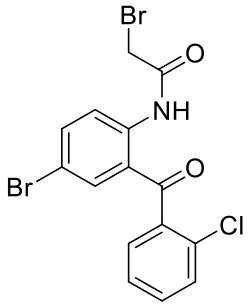

A homogenous solution of benzophenone **4** (100 g, 324.6 mmol) was obtained by dissolving it in dry CH_2Cl_2 (300mL) in a 3-neck flask. It was stirred it until the solution was obtained. After that, solid $NaHCO_3$ (54.54g, 649.2 mmol) was slowly added to the solution and the mixture was cooled to 0^{o}C (ice bath). The bromoacetyl bromide (42.55 g, 486.96 mmol; dissolved in 100 mL of dry CH_2Cl_2) was added dropwise at 0^{o}C. The mixture was allowed to stir at rt until the starting material was consumed as indicated by TLC (Silica gel:EtOAc/hexanes, 2:1). Then the reaction was quenched by adding ice-water (1000 mL) to the mixture. Then the organic

layer was separated, and the water layer was extracted with CH_2Cl_2 (3 x 500 mL). The organic layers were combined and washed (800 mL each) sequentially with a sat'd aq $NaHCO_3$ solution, water, 10% HCl, brine and then dried (Na_2SO_4). The organic solution was then reduced to 1/3 of its original volume by concentration under reduced pressure Then it was directly used in the next step without any further purification. **^{1}H NMR** (500 MHz, CDCl3) δ 12.02 (s, 1H), 8.70 (dd, J = 9.0, 3.0 Hz, 1H), 7.72 (dd, J = 9.0, 2.4 Hz, 1H), 7.54 – 7.48 (m, 3H), 7.43 (ddd, J = 7.7, 4.8, 3.7 Hz, 1H), 7.40 – 7.36 (m, 1H), 4.08 (s, 2H). **^{13}C NMR** (126 MHz, CDCl3) δ 197.86 (s), 165.44 (s), 139.62 (s), 138.32 (s), 137.71 (s), 136.37 (s), 131.89 (s), 131.11 (s), 130.38 (s), 128.95 (s), 127.02 (s), 123.94 (s), 122.57 (s), 115.77 (s), 29.46 (s). **HRMS** (ESI/IT-TOF) m/z: $[M + H]^+$ Calcd for C15H10Br2ClNO2 429.8814 found 429.8805

N-(4-bromo-2-(2-chlorobenzoyl)phenyl)-2-chloroacetamide(FR-I-99):

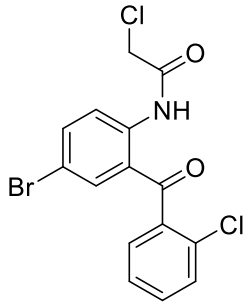

In a homogenous mixture of 2-amino-5-bromophenyl)(2-chlorophenyl)methanone (100 g, 321.97 mmol) and dicholoromethane (1000 ml) , sodium bicarbonate (54 g, 642.7 mmol) was added in one portion at rt. Then the solution was cooled to 0^o C and choloroacetyl chloride (38.41 ml, 482.9 mmol) was added dropwise using an additional funnel. The reaction mixture was allowed to stir for 4 h at rt. After completion of the reaction, which was confirmed by TLC using silica gel 20% ethyl acetate/ hexane. To quench the reaction water (500 mL) was added dropwise over 30

min. The mixture which resulted was extracted with dicholoromethane (500 mL). After washing with 5% of sodium bicarbonate solution and 10% sodium chloride solution. The organic layer was dried (Na2SO4) combined and concentrated under reduced pressure which results off white solid powder. After removing all solvent, ethanol(500mL) was added to the white powder and made a slurry which was heated at 50-55 ^{o}C for 30 min. After cooling down to room temperature the solid was filtered off, washed with ethanol and the residue was dried under vacuum (40^{o} C). Total yield 115g, 92%.**^{1}H NMR** (500 MHz, CDCl3) δ 12.18 (s, 1H), 8.73 (d, J = 9.0 Hz, 1H), 7.72 (dd, J = 9.0, 2.4 Hz, 1H), 7.51 (dd, J = 4.5, 1.5 Hz, 3H), 7.43 (ddd, J = 8.5, 4.7, 3.8 Hz, 1H), 7.39 – 7.37 (m, 1H), 4.26 (s, 2H). **^{13}C NMR** (126 MHz, CDCl3) δ 197.79 (s), 165.84 (s), 139.34 (s), 138.31 (s), 137.73 (s), 136.38 (s), 131.89 (s), 131.12 (s), 130.37 (s), 128.97 (s), 127.02 (s), 124.08 (s), 122.60 (s), 115.84 (s), 43.23 (s). **HRMS** (ESI/IT-TOF) m/z: $[M + H]^{+}$ Calcd C15H10BrCl2NO2 for 384.943 found 384.942

7-bromo-5-(2-chlorophenyl)-1,3-dihydro-2H-benzo[e][1,4]diazepin-2-one(FR-I-20): (8)

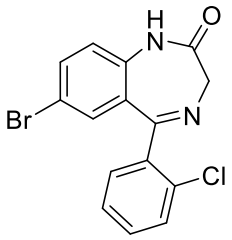

Methanol (800 mL) was placed a 1000 mL flask and put in an ice-brine mixture in a cooling bath and cooled to -10^{o}C. Then it was saturated with anhydrous ammonia gas. The organic solution from above was then added to the saturated methanolic-ammonia solution at 0^{o}C. The mixture was left to warm to rt and then gradually heated to reflux until the starting material was consumed, as

indicated by analysis by TLC (silica gel). Then the reaction mixture was cooled to rt and the solvent was removed under reduced pressure. The solid which was remained was washed with water and EtOAc and then filtered to produce the amide (8) which is an off-white colored solid and the yield was 91%**1H NMR** (500 MHz, CDCl3) δ 9.54 (s, 1H), 7.58 (td, 1H), 7.55 – 7.52 (m, 1H), 7.45 – 7.38 (m, 3H), 7.22 (d, J = 2.1 Hz, 1H), 7.09 (d, J = 8.6 Hz, 1H), 4.41 (s, 2H). **13C NMR** (126 MHz, CDCl3) δ 171.20 (s), 169.27 (s), 138.33 (s), 137.01 (s), 136.98 (s), 134.83 (s), 133.23 (s), 132.16 (s), 131.04 (s), 130.22 (s), 129.58 (s), 127.05 (s), 122.76 (s), 116.73 (s), 56.53 (s). **HRMS** (ESI/IT-TOF) m/z: $[M + H]^+$ Calcd for

7-bromo-5-(2-chlorophenyl)-1,3-dihydro-2H-benzo[e][1,4]diazepin-2-one(FR-I-20):

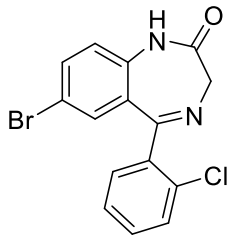

A 3L dry round bottom flask was charged with N-(4-bromo-2-(2-chlorobenzoyl)phenyl)-2-chloroacetamide (110g, 284.2 mmol), hexamethylenetetramine (HMTM, 87.65g ,625.24 mmol) , ammonium acetate (48.19 g, 625.29 mmol) and isopropanol (2000 mL). The mixture was heated to reflux at 82^o for 4h. The reaction progress was monitored by the TLC using silica gel 40% Ethyl acetate and hexane. After completion of the reaction the mixture was concentrated under reduced pressure. When half of the solvent had been removed, the water was added to the solution and the solid was filtered off. The solid was further washed with isopropanol : water(50:50, 200 mL) and the residue was dried under vacuum (40^o C) to get off white solid(95.95g, 95%).**1H NMR** (500 MHz, CDCl3) δ 9.54 (s, 1H), 7.58 (td, 1H), 7.55 – 7.52 (m, 1H), 7.45 – 7.38 (m, 3H), 7.22 (d, J =

2.1 Hz, 1H), 7.09 (d, J = 8.6 Hz, 1H), 4.41 (s, 2H). **13C NMR** (126 MHz, CDCl3) δ 171.20 (s), 169.27 (s), 138.33 (s), 137.01 (s), 136.98 (s), 134.83 (s), 133.23 (s), 132.16 (s), 131.04 (s), 130.22 (s), 129.58 (s), 127.05 (s), 122.76 (s), 116.73 (s), 56.53 (s). **HRMS** (ESI/IT-TOF) m/z: $[M + H]^+$ Calcd for.

Ethyl 8-bromo-6-(2-chlorophenyl)-4H-benzo[f]imidazo[1,5-a][1,4]diazepine-3-carboxylate (FR-I-45): (9)

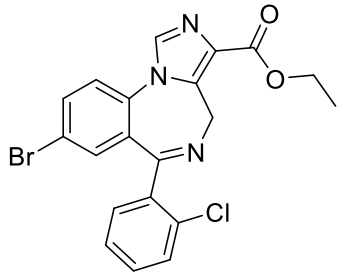

The homogenous solution of7-bromo-5-(2-chlorophenyl)-1,3-dihydro-2H-benzo[e][1,4]diazepin-2-one (90g, 257.42 mmol) and dry tetrahydrofuran (1200 mL) was cooled to -20^o C by using a dry ice / isopropyl alcohol. Potassium *t* butoxide (37.55g, 334.6 mmol) was dissolved in dry tetrahydrofuran and added to the previous reaction mixture dropwise over 30 min maintaining the temperature at -20^o- -15^o C. After addition, the reaction mixture was stirred for another 1h at -20^o C. Diethyl chlorophosphate (52.18 mL, 360.40 mmol) was added dropwise to the reaction mixture maintaining the temperature at -20^o C over 30 min time period. The reaction mixture was allowed to stir for another 4 h at -20 ^{o}C. At this point the completion of reaction was confirmed by TLC using silica gel (ethyl acetate / hexane, 40:60, 1% triethylamine). The ethyl isocyanoacetate (36.052 mL, 334.65 mmol) was added dropwise over 15 minutes at -20^o C, After this addition, a solution of potassium *t* butoxide (37.55 g, 334.6 mmol) in THF was added and the reaction mixture brought to room temperature and stirred for 12 h. The completion of the reaction

was confirmed by TLC using silica gel (ethyl acetate /hexane; 40:60). To quench the reaction, 5% aq sodium bicarbonate (1000 mL) was added and the aq layer separated from the biphasic mixture which is followed by extraction of the water layer with dichloromethane (1000 mL x 2). The organic layers were combined and washed with 10% aq sodium chloride solution (1000 mL), 5% of sodium bicarbonate solution and dried over Na_2SO_4. After removing the solvent under reduced pressure, *t*-butyl methyl ether was added to the brownish residue which resulted in a slurry. This slurry was stirred for 30 min at 50-55^o C. After cooling to rt the slurry was stirred overnight and then the solid was filtered off and washed with *t* butyl methyl ether. For purification, ethanol was added to the former solid and it was heated to reflux for 1 h at 60^o C. After cooling to rt ,the solid was filtered with cold ethanol and dried under vacuum which gave a light brown solid. (65 g ,55%)**^{1}H NMR** (500 MHz, $CDCl_3$) δ 7.94 (s, 1H), 7.76 (dt, 1H), 7.59 – 7.54 (m, 1H), 7.49 (d, *J* = 8.6 Hz, 1H), 7.41 – 7.38 (m, 2H), 7.33 (dd, 2H), 6.09 (d, *J* = 14.8 Hz, 1H), 4.42 (q, *J* = 5.9 Hz, 2H), 4.14 (d, *J* = 8.8 Hz, 1H), 1.43 (t, *J* = 7.1 Hz, 3H). **^{13}C NMR** (126 MHz, CDCl3) δ 167.58 (s), 162.80 (s), 138.44 (s), 138.26 (s), 135.09 (s), 134.20 (s), 133.88 (s), 132.93 (s), 132.55 (s), 131.18 (s), 130.94 (s), 130.49 (s), 130.16 (s), 129.60 (s), 127.19 (s), 124.03 (s), 121.25 (s), 60.85 (s), 44.85 (s), 14.44 (s). **HRMS** (ESI/IT-TOF) m/z: $[M + H]^+$ Calcd for C20H15BrClN3O2 444.0109 and found 444.0104.

Ethyl 6-(2-chlorophenyl)-8-((triisopropylsilyl)ethynyl)-4H-benzo[f]imidazo[1,5-a][1,4]diazepine-3-carboxylate (FR-II-29): (10)

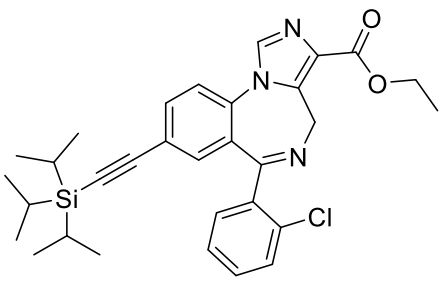

A catalyst was prepared by adding palladium acetate (1.59g, 7.08mmol) and tri-o-tolylphosphine (4.312g, 14.16 mmol) to dry acetonitrile (200 mL) and then stirring the slurry for 30 min at rt. Then the following reagents were added to the mixture sequentially: ethyl 8-bromo-6-(2-chlorophenyl)-4H-benzo[f]imidazo[1,5-a][1,4]diazepine-3-carboxylate (63g, 141.66 mmol), triethylamine (39.819 mL, 283.33 mmol), (triisopropylsilyl)acetylene (41.31 mL, 184.16 mmol) and additional dry acetonitrile (400 mL). Then the mixture was heated to 75 ^{o}C to reflux and held for 4 h until the reaction was complete as confirmed by analysis by TLC (silica gel; 40% EtOAc /hexane). Then the reaction mixture was allowed to cool to rt and silica gel (25 g) was added. Then the mixture was stirred for 30 min and the spent catalyst collected on the silica gel and was filtered off a celite, silica gel plug. The catalyst was then washed with acetonitrile (100 mL x 2). Then solvent was removed under reduced pressure. The resulting residue was dissolved in DCM (700 mL) and 5% aq solution of $NaHCO_3$ (700 mL) was added. This resulted in a biphasic mixture. This mixture was allowed to stand for 15 min until the layers separated. The aq layer was removed to leave the dichloromethane layer (700 mL). the organic layers were washed with 5% aq $NaHCO_3$ solution (700 mL) and then 10% aq NaCl solution (700 mL). The organic layer was then dried (Na_2SO_4), concentrated under reduced pressure and then purified by flash chromatography with

silica gel (600 g) and EtOAc/hexanes (1:1). Then the pure fractions were pooled and concentrated under reduced pressure. The resulting oil was dried at 40 ^{o}C for 2 h under reduced pressure. This resulted into the final product as a clear, golden oil (64.2 g, 106%, HNMR analysis displayed 90wt% product, 10wt% solvents); ***Rf*** = 0.6 (100% EtOAc); **1H NMR** (500 MHz, CDCl3) δ 7.96 (s, 1H), 7.71 (dd, J = 8.3, 1.8 Hz, 1H), 7.59 (dd, J = 5.8, 3.2 Hz, 1H), 7.54 (d, J = 8.3 Hz, 1H), 7.42 – 7.39 (m, 2H), 7.35 – 7.33 (m, 1H), 7.26 (d, J = 1.7 Hz, 1H), 6.17 (d, J = 7.0 Hz, 1H), 4.44 (q, 2H), 4.14 (d, J = 9.3 Hz, 1H), 1.44 (t, J = 7.1 Hz, 3H), 1.15 – 1.07 (m, 3H), 1.11 (s, 18H). **13C NMR** (126 MHz, CDCl3) δ 168.28 (s), 162.86 (s), 138.74 (s), 138.37 (s), 135.53 (s), 134.26 (s), 134.23 (s), 133.19 (s), 132.60 (s), 130.95 (s), 130.86 (s), 130.08 (s), 129.52 (s), 128.96 (s), 127.06 (s), 123.28 (s), 122.39 (s), 104.53 (s), 94.39 (s), 60.82 (s), 44.85 (s), 18.60 (s), 14.45 (s), 11.22 (s). **HRMS** (ESI/IT-TOF) m/z: $[M + H]^{+}$ Calcd for C31H36ClN3O2Si was 546.2334 and found 546.233.

Ethyl 6-(2-chlorophenyl)-8-ethynyl-4H-benzo[f]imidazo[1,5-a][1,4]diazepine-3-carboxylate (FR-I-59): (11)

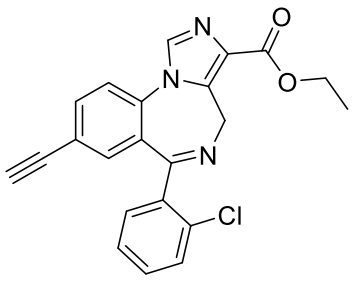

A mixture was prepared by adding ethyl 6-(2-chlorophenyl)-8-((triisopropylsilyl)ethynyl) -4H-benzo[f]imidazo[1,5-a][1,4]diazepine-3-carboxylate (**10)**, 60.5 g, 110.76 mmol) and water (6.0 mL) to a solution of THF (600 mL). Then this mixture was cooled to -20 ^{o}C using a dry ice / IPA bath. The tetrabutylammonium fluoride hydrate, 1M in THF (132.92 mL, 132.92 mmoL) was

added dropwise over 30 min at -20 to -15 ^{o}C. Then the mixture was brought to rt and stirred for additional 1 h until the reaction was complete, as confirmed by analysis by TLC (silica gel, 100% EtOAc; ***Rf: 10*** = 0.6, ***Rf: 11*** = 0.4). Then EtOAc (600 mL) and 10% aq NaCl (600 mL) was added to the mixture for dilution. This formed a biphasic mixture which was allowed to stand for 15 min until the layers separated. The aq layer was extracted with EtOAc (600 mL) and the organic layer was dried (Na_2SO_4). The organic layer was concentrated under reduced pressure to remove the solvents. The remaining residue was slurried with methanol (250 mL) for 30 min while maintaining a temperature of 50 – 55 ^{o}C. Then water was added to the slurry and stirred for an additional 30 min maintaining the temperature at 50 – 55 ^{o}C. Then the mixture was cooled to 20 – 25 ^{o}C and held at that for 2 h. Then the solid was filtered and washed with methanol/water (1:1, 50 mL x 4). Then it was further washed with hexanes (50 mL x 3). The subsequently solid, which resulted, was dried at 40 ^{o}C under vacuum to obtain the final white crystalline solid product. (yield 94% ,40.4 g) **1H NMR** (500 MHz, CDCl3) δ 7.96 (s, 1H), 7.74 (dd, J = 8.3, 1.8 Hz, 1H), 7.57 (d, J = 8.3 Hz, 2H), 7.42 – 7.36 (m, 2H), 7.33 (dd, J = 3.6, 1.8 Hz, 2H), 6.13 (d, J = 22.9 Hz, 1H), 4.47 (q, J = 35.6, 11.4 Hz, 2H), 4.20 (d, J = 15.6 Hz, 1H), 3.16 (s, 1H), 1.44 (t, J = 7.1 Hz, 3H). **13C NMR** (126 MHz, CDCl3) δ 168.14 (s), 162.83 (s), 138.67 (s), 138.32 (s), 135.37 (s), 134.75 (s), 134.26 (s), 133.84 (s), 132.58 (s), 131.05 (s), 130.92 (s), 130.13 (s), 129.58 (s), 129.02 (s), 127.12 (s), 122.55 (s), 121.91 (s), 81.41 (s), 79.83 (s), 60.85 (s), 44.86 (s), 14.44 (s). **HRMS** (ESI/IT-TOF) m/z: $[M + H]^+$ Calcd for C22H16ClN3O2 is 390.1004 and found 390.0983.

8-bromo-6-(2-chlorophenyl)-4H-benzo[f]imidazo[1,5-a][1,4]diazepine-3-carbaldehyde (FR-II-58) (13)

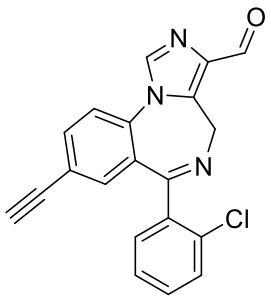

Potassium *tert*-butoxide(1.3 g , 2.57 mmol) was dissolved in dry THF and cooled it to 0^{o} C . DIBALH (4.5mL, 1.0 M in hexane, 4.50mmol) was added dropwise to the homogenous solution of potassium *tert*-butoxide at 0 °C. The mixture was allowed to stir at rt for 2 h.

In a 100 ml flask, the ethyl ester (11) (2 g) was dissolved in dry DCM (10 mL) at 0 °C. The ice-water bath was removed, and PDBBA solution was added in one portion with vigorous stirring. After adding the PDBBA solution the color of the reaction mixture changes light brown to dark black. The reaction was monitored by TLC (silica gel) after each minute and was completed in 5 min, and this was followed by hydrolysis of the mixture in 1N aq HCl at 0 °C. Water (20mL) was added to the mixture, and it was stirred for 0.5 h. The resulted aluminum salt was formed and filtered off on a celite pad. The filtrate was extracted with DCM (3 x 50 mL). All the organic layers were combined and concentrated with reduced pressure, and this was followed by washing with brine and dried (Na_2SO_4). The solid residue was dissolved in a mixture of DCM (100 mL) and EtOAc (100 mL) at 50 °C. The filtrate was combined and further purified by flash chromatography (silica gel, etOAc and 1% of each TEA and MeOH) to afford additional aldehyde as a white solid (1.4 g).^{1}H NMR (500 MHz, CDCl3) δ 10.08 (s, 1H), 8.00 (s, 1H), 7.79 (dd, J = 8.6, 2.2 Hz, 1H), 7.61 – 7.58 (m, 1H), 7.51 (d, J = 8.6 Hz, 1H), 7.44 – 7.40 (m, 2H), 7.37 – 7.33 (m, 2H), 6.12 (d, J

= 20.6 Hz, 1H), 4.44 (d, J = 12.6 Hz, 1H). 3.18 (s, 1H) ^{13}C NMR (126 MHz, CDCl3) δ 186.71 (s), 167.76 (s), 138.28 (s), 137.72 (s), 136.91 (s), 135.22 (s), 135.12 (s), 133.46 (s), 133.05 (s), 132.53 (s), 131.33 (s), 131.01 (s), 130.64 (s), 130.22 (s), 127.26 (s), 124.01 (s), 121.59 (s), 80.51 (s), 79.67 (s) 44.23 (s). **HRMS** (ESI/IT-TOF) m/z: $[M + H]^+$ Calcd for C20H12ClN3O was 346.0789 and found 346.0654.

5-(6-(2-chlorophenyl)-8-ethynyl-4H-benzo[f]imidazo[1,5-a][1,4]diazepin-3-yl)oxazole(FR-II-60) (14)

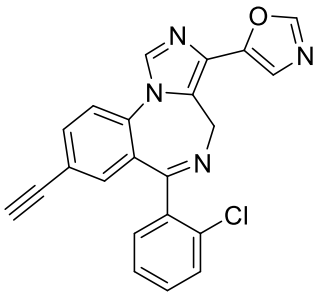

The toluenesulfonylmethyl isocyanide (TosMIC, 1.06 g), K_2CO_3 (1.89 g) and the aldehyde (1.4.g) were placed in a dry two neck round bottom flask. Dry MeOH (100 mL) was added to the mixture under an argon atmosphere at rt. The reaction mixture was allowed to heat to reflux for 2 h. After completion of the reaction on analysis by TLC (silica gel, EtOAc and 1% of each TEA and MeOH), the reaction mixture was quenched with cold water (30 mL) and extracted with EtOAc (3 x 100 mL). The organic layers were combined, and this was followed by washing with brine. The solution was then dried (Na_2SO_4) and concentrated under reduced pressure to dryness and further purified by flash chromatography (silica gel, EtOAc and 1% of each TEA and MeOH) to afford additional oxazole as a white solid (800 mg).^{1}H NMR (500 MHz, $CDCl_3$) δ 8.02 (s, 1H), 7.92 (s, 1H), 7.74 (dd, *J* = 8.3, 1.8 Hz, 1H), 7.58 (t, *J* = 6.0 Hz, 2H), 7.47 (s, 1H), 7.42 – 7.38 (m, 2H), 7.36 – 7.32 (m, 2H), 5.72 (d, *J* = 17.4 Hz, 1H), 4.30 (d, *J* = 26.0 Hz, 1H), 3.16 (s,

1H). ^{13}C NMR (126 MHz, CDCl3) δ 168.15 (s), 149.82 (s), 146.53 (s), 138.83 (s), 135.46 (s), 135.06 (s), 134.92 (s), 134.04 (s), 132.58 (s), 131.04 (s), 130.88 (s), 130.18 (s), 129.81 (s), 128.85 (s), 127.65 (s), 127.12 (s), 122.62 (s), 122.37 (s), 121.58 (s), 81.51 (s), 79.67 (s), 45.01 (s). **HRMS** (ESI/IT-TOF) m/z: $[M + H]^+$ Calcd for C22H13ClN4O was 385.0851 and found 385.0836

5-(8-bromo-6-(2-chlorophenyl)-4H-benzo[f]imidazo[1,5-a][1,4]diazepin-3-yl)-3-methyl -1,2,4-oxadiazole:(FR-III-48) (15)

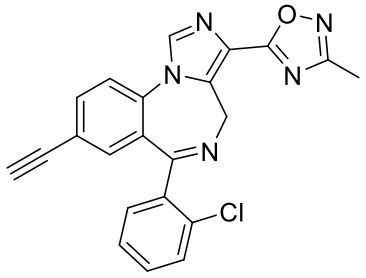

In a flask with 3Å molecular sieves isopropyl oxime (0.919g, 8.99 mmol) was added to the dry THF under argon pressure. Sodium hydride ((60% dispersion in mineral oil, 59.36 mg, 2.47 mmol) was added to the reaction mixture and stirred for 1 hour. In another flask the Br-ethyl ester, (11) (1g, 2.24 mmol) was dissolved in dry THF. The former homogenous mixture was added to the first one dropwise and allowed to be stirred for 2 h. The completion of the reaction was confirmed by checking TLC when all the starting material consumed. (Silica gel, 40% etOAc/ hexane). $NaHCO_3$ solution (20 mL) was added to quench the reaction. Then etOAc (100 mL) and 10% aq solution NaCl (100 mL) was added to the mixture and form a biphasic solution which allowed to stand for 10 minutes to separate the layers. The organic layers all combined and dried over Na_2SO_4. The organic layers removed under the reduced pressure to result a brownish crude. The crude was purified with column chromatography to afford an off-white solid (900 mg, 82.56%) ^1H NMR (500 MHz, CDCl3) δ 8.09 (s, 1H), 7.77 (dd, J = 8.3, 1.8 Hz, 1H), 7.63 (d, J = 8.3 Hz, 1H), 7.60

(dd, J = 4.9, 2.7 Hz, 1H), 7.40 (dd, J = 5.8, 3.5 Hz, 2H), 7.36 (d, J = 1.8 Hz, 1H), 7.33 (dd, J = 5.9, 3.3 Hz, 1H), 3.18 (s, 1H), 2.47 (s, 3H). ^{13}C NMR (126 MHz, CDCl3) δ 170.73 (s), 168.36 (s), 167.45 (s), 138.59 (s), 136.15 (s), 135.60 (s), 135.50 (s), 134.50 (s), 133.98 (s), 132.56 (s), 131.15 (s), 130.97 (s), 130.15 (s), 129.10 (s), 127.13 (s), 124.88 (s), 122.51 (s), 122.18 (s), 81.33 (s), 80.01 (s), 44.70 (s), 14.20 (s).**HRMS** (ESI/IT-TOF) m/z: $[M + H]^+$ Calcd for C22H14ClN5O was 400.0847 and found 400.0829.

5-(6-(2-chlorophenyl)-8-ethynyl-4H-benzo[f]imidazo[1,5-a][1,4]diazepin-3-yl)-3-ethyl-1,2,4-oxadiazole (FR-I-75) (16)

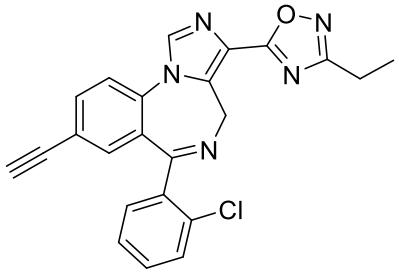

In a flask charged with 3Å molecular sieves N'-hydroxypropionimidamide (904.06 mg, 10.26 mmol) was added to dry THF under argon pressure. Sodium hydride ((60% dispersion in mineral oil,67.72 mg, 2.82 mmol) was added to the reaction mixture and it was allowed to stir for 1 hour. In another flask the ethyl ester, (11) (1g, 2.565 mmol) was dissolved in dry THF. The former homogenous mixture was added to the first one dropwise and allowed to be stirred for 2 h. The completion of the reaction was confirmed by checking by TLC when all the starting material was consumed. (Silica gel, 40% etOAc/ hexane). Aqueous $NaHCO_3$ solution (20 mL) was added to quench the reaction. Then EtOAc (100 mL) and 10% aq NaCl (100 mL) solution were added to the mixture, and this resulted in a biphasic solution which was allowed to stand for 10 min to separate the layers. The organic layers were all combined and dried over Na_2SO_4. The organic

layer was removed under the reduced pressure to result a brownish colored crude solid. The solid was purified by column chromatography to afford an off-white solid (700 mg, 61%)^{1}H NMR (500 MHz, $CDCl_3$) δ 8.09 (s, 1H), 7.77 (dd, *J* = 8.3, 1.8 Hz, 1H), 7.62 (d, *J* = 8.3 Hz, 2H), 7.60 (dd, *J* = 5.6, 3.5 Hz, 1H), 7.43 – 7.39 (m, 2H), 7.36 (d, *J* = 1.8 Hz, 1H), 7.35 – 7.32 (m, 1H), 6.20 (d, *J* = 7.7 Hz, 1H), 4.32 (d, *J* = 16.2 Hz, 1H), 3.18 (s, 1H), 2.84 (q, *J* = 7.6 Hz, 2H), 1.40 (t, *J* = 7.6 Hz, 3H). ^{13}C NMR (126 MHz, CDCl3) δ 171.90 (s), 170.68 (s), 168.36 (s), 138.62 (s), 136.11 (s), 135.56 (s), 135.50 (s), 134.54 (s), 133.99 (s), 132.56 (s), 131.15 (s), 130.93 (s), 130.16 (s), 129.07 (s), 127.15 (s), 125.04 (s), 122.51 (s), 122.15 (s), 81.34 (s), 79.99 (s), 44.73 (s), 19.76 (s), 11.55 (s). **HRMS** (ESI/IT-TOF) m/z: $[M + H]^+$ Calcd for C21H14ClN3O2 was 376.0847 and found 376.0828.

5-(6-(2-chlorophenyl)-8-ethynyl-4H-benzo[f]imidazo[1,5-a][1,4]diazepin-3-yl)-3-isopropyl-1,2,4-oxadiazole (FR-III-51) (17)

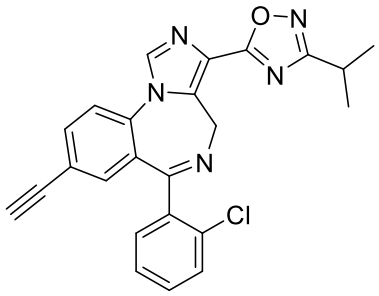

To a flask 3Å molecular sieves were charged and this was followed by the addition of isopropyl oxime (1.047g, 10.25 mmol). It was added to the dry THF mixture under argon pressure. Sodium hydride ((60% dispersion in mineral oil, 67.7mg, 2.82 mmol) was added to the reaction mixture and it was allowed to stir for 1 hour at rt. In another flask the ethyl ester, (11) (1g, 2.565 mmol) was dissolved in dry THF. The latter homogenous mixture was added to the first one dropwise and the mixture was allowed to be stir for 2 h. The completion of the reaction was

confirmed by checking by TLC, when all the starting material had been consumed. (Silica gel, 40% etOAc/ hexane). $NaHCO_3$ solution (20 mL) was added to quench the reaction. Then EtOAc (100 mL) and 10% aq NaCl (100 mL) solution were added to the mixture to provide a biphasic solution, which allowed to stand for 10 minutes to separate the layers. The organic layers all combined and dried over Na_2SO_4. The organic layers combined and removed under the reduced pressure to provide a brownish colored crude solid. The crude was purified with column chromatography to afford an off-white colored solid (850 mg, 77%). ^{1}H NMR (500 MHz, CDCl3) δ 8.09 (s, 1H), 7.77 (dd, J = 8.3, 1.8 Hz, 1H), 7.62 (d, J = 8.4 Hz, 1H), 7.60 (t, 1H), 7.43 – 7.39 (m, 2H), 7.36 (d, J = 1.8 Hz, 1H), 7.34 (dd, 1H), 6.15 (d, 1H), 4.29 (d, 1H), 3.24 – 3.15 (m, 1H), 3.18 (s, 1H), 1.42 (s, 3H), 1.41 (s, 3H). ^{13}C NMR (126 MHz, CDCl3) δ 175.34 (s), 170.59 (s), 168.35 (s), 138.64 (s), 136.08 (s), 135.52 (s), 135.50 (s), 134.58 (s), 134.00 (s), 132.56 (s), 131.14 (s), 130.88 (s), 130.18 (s), 129.05 (s), 127.16 (s), 125.16 (s), 122.50 (s), 122.13 (s), 81.35 (s), 79.98 (s), 44.77 (s), 26.76 (s), 20.62 (s).**HRMS** (ESI/IT-TOF) m/z: $[M + H]^+$ Calcd for C24H18ClN5O was 428.1273 and found 428.1253.

Methyl 6-(2-chlorophenyl)-8-ethynyl-4H-benzo[f]imidazo[1,5-a][1,4]diazepine-3-carboxylate (FR-I-98) (19)

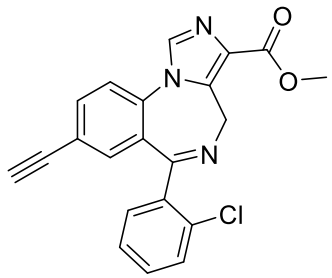

To the homogenous mixture of **(11)** (1g, 2.24 mmol) and methanol (80 mL), sodium methoxide was added, and the mixture heated at 60-65^{o} C to reflux for 0.5 h. The reaction completion was confirmed by the TLC (silica gel 4:1, etOAc: hexane), when there is no starting material left which took approximately 1 h. The reaction mixture was cooled to rt and a saturated solution of sodium bicarbonate (20 mL) and water (60 mL) was added to quench the reaction. After removing the methanol under reduced pressure, the reaction mixture was extracted with ethyl acetate (3x100 mL). After combining all the organic layers and washed with brine and dried over Na_2SO_4. The solvent was removed under the reduced pressure to provide a brownish colored crude, which was purified followed by a flash column chromatography (silica gel, 40% etOAc/ hexane) to afford an off-white powder product. (720 mg, 75%)**1H NMR** (500 MHz, CDCl3) δ 7.97 (s, 1H), 7.74 (dd, J = 8.3, 1.8 Hz, 1H), 7.59 (d, J = 8.3 Hz, 2H), 7.43 – 7.37 (m, 2H), 7.35 – 7.31 (m, 2H), 6.08 (d, J = 4.8 Hz, 1H), 4.18 (d, J = 5.0 Hz, 1H), 3.96 (s, 3H), 3.17 (s, 1H). **^{13}C NMR** (126 MHz, CDCl3) δ 168.17 (s), 163.21 (s), 138.65 (s), 138.34 (s), 135.38 (s), 134.70 (s), 134.32 (s), 133.86 (s), 132.58 (s), 131.07 (s), 130.93 (s), 130.13 (s), 129.35 (s), 129.04 (s), 127.12 (s), 122.54 (s), 121.96 (s), 81.40 (s), 79.85 (s), 51.89 (s), 44.83 (s) **HRMS** (ESI/IT-TOF) m/z: $[M + H]^+$ Calcd for C21H14ClN3O2 was 376.0847 and found 376.0828.

6-(2-chlorophenyl)-8-ethynyl-N-methyl-4H-benzo[f]imidazo[1,5-a][1,4]diazepine-3-carboxamide (FR-I-70) (20)

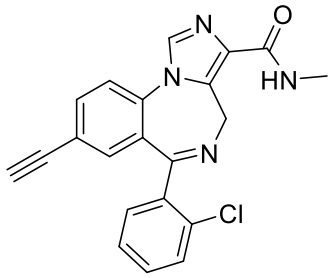

6-(2-chlorophenyl)-8-ethynyl-*N*-methyl-4*H*-benzo[*f*]imidazo[1,5-*a*][1,4]diazepine-3-carboxamide

The ethyl ester (11) (1g, 2.56 mmol) was dissolved in excess amount of methyl amine (0.729 mL, 15 mmol) and the reaction was allowed to run for 16 h. The reaction completion was confirmed by TLC. The methyl amine removed under reduced pressure. The ethyl acetate was added to the solution and extracted with brine. All the organic layer combined and reduced under pressure.^{1}H NMR (500 MHz, CDCl3) δ 7.85 (s, 1H), 7.72 (dd, J = 8.3, 1.8 Hz, 1H), 7.61 (dd, J = 5.8, 3.3 Hz, 1H), 7.54 (d, J = 8.3 Hz, 1H), 7.41 – 7.37 (m, 2H), 7.33 – 7.30 (m, 2H), 7.14 (s, 1H), 6.11 (d, 1H), 3.90 (d, 1H), 3.15 (s, 1H), 2.99 (d, J = 5.0 Hz, 3H). ^{13}C NMR (126 MHz, CDCl3) δ 167.65 (s), 163.16 (s), 138.90 (s), 135.61 (s), 135.18 (s), 134.96 (s), 133.84 (s), 132.85 (s), 132.54 (s), 131.94 (s), 131.15 (s), 130.92 (s), 130.02 (s), 129.15 (s), 127.07 (s), 122.41 (s), 121.66 (s), 81.53 (s), 79.61 (s), 44.63 (s), 25.65 (s). **HRMS** (ESI/IT-TOF) m/z: $[M + H]^{+}$ Calcd for C22H13ClN4O was 375.1007 and found 375.0984.

8-bromo-6-(2-chlorophenyl) -4H-benzo[f]imidazo[1,5-a][1,4]diazepine-3-carboxylic acid: (23)

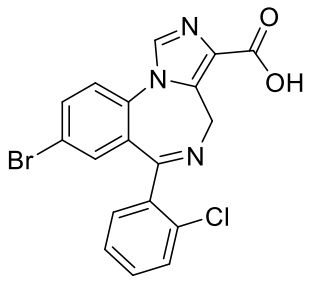

Ethyl ester (300 mg, 77 mmol) was dissolved in ethanol (100 mL). After adding sodium hydroxide (8.48 mmol), the solution was heated to 55 °C at reflux for 1 h. When the reaction was complete, this was confirmed by checking TLC (silica gel), the solution was cooled to rt and water was added to dilute the solution. One half of the solvent was removed under reduced pressure. The remaining 50% of the solution was stirred at rt and then hydrochloric acid was added dropwise (pH = 4) until the product began to precipitate from the solution. The filtration of the solution gave a white solid product **17**. **^{1}H NMR** (300 MHz, CD_3OD) δ 9.0 (s, 1H), 8.88 (t, *J* = 23.8 Hz, 1H), 8.6 (s, 1H), 8.4 (m, *J* = 4.2, 1.8 Hz, 2H), 8.0 (d, *J* = 16.3 Hz, 1H), 7.8 (d, *J* = 18 Hz, 1H), 7.6(d, *J* = 13 Hz, 1H) 6.0 (m, *J* = 10.4 Hz, 1H), 4.57 (m, 2H), 4.27 (d, *J* = 10.0 Hz, 1H); **^{13}C NMR** (75 MHz, CD_3OD) δ 168.88, 163.88, 151.95, 138.16, 136.41, 135.43, 133.38, 132.62, 130.77, 129.48, 128.49, 127.77, 124.67, 124.0, 122.45, 120.89, 83.0, 82.42, 44.7; **LC-MS** calcd for $C_{18}H_{12}BrClN_3O_2$ $(M + H)^+$ 416,418,420 ; **HRMS** calcd for $C_{18}H_{12}BrClN_3O_2$ $(M + H)^+$ 415.9417. found 415.9814

8-bromo-6-(2-chlorophenyl)-4H-benzo[f]imidazo[1,5-a][1,4]diazepine-3-carboxylic-1,4,4-d3 acid (24)

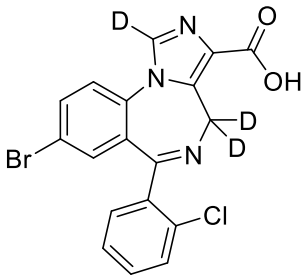

The Choloro-bromo substituted acid was dissolved in CH_3OD and the base potassium carbonate (2 eq) was added to the solution with stirring. The solution was heated to reflux for 6 h. After completion of the reaction, by TLC (Silica gel) the solvent was removed under reduced pressure. D_2O was added to the solution to dilute the reaction mixture and it was then cooled to 0 ^oC. Deuterated hydrochloric acid was added dropwise until the product precipitated out of the solution. After filtration this afforded a white solid **18**. **^{1}H NMR** (300 MHz, CD_3OD) δ 9.0 (s, 1H), 8.88 (t, *J* = 23.8 Hz, 1H), 8.6 (s, 1H), 8.4 (m, *J* = 4.2, 1.8 Hz, 2H), 8.0 (d, *J* = 16.3 Hz, 1H), 7.8 (d, *J* = 18 Hz, 1H), 7.6(d, *J* = 13 Hz, 1H) , 4.27 (d, *J* = 10.0 Hz, 1H) **^{13}C NMR** (75 MHz, CD_3OD) δ 168.88, 163.88, 151.95, 138.16, 136.41, 135.43, 133.38, 132.62, 130.77, 129.48, 128.49, 127.77, 124.67, 124.0, 122.45, 120.89, 83.0, 82.42, 44.7; **LC-MS** Calc. for $C_{18}H_9D_3BrClN_3O_2$ $(M + H)^+$ 419,421,423 found 419, 421,423; **HRMS** calcd for $C_{18}H_9D_3BrClN_3O_2$ $(M + H)^+$ 418.9577, ,420.9887,421.9777found 418.9414, 420.9775,421.9767.

6-(2-chlorophenyl)-8-ethynyl-4H-benzo[f]imidazo[1,5-a][1,4]diazepine-3-carboxylic acid (26)

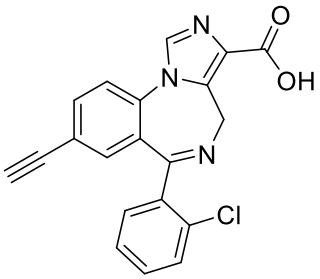

Ethyl ester (300 mg, 77 mmol) was dissolved in ethanol (100 mL). After adding sodium hydroxide (8.48 mmol), to the solution it was heated at reflux for one h. When the reaction was complete on checking TLC (Silica gel) the solution was cooled to rt and water was added to dilute the solution. One half of the solvent was removed under reduced pressure until 50% of the solution remained. The solution which remains was stirred at rt and hydrochloric acid was added dropwise until the product began to precipitate from the solution. The product was filtered to give a white solid . **^{1}H NMR** (300 MHz,CDCL3) δ 8.86 (s, 1H), 8.34 (t, *J* = 7.5Hz, 1H), 7.94 (s, 1H), 7.84(m, *J* = 4.2, 1.8 Hz, 2H), 7.63(d, *J* = 12 Hz, 1H), 7.52(d, *J* = 18 Hz, 1H), 7.15 (m, *J* = 10.4 Hz, 1H),6.89(s,1H) 4.57 (m, 2H),3.89 (s,1H); **^{13}C NMR** (75 MHz, $CDCl_3$) δ 168.6, 160.32, 156.64, 148.77, 138.43, 137.60, 136.23, 135.92, 135.57, 135.15, 129.12, 127.19, 125.47, 124.20, 123.86, 120.35, 82.98, 82.42, 45.10; **LC-MS** Calc 361 found 361. for $C_{20}H_{13}ClN_3O_2$ $(M + H)^+$ 360.9967 (calc) found 360.9959.

6-(2-chlorophenyl)-8-ethynyl-4H-benzo[f]imidazo[1,5-a][1,4]diazepine-3-carboxylic-1,4,4-d3 acid (27)

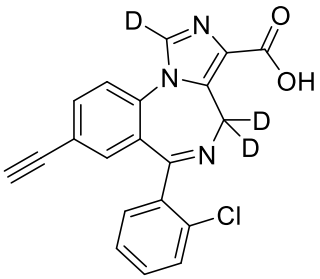

The acid was dissolved in methanol-D and potassium carbonate was added to the solution with stirring under argon . The solution was heated to reflux for 6 h under argon. After completion of the reaction, the solvent was removed under reduced pressure. D_2O was then added to the solution to dilute the reaction mixture and it was cooled to 0^o C. The deuterated hydrochloric acid was added dropwise until the product precipitated from the solution. After filtration the product was obtained as a white solid **21**. **^{1}H NMR** (300 MHz,$CDCl_3$) δ 8.86 (s, 1H), 8.34 (t, *J* = 7.5Hz, 1H), 7.94 (s, 1H), 7.84 (m, *J* = 4.2, 1.8 Hz, 2H), 7.63(d, *J* = 12 Hz, 1H), 7.52(d, *J* = 18 Hz, 1H), 7.15 (m, *J* = 10.4 Hz, 1H), 3.89 (s,1H); **^{13}C NMR** (75 MHz, $CDCl_3$) δ 167.2, 162.42, 156.64, 148.77, 138.43, 137.60, 136.23, 135.92, 135.57, 135.15, 129.12, 127.19, 125.47, 124.20, 123.86, 120.35, 82.98, 82.42, 45.10; **LC-MS** calcd for $C_{20}H_{10}D_3ClN_3O_2$ $(M + H)^+$ 364 found 364; **HRMS** calcd for $C_{20}H_{10}D_3ClN_3O_2$ $(M + H)^+$ 363.9980, 365.9986, 367.9765 (calc): found 363.9975 , 365.9879 , 367.9758.

5-(8-(ethynyl-d)-6-(pyridin-2-yl)-4H-benzo[f]imidazo[1,5-a][1,4]diazepin-3-yl-1,4,4-d3)oxazole-2,4 d2: (4a)

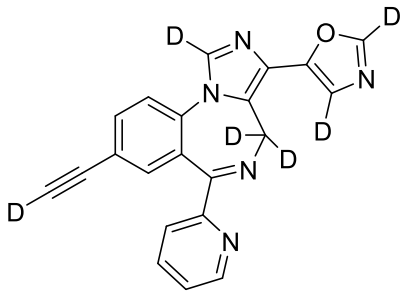

The toluenesulfonylmethyl isocyanide (TosMIC, 150.02 mg, 0.77 mmol), K_2CO_3 (265.5 mg, 1.92 mmol) and the aldehyde (200 mg, 45.5 mmol) were placed in a dry two neck round bottom flask. Dry CD_3OD (10 mL) was added to the mixture under an argon atmosphere at rt. The reaction mixture was allowed to heat to reflux for 2 h. After completion of the reaction on analysis by TLC (silica gel, EtOAc and 1% TEA), the reaction mixture was quenched with D_2O (10 mL) and extracted with EtOAc (3 x 100 mL). The organic layers were combined and dried over Na_2SO_4. Excess solvent was removed under reduced pressure and further purified by flash chromatography (silica gel, EtOAc:hexane, 3:1) to afford oxazole (d_6-KRM-II-81) as a white solid (228.86 mg, 78% yield). R_f = 0.3 (EtOAc and 1% of each MeOH and TEA); **^{1}H NMR** (300 MHz, $CDCl_3$): δ 8.60 (d, *J* = 4.5 Hz, 1H), 8.04 (d, *J* = 7.9 Hz, 1H), 7.85-7.76 (m, 2H), 7.59-7.55 (m, 2H), 7.38 (t, *J* = 6 Hz, 1H), 3.17 (s, 0.3H); **LC-MS** calcd $C_{21}H_8D_6N_5O$ $(M + H)^+$ 358 found 358.

5-(8-(ethynyl-d)-6-(pyridin-2-yl)-4H-benzo[f]imidazo[1,5-a][1,4]diazepin-3-yl1,4d3)oxazole-2,4 d2: (4b)

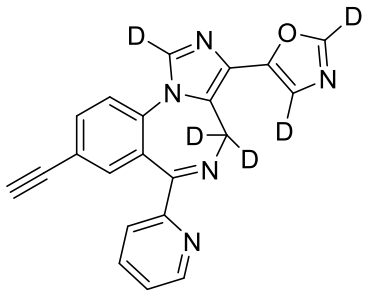

Compound **3** (100 mg, 0.28 mmol) was dissolved in methanol (10 mL) and the mixture heated to 50 °C for 30 min with stirring to afford compound **4** (d_5-KRM-II-81) (85 mg, yield 95%). R_f = 0.3 (EtOAc and 1% of each MeOH and TEA); **^{1}H NMR** (300 MHz, $CDCl_3$): δ 8.60 (d, *J* = 4.5 Hz, 1H), 8.04 (d, *J* = 7.9 Hz, 1H), 7.85-7.76 (m, 2H), 7.59-7.55 (m, 2H), 7.38 (t, *J* = 6 Hz, 1H), 3.17 (s, 1H); **LC-MS** calcd $C_{21}H_9D_5N_5O$ $(M + H)^+$ 357 found 357; **HRMS** (ESI) calcd for $C_{21}H_9D_5N_5O$ $(M + H)^+$ 357.1512, found 357.1489.

5-(8-(ethynyl-d)-6-(pyridin-2-yl)-4H-benzo[f]imidazo[1,5-a][1,4]diazepin-3-yl-1,4,4-d3)oxazole-2,4 d2: (4c)

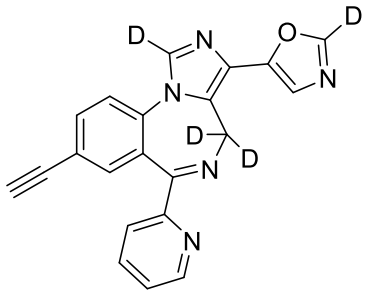

The oxazole **5** (50 mg, 0.14 mmol) and K_2CO_3 (19 mg, 0.14 mmol) was placed in a round bottom flask. Dry CD_3OD (5 mL) was added to the mixture under an argon atmosphere at rt. The

reaction mixture was allowed to stir for 2 h at reflux. The excess solvent was evaporated. Ethyl acetate was added to the solution and it was filtered through celite. Excess of solvent was removed under reduced pressure to afford oxazole **6** as a white solid (89 mg, 89% yield). Compound **6** was dissolve in methanol 10 mL and heated to 50 °C for 30 min with stirring to final afford compound **7** (d_4-KRM-II-81) (85 mg, yield 95%). Compound **6** R_f = 0.3 (EtOAc and 1% of each MeOH and TEA); Compound **6** **^{1}H NMR** (300 MHz, $CDCl_3$): δ 8.60 (d, *J* = 4.5 Hz, 1H), 8.04 (d, *J* = 7.9 Hz, 1H), 7.85-7.76 (m, 2H), 7.59-7.55 (m, 2H), 7.45 (s, 1H), 7.38 (t, *J* = 6 Hz, 1H), 3.17 (s, 0.63H); Compound **6** **LC-MS** calcd $C_{21}H_9D_5N_5O$ $(M + H)^+$ 357 found 357; Compound **7** R_f = 0.3 (EtOAc and 1% of each MeOH and TEA); Compound **7** **^{1}H NMR** (300 MHz, $CDCl_3$): δ 8.60 (d, *J* = 4.5 Hz, 1H), 8.04 (d, *J* = 7.9 Hz, 1H), 7.85-7.76 (m, 2H), 7.59-7.55 (m, 2H), 7.45 (s, 1H), 7.38 (t, *J* = 6 Hz, 1H), 3.16 (s, 1H); Compound **7** **LC-MS** calcd for $C_{21}H_{10}D_4N_5O$ $(M + H)^+$ 356 found 356; **HRMS** (ESI) calcd for $C_{21}H_{10}D_4N_5O$ $(M + H)^+$ 356.1449, found 356.1423.

2.16. Methods

Dorsal Root Ganglion Electrophysiology (Dr. Kevin Freeman, University of Mississippi Medical Center)

A culture of dorsal root ganglia (DRG) sensory neurons was prepared following the method of (Bleakman et al., 1996). The ganglia were isolated from 2-month-old rats weighing 235 - 310 g and then digested enzymatically with type II collagenase (3 mg/mL), at a temperature of 37 ºC for 50 min. After that, the mechanical dissociation of the tissues was performed using a set of fire-polished sterile glass pipettes of decreasing diameters and plated on Nunc 35 x 10 tissue culture dishes. The tissue was incubated in Nb Active1 (Brainbits LLC, Springfield, IL), 5% dialyzed fetal bovine serum and 0.25% Glutamax (Gibco). The tissue incubators were always maintained at (37

^{o}C, 5% CO_2) and not used beyond seven days. DRG neurons were recorded at rt using the voltage clamp methods of Cerne et al. (2016). Cells were clamped at -80mV voltage throughout the procedure. GABA currents were initiated by 4 s perfusion (GABA concentration: EC10; ValveBank II eight channel perfusion system, AutoMate Scientific, Berkeley, CA). Test compounds were dissolved in DMSO to prepare stock solutions and further diluted by the GABA EC10 or the external solution to make sure that the DMSO concentrations were less than 0.1% (v/v). Perfusion of the test compound was performed for 2 min and then GABA was co-administered for 4 s. The perfusion of Nunc 35 x 10 tissue culture dishes was continued using a gravity flow perfusion system throughout the recording, following the method reported by Witkin et al. (2019). The recorded data was first normalized using the GABA EC10 current amplitudes as the baseline and then the mean and standard error of the mean (SEM) were reported. The data was then fitted using the four-parameter logistic equation.

Marble Burying Assay (CRO)

The evaluation of the ligands was performed following the methods of marble-burying in mice (Li, et al., *Life Sci.*, **2006**, *78*, 1933 – 1939). Either 1% carboxymethyl cellulose vehicle or a test compound was administered to the mice i.p. 30 min prior to testing. A plastic tub (17 cm x 28 cm x 12 cm , with 5 mm sawdust shavings) was placed on the floor and then the mice were put in it (Harlan Sani-Chips, Harlan-Teklad, Indianapolis, IN). At the center of the tub, 20 blue marbles of 1.5 cm diameters were placed and the mice were left alone for 30 min. The number of murbles covered at least two-third in sawdust were recorded.

Vogel Conflict Assay (Dr. Jeffrey M. Witkin, CRO)

The evaluation of the ligands was performed in male Sprague-Dawley rats weighing between 200-300 grams (Harlan Industries, Indianapolis, IN) following the Vogel conflict assay methods of (Alt, et al., *Neuropharmacology*, **2007**, *52*, 1482 – 1487). Operant behavior test chambers were ENV-007 (Med Associates Inc., Georgia, Vermont, USA) 30.5 x 24.1 x 29.2 cm, for the assay. A Compaq computer running MED-PC Version IV (Med Associates Inc., Georgia, Vermont, USA) was used to record the data. For the first training session, water was withheld for 1 day. A duration of 6 min following the first lick was considered as the training. The two 3-min intervals were the unpunished and punished components respectively. In the first two training days, no shock was given during the punished component of the training. At the end of the session, the rats were returned to the home cages and provided with water for 30 min. Then water was again withheld for the next 24 h prior to the next session. For the third day onwards, the rats were administered i.p. with vehicle (0.5% Tween 80, 1% hydroxyethyl cellulose, 0.05% Dow anti-foam administered at 3 mL/kg), chlordiazepoxide (20 mg/kg at 1 mL/kg), Hz-166 (30 mg/kg at 3 mL/kg) or KRM-II-81 (3, 10, 30, or 60 mg/kg; 3 and 10 mg/kg at 1 mL/kg, 30 mg/kg at 3 mL/kg, and 60 mg/kg at 6 mL/kg) 30 min prior to testing (n = 6 – 8). On the third day, electric shocks were given in the punished session (100 msec, 0.5 mA) after every 20th lick (FR20). The number of licks during each session was recorded. The mean number of licks for each session was analyzed and compared to the control vehicle group. Dose-effect functions were analyzed by ANOVA. Then post-hoc Dunnett's test was performed with vehicle as the control. The statistical significance margin was set at ≤ 0.5.

6 Hz 44mA Seizure Model (ETSP/ NINDS)

The mice were administrated p.o. with KRM-II-81 (**2**). After two hours, a 6 Hz stimulation was delivered for 3 seconds using corneal electrodes (44 mA). The seizure was observed and recorded. Another group of mice were given higher doses of **1** and after 4 hr observed for possible motor impairment and toxicity.

Maximal Electroshock Seizure (MES) Model (ETSP)

The purpose of the MES assay is to investigate the anticonvulsant effects of the test compounds that either cause or alleviate seizures. For this stuty, male CD1 mice (Taconic Farms) weiging 21-32 g were used. A Wahlquist stimulator Model H with 0.2-sec stimulation via corneal electrodes was used in the procedure. Diazepam was dissolved in 1% hydroxyethylcellulose/0.25% Tween- 80/0.05% with Dow antifoam in water. KRM-II-81 (2) and HZ-166(1) were suspended in carboxymethylcellulose. The dose volumes for rats and mice were different. In the case of diazepam, rats were given 1 mL/kg and mice were given 10 ml/kg. In the cases of both KRM-II-81(2) and HZ-166(1) mice were administered with 10 mL/kg. For rats, the dose volumes of HZ-166 (1) and KRM-II-81(2) were 5 mL/kg and 1 mL/kg, respectively, below doses of 30 mg/kg; 3 mL/kg for doses of 30 mg/kg and 6 mL/kg for doses of 60 mg/kg. Mice were given diazepam (1, 3 or 6 mg/kg), **1** (3, 10 or 30 mg/kg) **2** (3, 10 or 30 mg/kg) or **14**(3, 10 or 30 mg/kg) i.p. 30 min before testing, and were observed for 10 sec after the electrical stimulus (10 uA). The convulsions were recorded (0 = no convulsion, 1 = clonus, 2 = tonic flexion, 3 = tonic extension). The animals were immediately euthanized following the test. The tonic extension at hindlimb was considered to be the primary endpoint. Fisher's probability test was used to analyze the proportion of mice showing convulsions.

Inverted Screen Test (ETSP)

This assay was performed with male Sprague Dawley rats weighing 90-110 g(Harlan Sprague Dawley, Indianapolis, IN). The deveice consisted of four 13 x 16 cm squares with round holes, perforated stainless steel mesh (18 holes/square inch, 3/16 inch diameter, ¼ inch staggered centers, 50% open area) mounted 15 cm apart on a metal rod and 35 cm above the table top. Test compounds diazepam (3 or 10 mg/kg), **2** (30 mg/kg) , **12, 1**(10 or 30 or 60 mg/kg) were administered to the rats and then were put back into the home cage. After 25 mins, inverted screen test was used for evaluation of the rats were evaluated. The evaluation was scored after 60 seconds as follows: 0 = climbed to the top of the screen, 1 = hanging on to the screen, 2 = fell off).

Pentylenetetrazole (PTZ)-Induced Seizure Threshold (ETSP)

For this procedue, male F-344 Harlan rats (Indianapolis, IN) were used. The animals were randomly administrated vehicle or test compounds. Rats were restrained inside a container with a winged infusion needle inserted into the lateral tail vein. Intravenous infusion of 10 mg/ml PTZ at 0.5 ml/min was administered until a clonic seizure occured, and the time required to the produce a seizure was recorded in seconds. The maximum time was set at 4 min at which point procedure ended. The infusion rate concentration of PTZ, time to clonic convulsion, and animal weight were recorded. The rats were euthanized at the end of the procedure.

Corneal Kindled Mouse Model (ETSP)

A group of male CF-1 mice were given a kindled electrical 3-s stimulation by corneal electrodes (3 mA, 60 Hz) two times daily for 10-14 days until they satisfied the criterion of Stage 5 seizures. If any mouse did not reach the criterion at that point, it was not included for the experiment. The test was started after 5-7 days since the last stimulation. Two groups of mice were

selected with each group consisting of 4 fully kindled mice. The groups were then administrated p.o. with different doses of KRM-II-81 (**2**) (1, 3, 8, 15, 25, 30 mg/kg). At the 2 hr mark, the Time of Peak Effect (TPE) was determined. Then the mice were returned to their home cage and allowed to rest for 3-4 days to wash out the test compoounds.

Lamotrigine (LTG)-Resistant Amygdala Kindled Rat Model (ETSP)

A group of male Sprague-Dawley rats (250-300 g) were used for this procedure. For each animal, an electrode was implanted into the left amygdala and then allowed to recover for 1 week. Then the animals were given a daily dose of 200 μAmp stimulus until they all reached at stage-4 or stage-5 seizures. The fully kindled animals were each administered i.p. with LTG (30 mg/kg) to induce resistant seizures. The they were stimulated to ensure the LTG-sensitivity of both the vehicle control group and the LTG-resistance group. Then LTG was allowed to wash out for 3 days. After 3 days, animals were administrated with different doses of KRM-II-81 (**2**) (1, 5, 10, 20, and 40 mg/kg). Then the animals were given the stimulus with the TPE determined at 1 hr. After concluding the test, the animals were sent back to their home cage and any test compounds were allowed to wash out for 3-4 days.

Model of Mesial Temporal Lobe Epilepsy (ETSP)

Kainic Acid (KA) (1 mmol in 100 mL) was administered by injection i.v. into the dorsal hippocampus of adult male C57BL/6J mice for 4 weeks to induce non-convulsive severe epilepsy. An electrode was implanted into the left hippocampus in male mice. After the 4 weeks, a group of 4 MTLE mice were administered with 15 mg/kg of KRM-II-81 by injection i.v. and digital EEG data was recorded for 20 minutes before and 90 min post administration. The number of HPDs were recorded 10 min before and 10 min after the PTE (Peak Time Effect).

Chronic Post-SE (KA) Spontaneously Seizing Rats: Stage 1 with IP Administration (ETSP)

A mild dose of kainic acid (KA) (7.5 mg/kg) was administered i.p. to rats hourly for up to 4 hours until the animal achieved Stage 5 seizures this to induce chronic epilepsy with status epilepticus. Milder doses can also be used if lower-stage convulsions are retained. Rats were administered with 3 mL of Ringers solution to prevent dehydration. This process was continued for 10 weeks at which point a wireless telemeter was impanted subdermally into the peritoneal space between the stomach and the head. The initial seizure rate in rats was recorded by EEG suites for over a week. Only the animals with the highest scores were chosen (n = 24). At the beginning of the test period (week 1), the baseline seizure rate was determined. In week 2, 20 mg/kg of KRM-II-81 (**2**) was administrated for 5 days (Monday-Friday). The animals were randomly divided into two groups (vehicle and test). The week 3 was the washout period where the rats were only monitored for 1 week with vehicle treatment. The cross-over paradigm was utilized to account for design variations. A second group of rats were treated similarly, but vehicle was followed by the treatment of **2**. A MATLAB algorithm developed to detect events (focal seizures and generalized seizures) was utilized to accumulate a list of detected events. The results were reported by seizure burden, frequency and Racine scores.

Evaluation of Seizure Protection in Resistant Epileptic Human Brain Tissue (Dr. Jeffrey M. Witkin; Elily and Co Wikin Consulting)

The tissue was prepared following the previously reported procedue (Zwart et al., 2014). Tissue slices were perfused by normal ACSF (NACSF) solution at 1.0 mL/min at 37 ° C for 1 h. If no spontaneous activity was detected, the tissue was then bathed in excitable ACSF (EACSF) solution containing 5 mM K^+ in order to induce a strong local field potential (LFP) activity in the

tissues. Then 10 μM of picrotoxin was added, and a baseline was established by recording the activity for 1 hr. After 1 hr, 30 μM of KRM-II-81(2) was added and activity-recording for an additional 1 hr was continued. For another batch, the same procedue as above was followed, but with 50 μM of AP-4 with all 60 channels activated. Time points were binned at 4 ms. A two-way ANOVA was carried out to evaluate the effectiveness of KRM-II-81(2) was effective and the dependency of this effectiveness on different channels, as described in Witkin et al.[89]

Acetic Acid and Lactic Acid-Induced Writhing Model (Dr. Lakeisha A. Lewter and Jun-Xu Li, University at Buffalo)

One of the two compounds 0.32% lactic acid or 0.6% acetic acid in water were administered to the mice. Acid-induced writhes were counted for 25 min from 5 or 10 min post-injection time points for acetic acid and lactic acid respectively. A writhe is defined as a contraction in the abdominal region followed by a stretch of hind limbs. Difference treatment groups of mice were administered with one of the three compounds via subcutaneous (s.c.) injections: morphine (0.1−3.2 mg/kg, 10 min pretreatment), KRM-II-18B (1−10 mg/kg, 30 min pretreatment), or KRM-II-81(2) (3.2−10 mg/kg, 30 min pretreatment). Also, the flumazenil blockade experiment was conducted by administering s.c. injections of flumazenil 15 min prior to the injections of each PAM.

CFA-Induced Inflammatory Pain Model by the Von Frey Test (Dr. Lakeisha A. Lewter and Jun-Xu Li, University at Buffalo)

Adult male Sprague-Dawley rats (Harlan, Indianapolis, IN, USA) were selected for this study. The rats were housed individually and kept in on a 12/12 h light/dark cycle. The light periods were used for the behavioral studies. The animals were only barred from food and water during

the experimental sessions. This study was conducted following the guidelines of the International Association for the Study of Pain (Zimmermann, 1983A) and was approved by the Institutional Animal Care and Use Committee, University at Buffalo, the State University of New York (Buffalo, NY), following the 2011 guide: Care and Use of Laboratory Animals (Institute of Laboratory Animal Resources on Life Sciences, National Research Council, National Academy of Sciences, Washington, DC).

Following the same procedure as previously described (Li et al., 2014), Complete Freund's Adjuvant (CFA) inoculations containing approximately 0.05 mg of Mycobacterium butyricum were used to induce inflammatory pain. CFA induces inflammation and increases paw thickness. For this experiment, the subjects were put under isoflurane anesthesia (2% isoflurane mixed with 100% oxygen at a flow rate of 5 L/min) and then 0.1 mL of CFA (Difco, Detroit, MI, USA) was injected into right hind paw of the subjects. Then after 48 hrs, mechanical nociception tests were conducted.

Two days after CFA treatment, the mechanical hyperalgesia was measured by von Frey filaments (1.4 g - 26 g; North Coast Medical, Morgan Hill, CA). Groups of 6 rats were placed in elevated boxes with mesh floors (IITC Life Science Inc., Woodland Hills, CA). The lowest filament (1.4 g) was applied perpendicularly to the medial plantar aspect of the right hind paw. Then increasingly higher filaments were used until the withdrawal of the hind paw (behavioral response) was observed. Filaments were maintained for approximately 2 seconds each time and cotinued until buckling occurred. Rats were administered the next dose of the drug every 20 min. Maximum threshod was observed at 26 g upon which point experiment was concluded.

From 2 days past the treatment, mechanical hyperalgesia was measured every 4 days for 12 days. On the first three intervals (days 1-3; 5-7; 9-11) rats were administered with either of the

PAMs (KRM-II-18B, KRM-II-81(2), or midazolam) or saline two times every day at 9:00AM-10:30AM and 5:00PM-6:30PM. On the days of mechanical hyperalgesia measurement, the animals were not administered the AM dose. The dosage for each PAMs is as follows: 3.2 mg/kg of KRM-II-18B; 5.6 mg/kg of KRM-II-81(2) and midazolam. On the days of mechanical hyperalgesia testing, cumulative dose-response curves contained KRM-II-18B (1.0-5.6 mg/kg), KRM-II-81(2) (1.0-5.6 mg/kg) , and midazolam (1.78-10 mg/kg).

For the preparation of drugs, KRM-II-18B and KRM-II-81(2) were dissolved into a mixture containing, 20% DMSO, 10% emulphor, and 70% saline, whereas midazolam (Akorn, Inc.) was dissolved in 0.9% saline. Doses were calculated as the weight of the drug in mg per kg of body weight. The drugs were administered intraperitoneally. Following pre-treatment of PAMs in the antagonist study, rats received injections at 20 min intervals, while the dosage of flumazenil (or saline) was gradually increased.

Formalin Assay (Dr. Jeffrey M. Witkin, Wikin Consulting)

Rats were introduced to the test chamber (SR-Lab Startle Response System, San Diego Instruments, San Diego, CA) and allowed to acclimate. A 5% formalin solution (50 μL) in 0.9% saline was administered by injection i.p. at the plantar surface of right hind paw. The pain-response was monitored and recorded by a force-transducer for a period of 50 minutes. The behavioral responses were observed where licking, resting, sniffing or any such events were counted. The response time is defined as time the rats spend licking the injected paw. Data were in two parts: the initial 5 minutes and the following 10-50 minutes, and analyzed separately by ANOVA and post-hoc Dunnett's test with $p < 0.05$ was considered a statistically significant difference.

SNL-Induced Hyperalgesia Model of Neuropathic Pain (Dr. Jeffrey M. Witkin, Wikin Consulting)

This procedure was performed using male Sprague-Dawley rats (Harlan Industries, Indianapolis, IN), with weights ranging 225 - 300 g. 90 – 104 days prior to testing, these rats underwent the SNL surgery following the procedures reported by Witkin et al., 2019. At first, baseline was obtained for each group of rats (n = 5). The rats were then administrated i.p. with either one of the following: vehicle (1% CMC), gabapentin (50 mg/kg) or **2** (30 mg/kg). The Paw Withdrawal Threshold (PWT) was determined by subjecting the rats to mechanical sensitization using Von Frey filaments. This process was repeated every hour throughout the 4 h testing period. The animals were monitored for any signs of response (e.g. licking, withdrawal or shaking the paw, etc.). Any exhibited response while either administering or immediately after removing the filament was considered a positive response. PWT measurement was carried out once every 15 min. The animals were administered by injection increasing doses of flumazenil or saline every 20 min immediately following the pre-treatment of drugs during the mechanical hyperalgesia study. For the second study, five rats were administered p.o. either one of the following: vehicle, **2**(10, 30, or 100 mg/kg), or gabapentin (75 mg/kg) 30 minutes prior to testing.

Chemotherapy Induced Neuropathic Pain (CINP) Models (Dr. Bronwyn Kivell, Victoria University of Wellington)

Male C57BL/6J mice (Victoria University of Wellington, Australia) were used for all the procedures involving this experiment.

Acute treatment: On the day 0, two pre-treatment groups were formed of 4 and 12 mice respectively. On days 0, 2, 4 and 6, the first group was administered i.p. the vehicle (one part

1:1:18 mix of kolliphor EL, ethanol and saline) and the second group with paclitaxel (4 mg/kg) in the vehicle. Therefore, the paclitaxel group received a cumulative paclitaxel dose of 16 mg/kg.

The mice were allowed to be accustomed to the experimental room for 1 hour in presence of the experimenter and then to the experimental chambers for at least 10 min. The mechanical hyperalgesia and thermal allodynia were measured the paclitaxel injections on days 0, 2 and 4 before, whereas on days 7, 11, 13 and on Day 15 it was done before the dose-response. The enclosure used for hyperalgesia and allodynia measurements was transparent, raised, and with a grated floor (to ensure proper access to the animals' paws). A von Frey anesthesiometer (IITC Inc., Life Science Instruments, Woodland Hills, CA, USA) was used for measuring the mechanical hyperalgesia. The center of the underside of a rear hind paw of the subject animal was applied with a measured and slowly increasing force. The force was immediately removed and recorded upon observing a reaction (e.g. removal of paw). This process was repeated for each hind paw, for three times on each measurement day. For the measurement of the thermal allodynia, acetone was applied to a hind paw with a syringe, and the time-length of the exhibited reaction (e.g. raising, licking, shaking or biting of the paw) was recorded. This process was repeated for each hind paw, two times on each measurement day.

Dose-response study: After two weeks, the pre-treatment process was concluded. On day 15, the Paclitaxel group of mice were distributed into three groups (n = 4 each). Each group would receive one of the following: KRM-II-81(2), MP-III-80 (3) and the vehicle. It was made sure that the experiementer was unaware as to which group the subject animal belonged to. During the study, each animal received six injections on 30 min intervals. The dosages for KRM-II-81(2) and MP-III-80 (3) injections were increased at each injection. The cumulative doses for both of the

drugs were: 0.1, 1, 5, 10, 15, 20 mg/kg. For each of the hind paws, mechanical hyperalgesia was measured twice and thermal allodynia was measured once, roughly 30 min post each injection.

Chronic neuropathic pain: For the chronic pain treatment, first the groups were decoded after the dose-response study on day 15. The mechanical hyperalgesia data (ED_{80} dose) was used to calculate the chronic treatment dosages for both drugs (KRM-II-81(2) and MP-III-80 (3)). During the chronic experiment, both test groups as well as the control group received a 1:2:7 ratio of KRM-II-81(2), MP-III-80 (3) or the vehicle in tween 80: dimethyl sulfoxide: saline. The animals pre-treated with paclitaxel then received chronic treatments of either of the drugs or the vehicle in groups of 4. The treatments were performed as blinded experiments.

From day 18 onwards, each of the hind paws of each of the subject animals was administered with an injection of chronic treatment, as well as three mehcnical hyperalgesia and two thermal allodynia measurements. During this entire interval, the mechanical hyperalgesia and thermal allodynia measurements were performed 30 min post-treatment on the even days and immediately after treatment on the odd days. This process was contninued until day 40.

Respiratory Depression (Dr. Kevin Freeman, University of Mississippi Medical Center)

A group of eight rats were selected for this procedure and allowed to become accustomed to the recording chamber 1 h prior to the testing, following a method proposed by Bassi et al. (2015). After 1 h, the chamber was opened and the animal was administered i.p. the vehicle or either of the drugs KRM-II-81(2) (1.0, 3.2, and 10 mg/kg, 30 min before testing) or alprazolam (0.32, 1.0, and 3.2 mg/kg, 15 min before testing). Immediately afterwards, the chamber was re-sealed after filling it with air (21% of O_2 and 0.04% CO_2). The pressure fluctuations within the chamber were measured for 1 min. After 1 min, 1 mm of air was pumped into the chamber for calibration of pressure. The measure of one-way ANOVA with Dunnett's multiple comparisons

was used to determine the pulmonary ventillation, following a plethysmography method reported by Bassi et al. (2015). Respiration frequency (f) and tidal volume (VT) were determined for each baseline in each drug condition by taking 1-min sample data containing rhythmic breathing acquired by PowerLab data acquisition software. Minute Volume was determined by the method of Bassi et al. (2015). The statistical tests were completed in Prism 6 (GraphPad Software, San Diego, CA).

Pain-Depressed Intracranial Self-Stimulation (ICSS model, Dr. Megan Moerke and Dr. Steve Nuggus, Virginia Commonwealth University

Following a procedure reported by Negus et al. (2012) a group of adult male Sprague-Dawley rats from Envigo (Indianapolis, IN) weighing 310-350 g was selected, and trained under a fixed-ratio 1 schedule of electrical brain. After obtaining the baseline, the animals were administrated i.p. with either vehicle or KRM-II-81(2) (0.32-10 mg/kg) (n=8) or 0.1-10 mg/kg ketorolac (n=6) or 0.32-10 mg/kg diazepam (n=6) without the dilute lactic acid. For each frequency trial, first the reinforcement rate of stimulations was normalized and then converted into percent Maximum Control Rate (% MCR), by calculating the mean of the observed maximal rates as compared to the baseline, following the process reported by Moerke et al., 2018.

Chapter 3: Cancer

3.1. Introduction

Medulloblastoma is known as a pediatric brain cancer (modulating paper) which has a high rate of mortality. It develops at the base of skull called the posterior fossa.[118, 119] Different kinds of standard-of-care including surgical resection, and this is followed by radiotherapy and chemotherapy, which cause neurocognitive side effects.[120-122] There are four different subgroups of medulloblastoma has reported according to the genomic studuies, wingless (WNT), sonic hedgehog (SHH), group 3, and group 4.[123-125] Among them WNT and SHH shows anomalous expression of genes related with the Wnt and Shh pathways which has a constancy g with genomic alterations[126-128] but group 3 and 4 do not show any sub-group specific genomic alteration. The group 3 subtype is the most lethal and 20% survival rate with standard care treatment. Although it was reported that the Group 3 subtype is *MYC*-driven but only one subset of the group 3 tumors exhibit *MYC* expression.[129] *TP53* wild-type group 3 medulloblastoma has a very poor diagnosis.[130, 131] The medulloblastoma subtype, subgroup 3 also has a high expression of the.[118, 119, 128] *GABRA5* gene.

QH-II-066 and KRM-II-008 are α5GABAR positive allosteric modulators and showed very high potency in cell viability assay by decreasing the expression of HOXA5 which is a homeobox transcription factor that controls p53 expression.[132] To understand the role of α5-$GABA_AR$ in group 3 cell viability, 763 primary medulloblastoma patient tumors has been studied by Dr. Soma Sengupta.

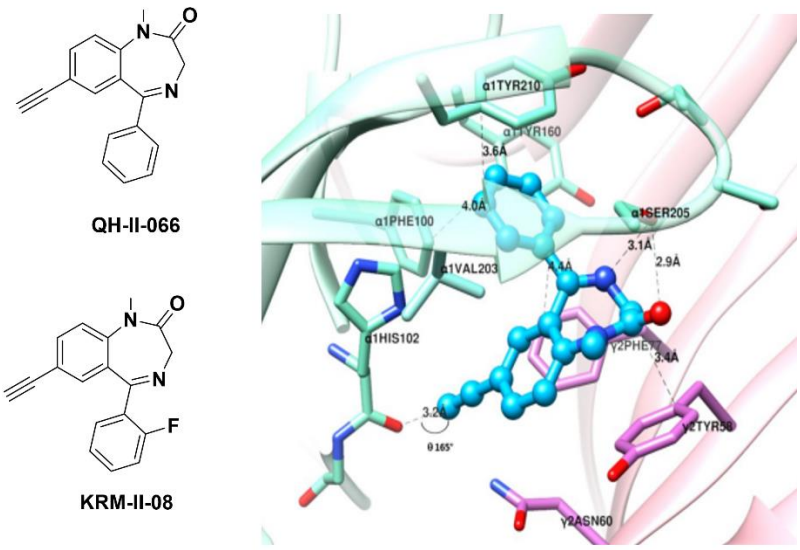

Figure 41. QH-II-066 at α^+ γ^- Interface of GABAA Receptor

The three most important interactions of (QH-II-066) was described by cryo-ER structures which help them to function as a PAM: i) bifurcated hydrogen bonding with α1Ser205 was 3.1A with the N atom in seven-member ring and 2.9A with the oxygen atom. ii) the hydrogen bonding with the backbone of α1His102 was less then the halogen bond formed by diazepam with α1His102 *via* the halogen bonding with the backbone carbonyl and the , iii) pi-pi stacking with α1Tyr210 and α1Phe100. The distance between the chlorine atom and carbonyl oxygen of α1His102 was 3.2 Å in the DZP bound cryo-ER structure (6HUP) and 3.8 Å in the case QH-II-066(6HUO). The σ-hole angle is 165 in both cyro-ER structures. The bifurcated hydrogen bond formed by QH-II-066 with α1Ser205 is shorter than that configured with bound DZP. The shorter hydrogen bond and bifurcated hydrogen bond interaction are consistent with same sedative effect of via α1β3γ2, but it is less than diazepam.(US patent, Cook et al 2006)

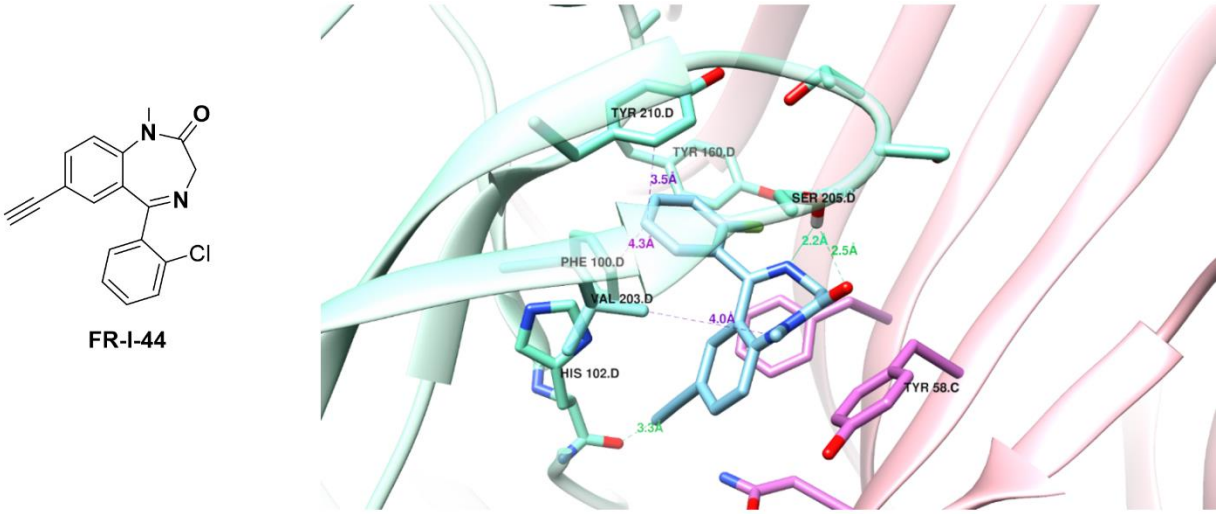

Figure 42. KRM-II-008 at $\alpha^{+}\gamma^{-}$ Interface of GABA$_A$ Receptor

The most important bifurcated hydrogen bonding with α1Ser205 was 2.2A with N atom in seven-member ring and 2.5A with the oxygen atom. ii) the hydrogen bonding with the backbone of α1His102, which is less than the halogen bond formed by diazepam with α1His102 *via* halogen bonding with the backbone carbonyl and, iii) pi-pi stacking with α1Tyr210 and α1Phe100.The bifurcated hydrogen bond formed by QH-II-066 with α1Ser205 is longer than that configured with bound KRM-II-008. As the hydrogen bond of KRM-II-008 is shorter than QH-II-066, so it exhibit more potent affinity for α1 than QH-II-066.

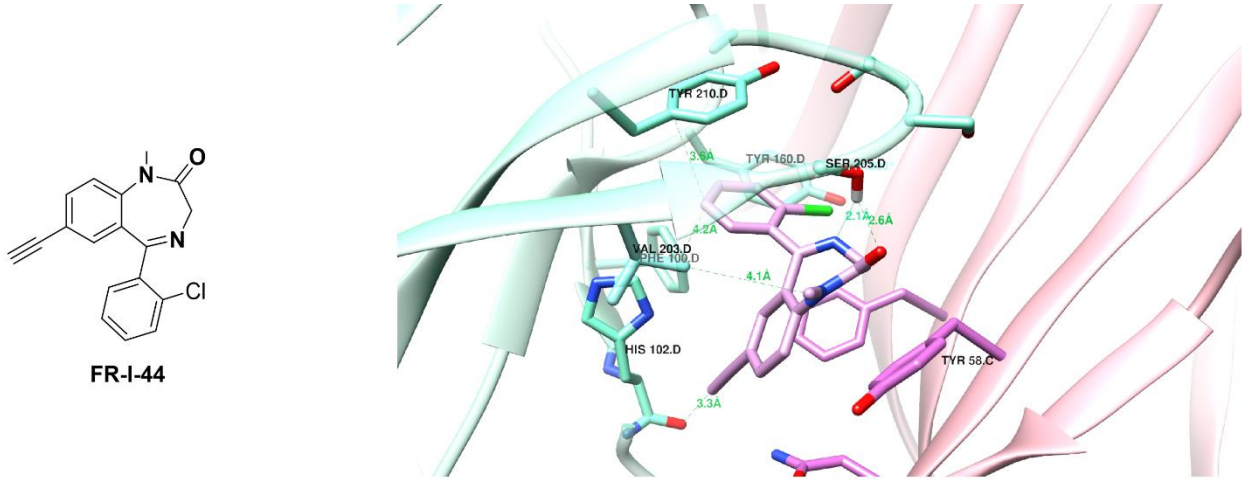

Figure 43. FR-I-44 at $\alpha^{+}\gamma^{-}$ Interface of $GABA_A$ Receptor

FR-I-44 shows same bonding affinity in the cryo-ER structure (6HUP) like KRM-II-008. Similar to KRM-II-008, it formed a hydrogen bond with the backbone of the α1His102 as it has ethylene function at its 8 position. The bifurcated hydrogen bonding with α1Ser205 was 2.1A with the N atom in seven-member ring and 2.6A with the oxygen atom this is almost similar like KRM-II-008. pi-pi stacking with α1Tyr210 and α1Phe100 also was observed here. The structural difference between QH-II-066, KRM-II-008 and FR-I-44 is the the substituent at 2' position. All these compounds showed affinity toward α1. And from the selectivity it matches the data, but this compound also has expression of α5 which is most important for this project. This modeling is an indication of some α1 mediated sedation. Since we know both QH-II-066 and KRM-II-008 are both active against group 3 medulloblastomas and diazepam is not, some α1 mediated sedation and anxiolytic effects of the active ligands is perfectly acceptable during the treatment with our ligand coupled with radiation and for this reason 2'Cl analogs of active anti-cancer ligand KRM-II-008 was synthesized and assayed.

The synthetic route of FR-I-44 and FR-I-43 is shown in the scheme 10. At first step the the benzophnenone which on SN_2 reaction with bromoacetal bromide produce acyl intermidiate followed by methanol cyclization lead to form the cyclized benzodiazepine.The copper free sonogahira reaction performed to produce TMS (trimethylsilyl) protected benzodiazepine. TBAF was used to deprotect TMS. CH_3I was used in the presence of potassium tert butaoxide to exchnage the H with methyl group and form the final product FR-I-44.

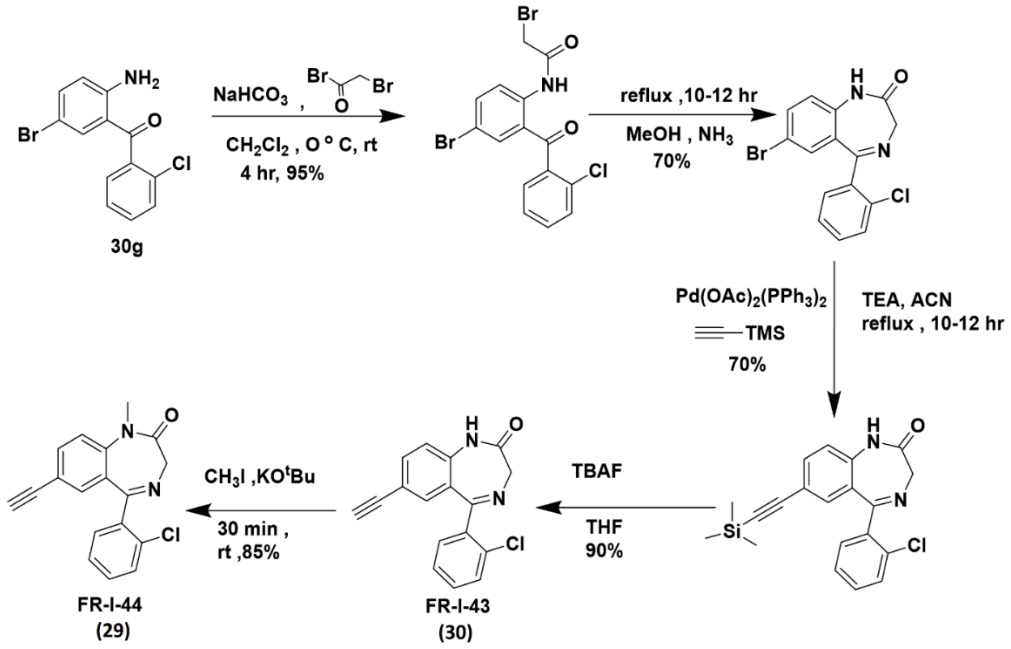

Scheme 10. The total synthesis of FR-I-44 and FR-I-43

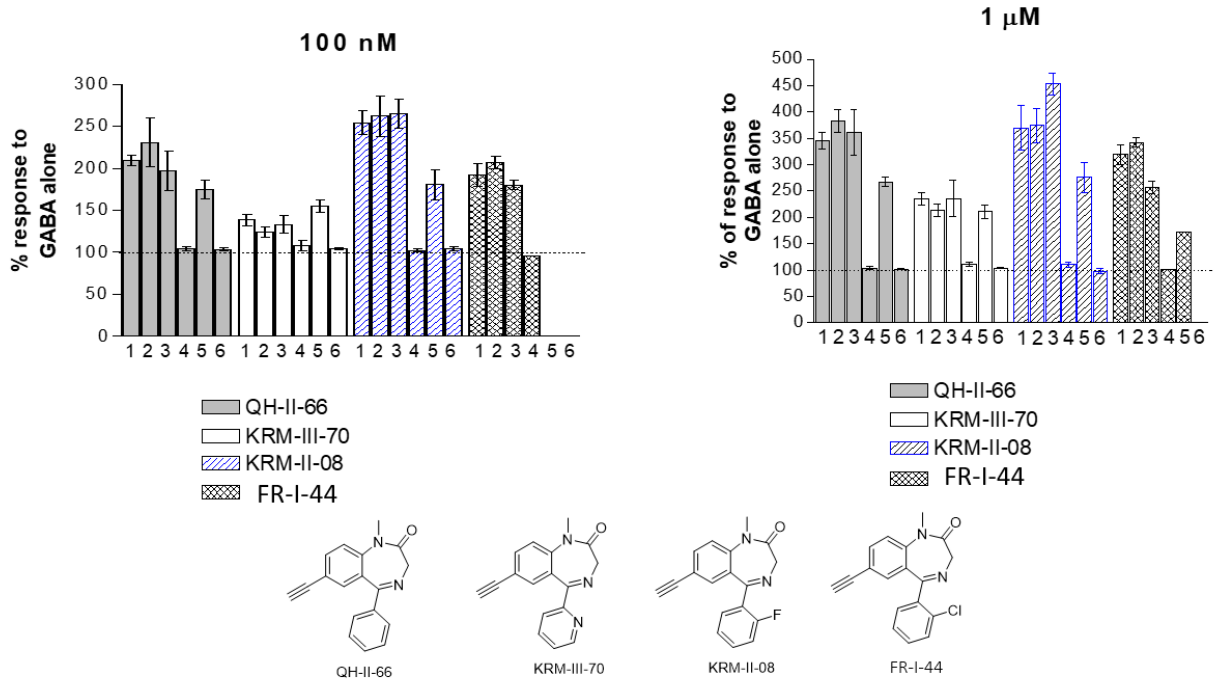

Figure 44. The efficacy of ligands expressed in HEK, α1-6,β3γ2 GABA ion channels with EC3 GABA.

3.2. Cytotoxicity Study

In both human embryonic kidney cells (HEK293T) and human liver cancer cell lines (HEPG2) the cytotoxicity assay was performed to study the toxicity of all analogs at the cellular level for the selection of safe lead compounds. The results are depicted in the following table:

	Code	HEK293 LD 50	HEPG2 LD 50
1	QH-II-66	174.6 ± 13	242.7 ± 10
2	KRM-III-70	>400	>400
3	KRM-II-08	257.5 ± 12.9	277.4 ± 15.5

4	FR-I-44(KRM-III-77)	138.5 ± 8.7	248.4 ± 32.5
5	NOR-KRM-II-08	210.1 ± 11.6	260.8 ± 13.5
6	FR-I-43	165.1 ± 22.9	130.9 ± 6.7
7	NOR-KRM-III-70	NA	NA
8	NOR-QH-II-66	NA	NA

Table 14. Cytotoxicity data of all synthesized analogs.

Ligands were incubated with HEK293T cells and HEPG2 cells, respectively, for 48 hours followed by detection of cell viability using a Cell-Titer Glo (Promega). The results were normalized using DMSO as a negative control and 3-dibutylamino-1-(4-hexyl-phenyl)-propan-1-one (150 mM in DMSO final concentration used as a positive control). Data was determined by three independent experiments carried out in quadruplet. The LD_{50} values in HEK293 and HEPG2 cell lines of each compound was presented in the last two columns, respectively. According to the LD_{50} value most of the compounds are non-toxic.

In HEPG2 cell lines the LD_{50} values for most of the compounds were greater than 200 µM (except FR-I-43) which indicate these compounds are safe and not cytotoxic. FR-I-43 also has LD_{50} value higher than 100 µM which is safe to use. In the clinical trial the concentration of the compound will be much less than 100 µM for safety. For further investigation, toxicity assays must be run for ADME with GMP material. In most cases, the LD_{50} value of the same compound is higher in the liver HEPG2 cell lines than the kidney HEK293 cell lines due to the presence of more metabolic enzymes in liver than in kidney. However, the LD_{50} value in HEK293 cells should be

studied more cautiously than the value in HEPG2 in order to avoid possible cytotoxicity that could trigger kidney problem. This will the part of the ADME toxicity study, if a drug is pushed forward to phase 1 chemical trials.

3.3. IC50 value

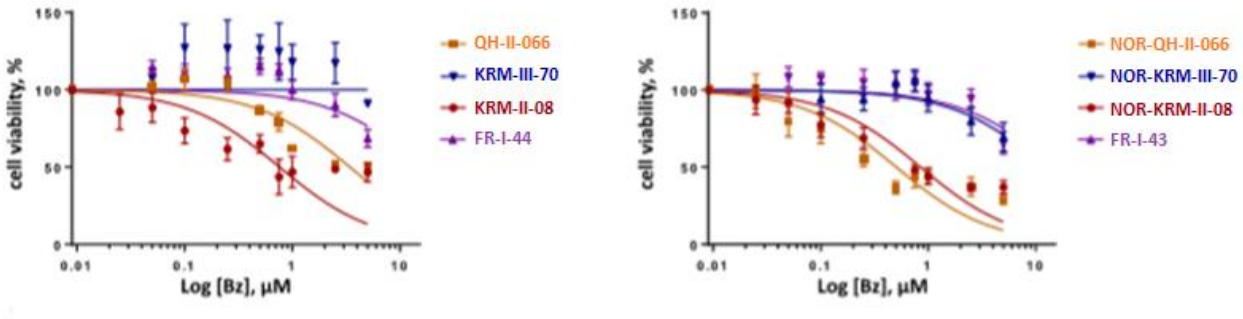

Figure 45. The potency of the ligands

Bz	IC_{50} (µM)
QH-II-066	3.4 ± 0.3
KRM-II-70	-
KRM-II-08	0.8 ± 0.1
FR-I-44	16.3 ± 3.4
NOR-QH-II-066	0.51 ± 0.06
NOR-KRM-III-70	12.16 ± 1.85
NOR-KRM-II-08	0.85 ± 0.09
FR-I-43	14.97 ± 2.54

Table 15. The IC50 value of the ligands in D283 cell line.

To verify the potency of different kinds of α5 preferring ligands were screened in D283 cell lines. All the benzodiazepines showed very good potency except KRM-II-70, it might bind to an alternative target such as the peripheral benzodiazepine channel TSPO. According to the IC50 value, QH-II-066, NOR QH-II-066, KRM-II-008 and NOR KRM-II-008 has great potency. 2'Cl compound, FR-I-43 and FR-I-44 has less potency in this particular cell line.

3.4. Gene expression of Medulloblastoma

As mentioned, to determine the expression of GABR and MYC in all subgroups of medulloblastoma, 763 resected tumor cells were analyzed. According to the online resources it was found that 1) In all subgroups of medulloblastoma there is a high expression of selective GABR genes. 2) The expression of GABAR varies by sub-group. [129] Some of the sub-groups have a high expression of GABAR expression than another sub-group 3. In group 3 and WNT tumors, the positive correlation between GABAR and MYC has been reported. In all subgroups of medulloblastoma tumor cell line has very high expression of GABRB3 but the degree of expression varies group to group. The degree of expression for GABRG2 also varies in subgroup but in group 3 and 4 the expression of GABRG2 was found the most. Again, the degree of GABR genes varies in SHHγ subtype that differentiate it from SHHα, SHHβ, SHHδ. The high expression of GABRA2 and GABRG1 were reported in all SHH subgroup[133] and in group 3 medulloblastoma, patients have a high expression of the GABRA5 gene.

To investigate the differences for both GABRA5 and MYC within group 3 and WNT subgroups, supervised heatmaps and boxplots were used. There is no statistically significant correlation between MYC and GABRA5 found in group 3 ($p = 0.202$) but in the group 3α subtype ($p = 0.006$), the positive correlation between MYC and GABRA5 were reported with loss of MYC

expression (11). In the group 3γ subtype ($p = 0.634$), there is no significant correlation between MYC and GABRA5 were found but it has a high MYC expression. In other group WNT tumor also has a high MYC expression but with poor expression of GABRA5 than in group 3.

It is very important to select the cell line which will replicate the molecular profile of group 3 patient tumors as well as those helps to investigate whether the benzodiazepine has any role in impairment of group 3 cell viability. Group 3 subtypes and other subgroups of medulloblastoma can be differentiated by the degree of expression of the GABRA5 gene. Generally, in group 3 tumors they have a high expression of MYC and low expression of N-MYC. Different kinds of patient derived lines Daoy, the D283 and D425 have been analyzed by qRT-PCR to investigate the expression of N/C-MYC and GABRA5. The SHH subgroup derived cell line is Daoy, D283 cell line was reported for group 3 medulloblastoma, TP53-wildtype (11) and also D425 is a group 3 medulloblastoma line, TP53-mutated [26]. From qRT-PCR, it was shown that Daoy, D283, and D425 these cell lines have very low and the same degree expression of N-MYC. Daoy cell lines did not have any expression for MYC where D283 and D425 had a higher expression of MYC. The high correlative expression of GABRA5, GABRB3, and GABRG2 had found in group 3 tumors. In the D283 cell line has high expression of the GABRA5 gene than any other GABRA gene. In term of the expression of GABRA5, the consistency was found between the D283 cell line and group 3 tumors. D283 cell line is generally used for group 3β or 3γ because group 3α has high expression for GABRA1 than GABRA5.

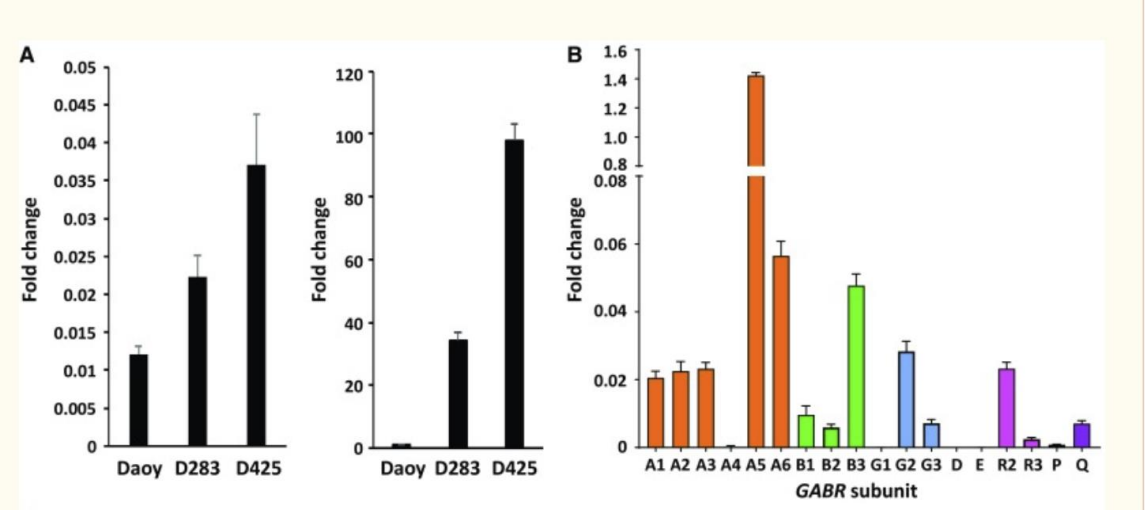

Figure 46. GABR expression MYC and in medulloblastoma and evidence for a functional α5-GABAA receptor in patient cell lines Daoy, D283, and D425 a. qRT-PCR of N-MYC (left) and MYC (right). b. in D283 qRT-PCR of GABR expression.

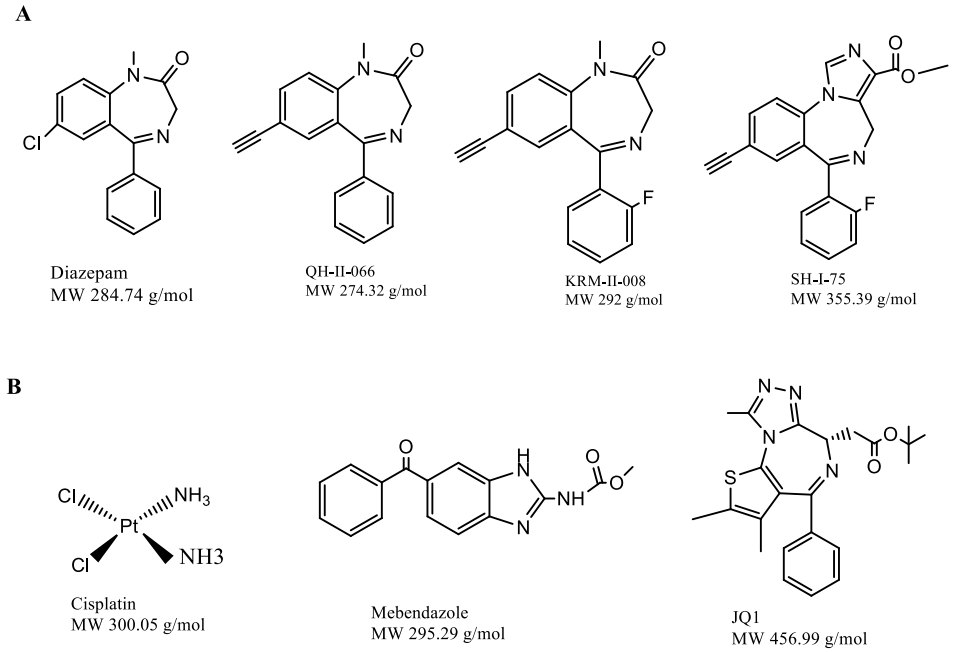

Figure 47. The structures of compounds for comparison in treatment of Medulloblastoma (A) Structurally α5 subtype selective benzodiazepine(B) The structures of the standard-of-case treatment compounds. JQ1 shares a similar structural similarity as the ligand SH-I-75

In several tumor models, the intratumor microdose efficacy of several benzodiazepines (**Figure 47**) which increase the action of GABA at 5-GABAA receptors were compared with different clinically relevant treatments, including cisplatin, mebendazole and the bromodomain

inhibitor JQ1. The medulloblastoma tumor cell lines were used to create nude mice flank xenografts (4). D425 and D283 tumor cell flank xenografts which have more expression of 5-GABAA receptor were found more delicate ($p < 001$) to benzodiazepine derivatives than DAOY flank xenografts which is a cell line which has a expression of non-5-GABAA receptor expressing medulloblastoma. This observation were determined by using microdevice technology.[134] The positive allosteric modulators of 5-GABAA receptors, KRM-II-008, was found more active at D425 tumors. Besides that, SH-I-75 and QH-II-066 also found sensitive towards the tumor via killing the tumor cell. With in 24 hour, KRM-II-008 has apoptosis rate 38% where for SH-I-75 it was 21% and for QH-II-066 was 13% in the exposed tumor cell. (**Figure 48**). In this tumor, KRM-II-008 is found more effective than all other standard-of-care treatments. In other tumor cell line D283, both KRM-II-008(AI = 32%) and QH-II-066(AI = 30%) showed high rate of apoptosis. On the other hand, on the non-5-GABAA receptor expressing tumor cell line DAOY (**Figure 48**), cisplatin,4 JQ1,[135] and mebendazole[136] exhibited a greater effect.

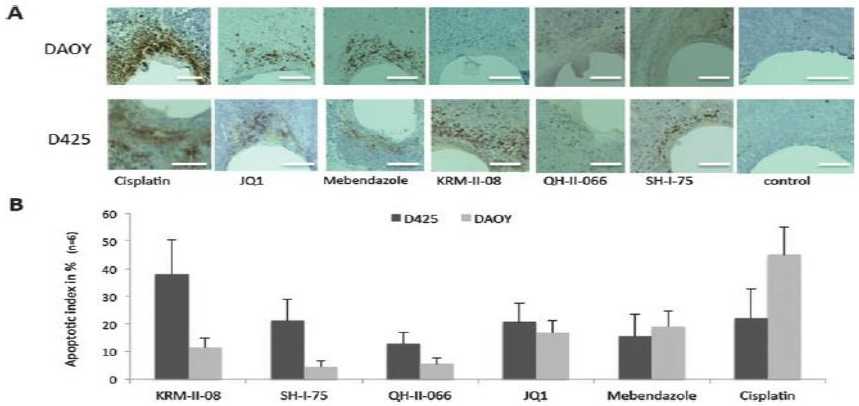

Figure 48. Representative images of D425 and DAOY tumor sections removed 24 hours after exposure to microdose of each drug from the device, showing distinct regions of apoptosis assessed by cleaved-caspase-3 expression (brown) after 24 hours. Scale bars, 250 μm. (B) Apoptotic index (%apoptotic cells/all cells in drug-affected tissue region) for human D425 and DAOY tumors exposed to KRM-II-08, SH-I-75, QH-II-066, JQ1, mebendazole and cisplatin (all 35% drug in PEG1450). Averages are taken from 6 spatially distinct reservoirs from at least 3 tumors please give ($p < 0.01$).

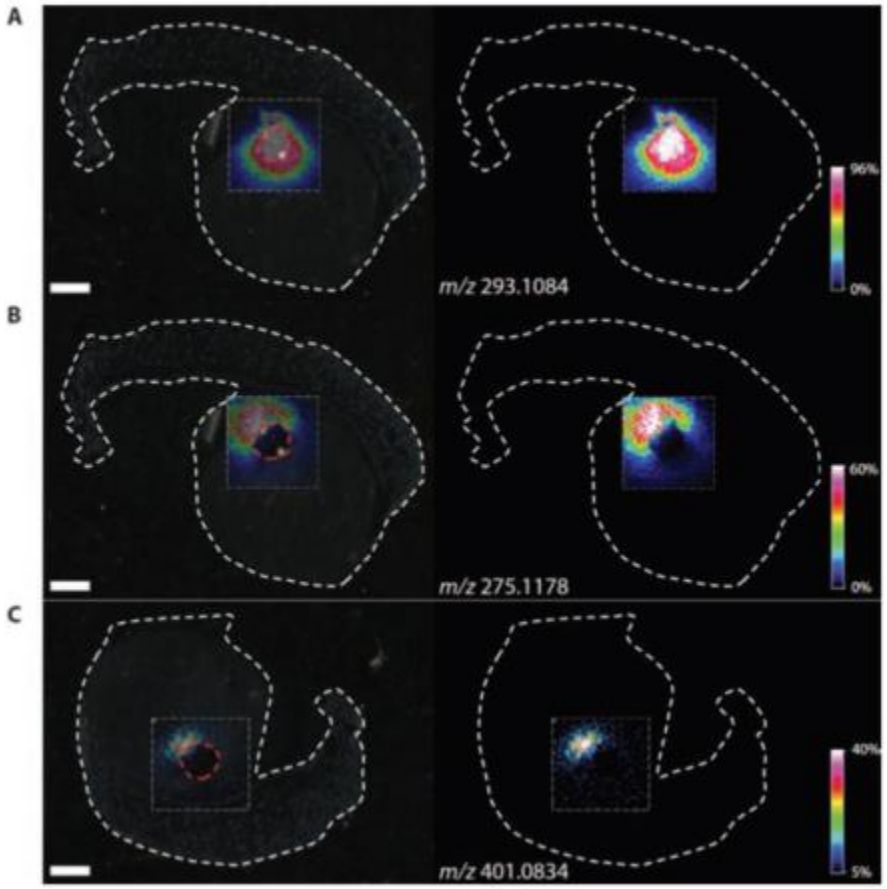

Figure 49. The molecular imaging of compound distribution in MALDI FTICR mass spectrometry. The distribution of three drugs in sections of a mouse flank tumor with an implanted device via Matrix-assisted laser desorption/ionization Fourier-transform ion cyclotron resonance (MALDI FTICR) mass spectrometric imaging (MSI): (A) KRM-II-08 (m/z 293.1084); (B) QH-II-066 (m/z 275.1178); and (C) a fragment of JQ1 (m/z 401.0834).

MALDI mass spectrometry imaging analyses1213 were used to determine the distribution of compounds released via the microdevice on cross-sectioned mouse frozen flank tissue. The distribution of KRM-II-08 (**Figure 49** (A)), QH-II-066 (**Figure 49** (B)), and JQ1 (**Figure 49** (C) were showed by using MALDI mass spectroscopy. FTICR analyzer (better than 1 ppm) was used to achieve the high mass accuracy measurement which confirmed the release of each compound from the microdevice. The ions the fragmentation parent molecule was found only in case of JQ1. An in-source fragmentation of the drug occurs due to the high laser intensity (i.e 35%). All the

compounds were distributed into the tumor tissue at maximum diffusion distances of 560 m for JQ1 and greater than 1150 m for KRM-II-08 and QH-II-066 (**Figure 49**) depending on the correlation eosin (H/E) and hematoxylin-stained serial section. In this analysis the area of drug exposure is related with the apoptosis induction.

3.5. Rotarod Test *via* Oral Gavage

In order to compare the sensorimotor coordination of the cyclized benzodiazepines (FR-I-44, FR-I-43 and KRM-II-08) were assessed on the rotarod test. To compare the sensorimotor coordination of the lead compound KRM-II-08 and 2' Cl compounds were assessed on the rotarod test. All compounds were given via oral gavage at 40 mg/kg in a vehicle of 2 % polyethylene glycol and 2.5 % hydroxypropylmethylcellulose solution. Diazepam used as the positive control (5 mg/kg), showed the greatest impairment of sensorimotor steadiness at 10 minutes, followed by 30 and 60 minutes on the rotarod. This result indicates that FR-I-43 and FR-I-44 both showed same type of motor impairment like the lead compound KRM-II-008 and with the higher dose the motor impairment increases.

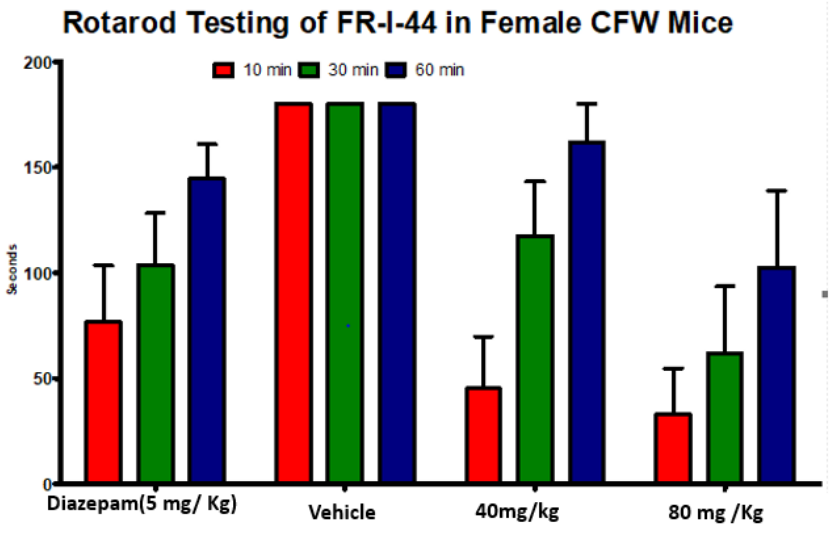

Figure 50. Rotarod data of FR-I-44

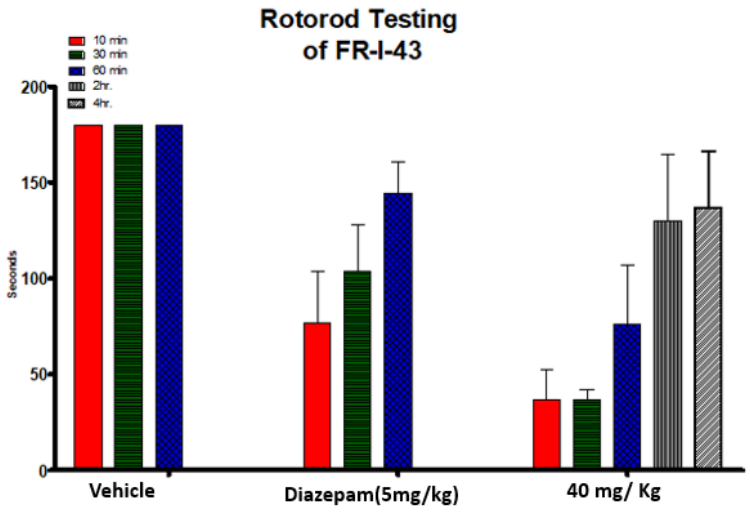

Figure 51. Rotarod data of FR-I-43

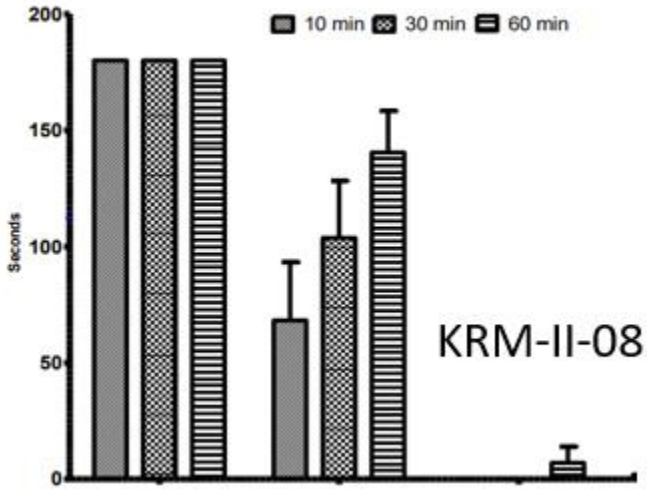

Figure 52. 3 Rotarod data of KRM-II-08

3.6. Discussion

To the efficacy of inducing tumor apoptosis *in vivo*, different kinds of new medulloblastoma drugs were tested by using medulloblastoma tumors. The α5 selective GABAA

receptors ligands were found to be very potent *in vivo* against the MYC subtype of medulloblastomas. In comparison with cisplatin, JQ1 and mebendazole, α5 selective ligand, KRM-II-008 and QH-II-066 found more effective in selective tumor cell line. Due to have less toxicity, all the benzodiazepines are safe to use in animal models and also in human for further study it can be use in clinical trials. It must be remembered that KRM-II-008, QH-II-066 and other active ligand will be combined with radiation or some other inhibitor, the so the anxiolytic and sedation properties are plus here in this cancer treatment. There is no chance of addiction as these will not be taken daily. It was reported that only Medulloblastoma tumor cell has shown only very expression for α5 selective GABAA receptors, for α1-GABAA receptor subtype it has very less expression and that is the reason why diazepam showed very less efficacy in inducing apoptosis medulloblastoma tumors cell. Further studies need to be done to check whether the receptor subtype(s) eliciting the beneficial effect against medulloblastoma growth and to clarify the exact mechanism of downstream events mediated by these compounds.[132]

3.7. Conclusion

In targeting Group 3 medulloblastomas tumor cell α5 selective GABAA receptors ligand showed very promising result among them KRM-II-08 and QH-II-066 showed better efficacy to induce the apoptosis of tumor cell than standard-of care treatment Cisplatin. The involvement of GABA pathway was found out in several other tumor types, including neuroblastoma[137, 138] and pancreatic cancer.[139] The IC50 value varies to different cell lines. Since we do not have a good Cyro er structure of the α5 subunit yet, we can not put FR-I-44 and diazepam.

3.8. Method

Implantable microdevice study targeting Group 2 medulloblastomas

In order to compare the efficacies of the conventional treatments with that of the KRM-II-08, a high-throughput localized intratumor drug delivery and efficacy testing was developed using a newly developed implantable microdevice.[140]

The subject for this study were 6-8 week-old female athymic nude mice (Charles River Laboratories). Medulloblastoma cell lines (D425, D283 and DAOY) were passaged in Dulbecco's Modified Eagle Medium/Nutrient Mixture (DMEM/F-12 with 1% of 10,000 units/mL penicillin and 10,000 µg/mL streptymycin (Pen-Strep), 1% of 200 mM L-glutamine and 10% fetal bovine serum, following the guidelines described in an earlier work.[132] The mice were injected with tumor cells subcutaneously into the flank above the hind limbs and the tumors were then allowed to grow for 4-5 weeks until they were about 6-10 mm in size. The animals were handled carefully in accordance with the guidelines approved by the Committee on Animal Care of the Massachusetts Institute of Technology.

The device implants (microdose drug delivery devices) were manufactured as described in a previous work.[134] First, cylindrical devices (0.82 mm diameter and 4 mm length) were manufactured, then 8-12 circular reservoirs (230 µm diameter and 250 µm length) were created on the outer layer of each device and finally, the reservoirs were filled with drug-polymer mixtures.

The mice were implanted with the devices directly into the tumor by a spinal biopsy needle and then pushed into the tissue using a retractable needle obturator. The devices were allowed to remain inside the tumors for 24 h. Three benzodiazepine drugs were tested: QH-II-066, KRM-II-08 and SH-I-75. The other drugs used for comparison were JQ1, Mebendazole, Cisplatin and Diazepam. Each drug reservoir contained 1 µg drug of one of the kinds.

The tumor was excised after the 24 h period and the tissue was fixed with 10% formalin and perfused with paraffin. The tissue samples were collected from each reservoir in such way. Standard immunohistochemistry was used to score the sections following a blinded process. Flash frozen samples were placed at -20 ^{o}C for 1 h and then sectioned (12 μm thickness) for mass spectrometry.

3.9. Results

The intratumor microdose efficacy of the benzodiazepines were compared. The α5-$GABA_A$ receptors expressing the D425 and D283 have been found considerably more sensitive to benzodiazepine derivatives. D425 tumors were the most sensitive to KRM-II-08, as well as highly sensitive to SH-I-75 and QH-II-066. Exposure to KRM-II-08 was found to cause apoptosis in roughly 38% of the cells within 1 day of time, whereas the same measure was 21% and 13% for SH-I-75 and QH-II-066 respectively.

3.10. Experimental

5-(2-chlorophenyl)-7-((trimethylsilyl)ethynyl)-1H-benzo[e][1,4]diazepin-2(3H)-one.(4): (28)

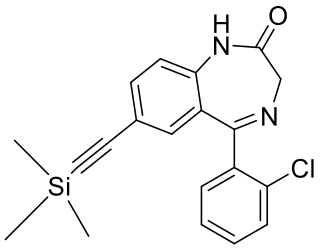

The amide (7 g, 20 mmol) from previous step was dissolved in triethylamine (250 mL) and acetonitrile (250 mL). The mixture was degassed under vacuum and argon. Trimethylsilylacetylene (2.16 g, 22 mmol) and bis(triphenylphosphine)-palladium (II) acetate

(.75g, 1 mmol) were added to the reaction mixture. A reflux column was attached and the mixture was degassed under vacuum and argon repeatedly for four times. The solution was then heated to reflux under argon and stirred overnight until the starting material was fully consumed, as indicated by analysis by TLC (silica gel). The reaction mixture was cooled to rt, filtered through celite and the celite washed with EtOAc. The filtrate was concentrated under reduced pressure. The black residue which resulted was purified by a wash column (silica gel, EtOAc/hexanes 2:1 with 1% each E_3N and CH_3OH) to afford **4** as an off-white. ^1H NMR (300 MHz, $CDCl_3$): δ 8.66(br s, 1H), 7.72-7.65(m, 2H), 7.58-7.46(m, 3H), 7.19(s, 1H), 7.07(d, J = 8.1 Hz, 1H), 4.47 (d, J = 4.8 Hz, 2H), 0.25(s, 9H); ^{13}C NMR (75 MHz, $CDCl_3$): δ 170.8, 169.8, 138.6, 137.5, 135.2, 133.3, 133.01, 131.0, 130.9, 130.6, 130.2, 127.9, 127.0, 120.9, 119.0, 105, 95.3, 56.5, -0.16; **HRMS** (ESI/IT-TOF) m/z: $[M + H]^+$ Calcd for

7-ethynyl-5-(2-Chlorophenyl)-1H-benzo[e][1,4]diazepin-2(3H)-one (5) or FR—01-43) (30)

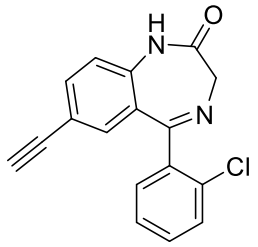

Intermediate (6 g, 16 mmol) was dissolved in THF (300ml) and cooled to 0^0C. After that tetrabutylammonium fluoride hydrate (1 M solution in THF, 51.4 mmol) was added to the solution. The reaction mixture was stirred at 0^oC to room temperature until the starting material was consumed as indicated by TLC (silica gel), in about 0.5h. The reaction was a quenched by adding water (500 mL), followed by extraction with EtOAc (5 x 500 mL). The combined organic extracts were washed with brine (2 x 500 mL), dried (Na_2SO_4), and the solvent was removed under reduced

pressure. The residue which resulted was purified by a wash column (silica gel, EtOAc/hexanes 4:1 and to afford pure as a white powder 5.5g (90% yield) ^{1}H NMR (500 MHz, CDCl3) δ 8.58 (s, 1H), 7.59 (dd, J = 8.4, 1.9 Hz, 1H), 7.56 – 7.53 (m, 1H), 7.43 – 7.38 (m, 4H), 7.24 (d, J = 1.8 Hz, 1H), 7.10 (d, J = 8.4 Hz, 1H), 4.41 (s, 3H), 3.05 (s, 1H). 13C NMR (126 MHz, CDCl3) δ 170.69 (s), 169.71 (s), 138.54 (s), 137.83 (s), 135.17 (s), 133.56 (s), 133.22 (s), 131.01 (s), 130.95 (s), 130.18 (s), 127.96 (s), 127.00 (s), 121.00 (s), 117.89 (s), 82.06 (s), 78.00 (s), 56.52 (s). **HRMS** (ESI/IT-TOF) m/z: $[M + H]^+$ Calcd for C17H11ClN2O is 295.0050 and found 295.1004.

7-ethynyl-5-(2-chlorophenyl)-1-methyl-1H-benzo[e][1,4]diazepin-2(3H)-one (6) or KRM-II-77: (29)

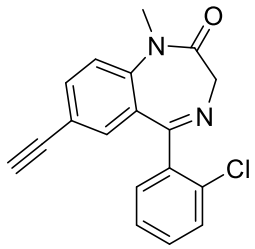

Potassium tert-butoxide (2.1 gram, 18 mmol) was dissolved in Dry THF. After 10-15 minutes (5) or FR-01-43 (5 g, 17 mmol) was added to the reaction mixture. After 5 minutes, methyl iodide (2.89g, 20 mmol) was added to the reaction mixture. The mixture was allowed to stir at rt until all starting material (5) was consumed, as indicated by TLC (silica gel). The reaction mixture was quenched by adding cold water followed by the extraction with (100 ml x 3) of ethyl acetate and after that the combined organic extract was washed with brine and dried with Na_2SO_4. The solvent was removed under reduced pressure. The residue was purified by column chromatography, (EtOAc/hexane 4:1) and the yield was 85%(4.25g) ^{1}H NMR (500 MHz, $CDCl_3$) δ 7.64 (dd, *J* = 8.5, 2.0 Hz, 1H), 7.61 – 7.59 (m, 1H), 7.45 – 7.41 (m, 2H), 7.39 (dd, *J* = 7.7, 5.1

Hz, 1H), 7.32 (d, *J* = 8.5 Hz, 1H), 7.20 (d, *J* = 1.9 Hz, 1H), 4.89 (d, *J* = 10.5 Hz, 1H), 3.85 (d, *J* = 10.5 Hz, 1H), 3.47 (s, 3H), 3.06 (s, 1H). ^{13}C NMR (126 MHz, CDCl3) δ 169.35 (s), 169.14 (s), 143.33 (s), 138.11 (s), 134.75 (s), 133.09 (s), 132.23 (s), 131.03 (s), 130.15 (s), 129.96 (s), 128.94 (s), 127.07 (s), 121.35 (s), 118.17 (s), 82.01 (s), 78.15 (s), 56.85 (s), 34.79 (s). **HRMS** (ESI/IT-TOF) m/z: $[M + H]^+$ Calcd for C18H13ClN2O is 309.0789 and found 309.0756.

Chapter 4: Chiral α5 or α2/3/5 Ligands for the Treatment of Schizophrenia and Depression

4.1. Introduction

One of the most challenging and prevalent CNS disorders known is schizophrenia. Roughly 1% of the world's population is estimated to suffer from it. The patients having this disorder can be divided into three major categories based on the symptoms exhibited: 1) positive symptoms (hallucinations, delusions, etc.), 2) negative symptoms (blunted affect, social dysfunction, lack of motivation, etc.) and 3) cognitive abnormalities (disruption of cognition, memory impairments, attention deficits, etc.).[141] Common treatments to manage the positive symptoms are a different range of antipsychotic drugs that prevent the over-activation of dopamine receptors.[142] The common drugs are frequently ineffective or insufficiently effective in managing symptoms is many patients with schizophrenia, especially those with negative symptoms and cognitive abnormalities.[143] Additionally, conventional antipsychotic drugs have severe side effects such as liver toxicity, addiction, sedation, weight gain, tolerance etc.[144] Therefore, it is desirable to develop a new and novel drug that can address all aspects of schizophrenia with little or no side effects. There has been published evidence that suggests that the disruption of a specific inhibitory neurotransmitter γ-aminobutyric acid (GABA) is very important in the pathophysiology of schizophrenia and depression.[145, 146]

In most physiological processes, one of the main features of importance is asymmetry. Most of the commonly used drugs are actually chiral molecules with two enantiomers- one provides the beneficial effect whereas the other often causes severe undesirable effects.[147, 148] From earlier developments of BZD/$GABA_A$ pharmacophore models,[19] a series of chiral molecules have

been synthesized and analyzed. Depicted in **Figure 53** is the structure of the main stereospecific $GABA_AR$ α5-selective positive allosteric modulator (PAM), SH-053-2`F-*R*-CH_3. The α5 subtype selectivity can be attributed to the (R)-methyl group at the C-4 position of imidazodiazepine . This feature facilitates potency at α5 subtypes, whereas the S-Ch_3 isomer has enhanced potency at α2, α3 and α5 subtypes. This α5-selective ligand can efficiently reduce the hyperactivity of dopamine in the methylazoxymethanol acetate schizophrenia model of Tony Grace.[149, 150] The ligand **1** was also found to axhibit anxiolytic and antidepressant effects in mice exposed to chronic mild stress. This effect was found to be sex-dependent wherein female mice showed significantly more response to the drug than male ones.[151] Moreover, several analogs have also been investigated and included in behavioral studies with improved potency (methyl amide MP-III-022, carboxylic acid SH-053-2`F-*R*-CH_3-acid, and others based on the antidepressant activity of ester **1**).[58, 63, 152, 153]

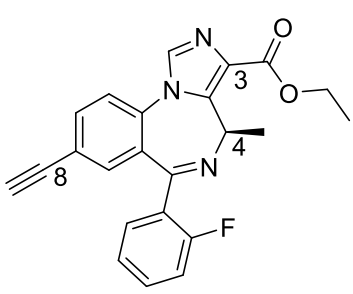

(SH-053-2'F-*R*-CH_3)
(31)

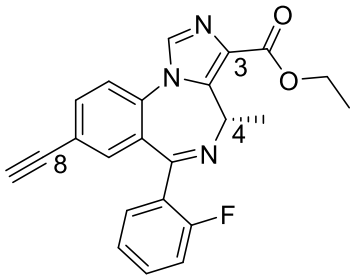

(SH-053-2'F-*S*-CH_3)
(32)

Figure 53. Structures of enantiotopic chiral lead imidazodiazepine ligands

It is essential to further study the effect of chirality at the C-4 position of imidazodiazepine in regard to the pharmacological response. Therefore, the enantiomer SH-053-2`F-*S*-CH_3 was synthesized and studied.[82] The S-enantiomer was found to be α2-, α3-, α5-β3γ2 subtype selective as mentioned above, while the R-enantiomer was an α5-subtype selective ligand. Since both enantiomers target the α5-subtype, it was essential to study them further in behavioral models assays. Upon performing a series of studies, the S-enantiomer was found to have anxiolytic effects

in animal models, whereas the R-enantiomer had minimal effect at considerably higher doses in rhesus monkeys.[83, 154] The S-enantiomer also exhibited promising results in relieving hyperactivity in animal models of schizophrenia in a completely different study.[155]

Although, both enantiomers showed potential in the treatment of schizophrenia-like symptoms, the S-enantiomer was found to metabolize at a very high rate in human liver microsomes, but R-enantiomer was stable in the same study.[156] Illustrated in the table is the result of this study.

Ligand	Liver microsomal stability (%-remaining) *Conditions*: 4 μM compound, 37 °C, 30 minutes			
	HLM[a]	DLM[b]	MLM[c]	RLM[d]
SH-053-2'F-*R*-CH_3	100.0	90.3	59.1	5.4
SH-053-2'F-*S*-CH_3	2.3	90.7	66.5	6.0

Error! Not a valid bookmark self-reference.**: *In vitro* liver microsomal stability of SH-053-2`F-*R*-$CH_3$ and SH-053-2`F-*S*-CH_3: The %-remaining after 30 minutes in [a]Human liver microsomes, [b]dog liver microsomes, [c]mouse liver microsomes, [d]rat liver microsomes.**

4.2. Analogs of the 2'-F S-CH_3 and R-CH_3 ligrands with a a 2'-Cl in place of the 2'-F group

According to the previously reported ligand based $GABA_AR$ pharmacophore/receptor model and SAR[19, 60] slight changes in the imidazole substituents could bring a effect on BzR/GABA(A)R subtype selectivity without destroying it. For example, the α5-subtype selective efficacy depends on the chiral methyl group at the C (4) position of the IMDZ ring. With the loss of the chiral methyl group at the C(4) position, the α5-subtype selective efficacy decreases. The

α1 subtype efficacy will increase with a halogen substituent at the C(8) position. The α5 selectivity of a IMDZ ring depends on different lipophilic groups at the C(8) position. To achieve the improved and extended physiological effects, the C (3) position has been optimized and this also increased the affinity and potency at α5-[157] or α2/3-[86, 158, 159] subtypes. Different kinds of 2'F S-CH_3 ligands had been synthesized (guanguan paper) with bioisosteres at the C(3) position which showed very good metabolic profiles for ongoing studies primarily for schizophrenia and depression. A novel analogs with a 2'Cl S-CH_3 analog in the place of 2'-F CH_3 group have been synthesized and characterized in order to evaluate this modification of the IMDZ ring.

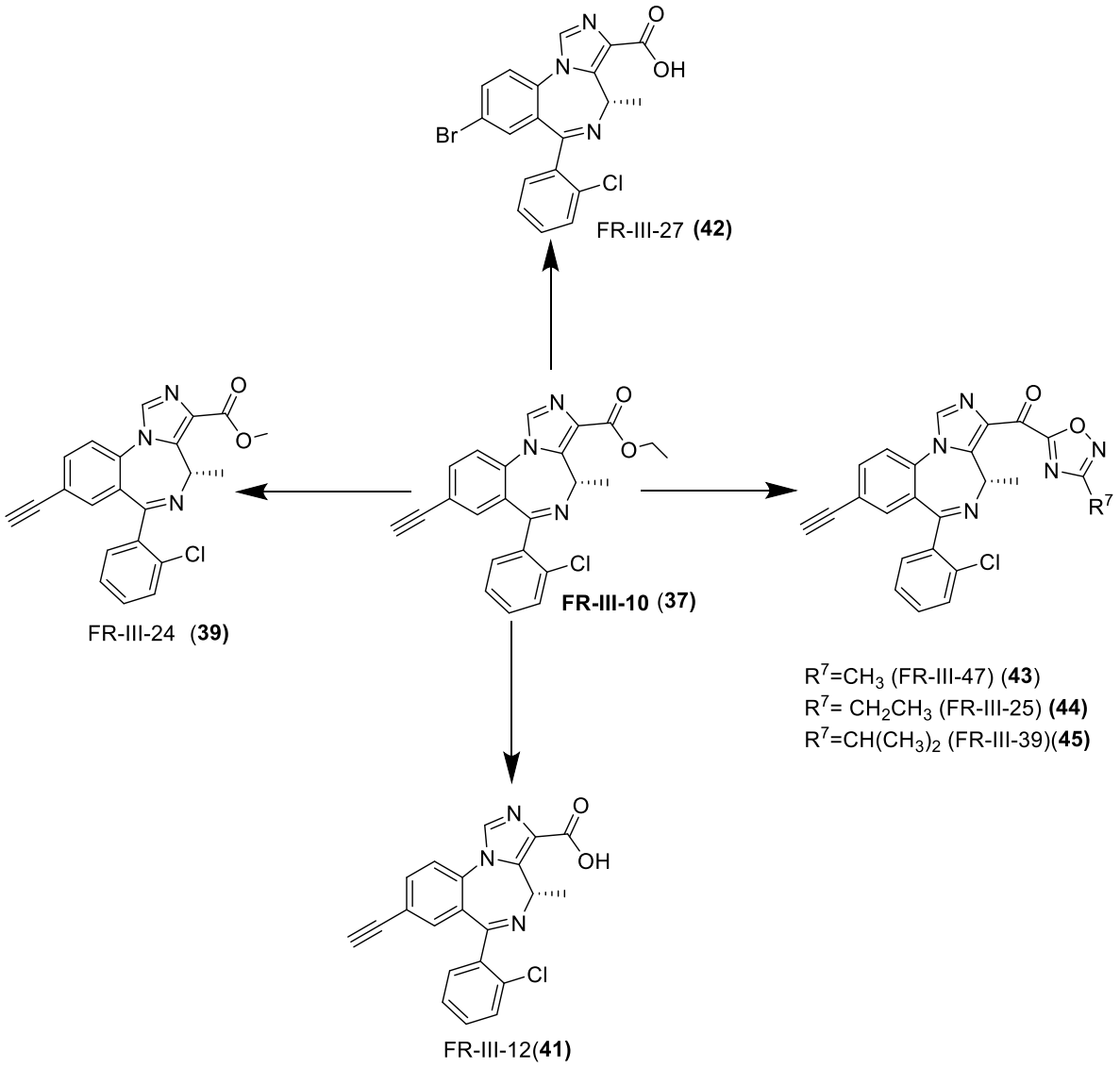

Figure 54. 2'-Cl S-CH_3 analogs prepared in this work to compare with the 2'-F compounds studied by G.Li.

4.3. Chemistry and Result

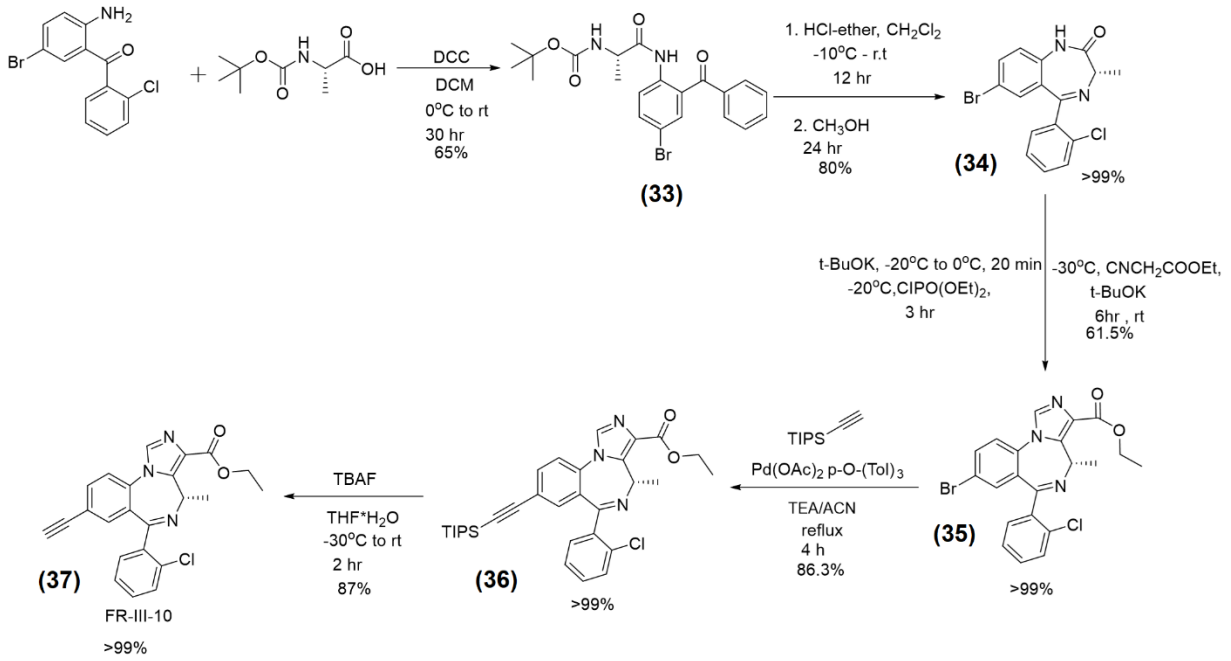

Scheme 11. Total synthesis of FR-III-10

In the first step, to make the amide (**33**), L-Boc-alanine was coupled with (2-amino-5-bromophenyl)(2-chlorophenyl)benzophenone with N,N'-dicyclohexylcarbodiimde (DCC) used as the coupling agent. The yield was 65% on a 100 g scale. In this coupling reaction, dissolving the DCC into dry DCM to form a homogenous mixture is compulsory before adding it to the mixture of L-Boc-alanine and starting material. The DCC was added to the prior mixture dropwise at 0^{o} C. To avoid the formation of the dimer of the DCC urea, DCC was added dropwise into the solution mixture. The yield of the reaction depended on the quality of DCC. To achieve a good yield, DCC must be stored properly. The next step was to deprotect the Boc group, which carried out by dissolving the amide in dry DCM and adding 4M HCl in ether dropwise at 0^{o} C. This is allowed to stir for 12h at room temperature. In the previous reactions HCl gas was used but for safety and also to quantify the amount of HCl, 4M HCl in ether was used. When the staring material was

consumed, the reaction was quenched and washed with aqueous $NaHCO_3$ solution. To cyclization to the 7 membered ring, the neutral path was employed. No base was used in this step to maintain the pH at 8.5. Instead of using a strong base, the previous route had been worked up with NaHCO3. But no base was used to prevent racemization of the 4-chiral S-CH_3group. For cyclization, only dry MeOH was used at room temparature. The yield was 80% and optical purity was checked in HPLC. The (**34**) was 99% optically pure.

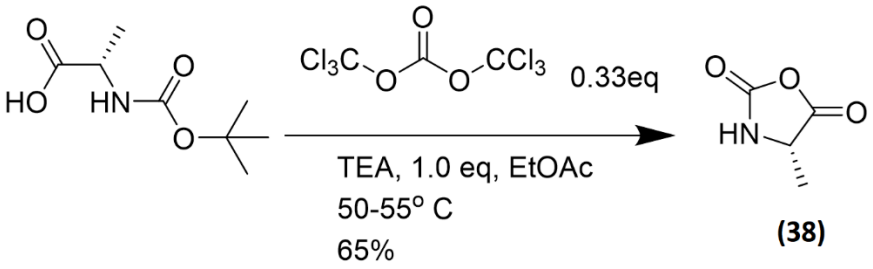

Scheme 12. Synthesis of NCA

To increase the yield and optical purity, A new route to synthesize the benzodiazepine core was explored. This new route was developed by Fier and Whitakker[160] at Merck and Co. They had used N-carboxyanhydrides (NCAs) by using neutral conditions and a non-polar solvent to synthesize optically pure amino acid derived benzodiazepines. Due to the unavailability of commercial L-amino acid NCAs, N-carboxy-L-alanine anhydride was synthesized. In the literature, phosgene gas[161, 162] or triphosgene[163, 164] was used with the free amino acid. For safety issues in large scale synthesis, triphosgene used. The reaction yield depends on the equivalents of the triphosgene employed. The yield of the reaction was very poor when only the free amino acid (1.0 eq) and triphosgene (0.3eq) used. To increase the yield, a new procedure was followed which was developed by Wilder and Mobashery.[165] In their work, they had used Boc-protected amino acids (1 eq) with triphosgene in the presence of triethylamine (1 eq). The yield was reported to be

55-60% on small scale. This procedure exhibited consistent yields (65%) on big scale. 100 g (2 times) (65% yield) of L-alanine-NCA crystalline solid were synthesized via this following procedure.

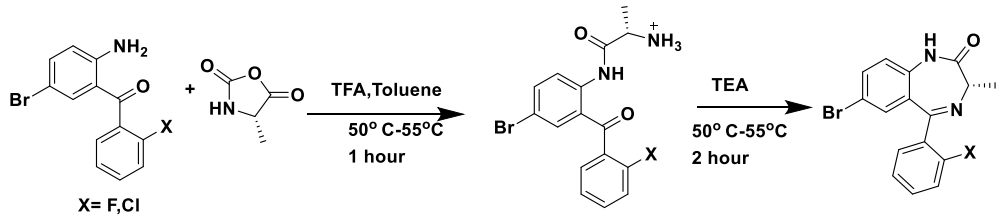

Scheme 13. Synthesis of the Benzodiazepine core using NCA

The next step was to synthesize the benzodiazepine. The L-alanine-NCA was reacted with the aminobenzophenone in toluene in the presence of trifluoroacetic acid (2 eq) which produced the β-amino amide intermediate as the trifluoroacetate salt. For the condensation of the primary amine with the benzophenone carbonyl group, two equivalence of triethylamine were added which produced the 99.5% optically pure benzodiazepine in 70% yield.

Among these two routes, the first one using L-Boc alanine is time consuming, but the overall yield and optically purity is almost identical to the second route. However, using trisphosgene in a large scale synthesis requires extra precautions and very dry solvent is needed for this NCA route. Consequently, the Boc amino acid route with DCC was employedin future routes which was much cheaper and safer.

In the next step the imidazole ring were installed to produce the imidazodiazepine(35). The S-CH_3 substituted benzodiazepine (34) was dissolved in THF and cooled to -20^o. After reaching the desired temperature, a homogenous mixture of potassium-*t*-butaoxide (1.3eq) in THF was added to the solution dropwise. The reaction was allowed to stir for 1h at -20 to -15^{o}C degree until the

completion of deprotection of amide from benzodiazepine. The next step required adding the diethylchlorophosphate (1.4 eq) in THF dropwise over 15 minutes. The reaction mixture was allowed to stir for another two hours at -20 to -15^{o}C. By confirming the complete formation of the iminophosphate intermediate by the TLC (silica gel), then ethyl isocyanoacetate (1.3 eq) was added dropwise in THF over 20 minutes. This was followed by the addition of a homogenous mixture of potassium-*t*-butaoxide in THF solution and the reaction was allowed to stir for 12 h at room temparature. After completion the reaction, which is confirmed by the TLC (silica gel), the reaction was quenched with 5% aq $NaHCO_3$ solution and *t*-butyl methyl ether was used for purification.

This chiral imidazodiazepine bromide was then reacted with TIPS-acetylene, palladium acetate, tri(O-tolyl)phosphine in one pot under refluxing conditions for 4 hours. The yield of this reaction was 86%. In previous cases, trimethylsilyl was required but degassing was needed to protect the palladium catalyst. In this Greg Fu-type process it was easy to manage for no degassing was needed, and the catalyst was produced *in situ*. Moreover, the TMS-analog has lower Rf value than new TIPS-product. Therefore, it was easy to separate the TIPS acetylene product from the bromo starting material in column chromatography**. To deprotect the TIPS,** (**36**) was dissolved in THF and tetra-*n*-butylammonium fluoride in THF was added dropwise at 0^{o} C to produce (**37**) in r 90 % yield, respectively.

To modify the ester group at the C-3 (37) as well as the chirality at the C (4) position, FR-III-24 was synthesized. MP-III-022 is a 2'F R methyl C-3 ester is α5 selective compound, The 2'Cl S methyl ester would be a good ligand for SAR to check how the chirality can affect the selectivity and other biological activities but in the 2'Cl series Yeunus Mian made this 2'Cl R-CH_3 isomer. To synthesize this compound, the lead compound FR-III-10 was dissolved in dry

methanol and sodium methoxide were added along with the compound and the mixture was held at 60º C, reflux for 2 hour. The yield of this reaction was good (82%), as expected for transesterification.

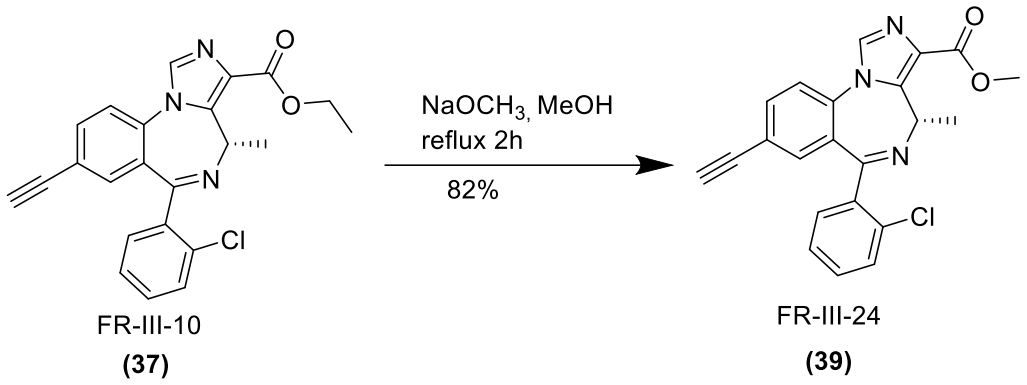

Scheme 14. Synthesis of the 2'Cl methylester (FR-III-24).

To make better clinical candidates, ester bioisosteres are widely used in drug design to replace the esters metabolic liability.[117] It had been reported that if the ester function was replaced by the substituted 1,2,4-oxadiazoles,[38, 46] the vitro and vivo stability would increased but also hydrophilicity of the ligands should improve often enhancing bioavailability.[20] Furthermore, the efficacy of this ester bioisosteres at BDZ receptor are sometimes more potent than the ester itself. To make the C(3)-substituted oxadiazole ligands, NaH was dissolved in dry THF and the corresponding amido oxime was added. This reaction mixture was allowed to stir at 0.5 hour and then the ester was added dropwise in THF. To avoid the isomerization of imine bond of the C(5)-C(6) to the C(4)-C(5) position, NaH was stirred with corresponding amido oxime before adding it to the ester. Otherwise the strong base generated could racemize the chirality at C(4) position. In addtion presence of excess NaH can reduce the yield of product by isomerization of the imine bond.

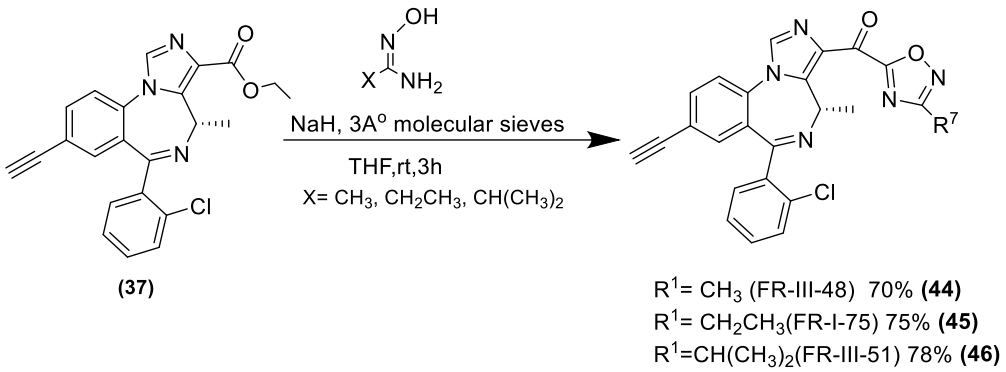

Scheme 15. Synthesis of Oxadiazoles.

Chapter 5: Asthma

5.1. Introduction

Asthma is an inflammatory disease which affects 334 million people in the world and it is prevalent in humans of all ages.[166] The number of affected people is projected to rise to 400 million in the next ten years.[167] The common symptoms of this condition may include cough, mucus formation,breathing problems, pain or discomfort in the chest etc.[166, 168, 169] There are numerous genetic, environmental and medical factors that can trigger an asthma attack.[166, 168, 169] People who have been diagnosed with the condition require proper care and efficient liftlong control of the condition, failure to which can lead to more complicated conditions like chronic obstructive pulmonary disease (COPD) which can even be fatal.[166] In the US alone, the total annual economic burden attributed to this condition is roughly 56 billion dollars.[170]

One of the biggest challenges is designing an effective approach for individual patients with asthma. All of the conventional treatments, as well as emerging potential treatments have ranges of undesired side effects. As asthmatic inflammation can be caused by many facors. Sometimes allergens interacting with macrophages, dendritic cells and mast cells can cause the activation of the CD4T lymphocytes at lymph noded which in turn can lead to eosinophilia.[167, 171-174] The development of asthmatic inflammation is a comlext problem, and it contains several pathways, inflammatory cells, proteins and mediators, and therefore, there is a vast range of therapies and treatments that are prescribed to treat different patients on a case-by-case basis.

All the existing treatments of the condition are used to merely manage the symptoms but none of them can actually cure the disease completely. This leaves the patients vulnerable to complications, and even death if they, at some point, fail to maintain their treatment regime or fail

to seek medical help promptly when needed. One of the main regimes of treatment is relieving bronchoconstriction, which is conventionally done with β_2-adrenergic agonists (bronchodilators). More recently, airway inflammations have been reported as a major cause of asthma which has led to the use of antri-inflammatory drugs such as corticosteroid-based treatments. A typical management plan for asthma might include a short-acting β_2 agonist (SABA) in the first step for initial relief, followed by a prescription of a low-dose corticosteroid accompanied by SABA in the second step. At the third step, the SABA will be replaced by a long-acting β_2-agonist (LABA). Based on the severity of the condition, as well as the medical history of the patient, there can also be steps 4 (medium dosage of corticosteroid and LABA) and 5 (high dosage of corticosteroid, LABA, and other add-ons such as biologic therapies injections, muscarinic antagonists, immunosuppressants, etc. [166, 175-180] In addition to the fact that none of the current therapies can cure asthma completely, these therapies often cause undesired problems like diabetes, cataracts, cadiovascular dysfunction, growth delay in children, CNS problems, etc. over long term use.[166, 168, 169, 175-180] Therefore, it is necessary to continue the research for synthesizing more potent drugs that can cure asthmatic inflammations and cause little or no undesired problems with bronchodialation as well.

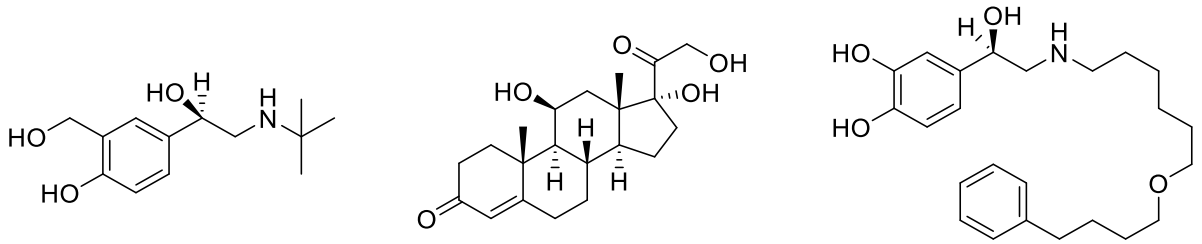

R-salbutamol (Ventolin) cortisol *R*-salmeterol (Serevent)

Figure 55. The Chemical structures of two SABAs: R-salbutamol (left), corticosteroid (center), and LABA: R-salmeterol (right).

5.2. Background

There is considerable amount of evidence in the literature that certain $GABA_AR$s are found in the brain and spinal neurons, as well as peripheral tissues and cells (e.g. liver, heart and lung). [1] The $GABA_AR$s found in the human lung have been reported to be related to the cholinergic outflow, which controls the muscle relaxant effects associated with asthmatic inflammation. [181, 182] One of the major questions that perplexed researchers for some time was where in the lung tissue were $GABA_AR$s specifically located and how they functioned. It was later reported that the subtypes α4, α5, β3and γ2 were found in the airway smooth musle (ASM) of guinea pigs and humans. It was also reported that the $GABA_AR$s enhanced muscle relaxation regulated by β-agonists via the potassium channels in the ASM of both guinea pigs and humans.[58, 59, 183, 184]

Moreover, the existing evidence strongly suggests that the $GABA_AR$s located in the airway epithelium controlled the overproduction of mucus, which is a possible complication of using $GABA_AR$ agonists- although this process was not mediated by the α4β3γ2 and α5β3γ2 subtypes. The subtypes in the airway epithelium that were found containing $GABA_AR$ were β2, β3 and π. On the other hand, α4, α5, β3, and γ2 proteins were found in the ASM. It is important to consider all factors relevant to the use of GABAergic signaling for treatment of airway inflammation caused by asthma, including the balance of ASM contractions and inflammation, the over-excretion of mucus, the immune response, etc.[183, 185] Moreover, the total receptor composition of the β3 subtypes is much lower in comparison to the others. Therefore, it is desirable to develop subtype-selective ligands for $GABA_AR$s that would ideally only interact with the subtypes expressed in the ASM. This would permit the treatment of asthma without either invoking an immune response or causing excessive mucus. The most promising candidates for this are the PAMs for $Bz/GABA_AR$ (in particular, the α4- or α5-subtype selective ones). These PAMs can not only mediate ASM

relaxation by binding with α and γ subunits, but also avoid the activation of $GABA_A$Rs containing β2/3- and π- subtypes that are associated with CNS side effects, mucus production and the immune response.

There have recently been considerable advancements in the development and testing of α4- and α5-subtype selective ligands with the goal of treating asthma. The α4 PAMS XHe-III-74 and CMD-45 were reported to possess the ability to relax tracheal rings in the ASM in guinea pigs, mice and humans even at low doses.[59, 186] Furthermore, XHe-III-74 successfully mediated acute bronchospasm in *in vivo* models.[186] These promising findings encouraged the development of several analogs of the XHe-III-74.[187, 188] Moreover, XHe-III-74EE and XHe-III-74A was reported to help with inflammation, ASM contraction, airway eosinophilia, airway hyperresponsiveness (AHR) and the production of excessive mucus.[188]

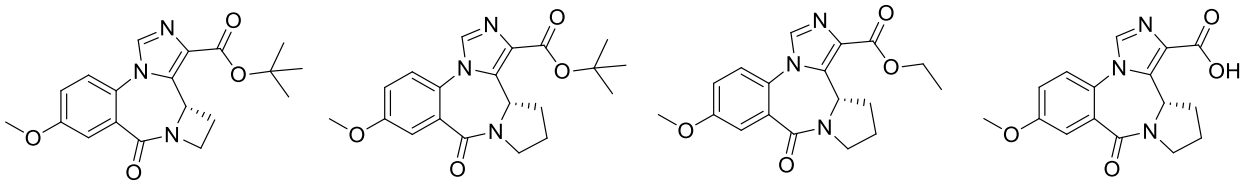

Figure 56. The structures of four α4- prefering ligands, CMD-45, XHe-III-74, XHe-III-74EE (ethyl ester) and XHe-III-74A (acid).

As mentioned before, both α4 and α5 subtypes are expressed in human ASM. Therefore, one of the interesting questions to answer was whether the α5 PAMs also have the ability to induce ASM relaxation similar to those mediated by the α4 subtypes. Thus, in a parallel line of research, the receptors in the ASM containing α5β3γ2- subtypes were also examined. The α5 subtype selective ligand SH-053-2'F-*R*-CH_3 was synthesized and found to alleviate bronchoconstrictions in human ASM and guinea pig trachial rings.[63, 83] Since this ligand was initially developed for

schizophrenia and MDD drug and was designed to cross the BBB to induce the desired CNS effects,[19, 60, 149-151] It was predictably found to cause mild sedation at higher doses.[189] However, the fact that SH-053-2'F-*R*-CH_3 was able to induce ASM relaxation provided an essential indication for the design of future ligand which will maintain the therapeutic benefits but avoid the BBB penetration and reduce the possibility of undesired CNS effects.

These important findings have led to the development of a series of ligands: Hz-166, SH-I-048A, SH-053-2'F-*R*-CH_3, SH-053-2'F-*R*-CH_3-acid, MP-III-004, MP-III-058 and their evaluation for their relaxation effects at ASM as well as electrophysiology of the $GABA_AR$ response in *Xenopus laevis* oocytes.

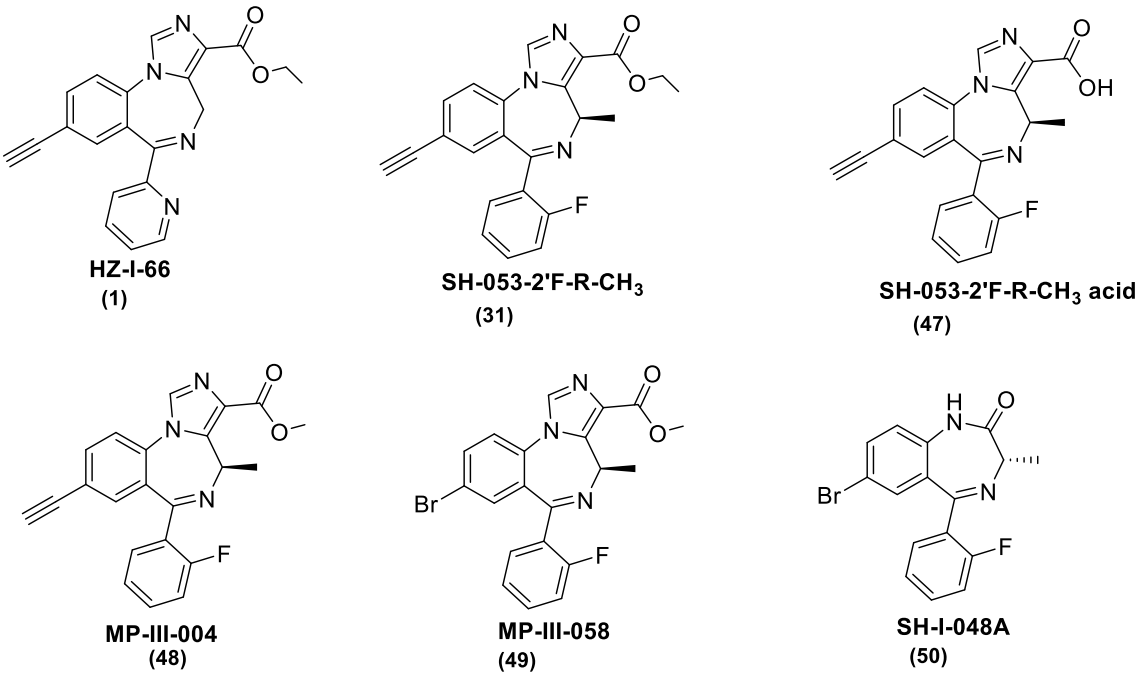

Figure 57. The structures of Hz-166, SH-I-048A, SH-053-2'F-R-CH_3, SH-053-2'F-R-CH_3-acid, MP-III-004 and MP-III-058

The α2/3 subtype selective ligand Hz-166 was merely used as a control in these studies since the efficacy at α5 subtypes is too low to cause ASM relaxation. An organ bath study was

performed, and no noticeable relaxation occurred with Hz-166 when compared to the vehicle. On the other hand, SH-I-048A is a BZD agonist with the S chirality at C4 which invoked $GABA_AR$ response at all α1-3,5 subtypes and was found to have the highest efficacy at α5 subtypes it did effect the best ASM relaxation. However, it was also found to be sedative, ataxic and able to penetrate the BBB.[190] This effect was not entirely unexpected due to the ligand's structural similarity to diazepam. Another promising candidate SH-053-2'F-*R*-CH_3-acid, which is the carboxylic acid of the ethyl ester, was found to be α5 subtype selective, but only resulted in low to moderate ASM relaxation similar to ethyl ester. Two other analogs MP-III-004 and C(8)-bromo methyl ester MP-III-058 also yielded similar results where the former was less effective than the parent compound and the latter was only marginally improved in comparison. But encouragingly enough, the C(8)-bromo methyl ester (MP-III-058) exhibited significant ASM relaxation which was very much comparable to SH-I-048A in its efficacy.

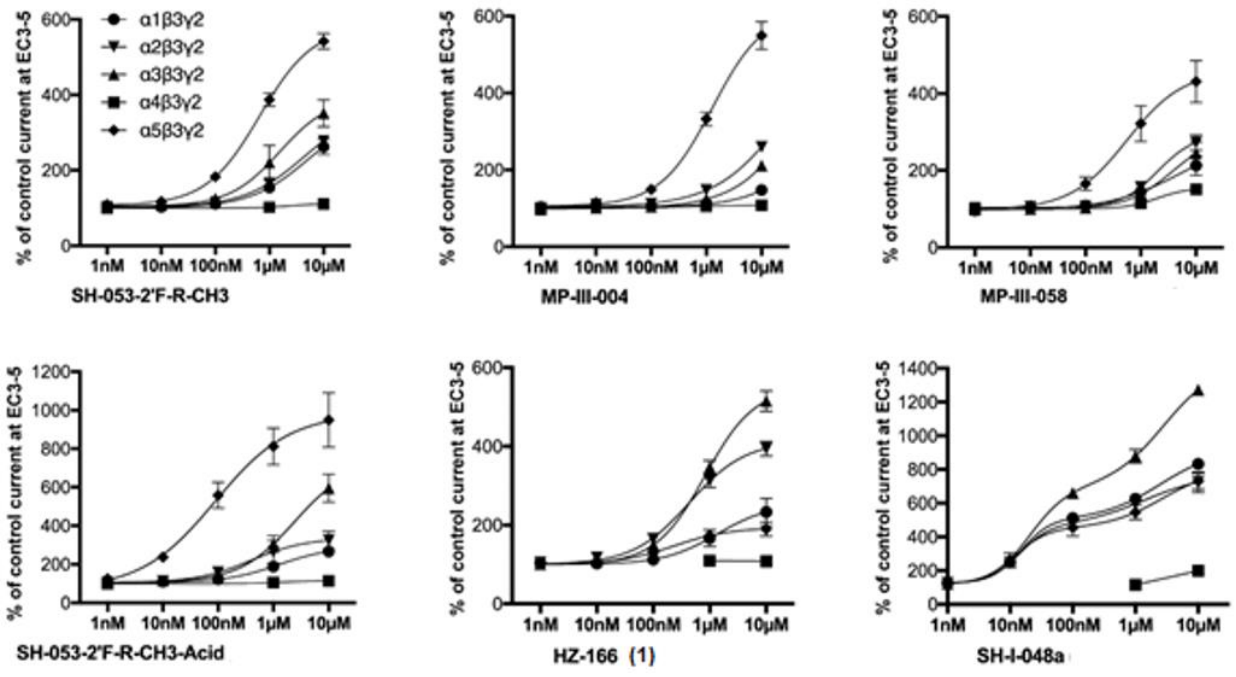

Figure 58. The oocyte efficacies of the Hz-166 (1), SH-I-048A, and the α5 subtype selective ligands.[191]

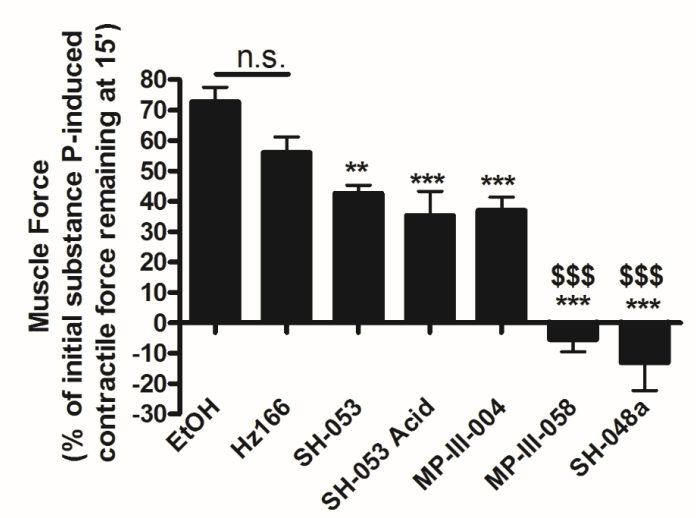

Figure 59. The alteration of airway muscle relaxation effects due to Hz-166 (1), SH-I-048A and α5-subtype selective ligands, from the precontracted guinea pig tracheal rings induced by substance P (1 μM) followed by vehicle (0.1% EtOH) or a test ligand (50 μM) in an organ bath. ** and * represent p< 0.01 and 0.001 respectively, as compared to vehicle control; $$$ p< 0.001 compared to SH-053, n = 6-17. SH-053 = SH-053-2'F-R-CH_3; SH-053 Acid = SH-053-2'F-R-CH_3-acid.[191]**

It was demonstrated by Dr. Arnold's group in a PK study that all the three esters SH-053-2'F-R-CH_3, MP-III-004 and MP-III-058 all had the ability to penetrate the BBB but the SH-053-2'F-R-CH_3-Acid showed only trace amounts present in rodent brain. However, since the esters should be metabolized to an active acid, it is believed that the ester function will be hydrolyzed in the liver or blood rapidly, and produce the acid as a metabolite. Also, the acid is unable to exhibit undesired CNS effects due to its increased hydrophilicity. It can not cross the BBB. The drug also has a good potential for oral administration.[153] To summarize, the SH-053-2'F-R-CH_3-Acid (47) is a potential drug for the treatment of asthma which has significantly reduced CNS effects and also shows the promise of being administered both as aerosol and oral medications.

5.3. Chemistry and Result

MYM-FR-II-88 was synthesized by Yeunus and myself. It is direct analog of GL-II-93. For future SAR it was a very important compound to evaluate. To synthesize of MYM-FR-II-88, the 2'Cl R-CH_3 ester was dissolved in dry ethanol and 4 eq of NaOH was added and heated to 50^o C. It is important to keep the temparature below 55^o C to prevent the recemization. The reaction was completed by 0.5 hour which was confirmed by the TLC (silica gel) and yield is 80%. The most important part of this synthesis was maintaing the pH when carboxylic acid was precipitated out from the reaction mixture. In the previous procedure, hydrochloric acid was used and it was reported by Roni, et al.[192] that there was a pH dependent equilibrium between the desired closed seven-membered ring and the open-ring acyclic benzophenone. If the pH was 3 or lower, then the seven member rings to open up. To control the P^H acetic acid was used instead of hydrochloric acid.

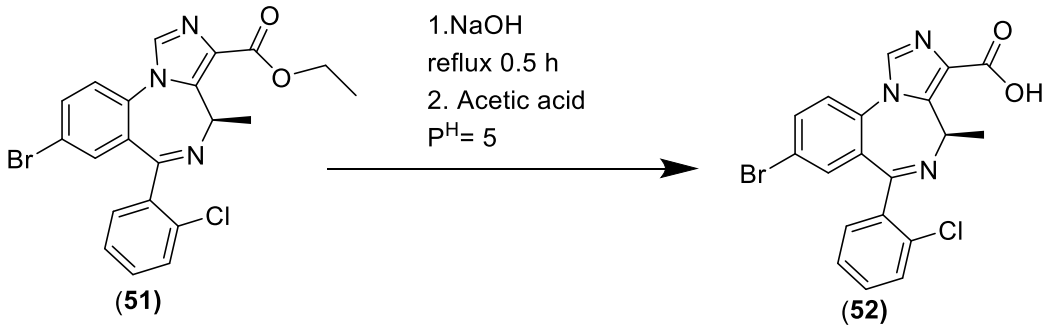

Figure 60. The structure of MYM-FR-II-88

Another important compound for the SAR was FR-III-45. It is an olefinic isomer. It is a racemic analog of FR-III-10. To synthesize this compound, the S or R CH_3 ester was dissolved in dry THF. Then potassium t-butoxide was added and heated it for 0.5h at 50^o C. The olefinic migration was confirmed by TLC and further confirmed by NMR.

The next step was to convert this C(4)-C(5) olefinic migrated ester FR-III-10 to carboxylic acid. To synthesize this compound, the general procedure for acid was followed. The ester was dissolved in dry ethanol and 4 eq NaOH was added. The acid was precipitate out by using 6 eq of acetic acid. The yield of this acid was 95%.

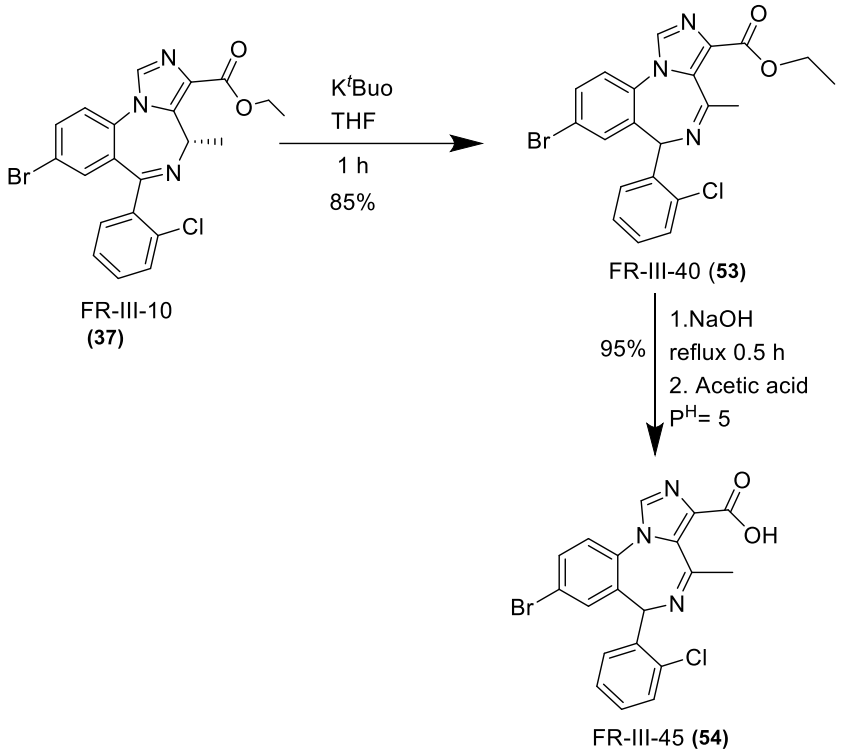

Scheme 16. The synthesis of FR-III-45

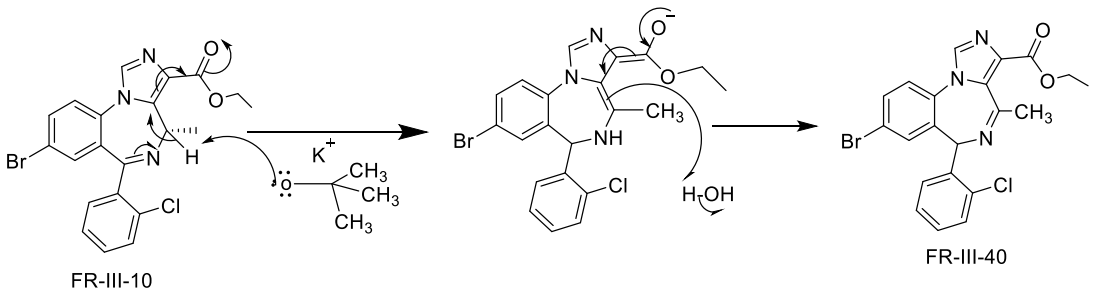

Figure 61. The proposed mechanism of the olefinic isomerization of FR-III-40.

5.4. No Motor Impairment in the Rotarod Study

FR-III-45 was asssesd in the rotarod(oral) test and there is no induction of sedative/ataxia activity at 40mg/kg nor the lossof righting reflex. This assay need to be run at 120mg/kg to ensure there is no sedation.

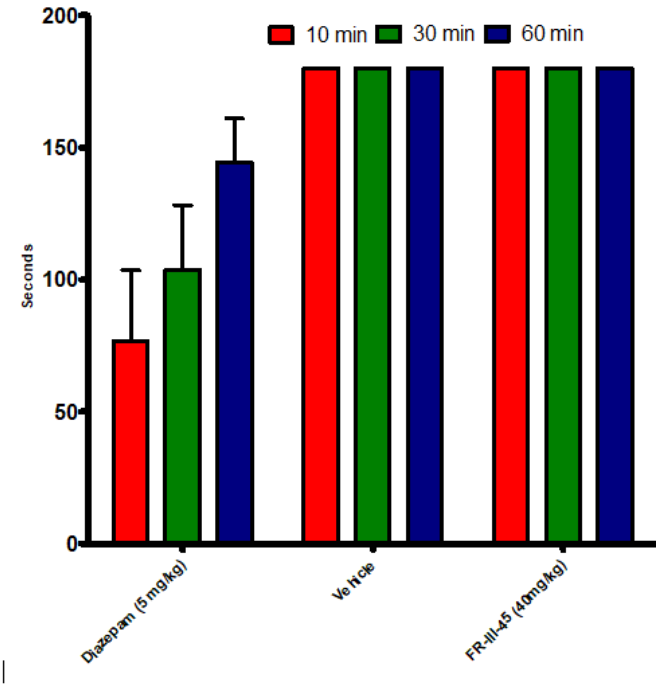

Figure 62. Rotarod data of FR-III-45 in CFW female mice.

In HEK293 cell, the LC_{50} and IC_{50} values reported 140.1 and 1.807 (µM) respectively. It is not cytotoxic at all.

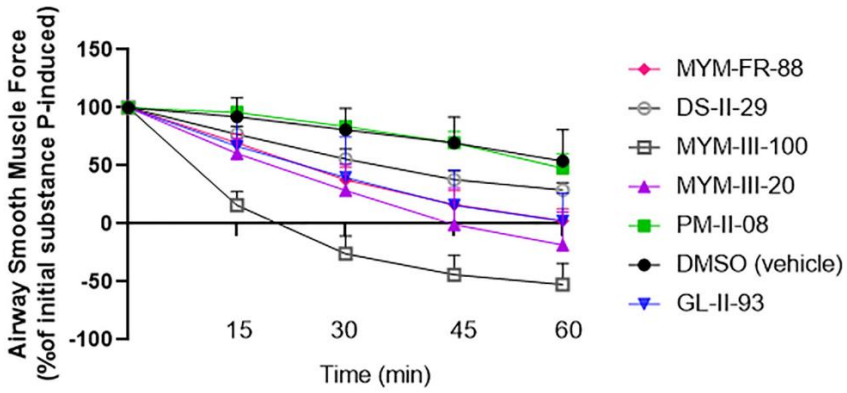

Figure 63. Relaxation of ex vivo guinea pig airway smooth muscle with Dr. Emala

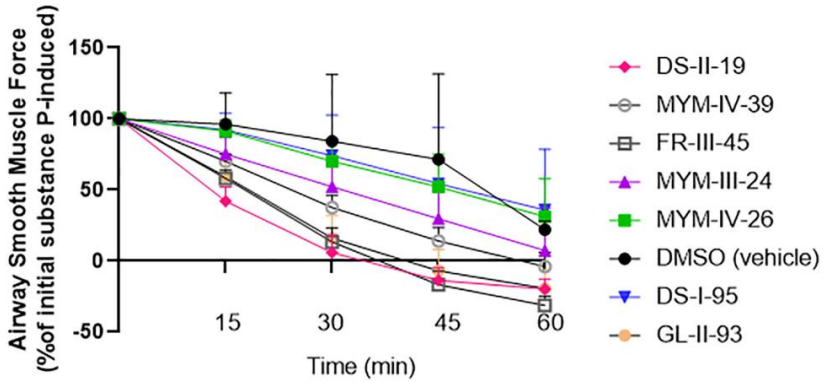

Figure 64. Relaxation of ex vivo guinea pig airway smooth muscle with Dr. Emala

GL-II-93 was very active in the organ bath assay for relaxation of pre-contracted ASM and was original lead compound. This experiment was done by Dr. Emala's group, in the medical school at Columbia University. In order to verify the data, differnet acid and ester analogs were evaluated in this asthma *ex vivo* model. Indeed MYM-FR-II-88 demonstrated in the **Figure 64**, did potently relax the condition of ASM on a pre-existing substance P-induced contraction on guinea pig tracheal rings. There are a couple of observations regarding the data above. In this series of experiments, the batch of MYM-FR-II-88 showed good potency was GL-II-93. But MYM-III-100 which was the C (8) bromo olefinic isomer of 2'F series acid showed better potency than GL-

II-93. After observing this data, FR-III-45 was made which was 2'Cl olefinic C(4)-C(5) migrated C(3) acid. It shows better potency than GL-II-93 but MYM-III-100 is slightly more active. However FR-III-45 and MYM-III-100 are equipotent within experimental error. There are a number of explanations that could explain this increase in activity, such as handling the mice differently, the experience of the person who ran the assay, etc. MYM-III-100 showed slightly more relaxation effect on ASM than FR-III-45 in the most recent experiments, as compared to the earlier published findings.

5.5. Discussion

Based on the accumulated evidence, research is ongoing on the synthesis and evaluation of different 2'Cl-S-CH_3 analogs and C(4) -C(5) olefenic isomer. To investigate the role of chirality in the structure in the drug's therapeutic properties in the treatment of asthma, the S-isomer of GL-II-093 was synthesized by modifying the chirality at the C(4) position. Several S-CH_3 chiral analogs with different functional groups (e.g. amide, oxadiazole) were also synthesized by changing substituents at the C(3) position. The carboxylic acids are non-toxic, as evidenced in the cytotoxicity data. The two most potent analogs that have been biologically evaluated to date are the 2'Cl C(8)-Br R and C(8)-Br R, olifinic migrated acid analogs in ASM Assay. These two analogs are more ppotent than **GL-II-93** since chloride substituents are very similar to fluoride substituents at 2' position. Therefore, the C(4)-C(5) olefinic C(2)-Cl analog FR-III-45 was evaluated in the organ bath assay where it showe considerable activity ASM relaxaion, and was found more potent than GL-II-93 and as potent as MYM-III-100.

5.6. Method

Binding Studies (PDSP)

The binding studies were performed according to the previously discussed methods. The HEK-293 cells (AmericanType Culture Collection ATCCs CRL-1574^{TM}) were kept in Dulbecco's modified Eagle medium (DMEM, high glucose, GlutaMAX^{TM} supplement, Gibco61965-059, ThermoFisher, Waltham, Massachusetts, USA), MEM (Non-Essential Amino Acids Gibco 11140-035, ThermoFisher, Waltham, Massachusetts, USA), 100U/ml Penicillin-Streptomycin (Gibco 15140-122, ThermoFisher, Waltham, Massachusetts, USA), and 10% fetal calf serum (Sigma-AldrichF7524, St. Louis, Missouri, USA) in 10 cm Cell culture dishes (Cell+, Sarstedt, Nürnbrecht, Germany) at 37 °C and 5% CO_2. cDNAs encoding rat $GABA_AR$ subunits, subcloned into pCI expression vectors, were used to transfect HEK-293 cells. The ratio of α(1,2,3 or 5) to β3 to γ2 plasmids used per 10 cm dish was 3 mg: 3 mg: 15 mg employed for transfection with $Ca_3(PO_4)_2$ precipitation.[193] Transfection was allowed to occur for 4-6 h and then the medium was changed. After a 72 d waiting period, cells were harvested by scraping into phosphate buffered saline. Centrifugation was performed for 10 min (12000 g, 4^o C) and then cells were resuspended in TC50 (50 mM Tris-citrate pH¼7.1), homogenized using Ultra-Turraxs (IKA, Staufen, Germany) and centrifuged again for 20 min (50000 g). Membranes were then washed thrice in TC50 and frozen at -20 ^{o}C.

Before examination, frozen membranes were thawed, suspended in TC50 and incubated for 90 min (4 ^{o}C) in a 500 mL solution. The solution was made of 150 mM NaCl, 50 mM Tris/citrate buffer, pH=7.1, and 2 nM [3H]-Flunitrazepam (Perkin Elmer New England Nuclear, Waltham, Massachusetts, USA). Additionally, the solution could also contain 5 mM diazepam

(Nycomed, Opfikon, Switzerland) or different concentrations of the test compounds (dissolved in DMSO, final DMSO concentration 0.5 %). Whatman GF/B filters were used to filter the membranes and then the GF/B filters were rinsed two times in 4 mL of ice-cold 50 mM Tris/citrate buffer. Then the filters were moved to scintillation vials, 3 mL Rotiszint Eco plus liquid scintillation cocktail was added and then scintillation counting was performed. The specific binding was calculated by determining non-specific binding by the 5 mM DZP and subtracting from the total [3H]-flunitrazepam binding. The equilibrium binding constant was determined for various receptor-subtypes by incubating membranes with various concentrations of 3H-flunitrazepam with or without 5 mM DZP. The equation used for analyzing the saturation binding was $Y = \mathrm{Bmax} * X/(\mathrm{KD} + X)$. A non-linear regression analysis was performed on the displacement curve using the equation $Y = 100/1 + 10^{(\log \mathrm{IC50} - x) * \mathrm{Hill-slope}}$ (log(inhibitor) vs. response-variable slope with Top = 100 % and Bottom = 0 %). Drug concentrations resulting into half-maximal inhibition of 3H-flunitrazepam binding (IC50) were transformed into K_i values by using the Cheng-Prusoff relationship[194] $\mathrm{Ki} = \mathrm{IC50}/(1 + (S/\mathrm{KD}))$ where S is the concentration of raioligand (2 nM).

KOR Stimulation Response Test (Dr. Petra Scholze, University of Vienna)

HitHunter Chinese hamster ovary cells (CHO-K1) (DiscoverX Corp., Fremont, CA) stablity expressing the human κ-opioid receptor (OPRK1, catalog no. 95-0088C2) were maintained in F-12 media with 800 μg/mL geneticin (Mirus Bio, Madison, WI), 10% fetal bovine serum (Life Technologies, Grand Island, NY), and 1% penicillin/streptomycin/L-glutamine (Life Technologies), then incubated (37 ^{o}C, 5% $C0_2$) in humidified incubator and allowed to grow. Using non-linear regression, forskolin-induced cAMP accumulation was analyzed and sigmoidal dose-response curves were generated for the cAMP accumulation assay. Later the data was normalized

by subtracting the vehicle data and adjusted to represent forskolin-only control values. Each ligand was tested in three parallel assays. The EC_{50} and E_{max} values were calculated by as means ± SEM and were expressed by the average of each experiment upon performing nonlinear regression analysis following the method previously reported by Riley et al.[195] and Crowley et al.[196].

Electrophysiological Recordings (Dr. Fisher, University of South Carolina School of Medicine)

Electrophysiological recordings were performed following a previously reported method.[197] The cDNAs for $GABA_AR$ subtypes (generously provided by Dr. David Weiss, the University of Texas Health Science Center, San Antonio, TX and Dr. Robert Macdonald, Vanderbilt University) were transfected into HEK-293T cell lines (GenHunter, Nashville, TN). Rat clones were used for all subtypes except α2, for which a human clone was used. Cells were transfected using $Ca_3(PO_4)_2$ precipitation. α-, β- and γ- Subtypes cDNA encoding plasmids (2 μg each) were added to the cells. The cells were then patch clamped (-50 mV). GABA was made into a bath solution either from stocks in water. The compounds to be tested were dissolved in DMSO and prepared into a bath solution. The DMSO level was not allowed to reach beyond 0.01%. Both solutions both with and without the compounds were applied to cells for 5 s. An axon 200B (Foster City, CA) patch clamp amplifier recorded the currents which were then analyzed. The concentration-response data was analyzed by fitting with the equation $\text{current} = (\text{min.current} + (\text{max.current} - \text{min.current}))/(1 + (10(\log(\text{EC50}) - \log(\text{modulator}))\text{n})$, with n being the Hill number. All data were normalized by the response to GABA alone for each cell and expressed as a percentage that response.

Pharmacokinetic Studies (Dr. Aleksandra Vidojevic and Dr. Miroslav Savic, University of Belgrade)

The subjects for this study were 15 young mice divided into 5 groups (n = 3 each) and each group was assigned a predetermined time interval (5, 20, 60, 180 or 720 min). The test compound was administered i.p. to the subject animals at a dosage of 10 mg/kg dosage (10 mL/kg). The brain concentrations were measured 20 min post each i.p. injection.

The animals were administered with ketamine solution (10% Ketamidor, Richter Pharma Ag, Wels Austria, dosed at 100 mg/kg i.p.) to anesthetize them at the predetermined time. Blood samples were collected by cardiac puncture and plasma samples collected by centrifugation (800 rcf, 10 min). Then the mice were decapitated, and the brains were weighed, homogenized in methanol (1.25 mL) and centrifuged (3400 rcf, 20 min). Using solid phase extraction by Oasis HLB cartridges (Waters Corporation, Milford, Massachusetts), compounds were extracted from both the plasma and the brain tissue. Sample was prepared and concentration measured by ultraperformance liquid chromatography-tandem mass spectrometry (UPLC–MS/MS) with Thermo Scientific Accela 600 UPLC system connected to a Thermo Scientific TSQ Quantum Access MAX triple quadrupole mass spectrometer (Thermo Fisher Scientific, San Jose, California), equipped with the electrospray ionization (ESI) source. Pharmacokinetic analysis was carried out with PK functions.

In vitro hydrolytic stability study in plasma

An *in vitro* hydrolytic stability test of the test compounds was carried out at 37 ^{o}C. The respective compound and the internal standard were both spiked with blank mouse plasma (SH-I-048A;

synthesized at the Department of Chemistry and Biochemistry, University of Wisconsin–Milwaukee, USA).

Plasma protein and brain tissue binding studies

The free fraction of GL-II-73, GL-II-74, and GL-II-75 in mouse plasma and brain tissue were determined by rapid equilibrium assay. The free concentrations of GL-II-73, GL-II-74, and GL-II-75 in the brain were obtained from rapid equilibrium dialysis (12.14%, 4.49% and 1.34%, respectively).

Griess Assay and Toxicity Assay (Amanda Nieman, UWM)

The non-activated mouse microglia (80 μL, 1x106 cells/mL) were placed in sterile 384 well plates. The remaining culture was activated with LPS (50 ng/mL) and IFNγ (150 U/mL) and distributed into the plates. 0.1 μL of 800 μM GABA was diluted in MilliQ water into a final concentration of 1 μM, and proper concentrations of relevant compounds (diluted in DMSO) were added. After an incubation period of 24 h at 37 ^{o}C, the assay plate was spun down. Then 40 μL of supernatant was transferred to another plate and analyzed by Griess assay (Promega, Madison, WI). TECAN Infinite M1000 plate reader was used to measure absorbance. The remaining 40 μL cells were analyzed for toxicity.

5.7. Experimental

Tert-butyl(S)-(1-((4-bromo-2-(2-chlorobenzoyl)phenyl)amino)-1-oxopropan-2-yl)carbamate (FR-I-90) (33)

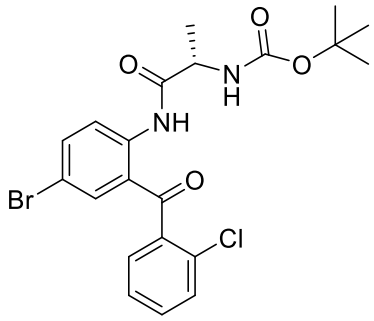

The (2-amino-5-bromophenyl)(2-Chlorophenyl)benzophenone (150 g, 482.96 mmol) and Boc-L-alanine (133.07 g, 470 mmol) were added to dry DCM (500 mL) in a 5 L round bottom flask at 0 ^{o}C and stirred continuously until completely dissolved. Afterwards, dicyclohexylcarbodiimide (DCC; 139.44 g, 676.144 mmol) was added to dry DCM (150 mL) in another container and a homogenous solution was formed. This solution was then added to the previous solution in a dropwise manner, over half an hour, all the while maintaining a constant temperature of 0 ^{o}C. The solution was stirred continuously for 22 h at rt. As a result, dicyclohexyl urea byproduct formed which was then filtered off and washed with DCM until the solid urea became completely colorless. The organic layers were combined and concentrated under reduced pressure. The crude solid was a yellow gum which was purified by a column chromatography (silica gel, DCM/hexane 1:1) to yield additional amide (225 g, 97 %): **^{1}H NMR** (300 MHz, $CDCl_3$) δ 11.68 (s, 1H), 8.71 (d, *J* = 9.0 Hz, 1H), 7.69 (dd, *J* = 9.0, 2.3 Hz, 1H), 7.64 – 7.53 (m, 2H), 7.51 – 7.42 (m, 1H), 7.35 – 7.27 (m, 1H), 7.21 (t, *J* = 9.1 Hz, 1H), 5.13 (s, 1H), 4.37 (s, 1H), 1.52 (d, *J* = 7.2 Hz, 3H), 1.45 (s, 9H); **^{13}C NMR** (75 MHz, $CDCl_3$) δ 195.47 (s), 172.42 (s), 159.56 (d, *J* = 253.2 Hz), 155.28

(s), 139.68 (s), 137.97 (s), 135.97 (d, *J* = 1.9 Hz), 133.62 (d, *J* = 8.4 Hz), 130.31 (d, *J* = 2.4 Hz), 126.77 (d, *J* = 14.5 Hz), 124.51 (s), 124.46 (s), 122.63 (s), 116.55 (d, *J* = 21.4 Hz), 114.95 (s), 80.26 (s), 51.86 (s), 28.26 (s), 18.58 (s) **HRMS** (ESI/IT-TOF) m/z: $[M + H]^+$ Calcd for C18H13ClN2O is 481.770 and found 481.750.

(*S*)-7-Bromo-5-(2-Chlorophenyl)-3-methyl-1,3-dihydro-2*H*-benzo[*e*][1,4]diazepin-2-one (FR-I-93) (34)

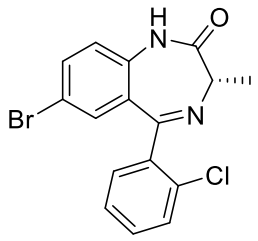

Amide (221.6 g, 467.2 mmol) was added to dry DCM (1 L) and the solution cooled to 0 ^oC. Then, anhydrous HCl (g) was slowly added over 2 h to saturate the solution. The solution was allowed to stir for 8 h at rt. After completion of the reaction, a sat aq solution of $NaHCO_3$ (2 x 500 mL) and water (2 x 300 mL) was added maintaining a pH of 8.5. The organic layers were combined and concentrated under reduced pressure which resulted into an oily mixture. The reaction mixture was dissolved in dry methanol (400 mL) and allowed to stir at rt overnight. The completion of the reaction was confirmed upon analysis by TLC (silica gel, EtOAc/hexanes, 7:3). The methanol was removed under reduced pressure. The concentrated oily mixture was dissolved in DCM and washed with water (2 x 400 mL). The organic layers were combined again and washed with brine (2 x 400 mL) and dried (Na_2SO_4). Then the organic layer was concentrated under reduced pressure which resulted in a yellow oily mixture. Then the mixture was purified on a column chromatography (silica gel, hexane/EtOAc 4:1) to yield benzodiazapine (230 g, 78 %): **$[\alpha]\ ^{26}_D$** = -

20.1 (c 0.71, EtOAc. **1H NMR** (500 MHz, CDCl3) δ 9.79 (s, 1H), 7.58 (dd, J = 8.6, 2.2 Hz, 1H), 7.55 – 7.49 (m, 1H), 7.42 – 7.35 (m, 3H), 7.22 (d, J = 2.2 Hz, 1H), 7.11 (d, J = 8.6 Hz, 1H), 3.83 (q, J = 6.5 Hz, 1H), 1.79 (d, J = 6.5 Hz, 3H). **^{13}C NMR** (126 MHz, CDCl3) δ 172.28 (s), 167.29 (s), 138.21 (s), 136.91 (s), 134.74 (s), 133.32 (s), 131.88 (s), 131.13 (s), 130.91 (s), 130.19 (s), 129.85 (s), 127.01 (s), 122.80 (s), 116.47 (s), 58.77 (s), 16.88 (s). **HRMS** (ESI/IT-TOF) m/z: [M + H]$^+$ Calcd for C16H12BrClN2O is 362.9879 and found 362.9894.

(S)-4-methyloxazolidine-2,5-dione (FR-III-18) (38)

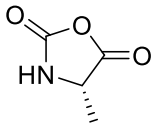

In a homogenous mixture of Boc-L-Alanine (100g, 528.5 mmol), triphosgene (62.7g, 211.4 mmol) and anhydrous ethyl acetate (4000mL), triethylamine (81.0mL, 581.4 mmol) was added dropwise over 60 min while maintaining the temperature between 25 – 30 o C and while observing the CO2(g) and HCl(g) evolution. The reaction mixture was then allowed to stir 1h at rt and this was followed by 2 h at reflux (65 – 70 o C) at which point the reaction was considered complete as gas evolution had stopped. The reaction mixture (a white slurry) was then cooled to rt. The white solid (TEA-HCl and residual L-Alanine) was removed by filtration which result a pale-yellow solution. The solid was washed with 2 portions of ethyl acetate (2 x 100 mL) and the filtrates were combined. The solvent was removed under reduced pressure which result a semisolid mass. The semi solid resulted mixture was then dissolved in dichloromethane (400 mL). Hexane (400mL) was added dropwise over 1 hr with vigorous stirring to precipitate the product. The resulted slurry was then put in a freezer at -20 o C for 12 hr for maximum product precipitation. The solid was filtered and washed with hexanes (250 mL x 2). The solid was dried under vacuum

at rt to afford the product as an off-white solid (34 g, 55.0%)**^{1}H NMR** (500 MHz, DMSO) δ 8.98 (s, 1H), 4.47 (q, J = 6.7 Hz, 1H), 1.28 (d, J = 58.3, 6.8 Hz, 3H). **^{13}C NMR** (126 MHz, DMSO) δ 172.85 (s), 152.15 (s), 53.27 (s), 17.18 (s). **HRMS (ESI/IT-TOF)**: m/z [M + H]+ calcd for C4H6NO3: 116.0348; found: 116.0350.

(*S*)-7-Bromo-5-(2-chlorophenyl)-3-methyl-1,3-dihydro-2H-benzo[*e*][1,4]diazepin-2-one (34)

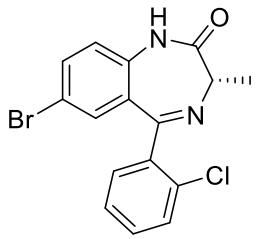

The 2-amino-5-bromo-2'-chlorobenzophenone (140.7 g, 478.4 mmol) was dissolved by adding the starting material to anhydrous toluene (2200 mL) and stirring at rt for 30 min. Then, the solid N-carboxy-L-alanine anhydride (66.0g, 574.0 mmol) was added to the mixture and heated at 50 – 55 ^{o}C over 1 h until the reaction was complete (intermediate TFA salt formation, <5% 2-amino-5-bromo-2'-chlorobenzophenone remained, ***Rf*** = 0.8 (100% EtOAc)) upon analysis by TLC (silica gel, EtOAc/hexanes 1:1). After completing the reaction, anhydrous triethylamine (133.3 mL, 956.7 mmol) was added dropwise for 30 min at 50 – 55 ^{o}C. Then the temperature of the reaction mixture was maintained at 50 – 55 ^{o}C for 2 h and then the completion of the reaction was confirmed by disappearance of intermediate TFA salt, ***Rf*** = 0.1 (100% EtOAc) and analysis by TLC (silica gel, EtOAc/hexanes, 1:1). Then the reaction mixture was cooled to rt and concentrated under reduced pressure. The resulting residue was dissolved in EtOAc (1500 mL) and water (1500 mL) which caused the formation of a biphasic mixture. This mixture was left for 15 min to settle until formation of layers and then the layers were separated. The organic layer was washed with

5% aq $NaHCO_3$ solution (1500 mL) and then with 10% aq NaCl solution (1500 mL). Then the layer was dried (Na_2SO_4, 50 g). The EtOAc was removed under reduced pressure and the residue was again dissolved in 10% EtOAc/heptane (25 mL x 2). Then the residue was dissolved by slurrying in 10% EtOAc/heptane (1700 mL) at 60 – 65 ^oC for 30 min. Then it was cooled to rt and held for 2 h. The solid product was filtered out and then washed with 10% EtOAc/heptane (50 mL x 2) and then with heptane (50 mL x 2). The resulting solid was then vacuum-dried at 35 – 40 ^oC to obtain the off-white solid product (127.0 g, 77.0%): ***Rf*** = 0.7 (100% EtOAc) **1H NMR** (500 MHz, CDCl3) δ 9.79 (s, 1H), 7.58 (dd, J = 8.6, 2.2 Hz, 1H), 7.55 – 7.49 (m, 1H), 7.42 – 7.35 (m, 3H), 7.22 (d, J = 2.2 Hz, 1H), 7.11 (d, J = 8.6 Hz, 1H), 3.83 (q, J = 6.5 Hz, 1H), 1.79 (d, J = 6.5 Hz, 3H). **^{13}C NMR** (126 MHz, CDCl3) δ 172.28 (s), 167.29 (s), 138.21 (s), 136.91 (s), 134.74 (s), 133.32 (s), 131.88 (s), 131.13 (s), 130.91 (s), 130.19 (s), 129.85 (s), 127.01 (s), 122.80 (s), 116.47 (s), 58.77 (s), 16.88 (s). **HRMS** (ESI/IT-TOF) m/z: $[M + H]^+$ Calcd for C16H12BrClN2O is 362.9879 and found 362.9894.

Ethyl (*S*)-8-bromo-6-(2-Chlorophenyl)-4-methyl-4*H*-benzo[f]imidazo[1,5-*a*][1,4]diazepine-3-carboxylate (FR-III-05) (35)

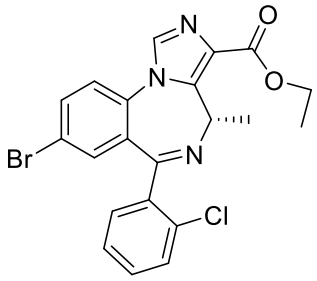

(*S*)-7-bromo-5-(2-chlorophenyl)-3-methyl-1,3-dihydro-2H-benzo[*e*][1,4]diazepin-2-one (90.0 g, 247.49 mmol) was added to anhydrous tetrahydrofuran (1200 mL) and then the mixture was cooled to -20 ^oC in dry ice / IPA bath. Another solution of potassium *t*-butoxide (36.1 g, 321.74 mmol) in

tetrahydrofuran (250 mL) was prepared separately, which was then added dropwise to the previous reaction mixture over 30 min at -20 to -15 ^{o}C. Then the reaction mixture was set to stir for 1 h while the temperature was maintained at -20 ^{o}C. Afterwards, Diethyl chlorophosphate (50 mL, 346.48 mmol) was added dropwise to the mixture for 15 min while the temperature was held at -20 to -15 ^{o}C. The reaction mixture was then again set to stir for 2 h at -20 ^{o}C. The completion of the reaction was confirmed by analysis by TLC (silica gel, 100% EtOAc). Upon completion, ethyl isocyanoacetate (35.16 mL, 321.73 mmol) was added to the reaction mixture dropwise over 15 min and then a solution of potassium *t*-butoxide (36.1 g, 321.74 mmol) in tetrahydrofuran (300 mL) over 30 min, maintaining a temperature of -20 to -15 ^{o}C, Then the mixture was allowed to warm to rt and set to stir for 12 h until the reaction was complete, confirmed by analysis by TLC (silica gel, 100% EtOAc). Then 5% aq sodium bicarbonate (2000 mL) and then ethyl acetate (2000 mL) was added to dilute the mixture, resulting in a biphasic mixture. This biphasic mixture was allowed to stand for 30 min at which point the layers were separated. The aq layer was extracted with ethyl acetate (1500 mL). Then the combination of organic layers was washed first with 10% aq $NaHCO_3$ solution (1500 mL) and later with 20% aq NaCl solution (2000 mL). Then the organic layer was dried (Na_2SO_4, 200 g) and concentrated under reduced pressure to remove solvents. The resulting solid residue was solvent exchanged to *t*-butyl methyl ether (150 mL x 2) and then slurried with *t*-butyl methyl ether (800 mL) at 50 – 55 ^{o}C for 30 min. Then it was cooled to rt and held for 12 h. Then the solid was filtered and washed with t-butyl methyl ether (100 mL x 4) and then dried under vacuum at a temperature of 35 – 40 ^{o}C which resulted in a white powder product (96.6 g, 60.7%); ***Rf*** = 0.4 (100% EtOAc); **^{1}H NMR** (500 MHz, CDCl3) δ 7.91 (s, 1H), 7.72 (d, J = 7.7 Hz, 1H), 7.48 (d, J = 8.6 Hz, 1H), 7.39 (dd, J = 10.2, 7.8 Hz, 3H), 6.69 (q, J = 6.0 Hz, 1H), 4.42 (q, J = 13.3, 6.4 Hz, 2H), 1.42 (t, J = 1.5 Hz, 3H), 1.34 (d, J = 5.8 Hz, 3H). **^{13}C NMR** (126

MHz, CDCl3) δ 162.90 (s), 141.51 (s), 139.34 (s), 134.81 (s), 134.72 (s), 134.17 (s), 132.84 (s), 132.35 (s), 130.95 (s), 130.85 (s), 130.69 (s), 130.17 (s), 129.84 (s), 129.69 (s), 127.18 (s), 123.52 (s), 120.96 (s), 60.85 (s), 50.15 (s), 14.99 (s), 14.42 (s). **HRMS** (ESI/IT-TOF) m/z: $[M + H]^+$ Calcd for C21H17BrClN3O2 is 458.0265 and found 458.0249.

Ethyl (*S*)-6-(2-Chlorophenyl)-4-methyl-8-((triisopropylsilyl)ethynyl)-4*H*-benzo[*f*]imidazo [1,5-*a*][1,4]diazepine-3-carboxylate [FR-III-04-TIPS] (36)

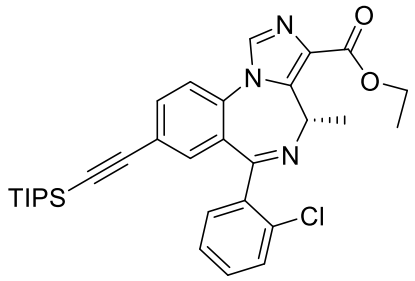

A mixture was prepared by adding palladium acetate (.978 g, 4.3 mmol) and tri-o-tolylphosphine (2.65g, 8.72 mmol) to acetonitrile (200 mL) and then stirring it for 30 min at rt. Then the following reagents were added to the mixture sequentially: ethyl (*R*)-8-bromo-6-(2-chlorophenyl)-4-methyl-4*H*-benzo[*f*]imidazo[1,5-*a*][1,4]diazepine-3-carboxylate (40g, 87.19 mmol), triethylamine (30.9 mL, 221.0 mmol), (triisopropylsilyl)acetylene (23.42 mL, 104.4 mmol) and additional acetonitrile (400 mL). Then the mixture was heated to 75 ^oC to reflux and held for 4 h until the reaction was complete, confirmed by analysis by TLC (silica gel; 40% EtOAc /Hexane). Then the reaction mixture was allowed to cool to rt and silica gel (25 g) was added. Then the mixture was stirred for 30 min and the spent catalyst on silica gel was filtered out and washed with acetonitrile (100 mL x 2). Then solvents were removed under reduced pressure. The resulting residue was dissolved in dichloromethane (700 mL) and 5% aq $NaHCO_3$ (700 mL). This resulted into a biphasic mixture. This mixture was allowed to stand for 15 min until the layers

separated. The aq layer was removed by dichloromethane (700 mL) and the organic layers were washed with 5% aq $NaHCo_3$ solution (700 mL) and then 10% aq NaCl solution (700 mL). The organic layer was then dried (Na_2SO_4), concentrated under reduced pressure and then purified by flash chromatography with silica gel (600 g) and EtOAc/hexanes (1:1). Then the pure fractions were pooled and concentrated under reduced pressure. The resulting oil was dried at 40 ^oC for 2 h under reduced pressure. This resulted into the final product as a clear, golden oil (64.2 g, 106%, HNMR analysis displayed 90wt% product, 10wt% solvents); ***Rf*** = 0.6 (100% EtOAc);

1H NMR (500 MHz, CDCl3) δ 7.92 (s, 1H), 7.65 (d, J = 8.0 Hz, 1H), 7.52 (d, J = 8.3 Hz, 3H), 7.40 – 7.35 (m, 4H), 7.18 (s, 1H), 6.66 (q, 1H), 4.40 (q, J = 13.1, 6.6 Hz, 3H), 1.42 (t, J = 7.1 Hz, 5H), 1.32 (d, J = 7.1 Hz, 3H), 1.15 – 1.06 (m, 3H), 1.10 (s, 18H).**^{13}C NMR** (126 MHz, CDCl3) δ 171.13 (s), 162.93 (s), 135.28 (s), 134.78 (s), 134.51 (s), 133.15 (s), 132.38 (s), 130.60 (s), 130.05 (s), 129.56 (s), 129.38 (s), 127.03 (s), 122.99 (s), 121.92 (s), 104.58 (s), 94.25 (s), 60.79 (s), 50.13 (s), 14.97 (s), 14.42 (s), 11.21 (s). **HRMS** (ESI/IT-TOF) m/z: $[M + H]^+$ Calcd for C32H38ClN3O2Si is 560.2495 found 560.2507.

Ethyl (*R*)-8-ethynyl-6-(2-fluorophenyl)-4-methyl-4*H*-benzo[*f*]imidazo[1,5-*a*][1,4]diazepine-3-carboxylate (FR-III-10) (37)

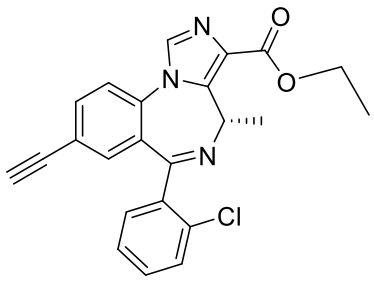

A mixture was prepared by adding ethyl (*S*)-6-(chlrophenyl)-4-methyl-8-((triisopropylsilyl) ethynyl)-4*H*-benzo[*f*]imidazo[1,5-*a*][1,4]diazepine-3-carboxylate (**FR-III-05**

TIPS, 60.5 g, 111.3 mmol) and water (6.0 mL) to tetrahydrofuran (600 mL). Then this mixture was cooled to -20 ^{o}C using a dry ice / IPA bath. Then tetrabutylammonium fluoride hydrate, 1M in THF (127.6 mL, 127.6 mmoL) was added dropwise over 30 min at -20 to -15 ^{o}C. Then the mixture was brought to rt and stirred for additional 1 h until the reaction was complete, confirmed by analysis by TLC (silica gel, 100% EtOAc; ***Rf: FR-III-05-TIPS*** = 0.6, ***Rf: FR-III-05*** = 0.4). Then EtOAc (600 mL) and 10% aq NaCl (600 mL) was added to the mixture for dilution. This formed a biphasic mixture which was allowed to stand for 15 min until layers separated. The aq layer was extracted with EtOAc (600 mL) and the organic layer was dried (Na_2SO_4). Then the organic layer was concentrated under reduced pressure to remove solvents. The remaining residue was slurried with methanol (250 mL) for 30 min while maintaining a temperature of 50 – 55 ^{o}C. Then water was added to the slurry and stirred for an additional 30 min maintaining the temperature at 50 – 55 ^{o}C. Then the mixture was cooled to 20 – 25 ^{o}C and held for 2 h. Then the solid was filtered and washed with methanol/water (1:1, 50 mL x 4). Then it was further washed with hexanes (50 mL x 3). The resulting solid was dried at 40 ^{o}C under vacuum to obtain the final white crystalline solid product (38.1 g, 88.6%): ***Rf*** = 0.4 (100% EtOAc); **^{1}H NMR** (500 MHz, CDCl3) δ 7.93 (s, 1H), 7.69 (d, J = 8.0 Hz, 1H), 7.57 (d, J = 8.3 Hz, 2H), 7.40 (dd, J = 5.7, 3.5 Hz, 3H), 7.27 (s, 1H), 6.68 (q, 1H), 4.42 (q, J = 14.7, 7.2 Hz, 2H), 3.15 (s, 1H), 1.63 (d, 1H), 1.43 (t, J = 7.1 Hz,3H), 1.33 (d, J = 7.0 Hz, 3H). **^{13}C NMR** (126 MHz, CDCl3) δ 162.91 (s), 141.62 (s), 139.60 (s), 135.16 (s), 135.02 (s), 134.80 (s), 133.75 (s), 132.84 (s), 131.95 (s), 131.82 (s), 130.72 (s), 130.12 (s), 129.66 (s), 129.49 (s), 127.11 (s), 122.07 (s), 121.65 (s), 81.44 (s), 79.73 (s), 60.84 (s), 50.14 (s), 15.00 (s), 14.42 (s).**HRMS** (ESI/IT-TOF) m/z: $[M + H]^{+}$ Calc C22H16ClN3O2 for is 458.0265 found 458.0249

(S)-6-(2-chlorophenyl)-8-ethynyl-4-methyl-4H-benzo[f]imidazo[1,5-a][1,4]diazepine-3-carboxylic acid(FR-III-12)(41)

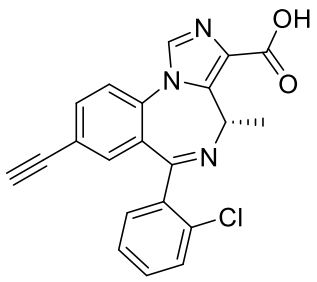

In a homogenous mixture of ethyl (s)-8-ethynyl-6-(2-Cholorophenyl)-4-methyl-4H-benzo[f]imidazo[1,5- a][1,4]diazepine-3-carboxylate (15.0 g, 37.22 mmol) and tetrahydrofuran (200 mL), a solution of lithium hydroxide (3.56 g, 148.8 mmol) and water (150 mL) was added dropwise by maintaing the temperature between 25 – 30 o C. The reaction mixture was then heated to 50 – 55 o C and allowed to run for 4 h, at which point the reaction completion was checked by TLC (silica gel; 100% ethyl acetate; the reaction temperature should maintain between 50- 55 o C and the reaction should not run longer than 4 hr otherwise the product might racemize. After cooling down to rt, water (150 mL) was added to the reaction mixture to dilute. Glacial acetic acid (10 mL, 160.85 mmol) was then added dropwise to the reaction mixture over 15 min, by keeping the temperature at 20 to 25 o C. The tetrahydrofuran was removed under reduced pressure. Methanol (150 mL) was added to the resulted semi solid slurry. The mixture was stirred at 40 – 45 o C for 30 min and kept in rt for maximum precipitation. The solid was filtered and washed with water (25 mL x 4). The solid was dried under vacuum at 35 – 40 o C to afford the product as an off-white powder (13.9 g, 92%).**^{1}H NMR** (500 MHz, MeOD) δ 8.28 (s, 1H), 7.85 (d, J = 8.4 Hz, 1H), 7.76 (d, J = 7.9 Hz, 1H), 7.63 – 7.55 (m, 1H), 7.50 (dd, J = 6.4, 3.1 Hz, 2H), 7.44 (d, J = 3.9 Hz, 1H), 7.17 (s, 1H), 6.64 (q, J = 7.0 Hz, 1H), 3.67 (s, 1H), 1.33 (d, J = 6.7 Hz, 3H). **13C NMR**

(126 MHz, MeOD) δ 167.12 (s), 165.60 (s), 139.81 (s), 139.21 (s), 135.54 (s), 135.32 (s), 135.04 (s), 133.30 (s), 131.86 (s), 130.90 (s), 130.48 (s), 129.66 (s), 128.94 (s), 127.09 (s), 122.78 (s), 121.84 (s), 80.69 (s), 80.05 (s), 49.90 (s), 13.76 (s). **HRMS** (ESI/IT-TOF) m/z: $[M + H]^+$ Calcd for 376.0987 found 376.0978

S)-8-bromo-6-(2-chlorophenyl)-4-methyl-4H-benzo[f]imidazo[1,5-a][1,4]diazepine-3-carboxylic acid (FR-III-27)(42)

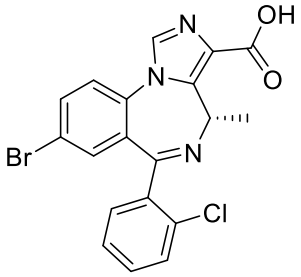

In a homogenous mixture of ethyl (S)-8-bromo-6-(2-chlorophenyl)-4-methyl-4H-benzo[f]imidazo[1,5-a][1,4]diazepine-3-carboxylate (10.0 g, 21.88 mmol) and tetrahydrofuran (200 mL), a solution of lithium hydroxide (2.09 g, 87.5 mmol) and water (100 mL) was added dropwise by maintaing the temperature between 25 – 30 o C. The reaction mixture was then heated to 50 – 55 o C and allowed to run for 4 h, at which point the reaction completion was checked by TLC (silica gel; 100% ethyl acetate; the reaction temperature should maintain between 50- 55 o C and the reaction should not run longer than 4 hr otherwise the product might racemize. After cooling down to rt, water (100 mL) was added to the reaction mixture to dilute. Glacial acetic acid (8.7 mL, 154.85 mmol) was then added dropwise to the reaction mixture over 15 min, by keeping the temperature at 20 to 25 o C. The tetrahydrofuran was removed under reduced pressure. Methanol (100 mL) was added to the resulted semi solid slurry. The mixture was stirred at 40 – 45 o C for 30 min and kept in rt for maximum precipitation. The solid was filtered and washed with

water (25 mL x 4). The solid was dried under vacuum at 35 – 40 o C to afford the product as an off-white powder (8.7g, 92%) (**^{1}H NMR** (500 MHz, DMSO) δ 12.77 (s, 1H), 8.40 (s, 1H), 7.91 (ddd, 10H), 7.62 (dd, J = 18.0, 9.8 Hz,1H), 7.56 – 7.29 (m, 3H), 7.15 (dd, 1H), 6.48 (q, J = 6.3 Hz, 1H),1.21 (d, J = 6.1 Hz, 3H). **^{13}C NMR** (126 MHz, DMSO) δ 164.84 (s), 164.66 (s), 140.93 (s), 139.67 (s), 136.71 (s), 135.44 (s), 134.52 (s), 132.08 (s), 131.60 (s), 130.68 (s), 130.14 (s), 129.40 (s), 127.97 (s), 125.57 (s), 120.19 (s), 49.84 (s), 15.18 (s).

(S)-5-(6-(2-chlorophenyl)-8-ethynyl-4-methyl-4H-benzo[f]imidazo[1,5-a][1,4]diazepin-3-yl)-3-isopropyl-1,2,4-oxadiazole (FR-III-39)(45)

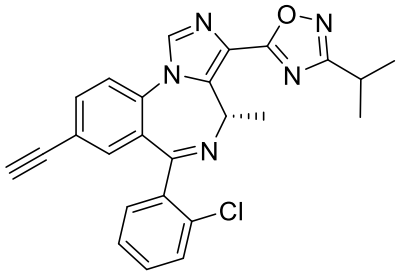

To a flask 3Å molecular sieves were charged and this was followed by the addition of isopropyl oxime (1.012g, 9.88 mmol). It was added to the dry THF mixture under argon pressure. Sodium hydride ((60% dispersion in mineral oil, 63.87mg, 2.729 mmol) was added to the reaction mixture and it was allowed to stir for 1 hour at rt. In another flask the ethyl ester, (1g, 2.488 mmol) was dissolved in dry THF. The latter homogenous mixture was added to the first one dropwise and the mixture was allowed to be stir for 2 h. The completion of the reaction was confirmed by checking by TLC, when all the starting material had been consumed. (Silica gel, 40% etOAc/ hexane). $NaHCO_3$ solution (20 mL) was added to quench the reaction. Then EtOAc (100 mL) and 10% aq NaCl (100 mL) solution were added to the mixture to provide a biphasic solution, which allowed to stand for 10 minutes to separate the layers. The organic layers all combined and dried

over Na_2SO_4. The organic layers combined and removed under the reduced pressure to provide a brownish colored crude solid. The crude was purified with column chromatography to afford an off-white colored solid (760 mg, 77%). **^{1}H NMR** (500 MHz, CDCl3) δ 8.06 (s, 1H), 7.72 (d, J = 7.9 Hz, 1H), 7.62 (d, J = 8.3 Hz, 1H), 7.54 (dd, J = 10.1, 4.2 Hz, 1H), 7.42 – 7.35 (m, 4H), 6.72 (q, 1H), 3.22 – 3.17 (m, 1H), 3.17 (s, 1H), 1.41 (d, J = 1.2 Hz, 3H), 1.39 (d, J = 1.4 Hz, 6H). **^{13}C NMR** (126 MHz, $CDCl_3$) δ 175.33 (s), 139.57 (s), 139.18 (s), 136.16 (s), 135.31 (s), 134.76 (s), 133.86 (s), 132.35 (s), 130.80 (s), 130.61 (s), 130.16 (s), 129.42 (s), 127.15 (s), 125.23 (s), 122.04 (s), 121.83 (s), 81.37 (s), 79.90 (s), 50.32 (s), 26.75 (s), 20.63 (s), 20.56 (s), 17.71 (s), 15.12 (s). **HRMS** (ESI/IT-TOF) m/z: $[M + H]^+$ Calcd for C25H20ClN5O is 442.1560 found 442.1539.

(S)-5-(6-(2-chlorophenyl)-8-ethynyl-4-methyl-4H-benzo[f]imidazo[1,5-a][1,4]diazepin-3-yl)-3-ethyl-1,2,4-oxadiazole(FR-III-25)(44)

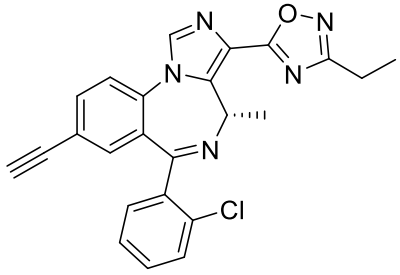

In a flask charged with 3Å molecular sieves N'-hydroxypropionimidamide (873.44 mg, 9.99 mmol) was added to dry THF under argon pressure. Sodium hydride ((60% dispersion in mineral oil, 63.87 mg, 2.77 mmol) was added to the reaction mixture and it was allowed to stir for 1 hour. In another flask the ethyl ester, (1g, 2.488 mmol) was dissolved in dry THF. The former homogenous mixture was added to the first one dropwise and allowed to be stirred for 2 h. The completion of the reaction was confirmed by checking by TLC when all the starting material was consumed. (Silica gel, 40% etOAc/ hexane). Aqueous $NaHCO_3$ solution (20 mL) was added to

quench the reaction. Then EtOAc (100 mL) and 10% aq NaCl (100 mL) solution were added to the mixture, and this resulted in a biphasic solution which was allowed to stand for 10 min to separate the layers. The organic layers were all combined and dried over Na_2SO_4. The organic layer was removed under the reduced pressure to result a brownish colored crude solid. The solid was purified by column chromatography to afford an off-white solid (770 mg, 71%)**^{1}H NMR** (500 MHz, $CDCl_3$) δ 8.06 (s, 1H), 7.72 (d, *J* = 7.9 Hz, 1H), 7.62 (d, *J* = 8.3 Hz, 1H), 7.54 (d, *J* = 18.7 Hz, 1H), 7.37 (ddd, *J* = 25.4, 10.5, 3.5 Hz, 4H), 6.72 (q, *J* = 7.0 Hz, 1H), 3.17 (s, 1H), 2.83 (q, *J* = 7.6 Hz, 2H), 1.39 (d, *J* = 7.6 Hz, 3H), 1.39 (t, *J* = 7.6 Hz, 3H). **13C NMR** (126 MHz, CDCl3) δ 171.89 (s), 139.48 (s), 139.23 (s), 136.19 (s), 135.31 (s), 134.73 (s), 133.90 (s), 133.38 (s), 132.37 (s), 130.80 (s), 130.70 (s), 130.15 (s), 129.45 (s), 127.13 (s), 125.52 (s), 125.12 (s), 122.03 (s), 121.86 (s), 81.37 (s), 79.91 (s), 50.27 (s), 19.75 (s), 15.11 (s), 11.53 (s). **HRMS** (ESI/IT-TOF) m/z: $[M + H]^+$ Calcd for C24H18ClN5O is 428.1367 found 428.1349.

(S)-5-(6-(2-chlorophenyl)-8-ethynyl-4-methyl-4H-benzo[f]imidazo[1,5-a][1,4]diazepin-3-yl)-3-methyl-1,2,4-oxadiazole(FR-III-47)(43)

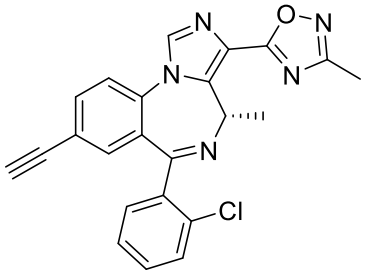

In a flask with 3Å molecular sieves isopropyl oxime (0.7344g, 9.92 mmol) was added to the dry THF under argon pressure. Sodium hydride (60% dispersion in mineral oil, 56.32 mg, 2.44mmol) was added to the reaction mixture and stirred for 1 hour. In another flask the Br-ethyl ester, (1g, 2.48 mmol) was dissolved in dry THF. The former homogenous mixture was added to

the first one dropwise and allowed to be stirred for 2 h. The completion of the reaction was confirmed by checking TLC when all the starting material consumed. (Silica gel, 40% etOAc/ hexane). $NaHCO_3$ solution (20 mL) was added to quench the reaction. Then etOAc (100 mL) and 10% aq solution NaCl (100 mL) was added to the mixture and form a biphasic solution which allowed to stand for 10 minutes to separate the layers. The organic layers all combined and dried over Na_2SO_4. The organic layers removed under the reduced pressure to result a brownish crude. The crude was purified with column chromatography to afford an off-white solid (900 mg, 82.56%)^{1}H NMR (500 MHz, $CDCl_3$) δ 8.06 (s, 1H), 7.73 (dd, *J* = 8.0 Hz, 1H), 7.62 (d, *J* = 8.3 Hz, 1H), 7.52 (d, *J* = 1.4 Hz, 1H), 7.42 – 7.35 (m, 3H), 6.72 (q, 1H), 3.17 (s, 1H), 2.47 (s, 3H), 1.39 (d, *J* = 6.9 Hz, 2H). 13C NMR (126 MHz, CDCl3) δ 167.45 (s), 139.47 (s), 139.21 (s), 136.22 (s), 135.31 (s), 134.71 (s), 133.89 (s), 133.39 (s), 132.39 (s), 131.04 (s), 130.80 (s), 130.70 (s), 130.15 (s), 129.49 (s), 127.12 (s), 125.01 (s), 122.02 (s), 121.87 (s), 81.37 (s), 79.91 (s), 50.22 (s), 15.08 (s), 11.66 . HRMS (ESI/IT-TOF) m/z: $[M + H]^+$ Calcd for C23H16ClN5O is 414.1116 found 414.1116.

Ethyl 8-bromo-6-(2-chlorophenyl)-4-methyl-6H-benzo[f]imidazo[1,5-a][1,4]diazepine-3-carboxylate(FR-III-40) (53)

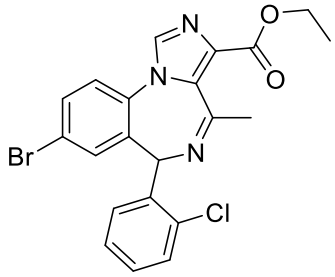

In **a container** ethyl (S)-8-bromo-6-(2-chlorophenyl)-4-methyl-4H-benzo[f]imidazo[1,5-a][1,4]diazepine-3-carboxylate was dissolved (1g, 2.188mmol) in dry THF (100 mL), potassium

t-butoxide (269.5 mg, 2.40 mmol) was added to the reaction mixture and heated for 0.5 h. The reaction completion was confirmed by TLC. After completion the reaction, THF was removed under reduced pressure. The semi solid residue was dissolved in ethyl acetate (100 mL) and extract with water (50x4). After extraction, all organic layer combined, washed with brine which followed by drying over Na_2SO_4. The organic layer reduced under pressure and the residue purified by column chromatography using silica gel 50% ethyl acetate /hexane (**1H NMR** (500 MHz, CDCl3) δ 8.42 (dd, J = 7.8, 1.5 Hz, 1H), 8.09 (s, 1H), 7.58 (dd, J = 8.4, 2.1 Hz, 1H), 7.54 (td, J = 7.4, 1.6 Hz, 1H), 7.45 – 7.37 (m, 3H), 6.85 (d, J = 1.9 Hz, 1H), 5.48 (s, 1H), 4.48 (qd, J = 7.1, 1.9 Hz, 2H), 2.59 (d, J = 1.0 Hz, 3H), 1.47 (t, J = 7.1 Hz, 3H).

8-bromo-6-(2-chlorophenyl)-4-methyl-6H-benzo[f]imidazo[1,5-a][1,4]diazepine-3-carboxylic acid (FR-III-45) (54)

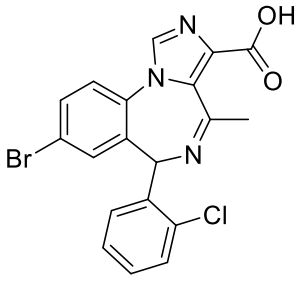

In a homogenous mixture of Ethyl 8-bromo-6-(2-chlorophenyl)-4-methyl-6H-benzo[f]imidazo[1,5-a][1,4]diazepine-3-carboxylate((1.0 g, 2.188 mmol) and tetrahydrofuran (200 mL), a solution of sodium hydroxide (.209 g, 8.75 mmol) and water (10 mL) was added dropwise by maintaing the temperature between 25 – 30 o C. The reaction mixture was then heated to 50 – 55 o C and allowed to run for 4 h, at which point the reaction completion was checked by TLC (silica gel; 100% ethyl acetate. After cooling down to rt, water (10 mL) was added to the reaction mixture to dilute. Glacial acetic acid (.87 mL, 15.485 mmol) was then added dropwise to

the reaction mixture over 15 min, by keeping the temperature at 20 to 25 o C. The tetrahydrofuran was removed under reduced pressure. Methanol (10 mL) was added to the resulted semi solid slurry. The mixture was stirred at 40 – 45 o C for 30 min and kept in rt for maximum precipitation. The solid was filtered and washed with water (5 mL x 4). The solid was dried under vacuum at 35 – 40 o C to afford the product as an off-white powder (800 mg, 89%) **^{1}H NMR** (500 MHz, DMSO) δ 8.58 (s, 1H), 8.35 (d, J = 7.5 Hz, 1H), 7.78 (dd, J = 24.3, 7.9 Hz, 2H), 7.62 (t, J = 7.3 Hz, 1H), 7.55 (d, J = 7.6 Hz, 1H), 7.50 (t, J = 7.2 Hz, 1H), 1.91 (s, 3H). **^{13}C NMR** (126 MHz, DMSO) δ 172.51 (s), 164.49 (s), 160.29 (s), 138.38 (s), 138.01 (s), 136.21 (s), 133.70 (s), 132.61 (s), 132.45 (s), 131.24 (s), 130.92 (s), 130.30 (s), 130.23 (s), 128.37 (s), 128.17 (s), 126.13 (s), 121.84 (s), 61.39 (s), 26.30 (s), 21.57 (s).

References

1. Watanabe, M.; Maemura, K.; Kanbara, K.; Tamayama, T.; Hayasaki, H., GABA and GABA Receptors in the Central Nervous System and Other Organs. In *International Review of Cytology*, Jeon, K. W., Ed. Academic Press: 2002; Vol. 213, pp 1-47.
2. Sieghart, W., Structure and pharmacology of gamma-aminobutyric acidA receptor subtypes. *Pharmacological Reviews* **1995,** *47* (2), 181.
3. Alexander, S. P. H.; Mathie, A.; Peters, J. A., Ion Channels. *British Journal of Pharmacology* **2011,** *164*, S137-S174.
4. Twyman, R. E.; Rogers, C. J.; Macdonald, R. L., Differential regulation of gamma-aminobutyric acid receptor channels by diazepam and phenobarbital. *Ann Neurol* **1989,** *25* (3), 213-20.
5. Hyland, N. P.; Cryan, J. F., A Gut Feeling about GABA: Focus on GABA(B) Receptors. *Frontiers in pharmacology* **2010,** *1*, 124-124.
6. Guidotti, A.; Auta, J.; Davis, J. M.; Dong, E.; Grayson, D. R.; Veldic, M.; Zhang, X.; Costa, E., GABAergic dysfunction in schizophrenia: new treatment strategies on the horizon. *Psychopharmacology (Berl)* **2005,** *180* (2), 191-205.
7. Luscher, B.; Shen, Q.; Sahir, N., The GABAergic deficit hypothesis of major depressive disorder. *Mol Psychiatry* **2011,** *16* (4), 383-406.
8. Sieghart, W.; Ernst, M., Heterogeneity of GABAA Receptors: Revived Interest in the Development of Subtype-selective Drugs. *Current Medicinal Chemistry - Central Nervous System Agents* **2005,** *5* (3), 217-242.

9. Bowser, D. N.; Wagner, D. A.; Czajkowski, C.; Cromer, B. A.; Parker, M. W.; Wallace, R. H.; Harkin, L. A.; Mulley, J. C.; Marini, C.; Berkovic, S. F.; Williams, D. A.; Jones, M. V.; Petrou, S., Altered kinetics and benzodiazepine sensitivity of a GABAA receptor subunit mutation [gamma 2(R43Q)] found in human epilepsy. *Proc Natl Acad Sci U S A* **2002,** *99* (23), 15170-5.

10. Munro, G.; Hansen, R. R.; Mirza, N. R., GABAA receptor modulation: Potential to deliver novel pain medicines? *European Journal of Pharmacology* **2013,** *716* (1), 17-23.

11. Barnard, E. A.; Skolnick, P.; Olsen, R. W.; Mohler, H.; Sieghart, W.; Biggio, G.; Braestrup, C.; Bateson, A. N.; Langer, S. Z., International Union of Pharmacology. XV. Subtypes of gamma-aminobutyric acidA receptors: classification on the basis of subunit structure and receptor function. *Pharmacol Rev* **1998,** *50* (2), 291-313.

12. Olsen, R. W.; Sieghart, W., GABA A receptors: subtypes provide diversity of function and pharmacology. *Neuropharmacology* **2009,** *56* (1), 141-8.

13. Wisden, W.; Laurie, D. J.; Monyer, H.; Seeburg, P. H., The distribution of 13 GABAA receptor subunit mRNAs in the rat brain. I. Telencephalon, diencephalon, mesencephalon. *J Neurosci* **1992,** *12* (3), 1040-62.

14. Fritschy, J. M.; Mohler, H., GABAA-receptor heterogeneity in the adult rat brain: differential regional and cellular distribution of seven major subunits. *J Comp Neurol* **1995,** *359* (1), 154-94.

15. Sieghart, W.; Sperk, G., Subunit Composition, Distribution and Function of GABA-A Receptor Subtypes. *Current Topics in Medicinal Chemistry* **2002,** *2* (8), 795-816.

16. Nutt, D., GABAA receptors: subtypes, regional distribution, and function. *J Clin Sleep Med* **2006,** *2* (2), S7-11.

17. Pirker, S.; Schwarzer, C.; Wieselthaler, A.; Sieghart, W.; Sperk, G., GABA(A) receptors: immunocytochemical distribution of 13 subunits in the adult rat brain. *Neuroscience* **2000,** *101* (4), 815-50.

18. Burt, D. R.; Kamatchi, G. L., GABAA receptor subtypes: from pharmacology to molecular biology. *The FASEB Journal* **1991,** *5* (14), 2916-2923.

19. Clayton, T.; Chen, J. L.; Ernst, M.; Richter, L.; Cromer, B. A.; Morton, C. J.; Ng, H.; Kaczorowski, C. C.; Helmstetter, F. J.; Furtmuller, R.; Ecker, G.; Parker, M. W.; Sieghart, W.; Cook, J. M., An updated unified pharmacophore model of the benzodiazepine binding site on gamma-aminobutyric acid(a) receptors: correlation with comparative models. *Curr Med Chem* **2007,** *14* (26), 2755-75.

20. Keramidas, A.; Moorhouse, A. J.; Schofield, P. R.; Barry, P. H., Ligand-gated ion channels: mechanisms underlying ion selectivity. *Progress in Biophysics and Molecular Biology* **2004,** *86* (2), 161-204.

21. Ramerstorfer, J.; Furtmuller, R.; Sarto-Jackson, I.; Varagic, Z.; Sieghart, W.; Ernst, M., The GABAA receptor alpha+beta- interface: a novel target for subtype selective drugs. *J Neurosci* **2011,** *31* (3), 870-7.

22. Varagic, Z.; Ramerstorfer, J.; Huang, S.; Rallapalli, S.; Sarto-Jackson, I.; Cook, J.; Sieghart, W.; Ernst, M., Subtype selectivity of α+β- site ligands of GABAA receptors: identification of the first highly specific positive modulators at α6β2/3γ2 receptors. *British journal of pharmacology* **2013,** *169* (2), 384-399.

23. Chiou, L.-C.; Tzeng, H.-R.; Fan, P.-C.; Sieghart, W.; Ernst, M.; Knutson, D. E.; Cook, J., A Novel Drug Target for Migraine: The GABAA Receptor α6 Subtype in Trigeminal Ganglia. *The FASEB Journal* **2019,** *33* (1_supplement), lb78-lb78.

24. Knutson, D. E.; Kodali, R.; Divović, B.; Treven, M.; Stephen, M. R.; Zahn, N. M.; Dobričić, V.; Huber, A. T.; Meirelles, M. A.; Verma, R. S.; Wimmer, L.; Witzigmann, C.; Arnold, L. A.; Chiou, L.-C.; Ernst, M.; Mihovilovic, M. D.; Savić, M. M.; Sieghart, W.; Cook, J. M., Design and Synthesis of Novel Deuterated Ligands Functionally Selective for the γ-Aminobutyric Acid Type A Receptor (GABAAR) α6 Subtype with Improved Metabolic Stability and Enhanced Bioavailability. *Journal of Medicinal Chemistry* **2018,** *61* (6), 2422-2446.

25. Vasović, D.; Divović, B.; Treven, M.; Knutson, D. E.; Steudle, F.; Scholze, P.; Obradović, A.; Fabjan, J.; Brković, B.; Sieghart, W.; Ernst, M.; Cook, J. M.; Savić, M. M., Trigeminal neuropathic pain development and maintenance in rats are suppressed by a positive modulator of α6 GABAA receptors. *European Journal of Pain* **2019,** *23* (5), 973-984.

26. Olsen, R. W.; Hanchar, H. J.; Meera, P.; Wallner, M., GABAA receptor subtypes: the "one glass of wine" receptors. *Alcohol* **2007,** *41* (3), 201-9.

27. Sawyer, E. K.; Moran, C.; Sirbu, M. H.; Szafir, M.; Van Linn, M.; Namjoshi, O.; Phani Babu Tiruveedhula, V. V. N.; Cook, J. M.; Platt, D. M., Little evidence of a role for the α1GABAA subunit-containing receptor in a rhesus monkey model of alcohol drinking. *Alcoholism, clinical and experimental research* **2014,** *38* (4), 1108-1117.

28. Ernst, M.; Brauchart, D.; Boresch, S.; Sieghart, W., Comparative modeling of GABA(A) receptors: limits, insights, future developments. *Neuroscience* **2003,** *119* (4), 933-43.

29. Haefely, W., The biological basis of benzodiazepine actions. *Journal of Psychoactive Drugs* **1983,** *15* (1-2), 19-39.

30. Haefely, W.; Facklam, M.; Schoch, P.; Martin, J. R.; Bonetti, E. P.; Moreau, J. L.; Jenck, F.; Richards, J. G., Partial agonists of benzodiazepine receptors for the treatment of epilepsy, sleep, and anxiety disorders. *Advances in biochemical psychopharmacology* **1992,** *47*, 379-394.

31. The benefits and risks of benzodiazepines. https://www.medicalnewstoday.com/articles/262809.

32. Hillestad, L.; Hansen, T.; Melsom, H.; Drivenes, A., Diazepam metabolism in normal man I. Serum concentrations and clinical effects after intravenous, intramuscular, and oral administrations. *Clin. Pharmacol. Therapeutics* **1974,** *16*, 479 - 484.

33. Stevenson, I. H.; Browning, M.; Crooks, J.; O'Malley, K., Changes in human drug metabolism after long-term exposure to hypnotics. *Br. Med. Journal* **1972,** *4*, 322 - 324.

34. Garattini, S.; Mussini, E.; Marucci, F.; Guaitani, A., Metabolic studies on benzodiazepines in various animal species. In *The Benzodiazepines*, Garattini, S.; Mussini, E.; Randall, L. O., Eds. Raven Press: New York, 1973; pp 75 - 97.

35. Rutherford, D. M.; Okoko, A.; Tyrer, P. J., Plasma concentrations of diazepam and desmethyldiazepam during chronic diazepam therapy. *Br. J. Clin. Pharmacol.* **1978,** *1978* (6).

36. Bond, A. J.; Hailey, D. M.; Lader, M. H., Plasma concentrations of benzodiazepines. *Br. J. Clin. Pharmacol.* **1977,** *4*, 51 - 56.

37. Moss, G. P., Nomenclature of fused and bridged fused ring systems (IUPAC Recommendations 1998). In *Pure and Applied Chemistry*, 1998; Vol. 70, p 143.

38. Hadingham, K. L.; Wingrove, P. B.; Wafford, K. A.; Bain, C.; Kemp, J. A.; Palmer, K. J.; Wilson, A. W.; Wilcox, A. S.; Sikela, J. M.; Ragan, C. I.; et al., Role of the beta

subunit in determining the pharmacology of human gamma-aminobutyric acid type A receptors. *Mol Pharmacol* **1993,** *44* (6), 1211-8.

39. Khom, S.; Baburin, I.; Timin, E. N.; Hohaus, A.; Sieghart, W.; Hering, S., Pharmacological properties of GABAA receptors containing gamma1 subunits. *Mol Pharmacol* **2006,** *69* (2), 640-9.

40. Bencsits, E.; Ebert, V.; Tretter, V.; Sieghart, W., A significant part of native gamma-aminobutyric AcidA receptors containing alpha4 subunits do not contain gamma or delta subunits. *J Biol Chem* **1999,** *274* (28), 19613-6.

41. Yang, W.; Drewe, J. A.; Lan, N. C., Cloning and characterization of the human GABAA receptor alpha 4 subunit: identification of a unique diazepam-insensitive binding site. *Eur J Pharmacol* **1995,** *291* (3), 319-25.

42. Korpi, E. R.; Seeburg, P. H., Natural mutation of GABAA receptor alpha 6 subunit alters benzodiazepine affinity but not allosteric GABA effects. *European journal of pharmacology* **1993,** *247* (1), 23-27.

43. Macdonald, R. L.; Olsen, R. W., GABAA Receptor Channels. *Annual Review of Neuroscience* **1994,** *17* (1), 569-602.

44. Study, R. E.; Barker, J. L., Diazepam and (--)-pentobarbital: fluctuation analysis reveals different mechanisms for potentiation of gamma-aminobutyric acid responses in cultured central neurons. *Proceedings of the National Academy of Sciences of the United States of America* **1981,** *78* (11), 7180-7184.

45. MacDonald, R. L., Benzodiazepine mechanisms of action. In *Antiepileptic Drugs,* Levy, R. H.; Mattson, R. H.; Meldrum, B. S.; Perucca, E., Eds. Lippincott Williams and Wilkins: Philadelphia, 2002; pp 179 - 186.

46. Killam, E. K.; Suria, A., Benzodiazepines. In *Antiepileptic Drugs: Mechanisms of Action*, Glaser, G. H.; Penry, J. K.; Woodbury, D. M., Eds. Raven Press: New York, 1980; pp 597 - 615.

47. Rogawski, M. A., Principles of antiepileptic drug action. In *Antiepileptic Drugs*, 5th ed.; Levy, R. H.; Mattson, R. H.; Meldrum, B. S.; Perucca, E., Eds. Lippincott Williams and Wilkins: Philadelphia, 2002; pp 3 - 22.

48. Rudolph, U.; Crestani, F.; Benke, D.; Brunig, I.; Benson, J. A.; Fritschy, J. M.; Martin, J. R.; Bluethmann, H.; Mohler, H., Benzodiazepine actions mediated by specific gamma-aminobutyric acid(A) receptor subtypes. *Nature* **1999,** *401* (6755), 796-800.

49. Low, K.; Crestani, F.; Keist, R.; Benke, D.; Brunig, I.; Benson, J. A.; Fritschy, J. M.; Rulicke, T.; Bluethmann, H.; Mohler, H.; Rudolph, U., Molecular and neuronal substrate for the selective attenuation of anxiety. *Science* **2000,** *290* (5489), 131-4.

50. Collinson, N.; Kuenzi, F. M.; Jarolimek, W.; Maubach, K. A.; Cothliff, R.; Sur, C.; Smith, A.; Otu, F. M.; Howell, O.; Atack, J. R.; McKernan, R. M.; Seabrook, G. R.; Dawson, G. R.; Whiting, P. J.; Rosahl, T. W., Enhanced learning and memory and altered GABAergic synaptic transmission in mice lacking the alpha 5 subunit of the GABAA receptor. *J Neurosci* **2002,** *22* (13), 5572-80.

51. Paul, J.; Yévenes, G. E.; Benke, D.; Di Lio, A.; Ralvenius, W. T.; Witschi, R.; Scheurer, L.; Cook, J. M.; Rudolph, U.; Fritschy, J.-M.; Zeilhofer, H. U., Antihyperalgesia by α2-GABAA receptors occurs via a genuine spinal action and does not involve supraspinal sites. *Neuropsychopharmacology : official publication of the American College of Neuropsychopharmacology* **2014,** *39* (2), 477-487.

52. He, X.; Huang, Q.; Ma, C.; Yu, S.; McKernan, R.; Cook, J. M., Pharmacophore/receptor models for $GABA_A$/BzR a2b3g2, a3b3g2 and a4b3g2 recombinant subtypes. Included volume analysis and comparison to a1b3g2, a5b3g2 and a6b3g2 subtypes. *Drug Des. Discov.* **2000,** *17*, 131 - 171.

53. Morris, H. V.; Dawson, G. R.; Reynolds, D. S.; Atack, J. R.; Stephens, D. N., Both alpha2 and alpha3 GABAA receptor subtypes mediate the anxiolytic properties of benzodiazepine site ligands in the conditioned emotional response paradigm. *Eur J Neurosci* **2006,** *23* (9), 2495-504.

54. Dias, R.; Sheppard, W. F.; Fradley, R. L.; Garrett, E. M.; Stanley, J. L.; Tye, S. J.; Goodacre, S.; Lincoln, R. J.; Cook, S. M.; Conley, R.; Hallett, D.; Humphries, A. C.; Thompson, S. A.; Wafford, K. A.; Street, L. J.; Castro, J. L.; Whiting, P. J.; Rosahl, T. W.; Atack, J. R.; McKernan, R. M.; Dawson, G. R.; Reynolds, D. S., Evidence for a significant role of alpha 3-containing GABAA receptors in mediating the anxiolytic effects of benzodiazepines. *J Neurosci* **2005,** *25* (46), 10682-8.

55. Yee, B. K.; Keist, R.; von Boehmer, L.; Studer, R.; Benke, D.; Hagenbuch, N.; Dong, Y.; Malenka, R. C.; Fritschy, J. M.; Bluethmann, H.; Feldon, J.; Möhler, H.; Rudolph, U., A schizophrenia-related sensorimotor deficit links α3-containing GABA_A receptors to a dopamine hyperfunction. *Proceedings of the National Academy of Sciences of the United States of America* **2005,** *102* (47), 17154.

56. Crestani, F.; Keist, R.; Fritschy, J. M.; Benke, D.; Vogt, K.; Prut, L.; Blüthmann, H.; Möhler, H.; Rudolph, U., Trace fear conditioning involves hippocampal alpha5 GABA(A) receptors. *Proceedings of the National Academy of Sciences of the United States of America* **2002,** *99* (13), 8980-8985.

57. Ralvenius, W. T.; Benke, D.; Acuna, M. A.; Rudolph, U.; Zeilhofer, H. U., Analgesia and unwanted benzodiazepine effects in point-mutated mice expressing only one benzodiazepine-sensitive GABAA receptor subtype. *Nat Commun* **2015,** *6*, 6803.

58. Mizuta, K.; Xu, D.; Pan, Y.; Comas, G.; Sonett, J. R.; Zhang, Y.; Panettieri, R. A., Jr.; Yang, J.; Emala, C. W., Sr., GABAA receptors are expressed and facilitate relaxation in airway smooth muscle. *Am J Physiol Lung Cell Mol Physiol* **2008,** *294* (6), L1206-16.

59. Gallos, G.; Yim, P.; Chang, S.; Zhang, Y.; Xu, D.; Cook, J. M.; Gerthoffer, W. T.; Emala, C. W., Sr., Targeting the restricted alpha-subunit repertoire of airway smooth muscle GABAA receptors augments airway smooth muscle relaxation. *Am J Physiol Lung Cell Mol Physiol* **2012,** *302* (2), L248-56.

60. Clayton, T.; Poe, M. M.; Rallapalli, S.; Biawat, P.; Savic, M. M.; Rowlett, J. K.; Gallos, G.; Emala, C. W.; Kaczorowski, C. C.; Stafford, D. C.; Arnold, L. A.; Cook, J. M., A Review of the Updated Pharmacophore for the Alpha 5 GABA(A) Benzodiazepine Receptor Model. *Int J Med Chem* **2015,** *2015*, 430248.

61. Cook, J.; Huang, S.; Edwankar, R.; Namjoshi, O. A.; Wang, Z. J. Selective agents for pain suppression. Sep. 16, 2014, 2014.

62. McKernan, R. M.; Rosahl, T. W.; Reynolds, D. S.; Sur, C.; Wafford, K. A.; Atack, J. R.; Farrar, S.; Myers, J.; Cook, G.; Ferris, P.; Garrett, L.; Bristow, L.; Marshall, G.; Macaulay, A.; Brown, N.; Howell, O.; Moore, K. W.; Carling, R. W.; Street, L. J.; Castro, J. L.; Ragan, C. I.; Dawson, G. R.; Whiting, P. J., Sedative but not anxiolytic properties of benzodiazepines are mediated by the GABAA receptor α1 subtype. *Nature Neuroscience* **2000,** *3*, 587.

63. Gallos, G.; Yocum, G. T.; Siviski, M. E.; Yim, P. D.; Fu, X. W.; Poe, M. M.; Cook, J. M.; Harrison, N.; Perez-Zoghbi, J.; Emala, C. W., Sr., Selective targeting of the alpha5-subunit of GABAA receptors relaxes airway smooth muscle and inhibits cellular calcium handling. *Am J Physiol Lung Cell Mol Physiol* **2015,** *308* (9), L931-42.

64. Davies, M.; Bateson, A. N.; Dunn, S. M. J., Structural Requirements for Ligand Interactions at the Benzodiazepine Recognition Site of the GABAA Receptor. *Journal of Neurochemistry* **1998,** *70* (5), 2188-2194.

65. Dunn, S. M. J.; Davies, M.; Muntoni, A. L.; Lambert, J. J., Mutagenesis of the Rat α1 Subunit of the γ-Aminobutyric Acid_A Receptor Reveals the Importance of Residue 101 in Determining the Allosteric Effects of Benzodiazepine Site Ligands. *Molecular Pharmacology* **1999,** *56* (4), 768.

66. Sigel, E.; Schaerer, M. T.; Buhr, A.; Baur, R., The Benzodiazepine Binding Pocket of Recombinant α1β2γ2 γ-Aminobutyric Acid_A Receptors: Relative Orientation of Ligands and Amino Acid Side Chains. *Molecular Pharmacology* **1998,** *54* (6), 1097.

67. Whitwam, J. G.; Amrein, R., Pharmacology of flumazenil. *Acta Anaesthesiol Scand Suppl* **1995,** *108*, 3-14.

68. Clayton, T. S. Ph.D. Thesis, Part I. Unified Pharmacophoric Protein Models of the Benzodiazepine Receptor Subtypes. Part II. Subtype Selective Ligands for a5 $GABA_A$/Bz Receptors. University of Wisconsin-Milwaukee, 2011.

69. Huang, Q.; He, X.; Ma, C.; Liu, R.; Yu, S.; Dayer, C. A.; Wenger, G. R.; McKernan, R.; Cook, J. M., Pharmacophore/Receptor Models for GABAA/BzR Subtypes (α1β3γ2, α5β3γ2, and α6β3γ2) via a Comprehensive Ligand-Mapping Approach. *Journal of Medicinal Chemistry* **2000,** *43* (1), 71-95.

70. Wong, G.; Koehler, K. F.; Skolnick, P.; Gu, Z. Q.; Ananthan, S.; Schonholze, P.; Hunkeler, W.; Zhang, W.; Cook, J. M., Synthetic and computer-assisted analysis of the structural requirements for selective, high affinity ligand binding to 'diazepam-insensitive' benzodiazepine receptors. *J. Med. Chem* **1993,** *36*, 1820 - 1830.

71. Gee, K. W.; Brinton, R. E.; Yamamura, H. I., CL-218872 antagonism of diazepam induced loss of righting reflex: Evidence for partial agonistic activity at the benzodiazepine receptor. *Life Sci.* **1983,** *32*, 1037 - 1040.

72. Lippke, K. P.; Schunack, W. G.; Wenning, W.; Muller, W. E., b-Carbolines as benzodiazepine receptor ligands. I. Synthesis and benzodiazepine receptor interactino of esters of b-carboline-3-carboxylic acid. *J. Med. Chem* **1983,** *26*, 499 - 503.

73. Haefely, W.; Martin, J. R.; Schoch, P., Novel anxiolytics that act as partial agonists at benzodiazepine receptors. *Trends Pharmacol. Sci.* **1990,** *11*, 452 - 456.

74. Hagen, T. J.; Guzman, F.; Schultz, C.; Cook, J. M., Synthesis of 3,6-disubstituted b-carbolines which possess either benzodiazepine antagonist or agonist activity. *Heterocycles* **1986,** *24*, 2845 - 855.

75. Allen, M. S.; Hagen, T. J.; Trudell, M. L.; Codding, P. W.; Skolnick, P.; Cook, J. M., Synthesis of novel 3-substituted b-carbolines as benzodiazepine receptor ligands: probing the benzodiazepine receptor pharmacophore. *J. Med. Chem* **1988,** *31*, 1854 - 1861.

76. Trudell, M. L.; Lifer, S. L.; Tan, Y. C.; Martin, M. J.; Deng, T.; Skolnick, P.; Cook, J. M., Synthesis of substituted 7,12-dihydropyrido[3,2-*b*:5,4-*b*'] diindoles: rigid planar benzodiazepine receptor ligands with inverse agonist/antagonist properties. *J. Med. Chem* **1990,** *33*, 2412 - 2420.

77. Yokoyama, N.; Ritter, B.; Neubert, A. D., 2-Arylpyrazolo[4,3-*c*]quinolin-3-ones: novel agonist, partial agonist, and antagonist of benzodiazepines. *J. Med. Chem* **1982,** *25*, 337 - 339.

78. Arbilla, S.; Depoortere, H.; Geroge, P.; Langer, S. Z., Pharmacological profile of the imidazopyridine zolpidem at benzodiazepine receptors and electrocorticogram in rats. *Naunym Schmiederbergs Arch. Pharmacol.* **1985,** *330*, 248 - 251.

79. Huang, Q.; Zhang, W.; Liu, R.; McKernan, R. M.; Cook, J. M., Benzo-fused benzodiazepines employed as topological probes for the study of benzodiazepine receptor subtypes. *Med. Chem. Res.* **1996,** *6*, 384 - 391.

80. van Rijnsoever, C.; Tauber, M.; Choulli, M. K.; Keist, R.; Rudolph, U.; Mohler, H.; Fritschy, J. M.; Crestani, F., Requirement of alpha5-GABAA receptors for the development of tolerance to the sedative action of diazepam in mice. *J Neurosci* **2004,** *24* (30), 6785-90.

81. Cook, J. M.; Huang, Q.; He, X.; Li, X.; Yu, J.; Han, D.; Lelas, S.; McElroy, J. F. Anxiolytic agents with reduced sedative and ataxic effects. Oct. 10, 2006, 2006.

82. Cook, J. M.; Zhou, H.; Huang, S.; Sarma, P. V. V. S.; Zhang, C., Stereospecific anxiolytic and anticonvulsant agents with reduced muscle-relaxant, sedative-hypnotic and ataxic effects. 2009.

83. Fischer, B. D.; Licata, S. C.; Edwankar, R. V.; Wang, Z. J.; Huang, S.; He, X.; Yu, J.; Zhou, H.; Johnson, E. M., Jr.; Cook, J. M.; Furtmuller, R.; Ramerstorfer, J.; Sieghart, W.; Roth, B. L.; Majumder, S.; Rowlett, J. K., Anxiolytic-like effects of 8-acetylene imidazodiazepines in a rhesus monkey conflict procedure. *Neuropharmacology* **2010,** *59* (7-8), 612-8.

84. Rivas, F. M.; Stables, J. P.; Murphree, L.; Edwankar, R. V.; Edwankar, C. R.; Huang, S.; Jain, H. D.; Zhou, H.; Majumder, S.; Sankar, S.; Roth, B. L.; Ramerstorfer, J.; Furtmüller, R.; Sieghart, W.; Cook, J. M., Antiseizure Activity of Novel γ-Aminobutyric Acid (A) Receptor Subtype-Selective Benzodiazepine Analogues in Mice and Rat Models. *Journal of Medicinal Chemistry* **2009,** *52* (7), 1795-1798.

85. Di Lio, A.; Benke, D.; Besson, M.; Desmeules, J.; Daali, Y.; Wang, Z. J.; Edwankar, R.; Cook, J. M.; Zeilhofer, H. U., HZ166, a novel GABAA receptor subtype-selective benzodiazepine site ligand, is antihyperalgesic in mouse models of inflammatory and neuropathic pain. *Neuropharmacology* **2011,** *60* (4), 626-32.

86. Poe, M. M.; Methuku, K. R.; Li, G.; Verma, A. R.; Teske, K. A.; Stafford, D. C.; Arnold, L. A.; Cramer, J. W.; Jones, T. M.; Cerne, R.; Krambis, M. J.; Witkin, J. M.; Jambrina, E.; Rehman, S.; Ernst, M.; Cook, J. M.; Schkeryantz, J. M., Synthesis and Characterization of a Novel γ-Aminobutyric Acid Type A (GABAA) Receptor Ligand That Combines Outstanding Metabolic Stability, Pharmacokinetics, and Anxiolytic Efficacy. *Journal of Medicinal Chemistry* **2016,** *59* (23), 10800-10806.

87. Li, G.; Golani, L. K.; Jahan, R.; Rashid, F.; Cook, J. M., Improved Synthesis of Anxiolytic, Anticonvulsant, and Antinociceptive alpha 2/alpha 3-GABA(A)-ergic Receptor Subtype Selective Ligands as Promising Agents to Treat Anxiety, Epilepsy, and Neuropathic. *Synthesis-Stuttgart* **2018,** *50* (20), 4124-4132.

88. Knutson, D. E.; Smith, J. L.; Ping, X.; Jin, X.; Golani, L. K.; Li, G.; Tiruveedhula, V. V. N. P. B.; Rashid, F.; Mian, M. Y.; Jahan, R., Imidazodiazepine Anticonvulsant, KRM-II-81, Produces Novel, Non-diazepam-like Antiseizure Effects. *ACS Chemical Neuroscience* **2020,** *11* (17), 2624-2637.

89. Witkin, J. M.; Smith, J. L.; Ping, X.; Gleason, S. D.; Poe, M. M.; Li, G.; Jin, X.; Hobbs, J.; Schkeryantz, J. M.; McDermott, J. S.; Alatorre, A. I.; Siemian, J. N.; Cramer, J. W.; Airey, D. C.; Methuku, K. R.; Tiruveedhula, V.; Jones, T. M.; Crawford, J.; Krambis, M. J.; Fisher, J. L.; Cook, J. M.; Cerne, R., Bioisosteres of ethyl 8-ethynyl-6-(pyridin-2-yl)-4H-benzo[f]imidazo [1,5-a][1,4]diazepine-3-carboxylate (HZ-166) as novel alpha 2,3 selective potentiators of GABAA receptors: Improved bioavailability enhances anticonvulsant efficacy. *Neuropharmacology* **2018,** *137*, 332-343.

90. Castel-Branco, M. M.; Alves, G. L.; Figueiredo, I. V.; Falcao, A. C.; Caramona, M. M., The maximal electroshock seizure (MES) model in the preclinical assessment of potential new antiepileptic drugs. *Methods Find Exp Clin Pharmacol* **2009,** *31* (2), 101-6.

91. An, X.-F.; Zhang, Y.; Winter, J. C.; Li, J.-X., Effects of imidazoline I2 receptor agonists and morphine on schedule-controlled responding in rats. *Pharmacology Biochemistry and Behavior* **2012,** *101* (3), 354-359.

92. Fuchs, P. N.; McNabb, C. T., The place escape/avoidance paradigm: a novel method to assess nociceptive processing. *Journal of integrative neuroscience* **2012,** *11* (01), 61-72.

93. LaBuda, C. J.; Fuchs, P. N., A behavioral test paradigm to measure the aversive quality of inflammatory and neuropathic pain in rats. *Experimental neurology* **2000,** *163* (2), 490-494.

94. Bonetti, E. P.; Pieri, L.; Cumin, R.; Schaffner, R.; Pieri, M.; Gamzu, E. R.; Müller, R. K. M.; Haefely, W., Benzodiazepine antagonist Ro 15-1788: neurological and behavioral effects. *Psychopharmacology* **1982,** *78* (1), 8-18.

95. Siemian, J. N.; Qiu, Y.; Zhang, Y.; Li, J.-X., Role of intracellular Ca 2+ signaling in the antinociceptive and discriminative stimulus effects of the imidazoline I 2 receptor agonist 2-BFI in rats. *Psychopharmacology* **2017,** *234* (22), 3299-3307.

96. Qiu, Y.; He, X.-H.; Zhang, Y.; Li, J.-X., Discriminative stimulus effects of the novel imidazoline I 2 receptor ligand CR4056 in rats. *Scientific reports* **2014,** *4* (1), 1-6.

97. Qiu, Y.; Zhang, Y.; Li, J.-X., Discriminative stimulus effects of the imidazoline I2 receptor ligands BU224 and phenyzoline in rats. *European journal of pharmacology* **2015,** *749*, 133-141.

98. Su, R.-B.; Ren, Y.-H.; Liu, Y.; Ding, T.; Lu, X.-Q.; Wu, N.; Liu, Z.-M.; Li, J., Agmatine inhibits morphine-induced drug discrimination in rats. *European journal of pharmacology* **2008,** *593* (1-3), 62-67.

99. García-Nafría, J.; Tate, C. G., Cryo-Electron Microscopy: Moving Beyond X-Ray Crystal Structures for Drug Receptors and Drug Development. *Annual Review of Pharmacology and Toxicology* **2020,** *60* (1), null.

100. Laverty, D.; Desai, R.; Uchanski, T.; Masiulis, S.; Stec, W. J.; Malinauskas, T.; Zivanov, J.; Pardon, E.; Steyaert, J.; Miller, K. W.; Aricescu, A. R., Cryo-EM structure of the human alpha1beta3gamma2 GABAA receptor in a lipid bilayer. *Nature* **2019,** *565* (7740), 516-520.

101. Liu, S.; Xu, L.; Guan, F.; Liu, Y. T.; Cui, Y.; Zhang, Q.; Zheng, X.; Bi, G. Q.; Zhou, Z. H.; Zhang, X.; Ye, S., Cryo-EM structure of the human alpha5beta3 GABAA receptor. *Cell Res* **2018,** *28* (9), 958-961.

102. Phulera, S.; Zhu, H.; Yu, J.; Claxton, D. P.; Yoder, N.; Yoshioka, C.; Gouaux, E., Cryo-EM structure of the benzodiazepine-sensitive alpha1beta1gamma2S tri-heteromeric GABAA receptor in complex with GABA. *Elife* **2018,** *7*.

103. Masiulis, S.; Desai, R.; Uchanski, T.; Serna Martin, I.; Laverty, D.; Karia, D.; Malinauskas, T.; Zivanov, J.; Pardon, E.; Kotecha, A.; Steyaert, J.; Miller, K. W.; Aricescu, A. R., GABAA receptor signalling mechanisms revealed by structural pharmacology. *Nature* **2019,** *565* (7740), 454-459.

104. Wongsamitkul, N.; Maldifassi, M. C.; Simeone, X.; Baur, R.; Ernst, M.; Sigel, E., α subunits in GABAA receptors are dispensable for GABA and diazepam action. *Scientific Reports* **2017,** *7* (1), 15498.

105. Weinbroum, A.; Rudick, V.; Sorkine, P.; Nevo, Y.; Halpern, P.; Geller, E.; Niv, D., Use of flumazenil in the treatment of drug overdose: a double-blind and open clinical study in 110 patients. *Crit Care Med* **1996,** *24* (2), 199-206.

106. Witkin, J. M.; Li, G.; Golani, L. K.; Xiong, W.; Smith, J. L.; Ping, X.; Rashid, F.; Jahan, R.; Cook, J. M.; Jin, X., The positive allosteric modulator of α2/3-containing GABAA receptors, KRM-II-81, is active in pharmaco-resistant models of epilepsy and reduces hyperexcitability after traumatic brain injury. *Journal of Pharmacology and Experimental Therapeutics* **2020,** *372* (1), 83-94.

107. Blažević, N.; Kajfež, F., A new ring closure synthesis of 1, 4-benzodiazepines. II. *Journal of Heterocyclic Chemistry* **1971,** *8* (5), 845-846.

108. Cepanec, I.; Litvić, M.; Pogorelić, I., Efficient synthesis of 3-hydroxy-1, 4-benzodiazepines oxazepam and lorazepam by new acetoxylation reaction of 3-position of

1, 4-benzodiazepine ring. *Organic process research & development* **2006,** *10* (6), 1192-1198.

109. Delépine, M., Sur l'hexamethylene-amine (suite). Solubilities, hydrate, bromure, sulfate, phosphate. *Bull. Soc. Chim. France (3)* **1895,** *13*, 352-361.

110. Chae, M. J.; Song, J. I.; An, D. K., Chemoselective Reduction of Esters to Aldehydes by Potassium Diisobutyl-t-butoxyaluminum Hydride (PDBBA). *Bull. Korean Chem. Soc.* **2007,** *28* (28), 2517-2518.

111. Patani, G. A.; LaVoie, E. J., Bioisosterism: A Rational Approach in Drug Design. *Chemical Reviews* **1996,** *96* (8), 3147-3176.

112. Namjoshi, O. A.; Wang, Z.-j.; Rallapalli, S. K.; Johnson, E. M.; Johnson, Y.-T.; Ng, H.; Ramerstorfer, J.; Varagic, Z.; Sieghart, W.; Majumder, S.; Roth, B. L.; Rowlett, J. K.; Cook, J. M., Search for α3β(2/3)γ2 Subtype Selective Ligands That are Stable on Human Liver Microsomes. *Bioorganic & medicinal chemistry* **2013,** *21* (1), 93-101.

113. Boström, J.; Hogner, A.; Llinàs, A.; Wellner, E.; Plowright, A. T., Oxadiazoles in Medicinal Chemistry. *Journal of Medicinal Chemistry* **2012,** *55* (5), 1817-1830.

114. Burger, A., Isosterism and bioisosterism in drug design. *Progress in drug research. Fortschritte der Arzneimittelforschung. Progres des recherches pharmaceutiques* **1991,** *37*, 287-371.

115. Watjen, F.; Baker, R.; Engelstoff, M.; Herbert, R.; MacLeod, A.; Knight, A.; Merchant, K.; Moseley, J.; Saunders, J., Novel benzodiazepine receptor partial agonists: oxadiazolylimidazodiazepines. *Journal of Medicinal Chemistry* **1989,** *32* (10), 2282-2291.

116. Chawla, G., 1, 2, 4-Oxadiazole as a privileged scaffold for anti-inflammatory and analgesic activities: A review. *Mini reviews in medicinal chemistry* **2018,** *18* (18), 1536-1547.

117. Li, G.; Stephen, M. R.; Kodali, R.; Zahn, N. M.; Poe, M. M.; Tiruveedhula, V. V. N. P. B.; Huber, A. T.; Schussman, M. K.; Qualmann, K.; Panhans, C. M.; Raddatz, N. J.; Baker, D. A.; Prevot, T. D.; Banasr, M.; Sibille, E.; Arnold, L. A.; Cook, J. M., Synthesis of chiral GABAA receptor subtype selective ligands as potential agents to treat schizophrenia as well as depression. *ARKIVOC* **2018,** *iv*, 158-183.

118. Pomeroy, S. L.; Loeffler, J. S.; Wen, P. Y.; Gajjar, A.; Eichler, A. F., Histopathology and molecular pathogenesis of medulloblastoma. *UpToDate. UpToDate; Waltham, MA:[Accessed on April 18, 2015].[Google Scholar]* **2013**.

119. Pomeroy, S. L.; Wen, P. Y.; Gajjar, A., Clinical presentation, diagnosis, and risk stratification of medulloblastoma. *Waltham, MA* **2014**.

120. Sturm, D.; Pfister, S. M.; Jones, D. T. W., Pediatric gliomas: current concepts on diagnosis, biology, and clinical management. *Journal of Clinical Oncology* **2017,** *35* (21), 2370-2377.

121. Marini, B. L.; Benitez, L. L.; Zureick, A. H.; Salloum, R.; Gauthier, A. C.; Brown, J.; Wu, Y.-M.; Robinson, D. R.; Kumar, C.; Lonigro, R., Blood-brain barrier–adapted precision medicine therapy for pediatric brain tumors. *Translational Research* **2017,** *188*, 27. e1-27. e14.

122. Wu, L.; Li, X.; Janagam, D. R.; Lowe, T. L., Overcoming the blood-brain barrier in chemotherapy treatment of pediatric brain tumors. *Pharmaceutical research* **2014,** *31* (3), 531-540.

123. Schwalbe, E. C.; Lindsey, J. C.; Nakjang, S.; Crosier, S.; Smith, A. J.; Hicks, D.; Rafiee, G.; Hill, R. M.; Iliasova, A.; Stone, T., Novel molecular subgroups for clinical classification and outcome prediction in childhood medulloblastoma: a cohort study. *The Lancet Oncology* **2017,** *18* (7), 958-971.

124. Cho, Y.-J.; Tsherniak, A.; Tamayo, P.; Santagata, S.; Ligon, A.; Greulich, H.; Berhoukim, R.; Amani, V.; Goumnerova, L.; Eberhart, C. G., Integrative genomic analysis of medulloblastoma identifies a molecular subgroup that drives poor clinical outcome. *Journal of Clinical Oncology* **2011,** *29* (11), 1424.

125. Northcott, P. A.; Korshunov, A.; Witt, H.; Hielscher, T.; Eberhart, C. G.; Mack, S.; Bouffet, E.; Clifford, S. C.; Hawkins, C. E.; French, P., Medulloblastoma comprises four distinct molecular variants. *Journal of clinical oncology* **2011,** *29* (11), 1408.

126. Kool, M.; Korshunov, A.; Remke, M.; Jones, D. T. W.; Schlanstein, M.; Northcott, P. A.; Cho, Y.-J.; Koster, J.; Schouten-van Meeteren, A.; Van Vuurden, D., Molecular subgroups of medulloblastoma: an international meta-analysis of transcriptome, genetic aberrations, and clinical data of WNT, SHH, Group 3, and Group 4 medulloblastomas. *Acta neuropathologica* **2012,** *123* (4), 473-484.

127. Northcott, P. A.; Shih, D. J. H.; Peacock, J.; Garzia, L.; Morrissy, A. S.; Zichner, T.; Stütz, A. M.; Korshunov, A.; Reimand, J.; Schumacher, S. E., Subgroup-specific structural variation across 1,000 medulloblastoma genomes. *Nature* **2012,** *488* (7409), 49-56.

128. Pugh, T. J.; Weeraratne, S. D.; Archer, T. C.; Krummel, D. A. P.; Auclair, D.; Bochicchio, J.; Carneiro, M. O.; Carter, S. L.; Cibulskis, K.; Erlich, R. L., Medulloblastoma exome sequencing uncovers subtype-specific somatic mutations. *Nature* **2012,** *488* (7409), 106-110.

129. Cavalli, F. M. G.; Remke, M.; Rampasek, L.; Peacock, J.; Shih, D. J. H.; Luu, B.; Garzia, L.; Torchia, J.; Nor, C.; Morrissy, A. S., Intertumoral heterogeneity within medulloblastoma subgroups. *Cancer cell* **2017,** *31* (6), 737-754. e6.

130. Gessi, M.; von Bueren, A. O.; Rutkowski, S.; Pietsch, T., p53 expression predicts dismal outcome for medulloblastoma patients with metastatic disease. *Journal of neuro-oncology* **2012,** *106* (1), 135-141.

131. Northcott, P. A.; Buchhalter, I.; Morrissy, A. S.; Hovestadt, V.; Weischenfeldt, J.; Ehrenberger, T.; Gröbner, S.; Segura-Wang, M.; Zichner, T.; Rudneva, V. A., The whole-genome landscape of medulloblastoma subtypes. *Nature* **2017,** *547* (7663), 311-317.

132. Sengupta, S.; Weeraratne, S. D.; Sun, H.; Phallen, J.; Rallapalli, S. K.; Teider, N.; Kosaras, B.; Amani, V.; Pierre-Francois, J.; Tang, Y., α5-GABAA receptors negatively regulate MYC-amplified medulloblastoma growth. *Acta neuropathologica* **2014,** *127* (4), 593-603.

133. Kallay, L.; Keskin, H.; Ross, A.; Rupji, M.; Moody, O. A.; Wang, X.; Li, G.; Ahmed, T.; Rashid, F.; Stephen, M. R., Modulating native GABA A receptors in medulloblastoma with positive allosteric benzodiazepine-derivatives induces cell death. *Journal of neuro-oncology* **2019,** *142* (3), 411-422.

134. Jonas, O.; Landry, H. M.; Fuller, J. E.; Santini, J. T.; Baselga, J.; Tepper, R. I.; Cima, M. J.; Langer, R., An implantable microdevice to perform high-throughput in vivo drug sensitivity testing in tumors. *Science translational medicine* **2015,** *7* (284), 284ra57-284ra57.

135. Bandopadhayay, P.; Bergthold, G.; Nguyen, B.; Schubert, S.; Gholamin, S.; Tang, Y.; Bolin, S.; Schumacher, S. E.; Zeid, R.; Masoud, S., BET bromodomain inhibition of MYC-amplified medulloblastoma. *Clinical Cancer Research* **2014,** *20* (4), 912-925.

136. Bai, R.-Y.; Staedtke, V.; Rudin, C. M.; Bunz, F.; Riggins, G. J., Effective treatment of diverse medulloblastoma models with mebendazole and its impact on tumor angiogenesis. *Neuro-oncology* **2015,** *17* (4), 545-554.

137. Roberts, S. S.; Mori, M.; Pattee, P.; Lapidus, J.; Mathews, R.; O'Malley, J. P.; Hsieh, Y. C.; Turner, M. A.; Wang, Z.; Tian, Q., GABAergic system gene expression predicts clinical outcome in patients with neuroblastoma. *Journal of clinical oncology* **2004,** *22* (20), 4127-4134.

138. Hiyama, E.; Hiyama, K.; Nishiyama, M.; Reynolds, C. P.; Shay, J. W.; Yokoyama, T., Differential gene expression profiles between neuroblastomas with high telomerase activity and low telomerase activity. *Journal of pediatric surgery* **2003,** *38* (12), 1730-1734.

139. Al-Wadei, H. A. N.; Al-Wadei, M. H.; Ullah, M. F.; Schuller, H. M., Celecoxib and GABA cooperatively prevent the progression of pancreatic cancer in vitro and in xenograft models of stress-free and stress-exposed mice. *PLoS One* **2012,** *7* (8), e43376.

140. Jonas, O.; Calligaris, D.; Methuku, K. R.; Poe, M. M.; Francois, J. P.; Tranghese, F.; Changelian, A.; Sieghart, W.; Ernst, M.; Pomeranz Krummel, D. A., First in vivo testing of compounds targeting group 3 medulloblastomas using an implantable microdevice as a new paradigm for drug development. *Journal of biomedical nanotechnology* **2016,** *12* (6), 1297-1302.

141. Frangou, S., Schizophrenia. Medicine, 2008; Vol. 36, pp 405-409.

142. Kapur, S.; Mamo, D., Half a century of antipsychotics and still a central role for dopamine D2 receptors. *Prog Neuropsychopharmacol Biol Psychiatry* **2003,** *27* (7), 1081-90.

143. Leucht, S.; Corves, C.; Arbter, D.; Engel, R. R.; Li, C.; Davis, J. M., Second-generation versus first-generation antipsychotic drugs for schizophrenia: a meta-analysis. *The Lancet* **2009,** *373* (9657), 31-41.

144. Longo, L. P.; Johnson, B., Addiction: Part I. Benzodiazepines-side effects, abuse risk and alternatives. *American family physician* **2000,** *61* (7), 2121.

145. Wassef, A.; Baker, J.; Kochan, L. D., GABA and schizophrenia: a review of basic science and clinical studies. *Journal of clinical psychopharmacology* **2003,** *23* (6), 601-640.

146. Fee, C.; Banasr, M.; Sibille, E., Somatostatin-Positive Gamma-Aminobutyric Acid Interneuron Deficits in Depression: Cortical Microcircuit and Therapeutic Perspectives. *Biological psychiatry* **2017,** *82* (8), 549-559.

147. Landoni, M. F.; Soraci, A., Pharmacology of chiral compounds 2-arylpropionic acid derivatives. *Current drug metabolism* **2001,** *2* (1), 37-51.

148. Patocka, J.; Ales, D., *Biomedical aspects of chiral molecules*. 2004; Vol. 2.

149. Gill, K. M.; Cook, J. M.; Poe, M. M.; Grace, A. A., Prior Antipsychotic Drug Treatment Prevents Response to Novel Antipsychotic Agent in the Methylazoxymethanol Acetate Model of Schizophrenia. *Schizophrenia Bulletin* **2014,** *40* (2), 341-350.

150. Gill, K. M.; Lodge, D. J.; Cook, J. M.; Aras, S.; Grace, A. A., A Novel α5GABA(A)R-Positive Allosteric Modulator Reverses Hyperactivation of the Dopamine System in the MAM Model of Schizophrenia. *Neuropsychopharmacology* **2011,** *36* (9), 1903-1911.

151. Piantadosi, S. C.; French, B. J.; Poe, M. M.; Timic, T.; Markovic, B. D.; Pabba, M.; Seney, M. L.; Oh, H.; Orser, B. A.; Savic, M. M.; Cook, J. M.; Sibille, E., Sex-Dependent Anti-Stress Effect of an alpha5 Subunit Containing GABAA Receptor Positive Allosteric Modulator. *Front Pharmacol* **2016,** *7*, 446.

152. Batinic, B.; Santrac, A.; Jancic, I.; Li, G.; Vidojevic, A.; Markovic, B.; Cook, J. M.; Savic, M. M., Positive modulation of alpha5 GABAA receptors in preadolescence prevents reduced locomotor response to amphetamine in adult female but not male rats prenatally exposed to lipopolysaccharide. *Int J Dev Neurosci* **2017,** *61*, 31-39.

153. Forkuo, G. S.; Nieman, A. N.; Yuan, N. Y.; Kodali, R.; Yu, O. B.; Zahn, N. M.; Jahan, R.; Li, G.; Stephen, M. R.; Guthrie, M. L.; Poe, M. M.; Hartzler, B. D.; Harris, T. W.; Yocum, G. T.; Emala, C. W.; Steeber, D. A.; Stafford, D. C.; Cook, J. M.; Arnold, L. A., Alleviation of Multiple Asthmatic Pathologic Features with Orally Available and Subtype Selective GABAA Receptor Modulators. *Molecular Pharmaceutics* **2017,** *14* (6), 2088-2098.

154. Savić, M. M.; Majumder, S.; Huang, S.; Edwankar, R. V.; Furtmüller, R.; Joksimović, S.; Clayton, T.; Ramerstorfer, J.; Milinković, M. M.; Roth, B. L.; Sieghart, W.; Cook, J. M., NOVEL POSITIVE ALLOSTERIC MODULATORS OF GABAA RECEPTORS: DO SUBTLE DIFFERENCES IN ACTIVITY AT α1 PLUS α5 VERSUS α2 PLUS α3 SUBUNITS ACCOUNT FOR DISSIMILARITIES IN BEHAVIORAL EFFECTS IN RATS? *Prog. Neuropsychopharmacol. Biol. Psychiatry* **2010,** *34* (2), 376-386.

155. Richetto, J.; Labouesse, M. A.; Poe, M. M.; Cook, J. M.; Grace, A. A.; Riva, M. A.; Meyer, U., Behavioral Effects of the Benzodiazepine-Positive Allosteric Modulator SH-053-2'F-S-CH3 in an Immune-Mediated Neurodevelopmental Disruption Model. *International Journal of Neuropsychopharmacology* **2015,** *18* (4), pyu055-pyu055.

156. Takai, S.; Matsuda, A.; Usami, Y.; Adachi, T.; Sugiyama, T.; Katagiri, Y.; Tatematsu, M.; Hirano, K., Hydrolytic Profile for Ester- or Amide-linkage by Carboxylesterases pI 5.3 and 4.5 from Human Liver. *Biological & Pharmaceutical Bulletin* **1997,** *20* (8), 869-873.

157. Batinić, B.; Santrač, A.; Jančić, I.; Li, G.; Vidojević, A.; Marković, B.; Cook, J. M.; Savić, M. M., Positive modulation of α5 GABAA receptors in preadolescence prevents reduced locomotor response to amphetamine in adult female but not male rats prenatally exposed to lipopolysaccharide. *International Journal of Developmental Neuroscience* **2017,** *61* (Supplement C), 31-39.

158. Fischer, B. D.; Schlitt, R. J.; Hamade, B. Z.; Rehman, S.; Ernst, M.; Poe, M. M.; Li, G.; Kodali, R.; Arnold, L. A.; Cook, J. M., Pharmacological and antihyperalgesic properties of the novel α2/3 preferring GABAA receptor ligand MP-III-024. *Brain Research Bulletin* **2017,** *131* (Supplement C), 62-69.

159. Witkin, J. M.; Cerne, R.; Wakulchik, M.; S, J.; Gleason, S. D.; Jones, T. M.; Li, G.; Arnold, L. A.; Li, J. X.; Schkeryantz, J. M.; Methuku, K. R.; Cook, J. M.; Poe, M. M., Further evaluation of the potential anxiolytic activity of imidazo[1,5-a][1,4]diazepin agents selective for α2/3-containing GABAA receptors. *Pharmacology Biochemistry and Behavior* **2017,** *157* (Supplement C), 35-40.

160. Fier, P. S.; Whittaker, A. M., An Atom-Economical Method To Prepare Enantiopure Benzodiazepines with N-Carboxyanhydrides. *Organic letters* **2017,** *19* (6), 1454-1457.

161. Bailey, J. L., 679. The synthesis of simple peptides from anhydro-N-carboxyamino-acids. *Journal of the Chemical Society (Resumed)* **1950**, 3461-3466.

162. Brenner, M.; Photaki, I., Zur Herstellung der Chlorid-hydrochloride der α-Aminosäuren. *Helvetica Chimica Acta* **1956,** *39* (6), 1525-1528.

163. Daly, W. H.; Poché, D., The preparation of N-carboxyanhydrides of α-amino acids using bis (trichloromethyl) carbonate. *Tetrahedron Letters* **1988,** *29* (46), 5859-5862.

164. Van Dijk-Wolthuis, W. N. E.; van de Water, L.; van de Wetering, P.; Van Steenbergen, M. J.; Kettenes-van den Bosch, J. J.; Schuyl, W. J. W.; Hennink, W. E., Synthesis and characterization of poly-L-lysine with controlled low molecular weight. *Macromolecular Chemistry and Physics* **1997,** *198* (12), 3893-3906.

165. Wilder, R.; Mobashery, S., The use of triphosgene in preparation of N-carboxy. alpha.-amino acid anhydrides. *The Journal of Organic Chemistry* **1992,** *57* (9), 2755-2756.

166. Papi, A.; Brightling, C.; Pedersen, S. E.; Reddel, H. K., Asthma. *The Lancet* **2018,** *391* (10122), 783-800.

167. Adcock, I. M.; Caramori, G.; Chung, K. F., New targets for drug development in asthma. *The Lancet* **2008,** *372* (9643), 1073-1087.

168. Trevor, J. L.; Chipps, B. E., Severe Asthma in Primary Care: Identification and Management. *The American Journal of Medicine* **2018,** *131* (5), 484-491.

169. McCracken, J. L.; Veeranki, S. P.; Ameredes, B. T.; Calhoun, W. J., Diagnosis and Management of Asthma in Adults: A Review. *Jama* **2017,** *318* (3), 279-290.

170. Nunes, C.; Pereira, A. M.; Morais-Almeida, M., Asthma costs and social impact. *Asthma research and practice* **2017,** *3*, 1-1.

171. Shimizu, T., Mucus, Goblet Cell, Submucosal Gland. In *Nasal Physiology and Pathophysiology of Nasal Disorders*, Önerci, T. M., Ed. Springer Berlin Heidelberg: Berlin, Heidelberg, 2013; pp 1-14.

172. Rydell-Törmänen, K.; Risse, P.-A.; Kanabar, V.; Bagchi, R.; Czubryt, M. P.; Johnson, J. R., Smooth muscle in tissue remodeling and hyper-reactivity: Airways and arteries. *Pulmonary Pharmacology & Therapeutics* **2013,** *26* (1), 13-23.

173. Barnes, P. J., Pharmacology of airway smooth muscle. *Am J Respir Crit Care Med* **1998,** *158* (5 Pt 3), S123-32.

174. Pascoe, C. D.; Wang, L.; Syyong, H. T.; Par; #xe9; , P. D., A Brief History of Airway Smooth Muscle's Role in Airway Hyperresponsiveness. *Journal of Allergy* **2012,** *2012*, 8.

175. Bush, A.; Pedersen, S.; Hedlin, G.; Baraldi, E.; Barbato, A.; de Benedictis, F.; Lødrup Carlsen, K. C.; de Jongste, J.; Piacentini, G., Pharmacological treatment of severe, therapy-resistant asthma in children: what can we learn from where? *European Respiratory Journal* **2011,** *38* (4), 947.

176. Kew, K. M.; Dahri, K., Long-acting muscarinic antagonists (LAMA) added to combination long-acting beta2-agonists and inhaled corticosteroids (LABA/ICS) versus LABA/ICS for adults with asthma. *Cochrane Database Syst Rev* **2016,** (1), Cd011721.

177. D'Urzo, A. D.; Chapman, K. R., Leukotriene-receptor antagonists. Role in asthma management. *Canadian family physician Medecin de famille canadien* **2000,** *46*, 872-879.

178. Barnes, P. J., Theophylline. *American Journal of Respiratory and Critical Care Medicine* **2013,** *188* (8), 901-906.

179. Polosa, R.; Morjaria, J., Immunomodulatory and biologic therapies for severe refractory asthma. *Respiratory Medicine* **2008,** *102* (11), 1499-1510.

180. Laxmanan, B.; Hogarth, D. K., Bronchial thermoplasty in asthma: current perspectives. *Journal of asthma and allergy* **2015,** *8*, 39-49.

181. Shirakawa, J.; Taniyama, K.; Tanaka, C., gamma-Aminobutyric acid-induced modulation of acetylcholine release from the guinea pig lung. *J Pharmacol Exp Ther* **1987,** *243* (1), 364-9.

182. Moore, C. T.; Wilson, C. G.; Mayer, C. A.; Acquah, S. S.; Massari, V. J.; Haxhiu, M. A., A GABAergic inhibitory microcircuit controlling cholinergic outflow to the airways. *J Appl Physiol (1985)* **2004,** *96* (1), 260-70.

183. Gallos, G.; Townsend, E.; Yim, P.; Virag, L.; Zhang, Y.; Xu, D.; Bacchetta, M.; Emala, C. W., Airway epithelium is a predominant source of endogenous airway GABA and contributes to relaxation of airway smooth muscle tone. *Am J Physiol Lung Cell Mol Physiol* **2013,** *304* (3), L191-7.

184. Gallos, G.; Gleason, N. R.; Zhang, Y.; Pak, S. W.; Sonett, J. R.; Yang, J.; Emala, C. W., Activation of endogenous GABAA channels on airway smooth muscle potentiates isoproterenol-mediated relaxation. *Am J Physiol Lung Cell Mol Physiol* **2008,** *295* (6), L1040-7.

185. Xiang, Y. Y.; Wang, S.; Liu, M.; Hirota, J. A.; Li, J.; Ju, W.; Fan, Y.; Kelly, M. M.; Ye, B.; Orser, B.; O'Byrne, P. M.; Inman, M. D.; Yang, X.; Lu, W. Y., A GABAergic system in airway epithelium is essential for mucus overproduction in asthma. *Nat Med* **2007,** *13* (7), 862-7.

186. Yocum, G. T.; Gallos, G.; Zhang, Y.; Jahan, R.; Stephen, M. R.; Varagic, Z.; Puthenkalam, R.; Ernst, M.; Cook, J. M.; Emala, C. W., Targeting the gamma-Aminobutyric Acid A Receptor alpha4 Subunit in Airway Smooth Muscle to Alleviate Bronchoconstriction. *Am J Respir Cell Mol Biol* **2016,** *54* (4), 546-53.

187. Jahan, R.; Stephen, M. R.; Forkuo, G. S.; Kodali, R.; Guthrie, M. L.; Nieman, A. N.; Yuan, N. Y.; Zahn, N. M.; Poe, M. M.; Li, G.; Yu, O. B.; Yocum, G. T.; Emala, C. W.; Stafford, D. C.; Cook, J. M.; Arnold, L. A., Optimization of substituted imidazodiazepines

as novel asthma treatments. *European Journal of Medicinal Chemistry* **2017,** *126* (Supplement C), 550-560.

188. Forkuo, G. S.; Guthrie, M. L.; Yuan, N. Y.; Nieman, A. N.; Kodali, R.; Jahan, R.; Stephen, M. R.; Yocum, G. T.; Treven, M.; Poe, M. M.; Li, G.; Yu, O. B.; Hartzler, B. D.; Zahn, N. M.; Ernst, M.; Emala, C. W.; Stafford, D. C.; Cook, J. M.; Arnold, L. A., Development of GABAA Receptor Subtype-Selective Imidazodiazepines as Novel Asthma Treatments. *Molecular Pharmaceutics* **2016,** *13* (6), 2026-2038.

189. Stamenic, T. T.; Poe, M. M.; Rehman, S.; Santrac, A.; Divovic, B.; Scholze, P.; Ernst, M.; Cook, J. M.; Savic, M. M., Ester to amide substitution improves selectivity, efficacy and kinetic behavior of a benzodiazepine positive modulator of GABAA receptors containing the alpha5 subunit. *Eur J Pharmacol* **2016,** *791*, 433-443.

190. Obradovic, A. L.; Joksimovic, S.; Batinic, B.; Radulovic, T.; Poe, M. M.; Namjoshi, O. A.; Cook, J. M.; Ramerstorfer, J.; Varagic, Z.; Sieghart, W.; Karovic, B.; Roth, B.; Savic, M. M., SH-I-048A, an *in vitro* nonselective super-agonist at the benzodiazepine site of $GABA_A$ receptors: the approximated activation of receptor subtypes may explain behavioral effects. *Brain Res.* **2014,** *1554*, 36 - 48.

191. Poe, M. M., Ph. D. Thesis: Synthesis of Subtype Selective Bz/GABAA Receptor Ligands for the Treatment of Anxiety, Epilepsy and Neuropathic Pain, as well as Schizophrenia and Asthma. University of Wisconsin Milwaukee. **2016**.

192. Roni, M. S. R.; Li, G.; Mikulsky, B. N.; Knutson, D. E.; Mian, M. Y.; Zahn, N. M.; Cook, J. M.; Stafford, D. C.; Arnold, L. A., The Effects of pH on the Structure and Bioavailability of Imidazodiazepine-3-Carboxylate MIDD0301. *Molecular pharmaceutics* **2020,** *17* (4), 1182-1192.

193. Chen, C.; Okayama, H., High-efficiency transformation of mammalian cells by plasmid DNA. *Molecular and cellular biology* **1987,** *7* (8), 2745.

194. Cheng, Y.-C.; Prusoff, W. H., Mouse ascites sarcoma 180 thymidylate kinase. General properties, kinetic analysis, and inhibition studies. *Biochemistry* **1973,** *12* (14), 2612-2619.

195. Riley, A. P.; Groer, C. E.; Young, D.; Ewald, A. W.; Kivell, B. M.; Prisinzano, T. E., Synthesis and κ-opioid receptor activity of furan-substituted salvinorin A analogues. *Journal of medicinal chemistry* **2014,** *57* (24), 10464-10475.

196. Crowley, R. S.; Riley, A. P.; Sherwood, A. M.; Groer, C. E.; Shivaperumal, N.; Biscaia, M.; Paton, K.; Schneider, S.; Provasi, D.; Kivell, B. M., Synthetic studies of neoclerodane diterpenes from salvia divinorum: identification of a potent and centrally acting μ opioid analgesic with reduced abuse liability. *Journal of medicinal chemistry* **2016,** *59* (24), 11027-11038.

197. Alexeev, M.; Grosenbaugh, D. K.; Mott, D. D.; Fisher, J. L., The natural products magnolol and honokiol are positive allosteric modulators of both synaptic and extra-synaptic GABAA receptors. *Neuropharmacology* **2012,** *62* (8), 2507-2514.

Appendix A

NMRs of FR-I-15

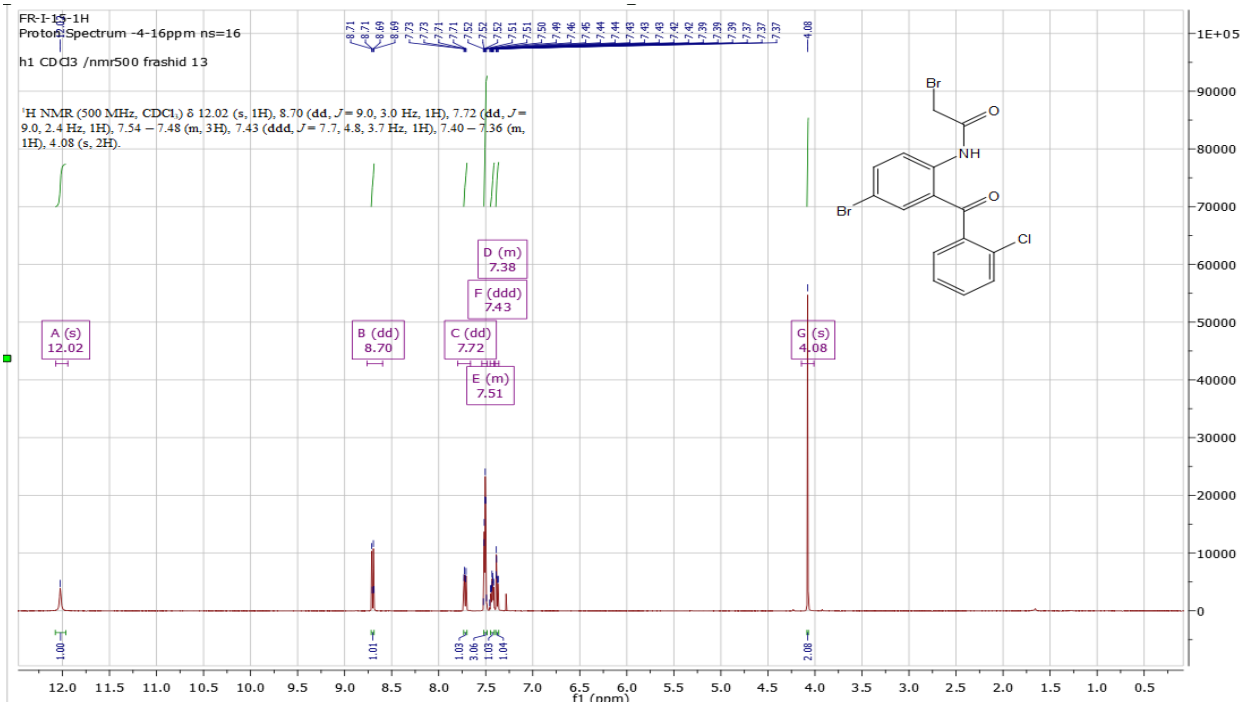

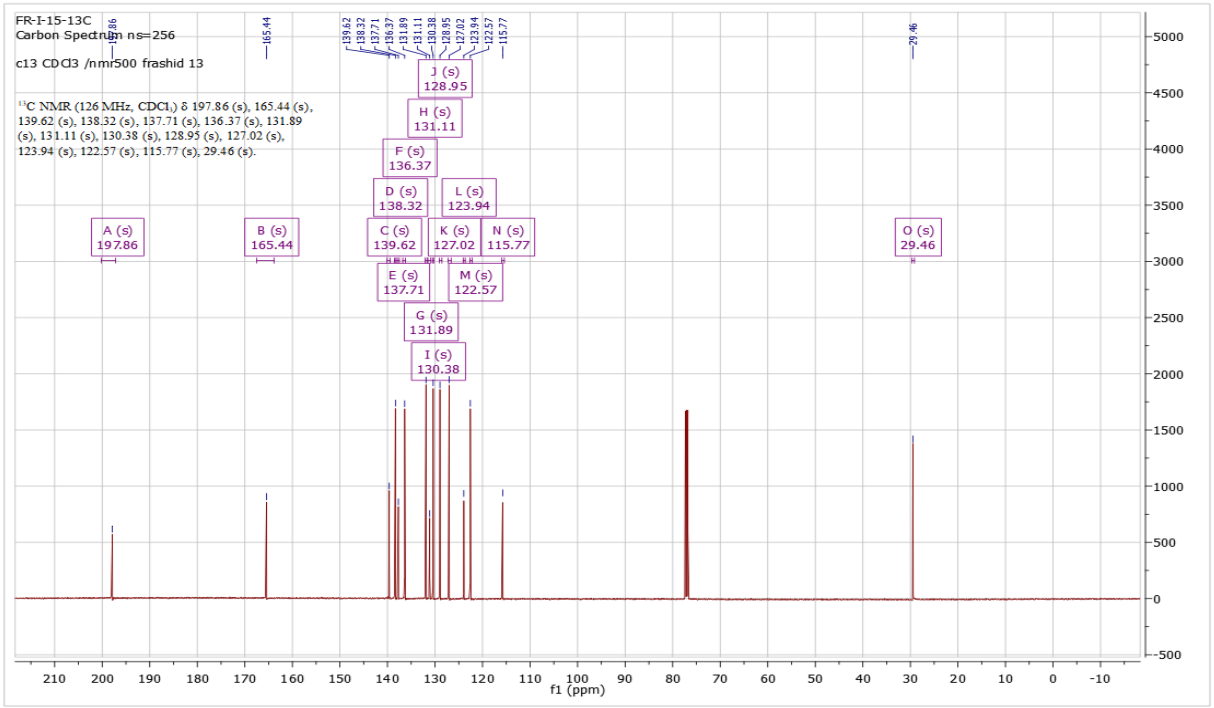

NMRs of FR-I-20

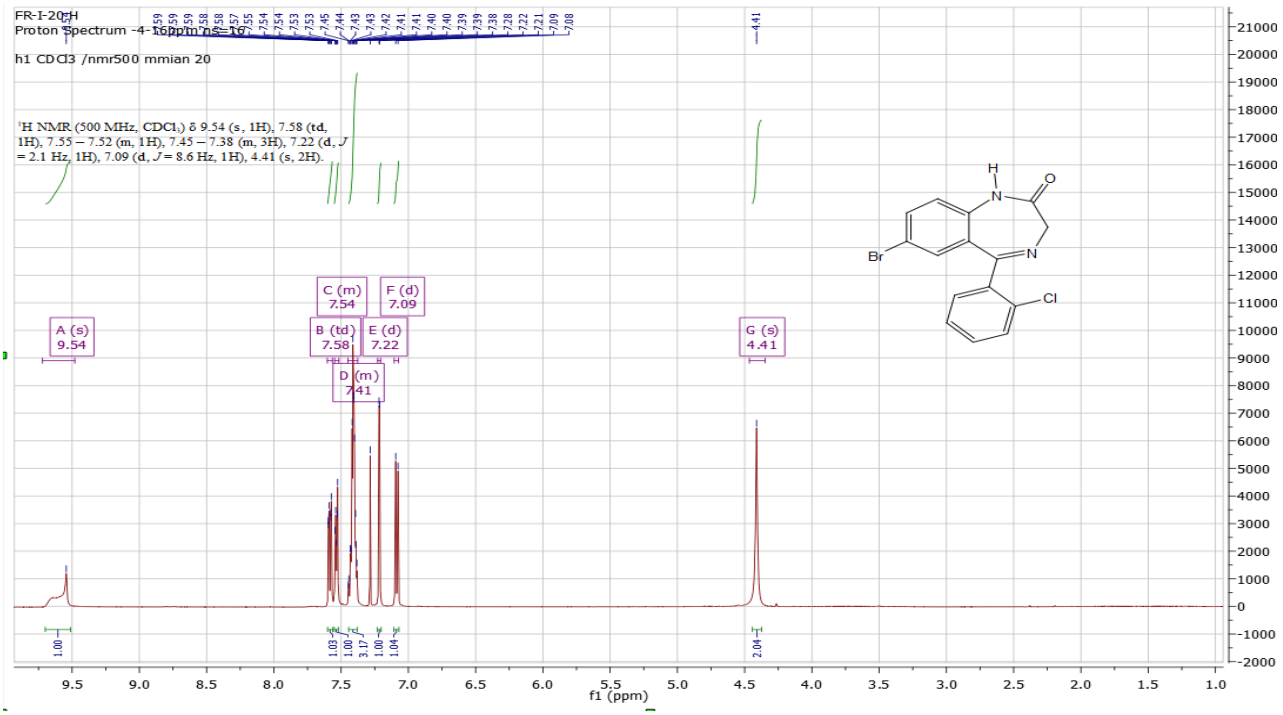

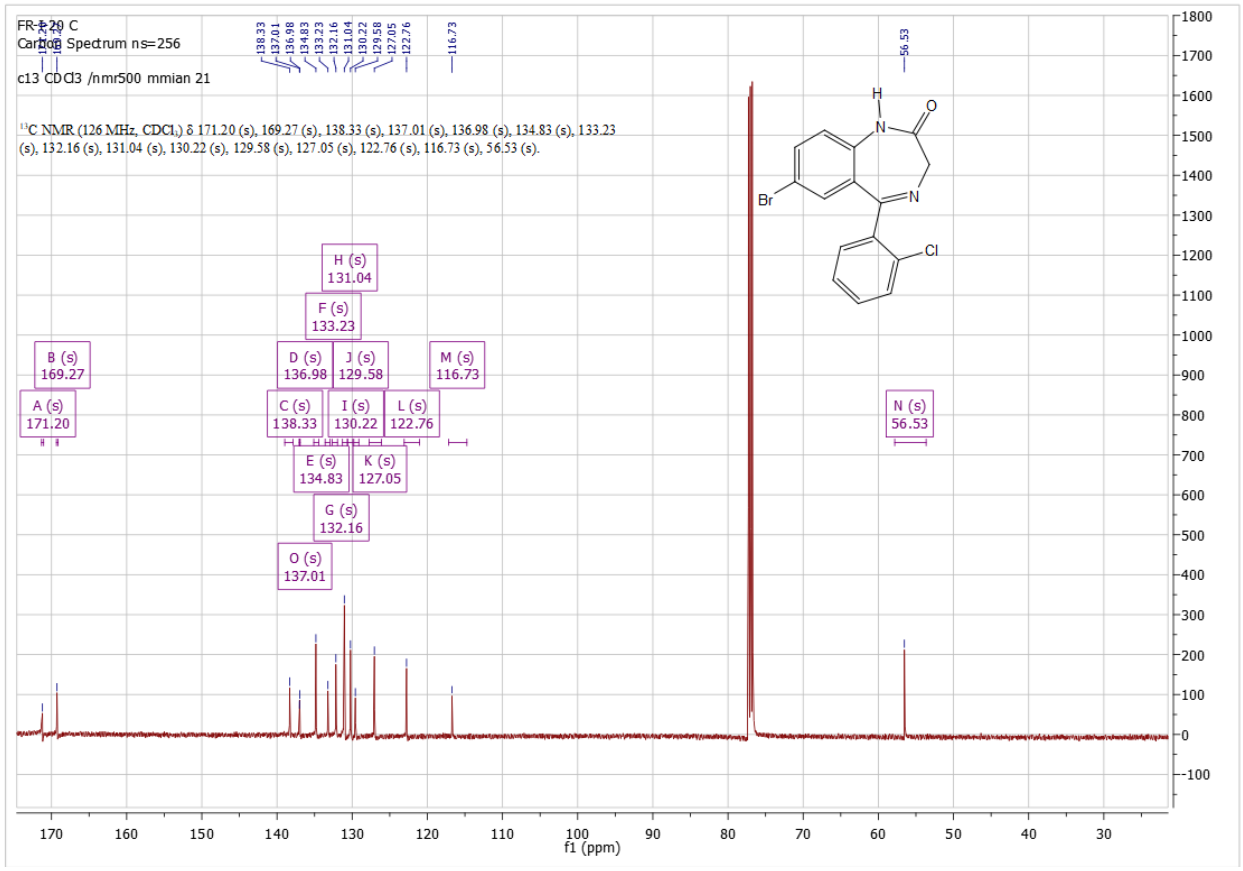

NMRs of FR-I-99

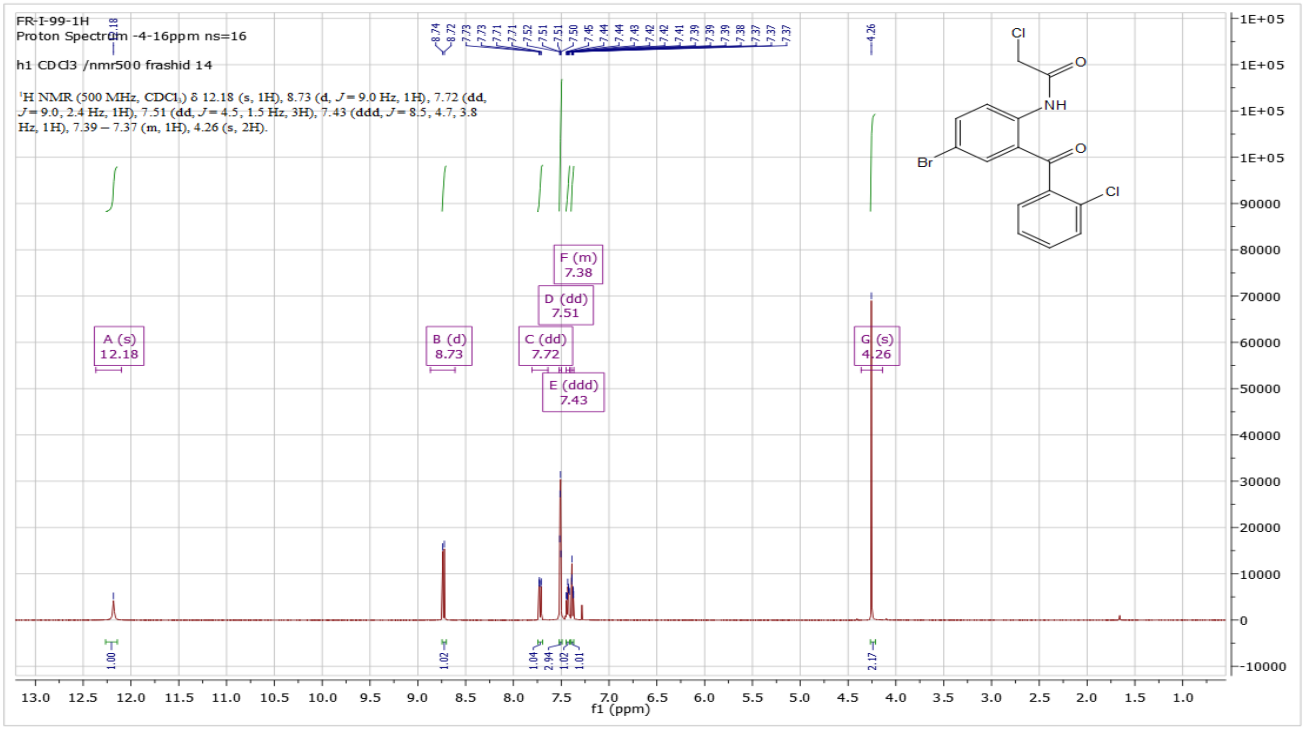

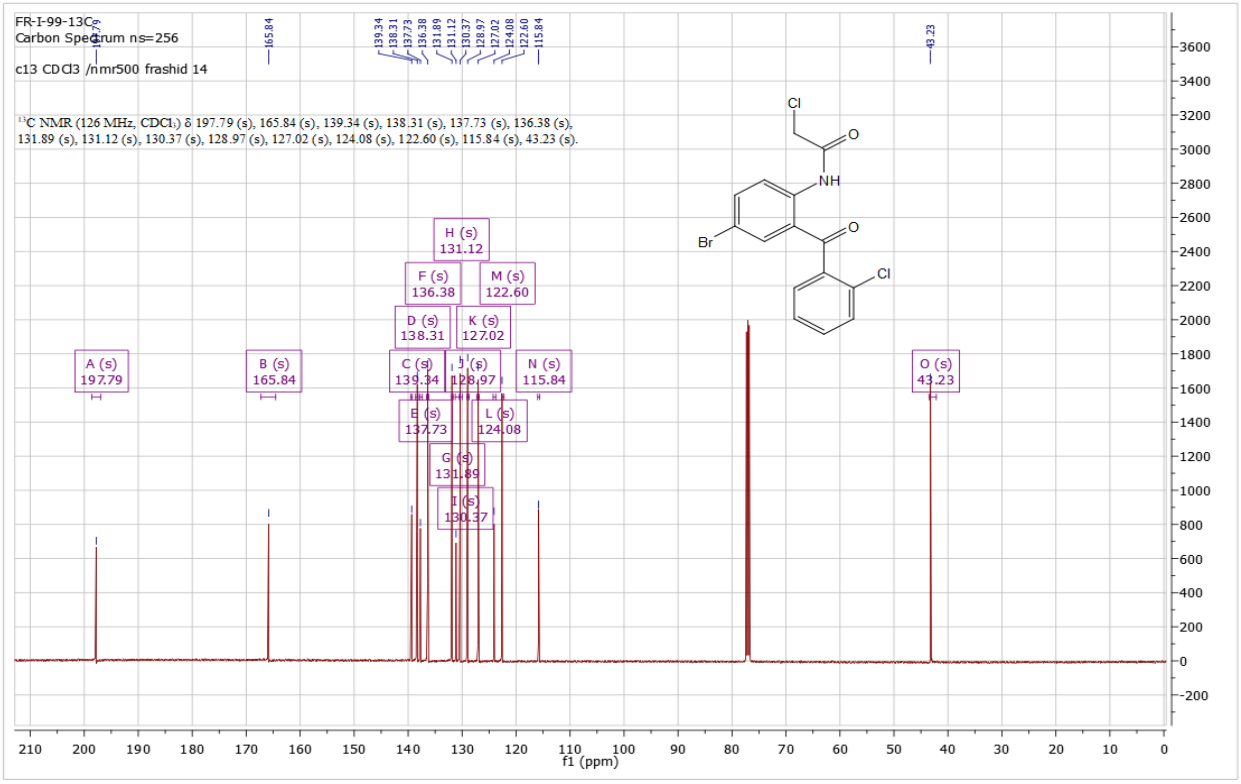

NMRs of FR-I-45

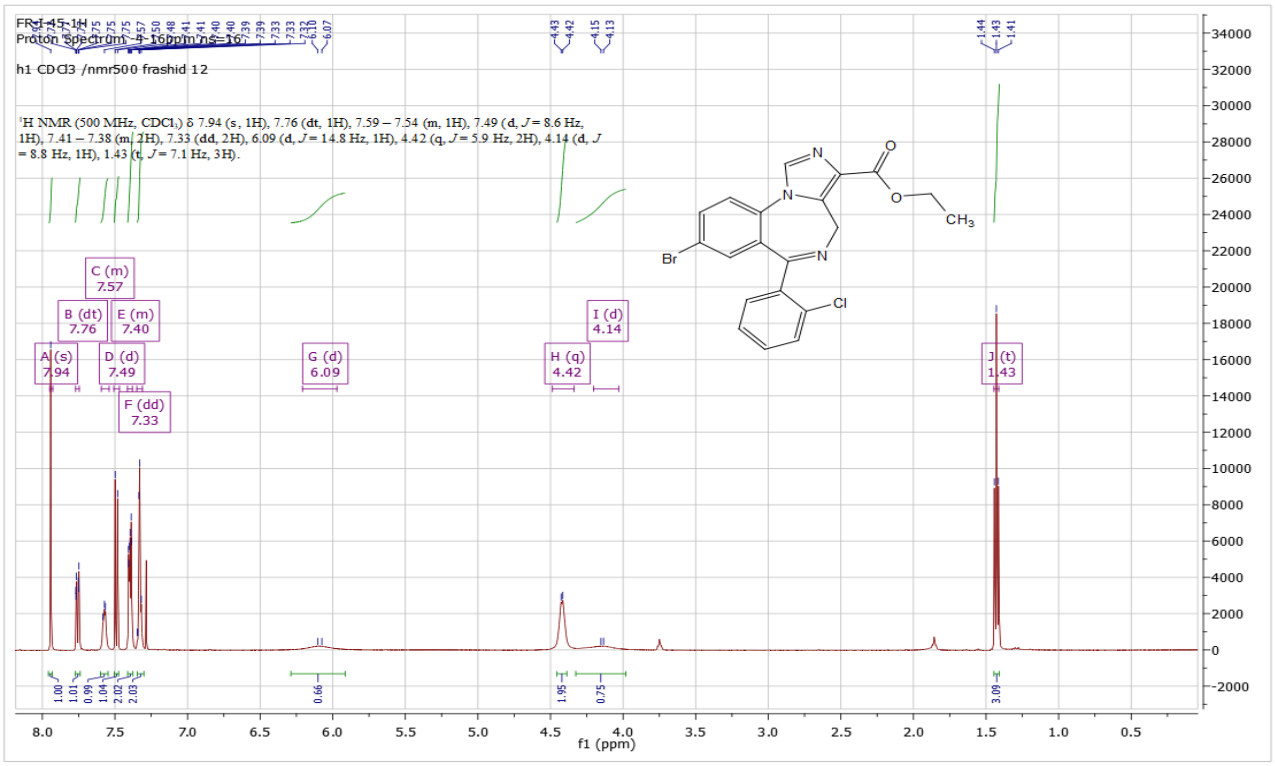

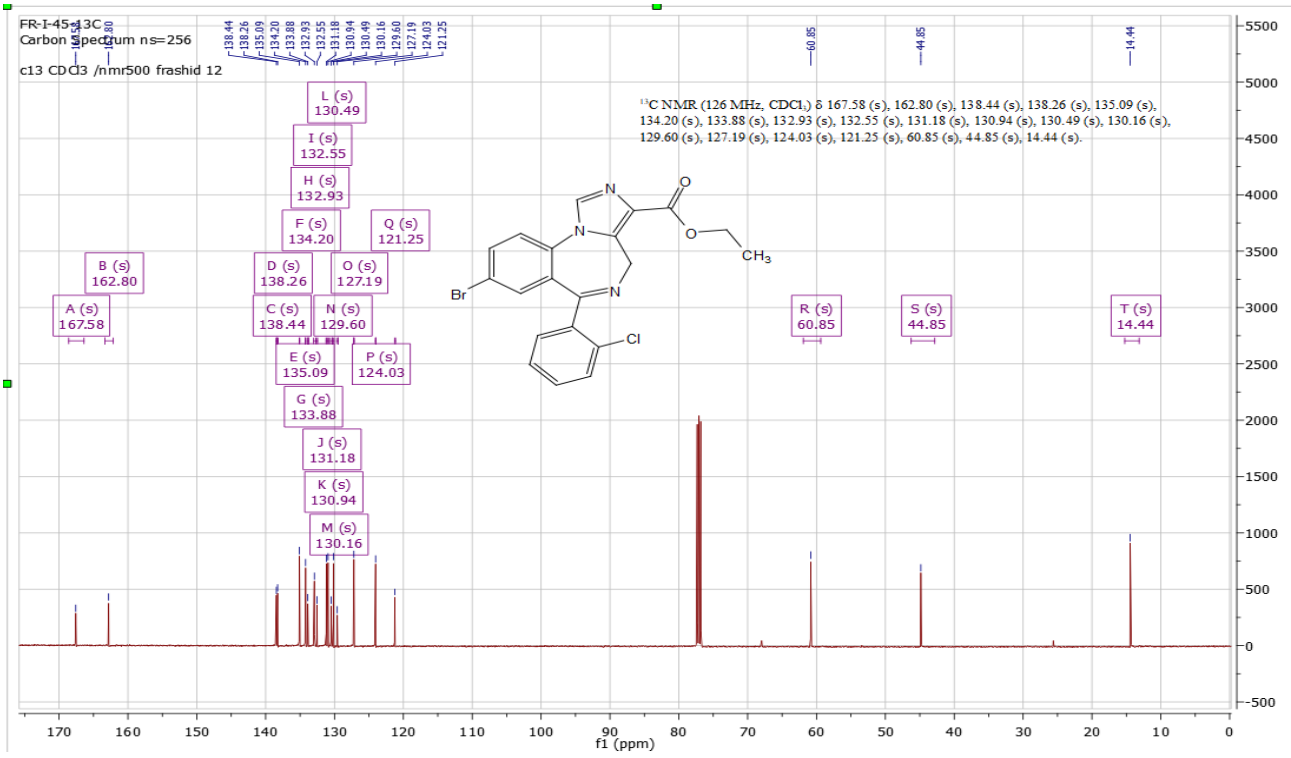

NMRs of FR-I-98

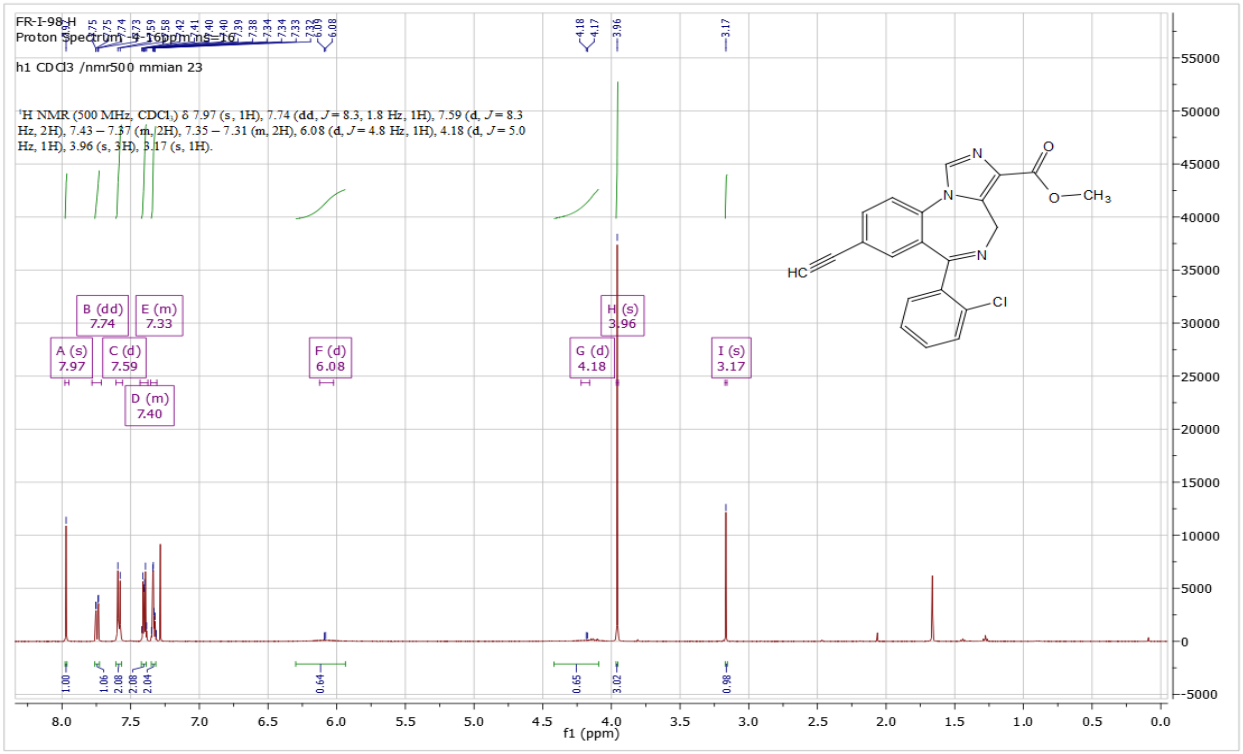

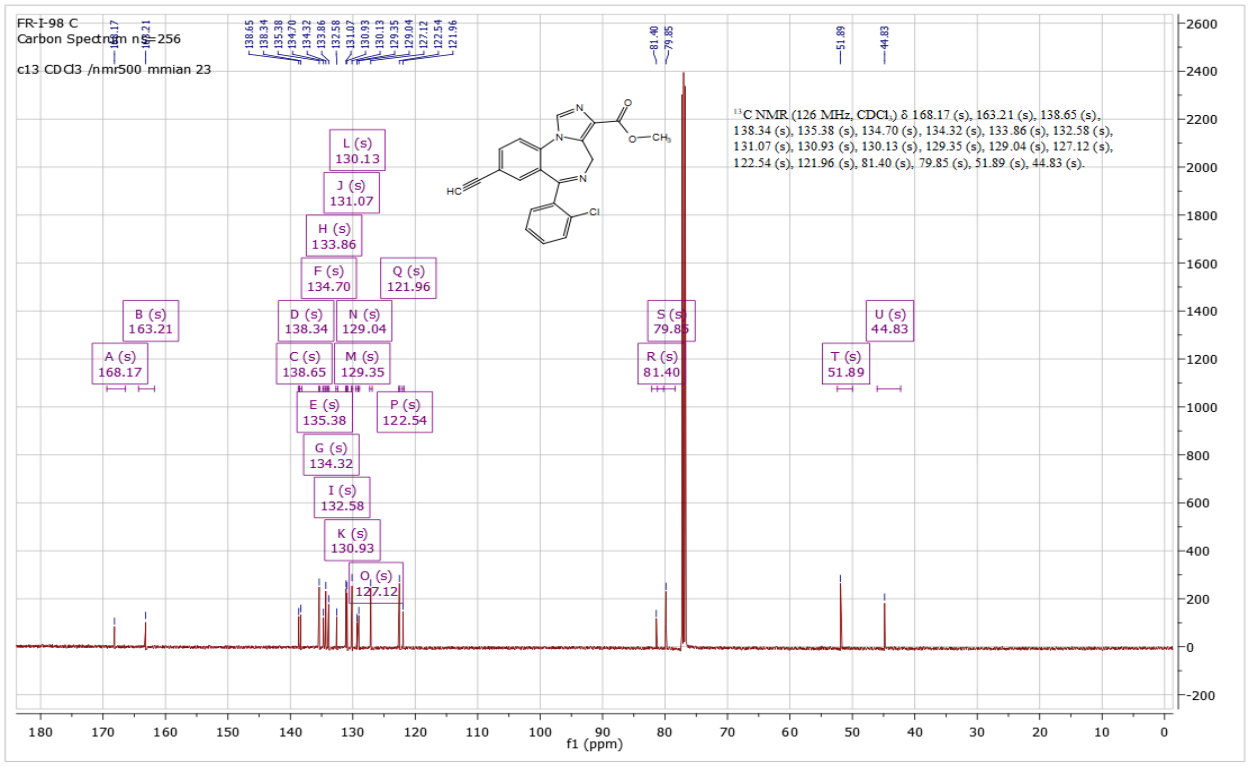

NMRs of FR_I_70

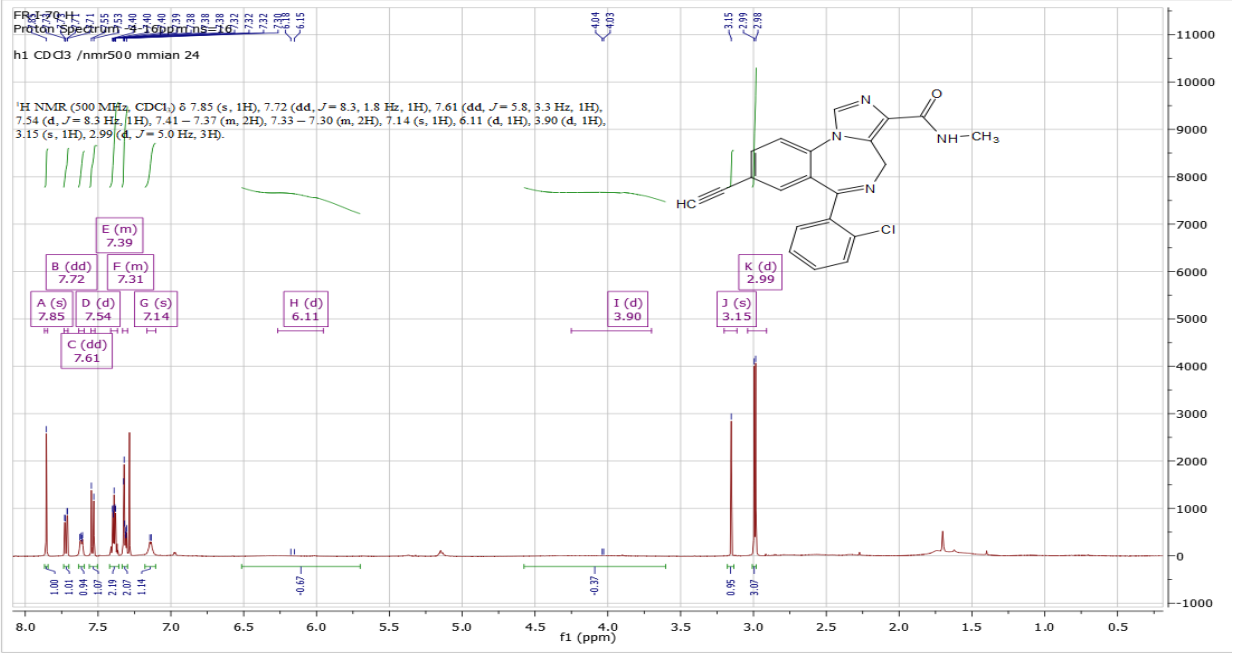

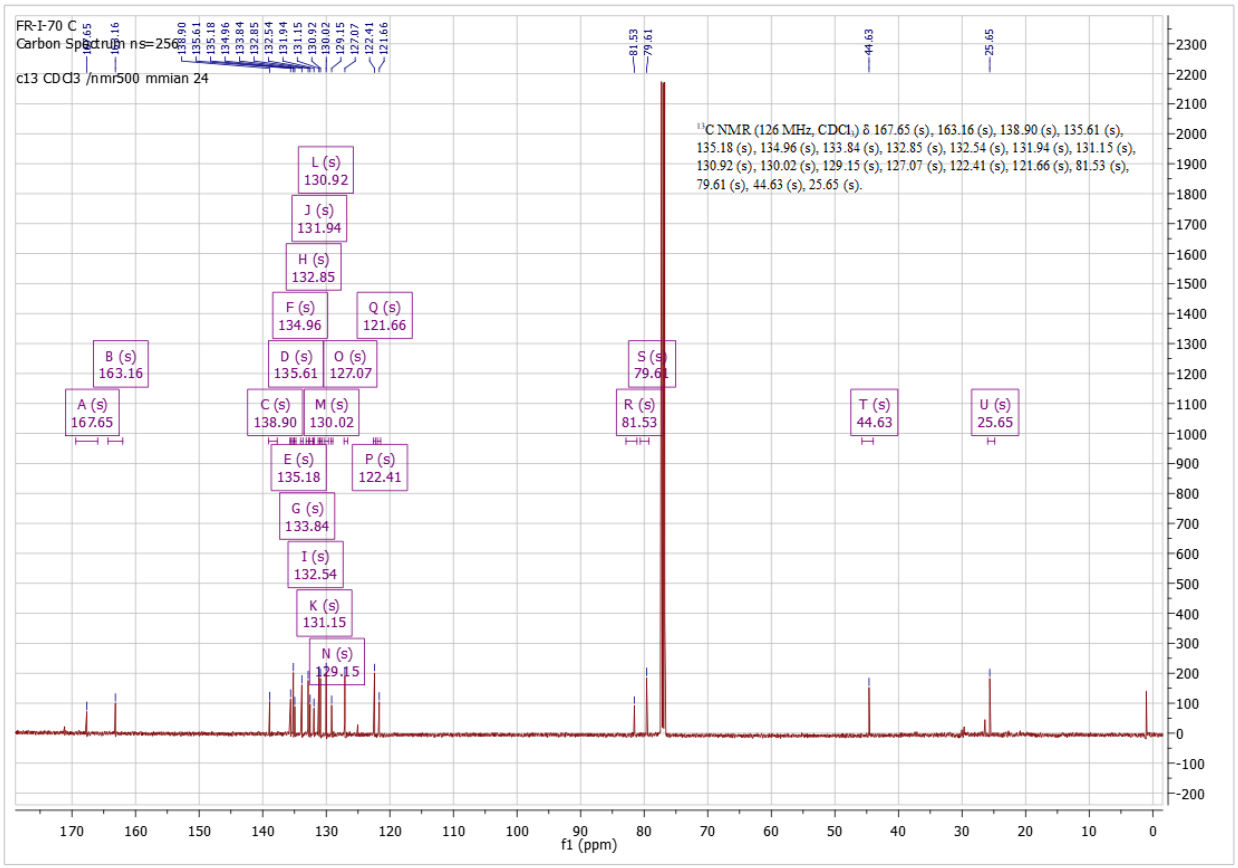

NMRs of FR-II-29

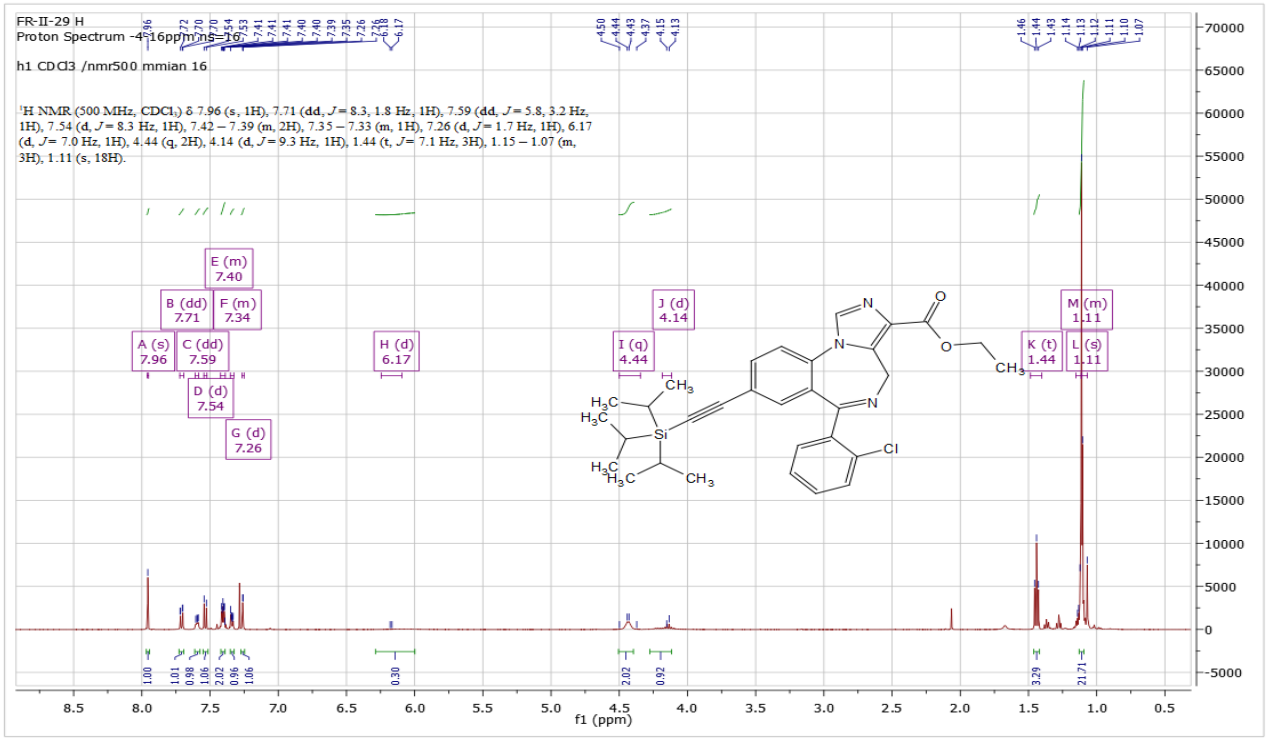

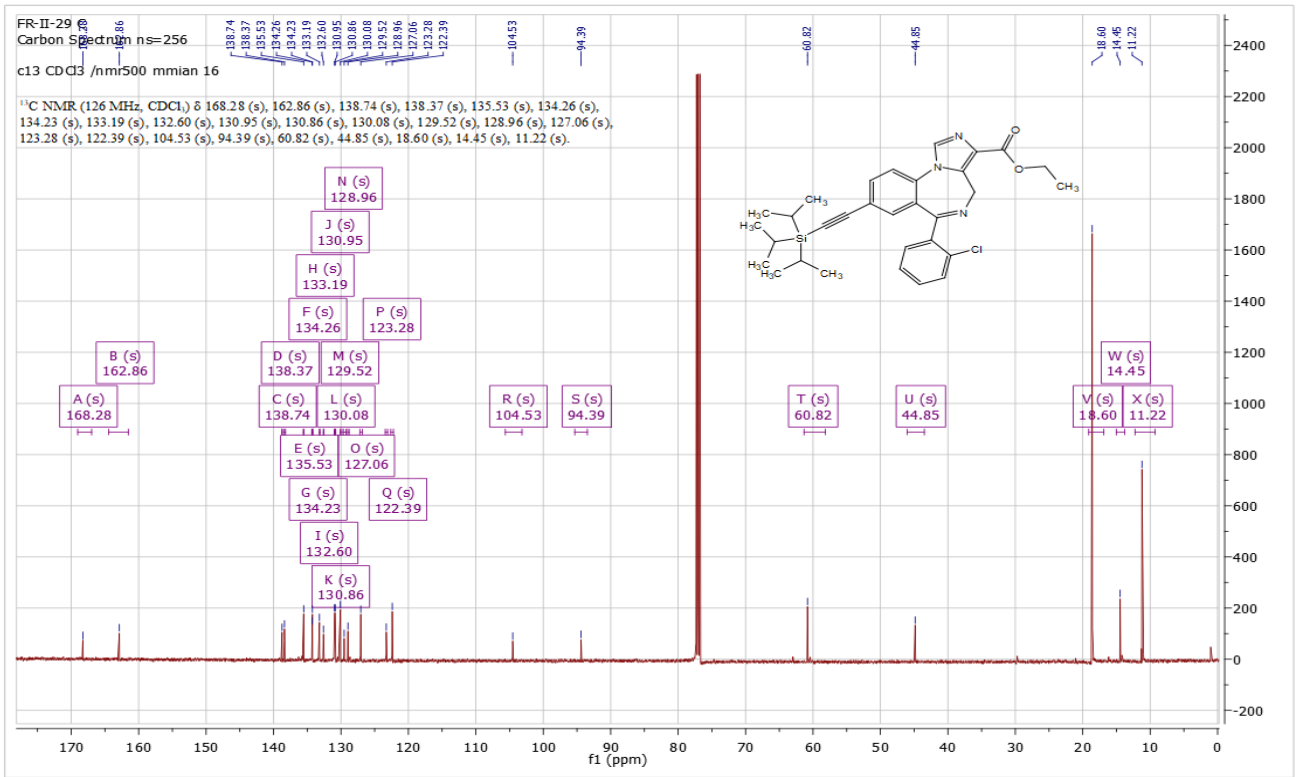

NMRs of FR-I-59

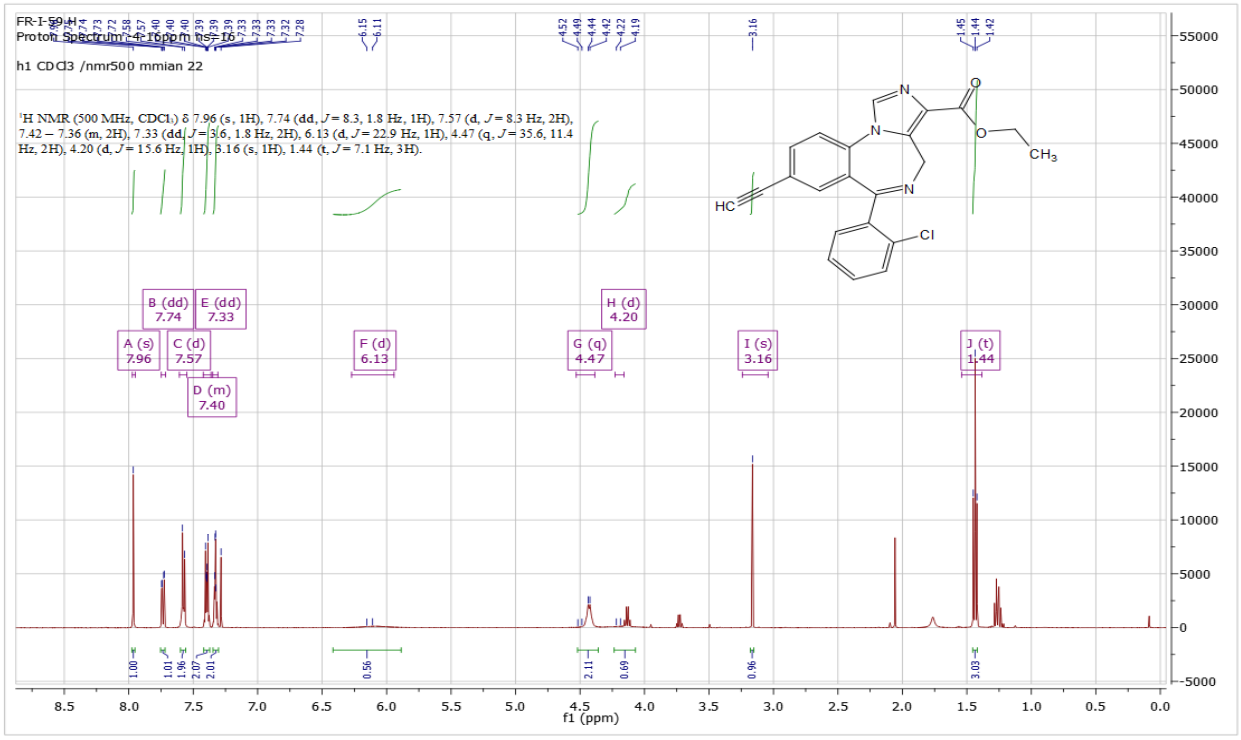

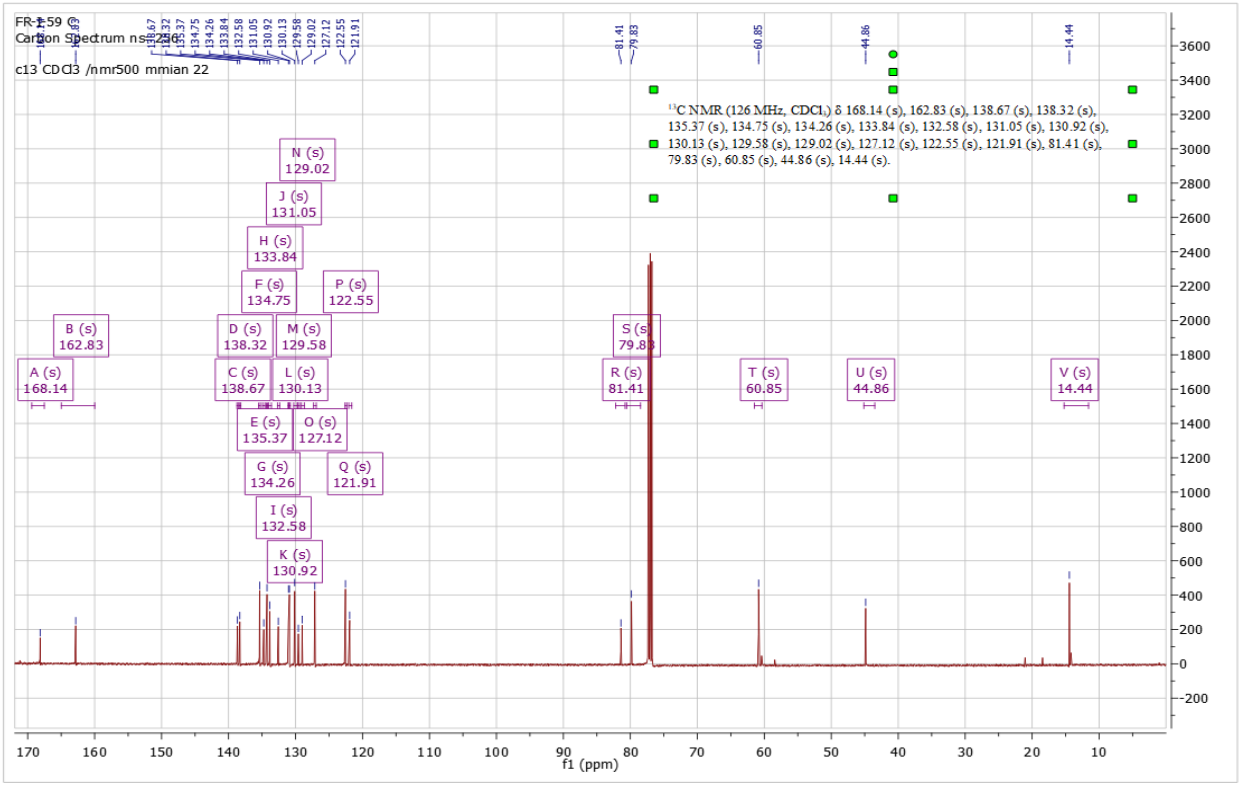

NMRs of FR-III-18

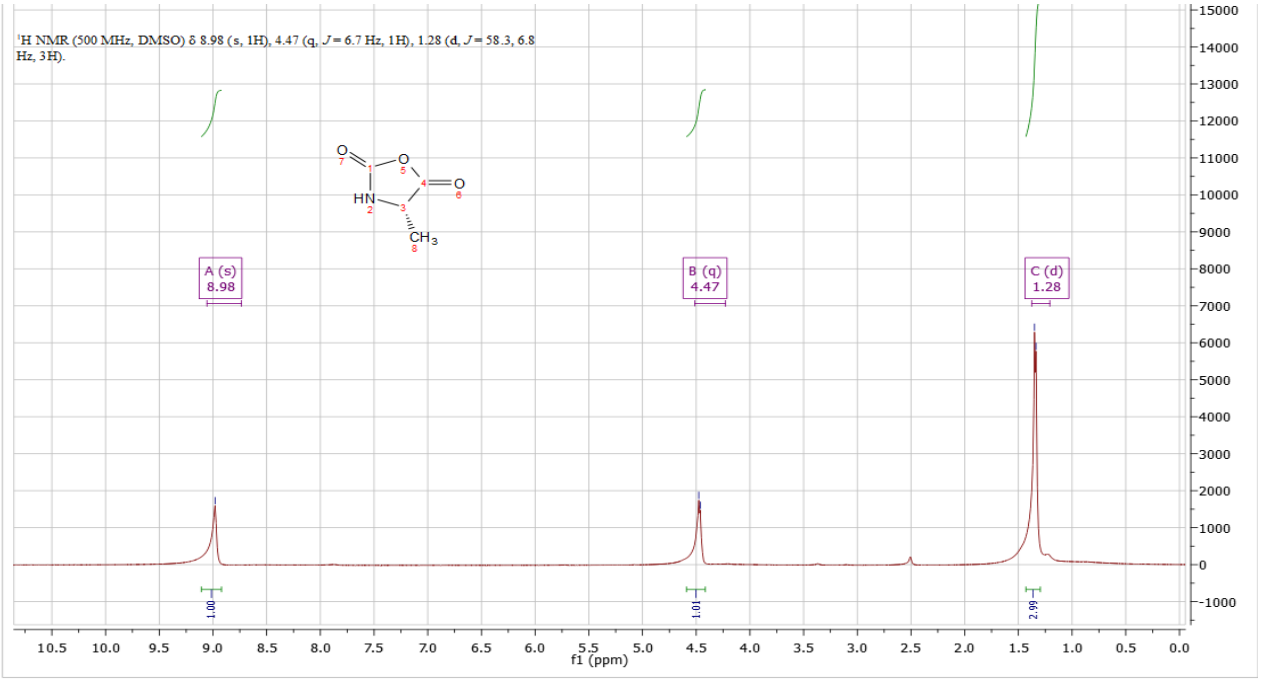

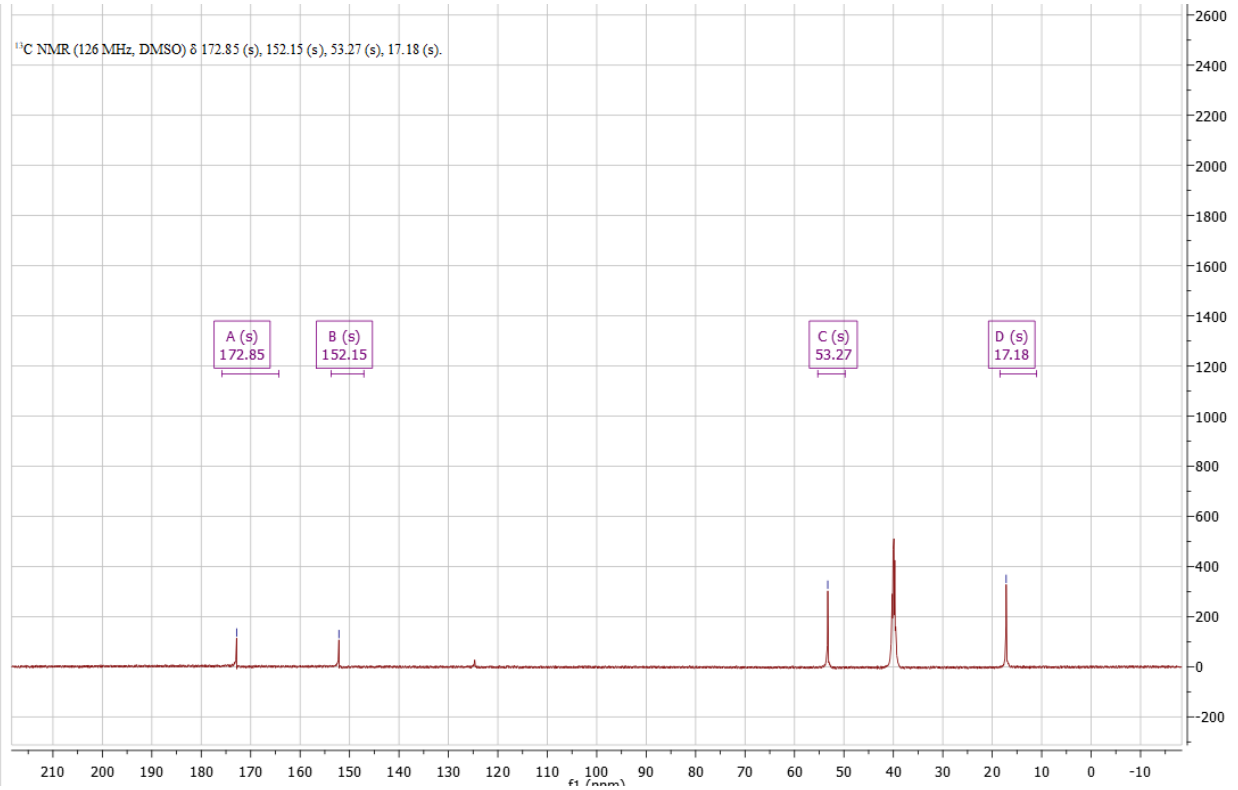

NMRs of FR-II-58

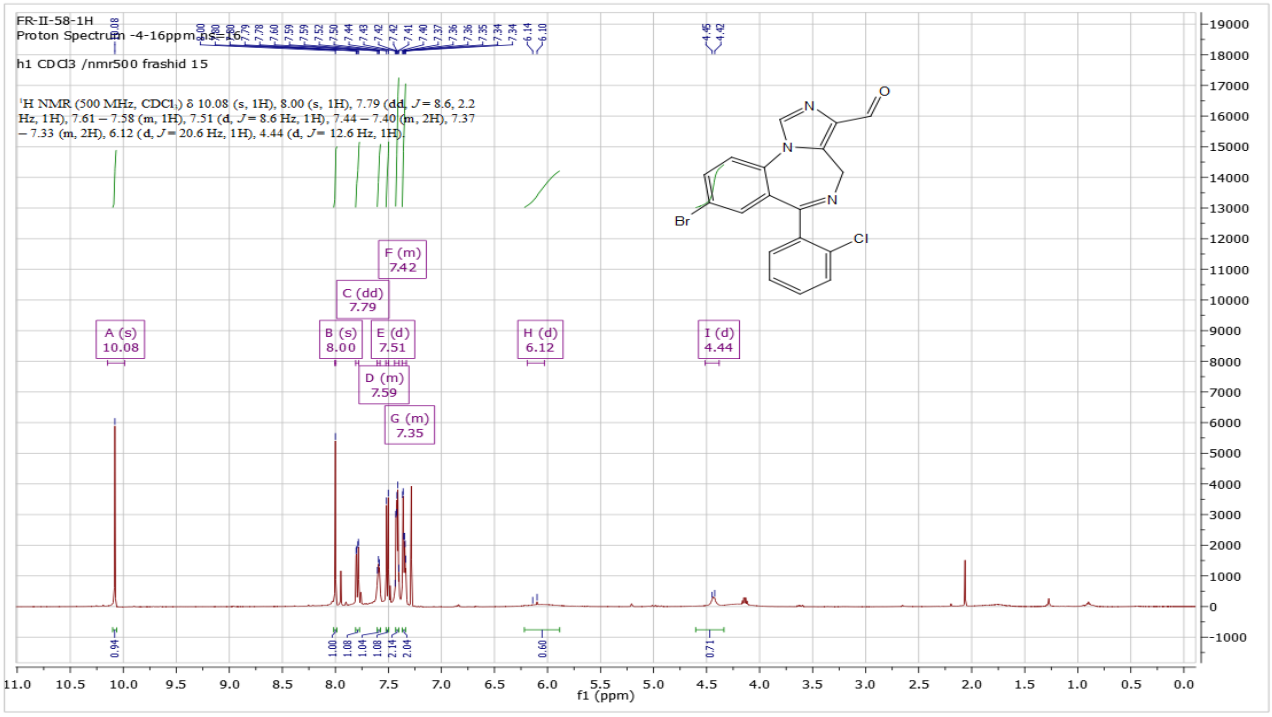

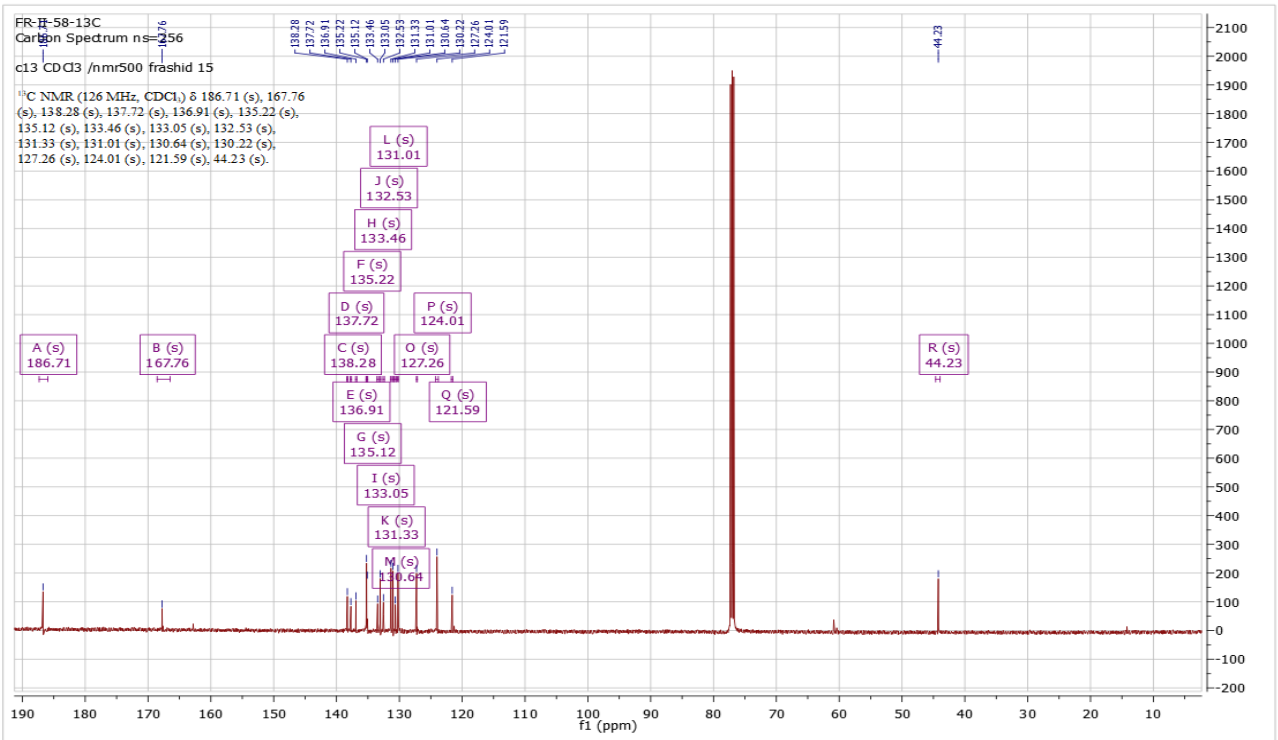

NMRs of FR-II-60

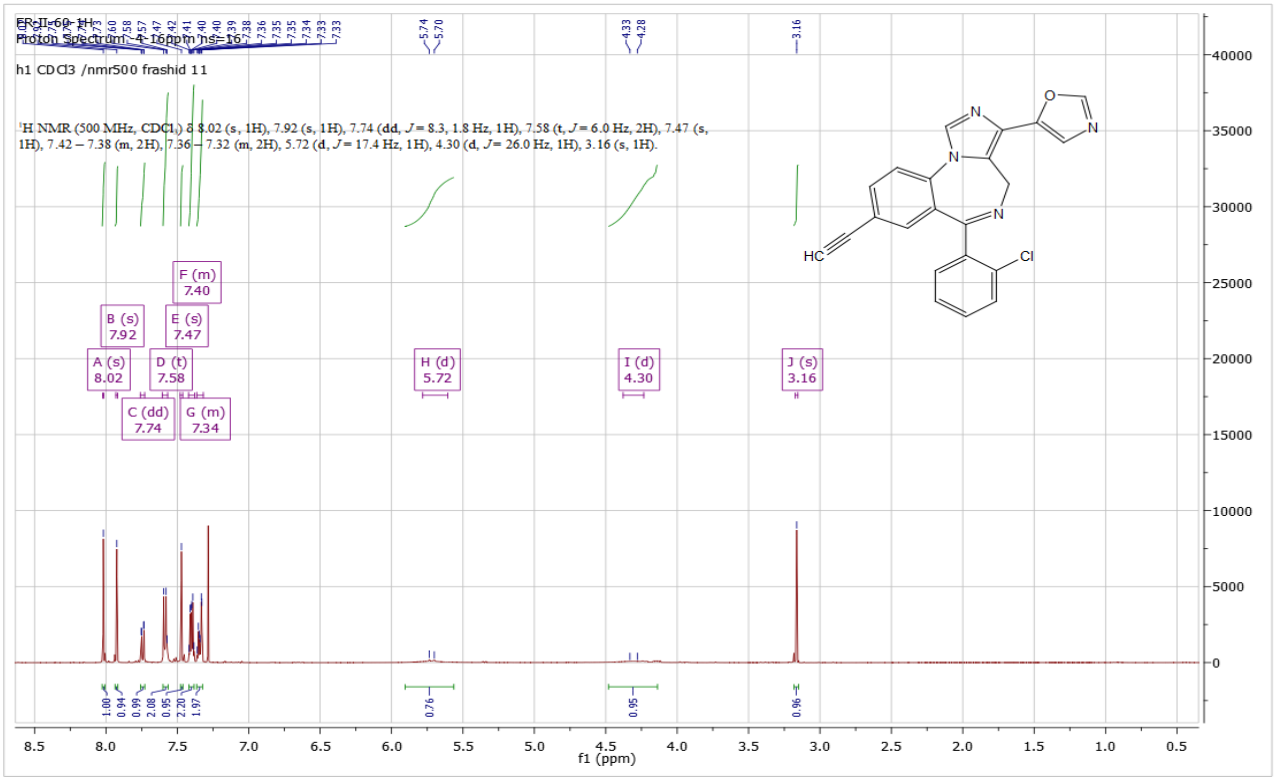

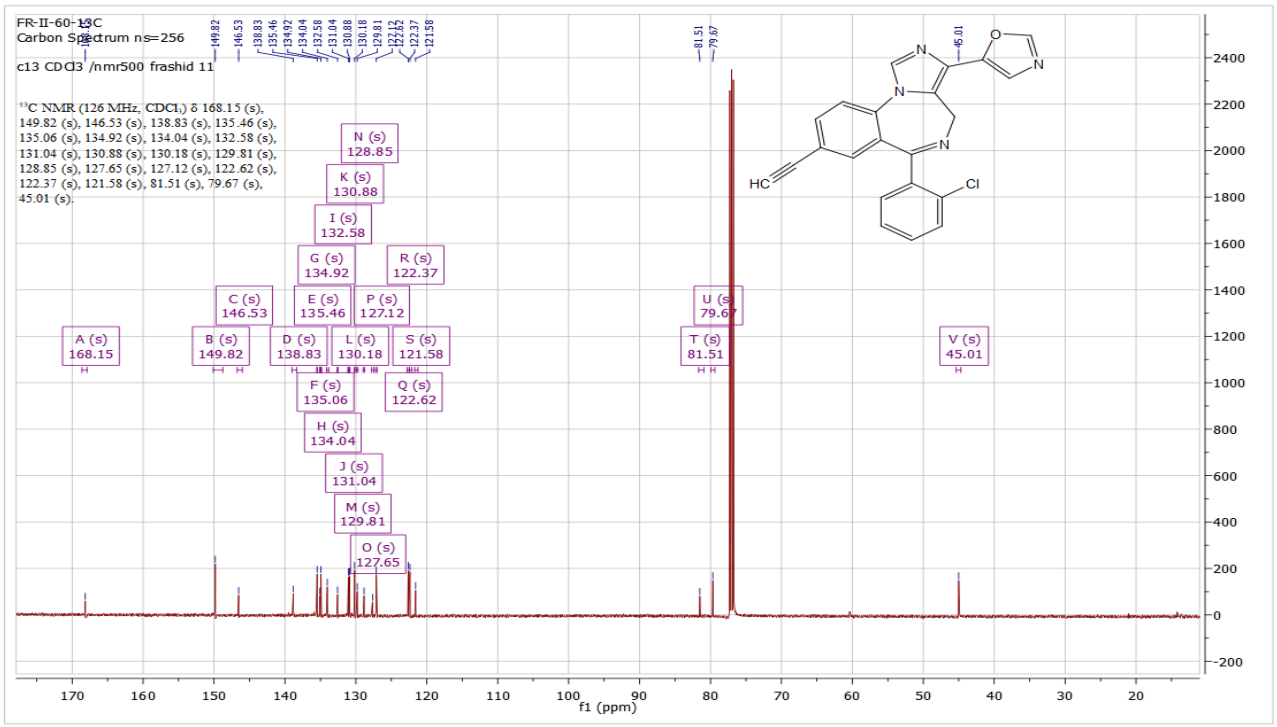

NMRs of FR-III-48

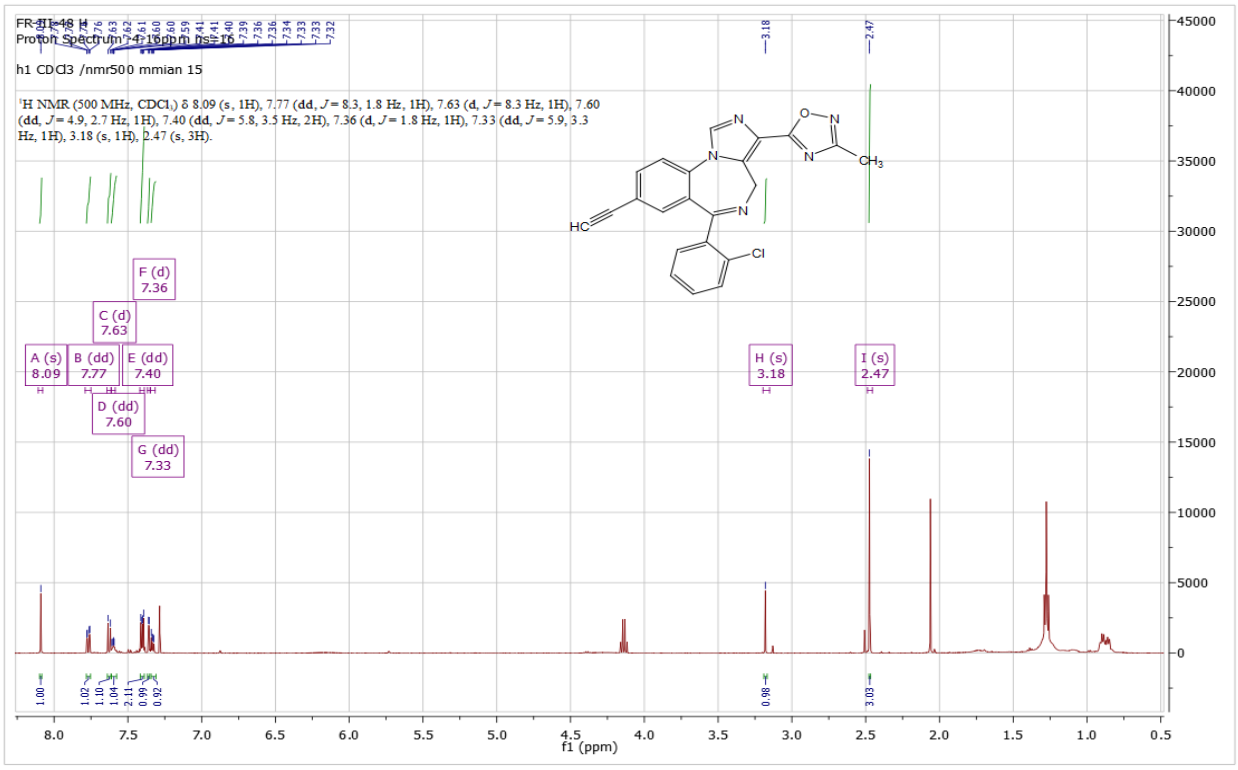

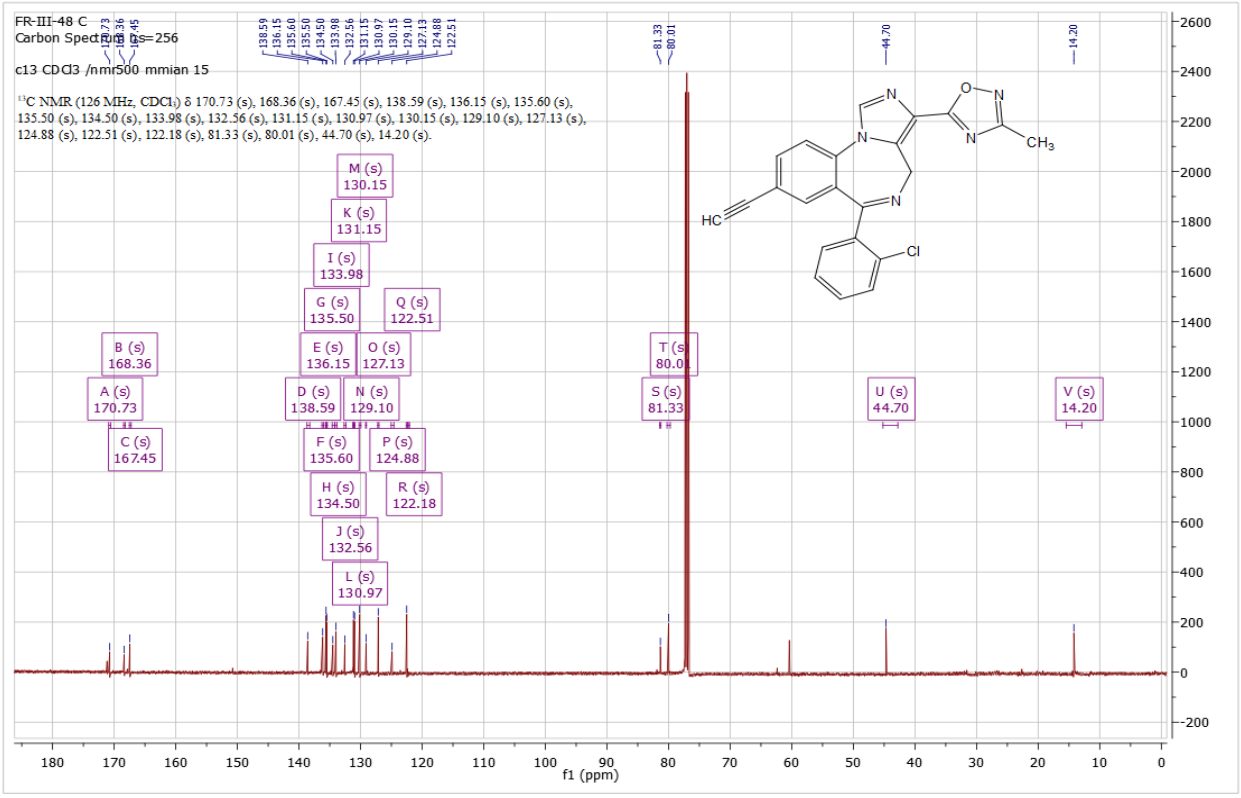

NMRs of FR-I-75

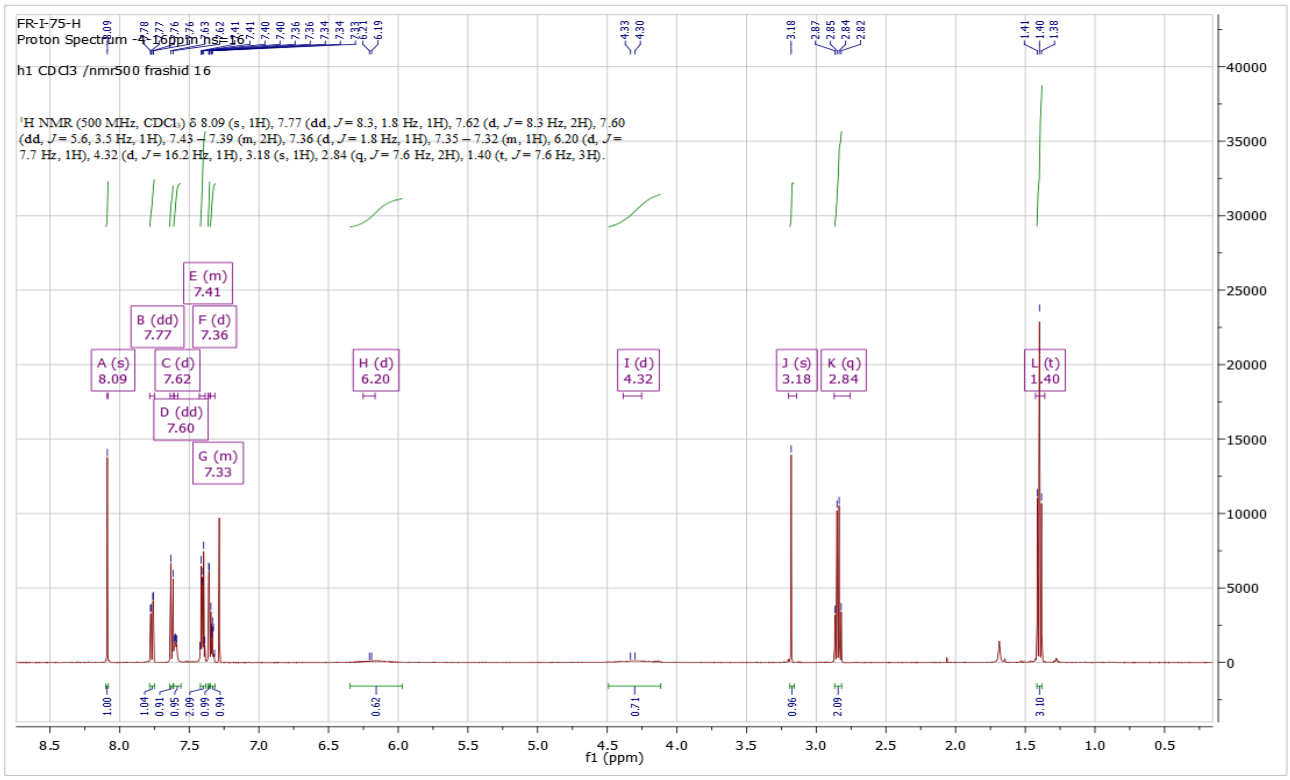

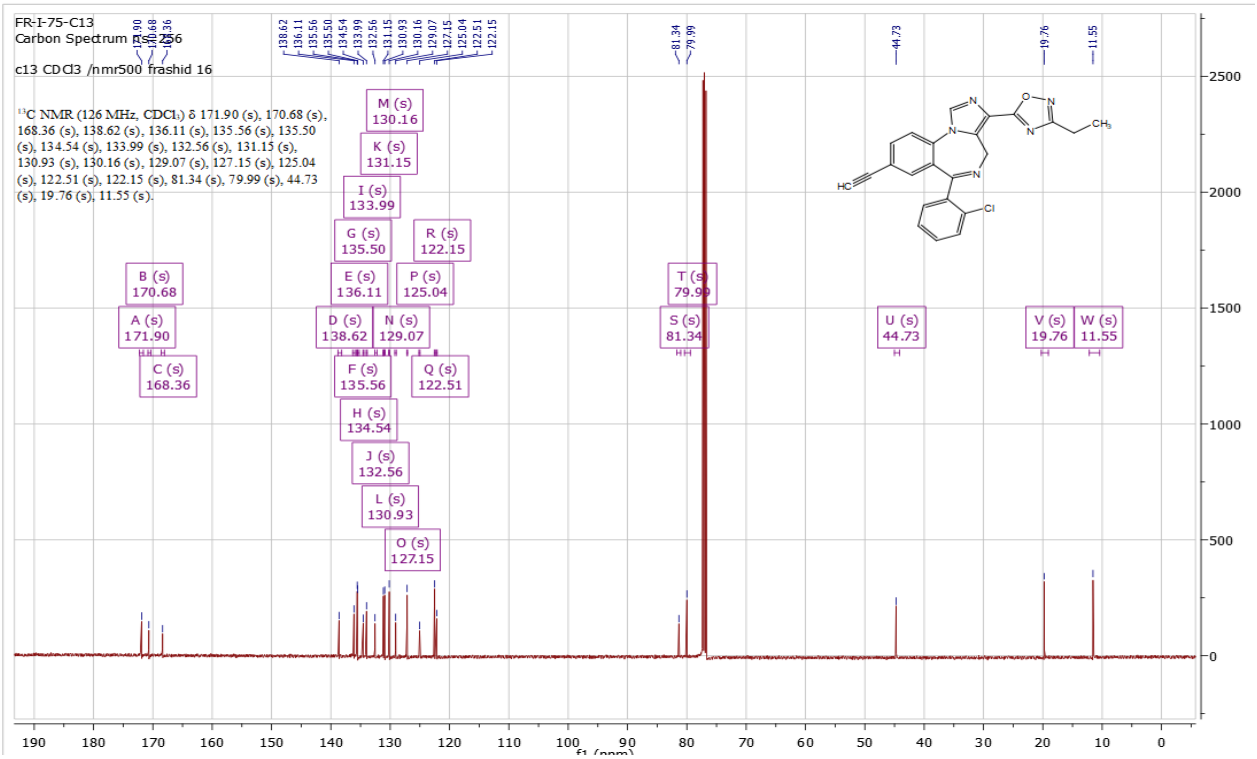

NMRs of FR-III-51

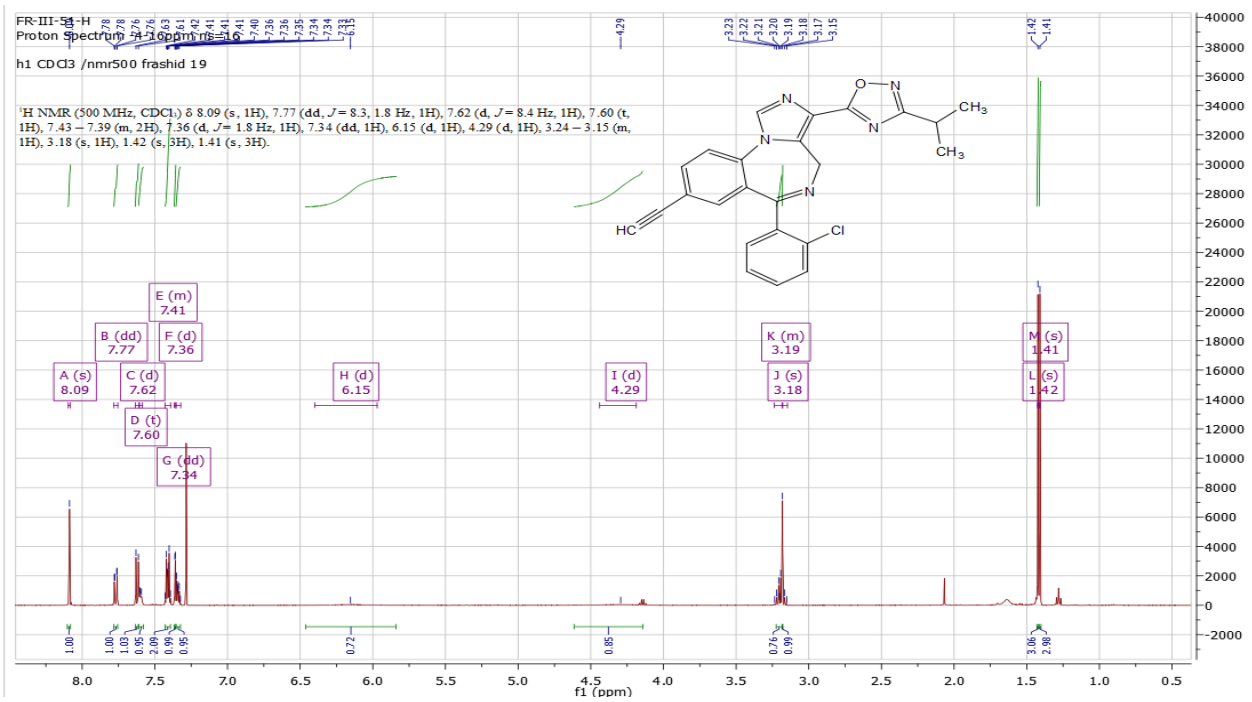

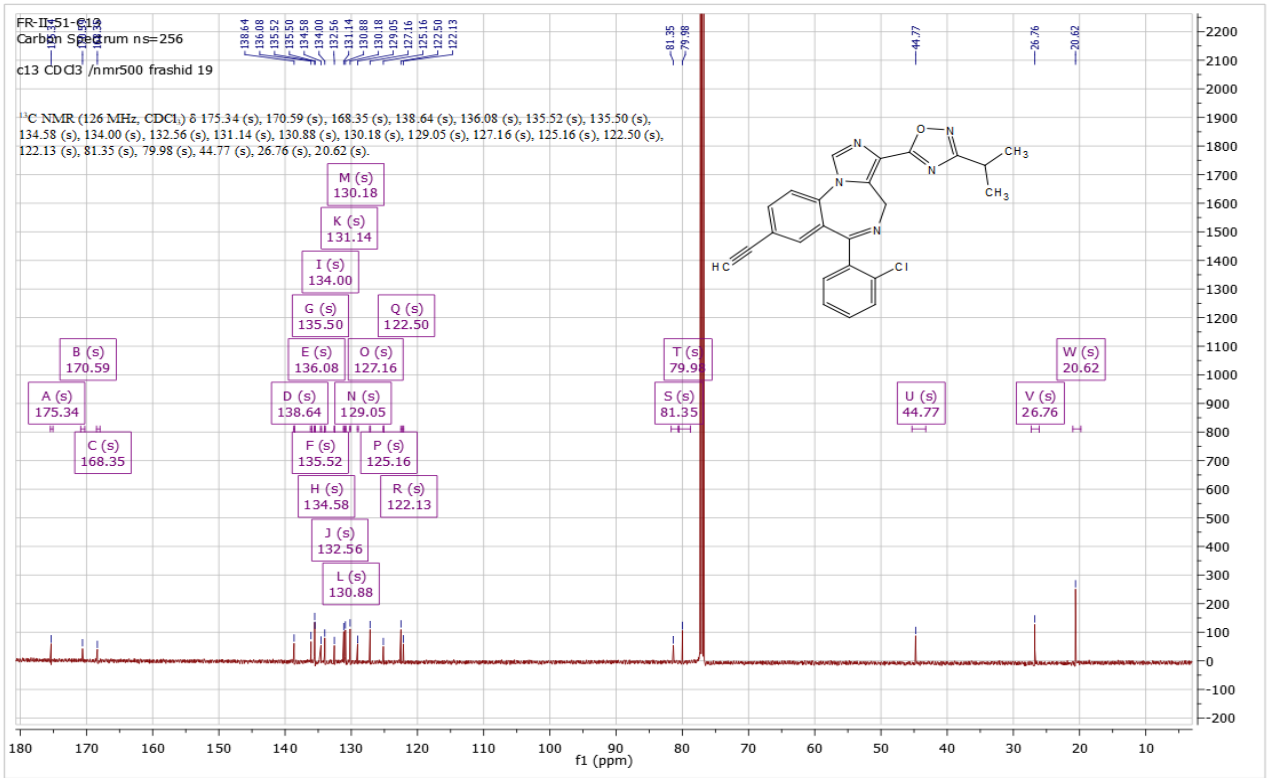

NMRs of FR-I-43

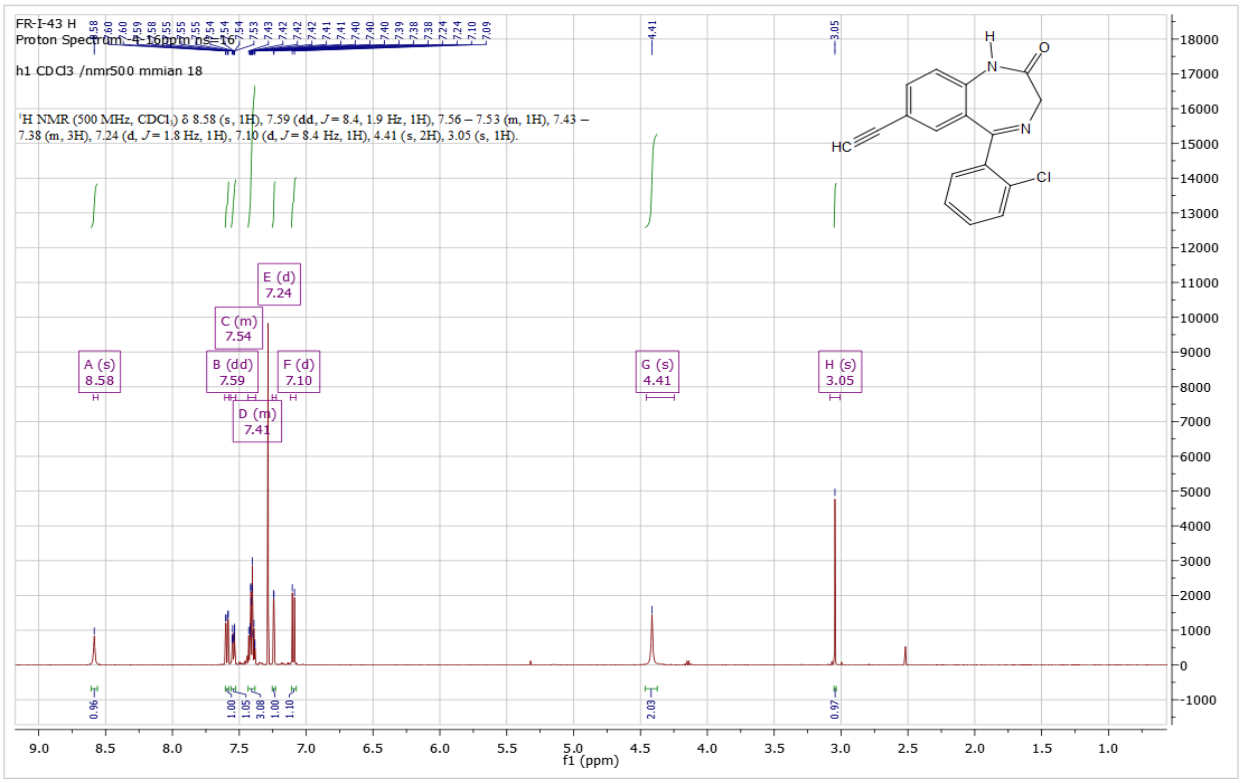

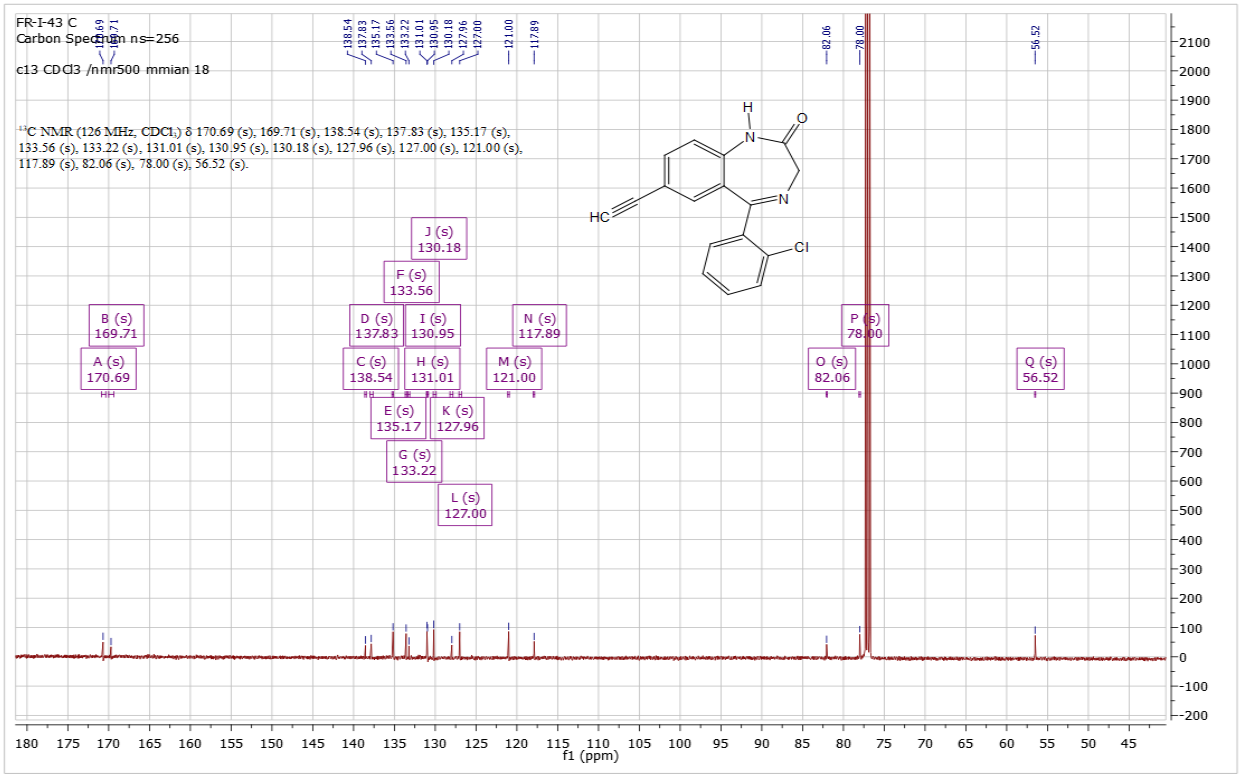

NMRs of KRM-III-77

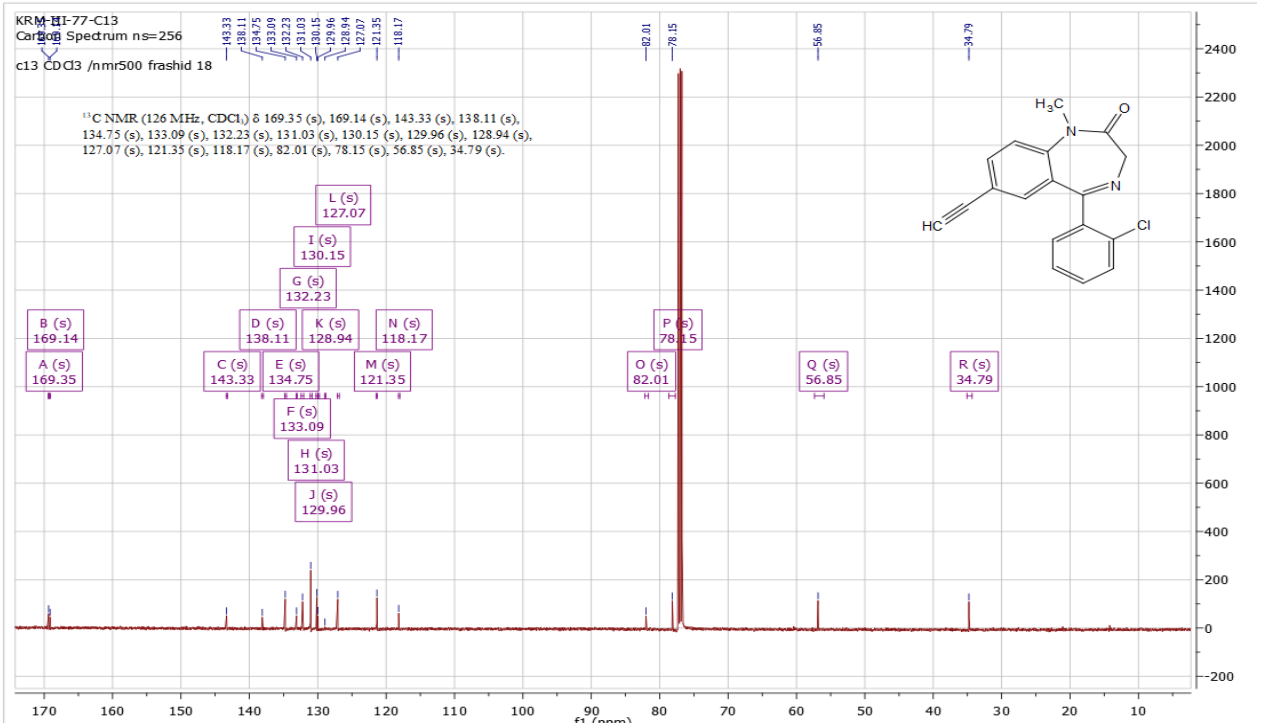

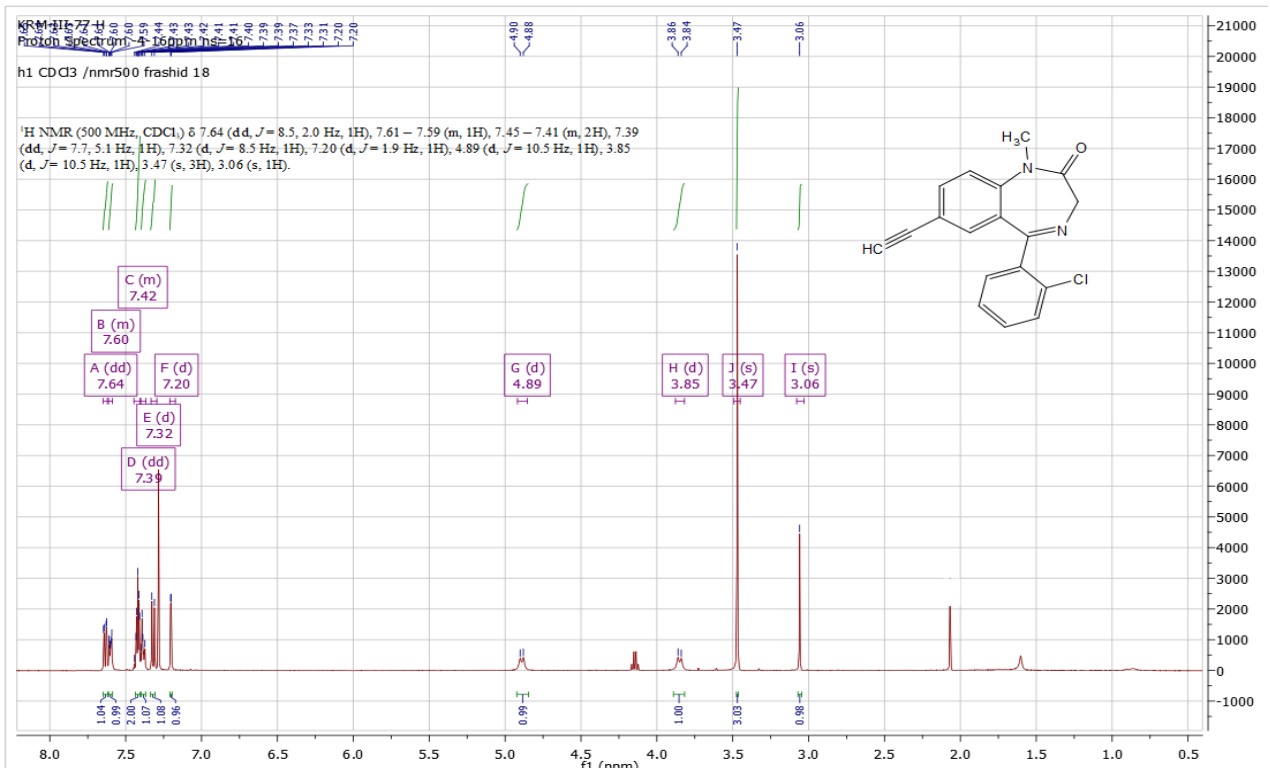

NMRs of FR-I-93

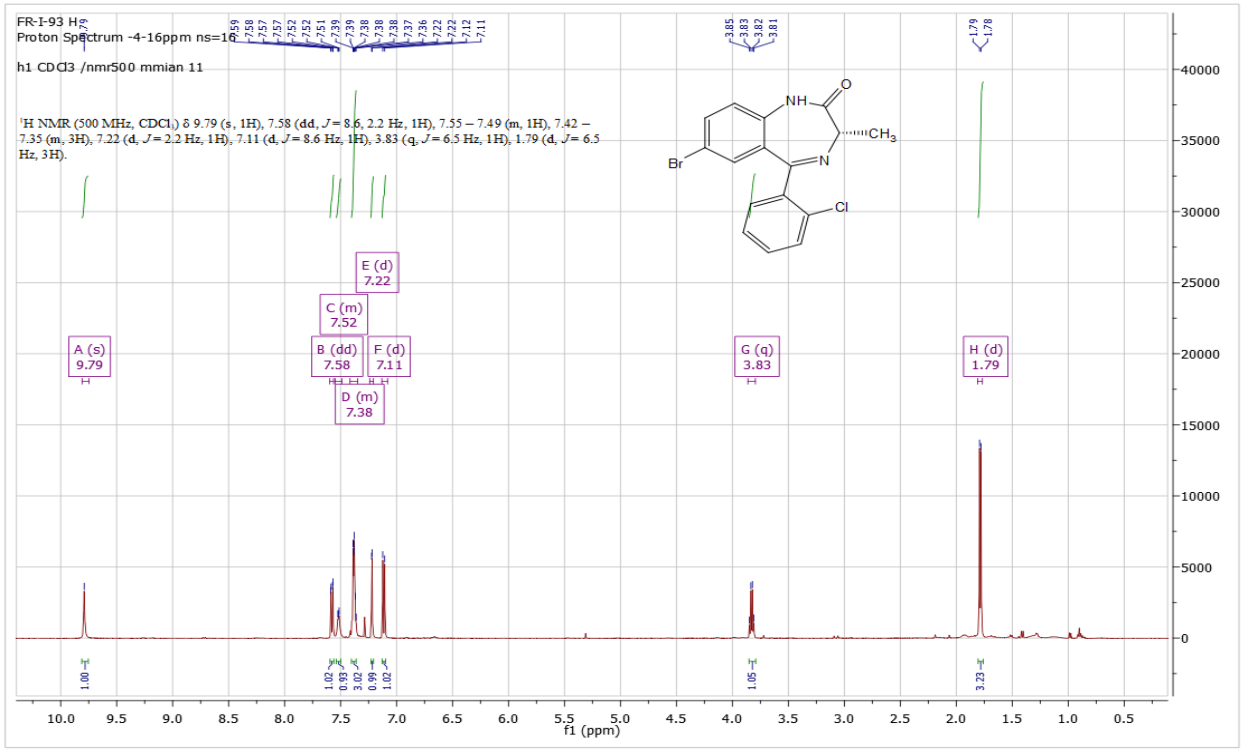

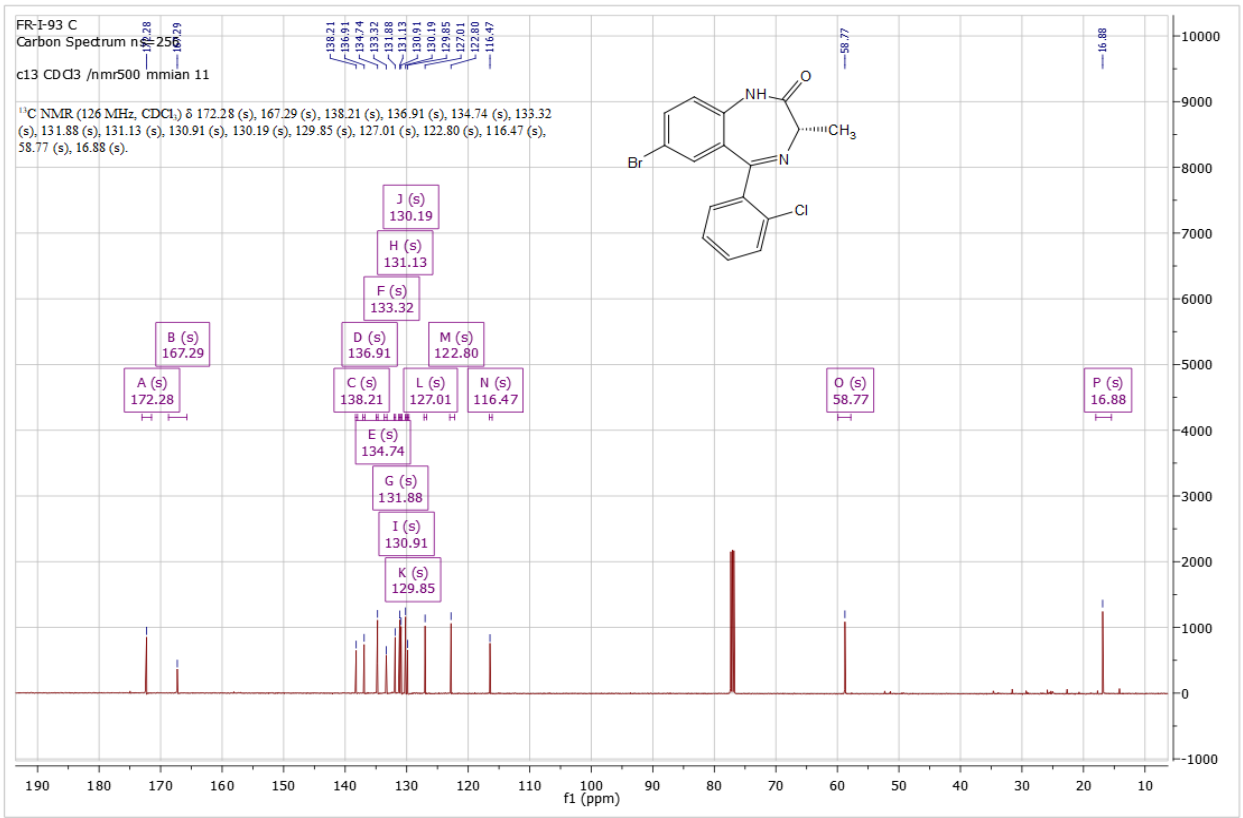

NMRs of FR-III-4

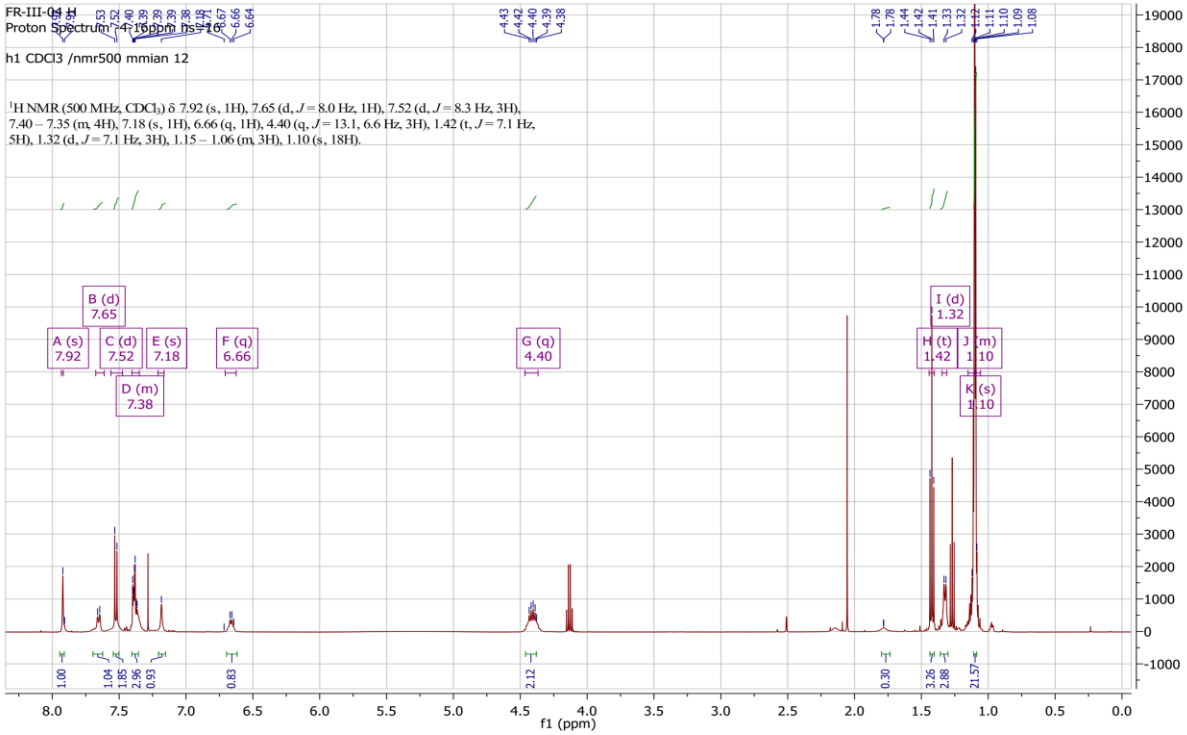

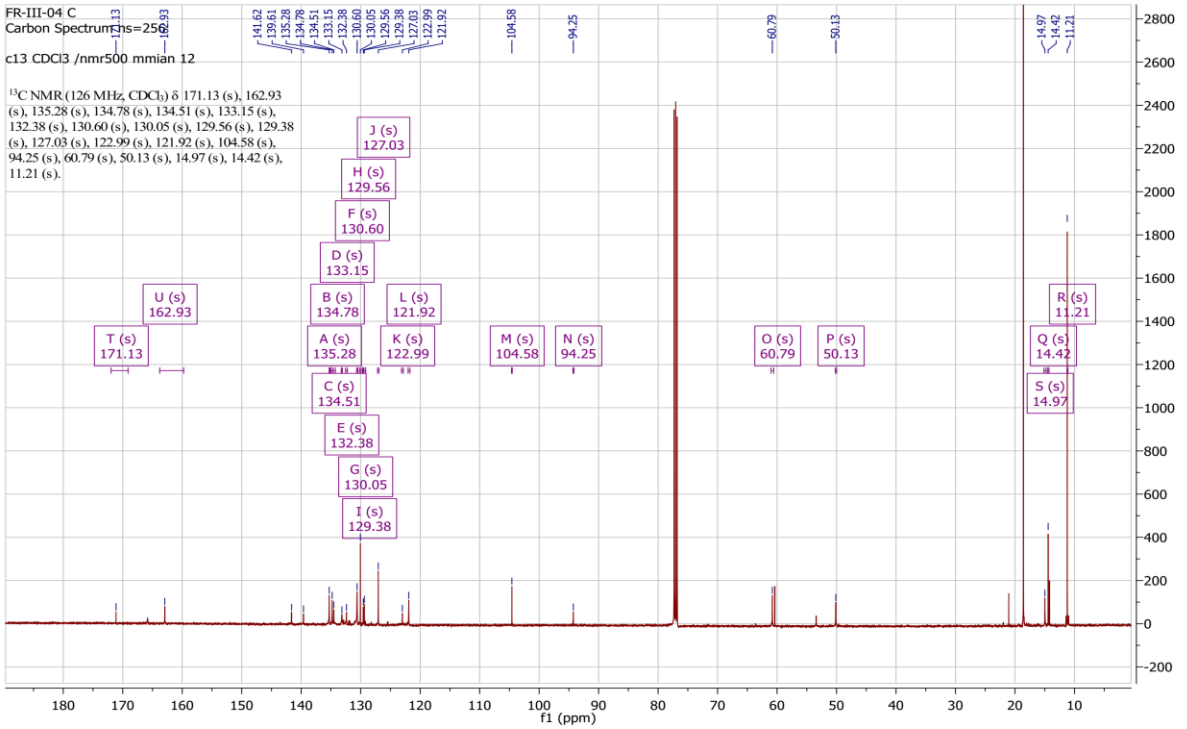

NMRs of FR-III-5

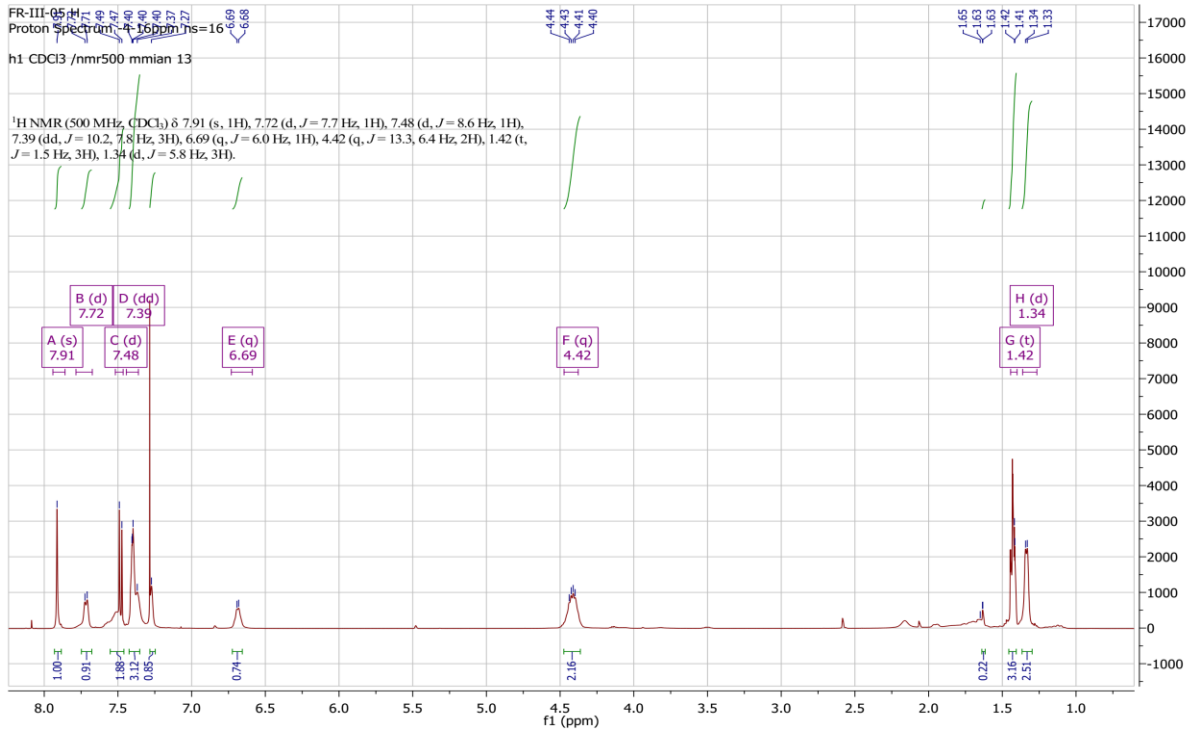

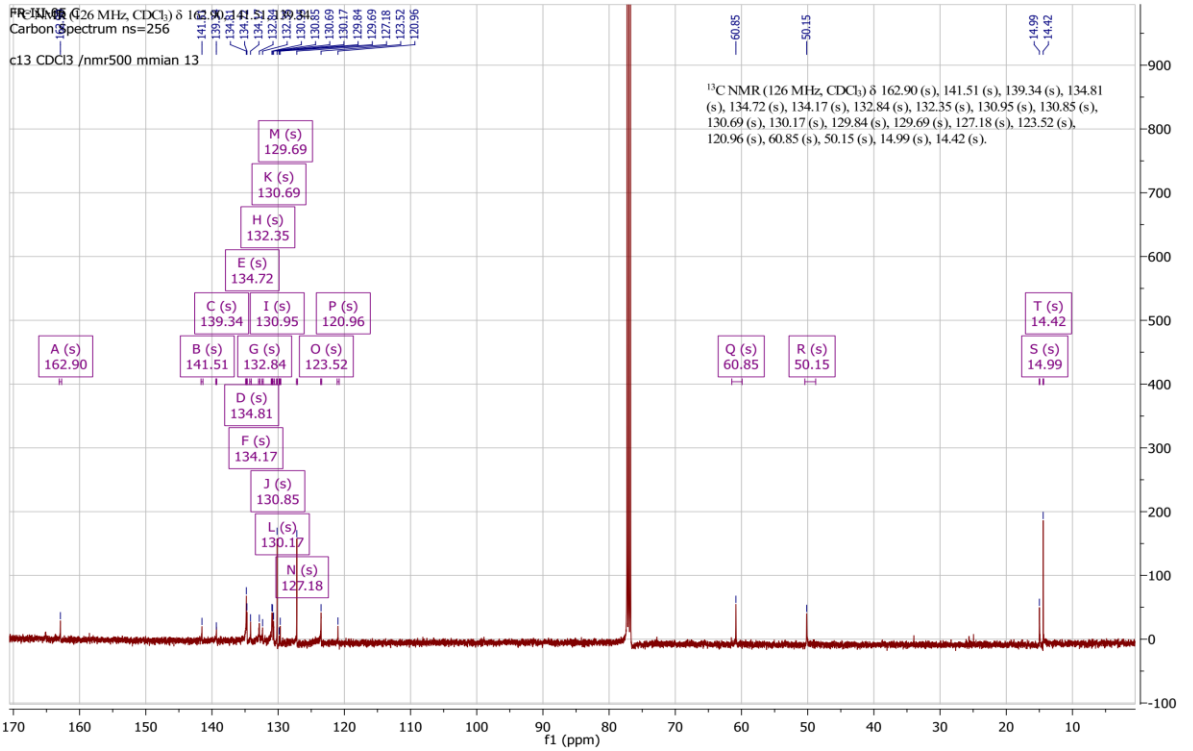

NMRs of FR-III-10

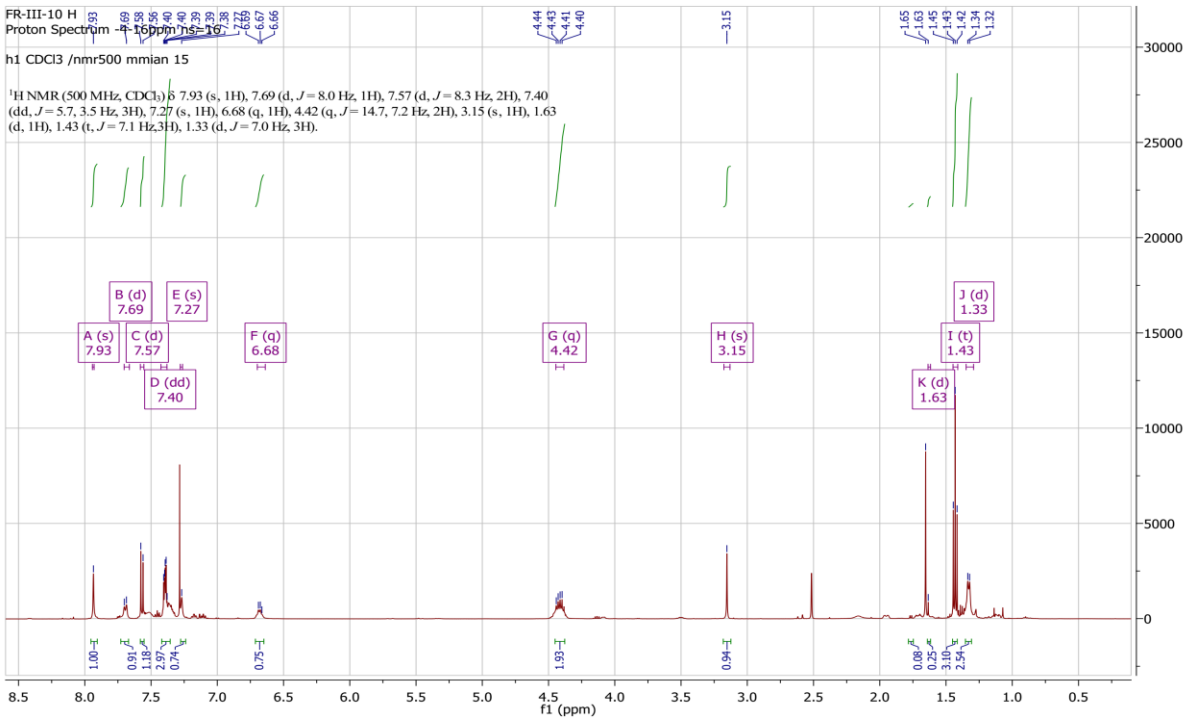

NMRs of FR-III-45

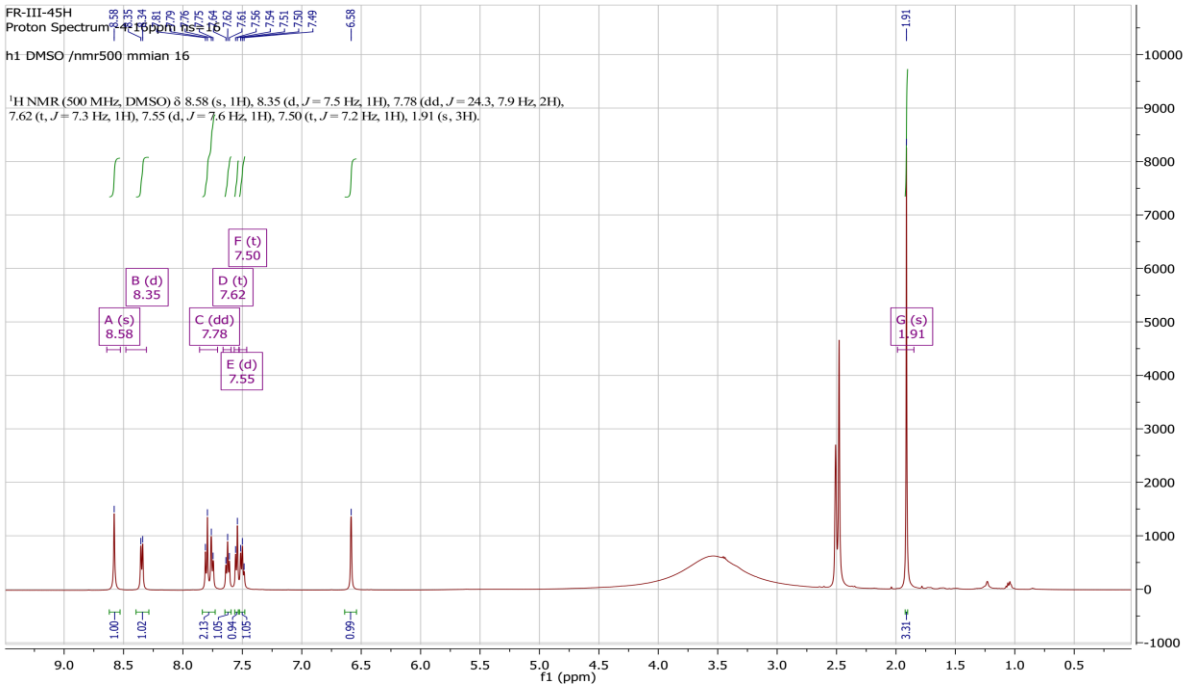

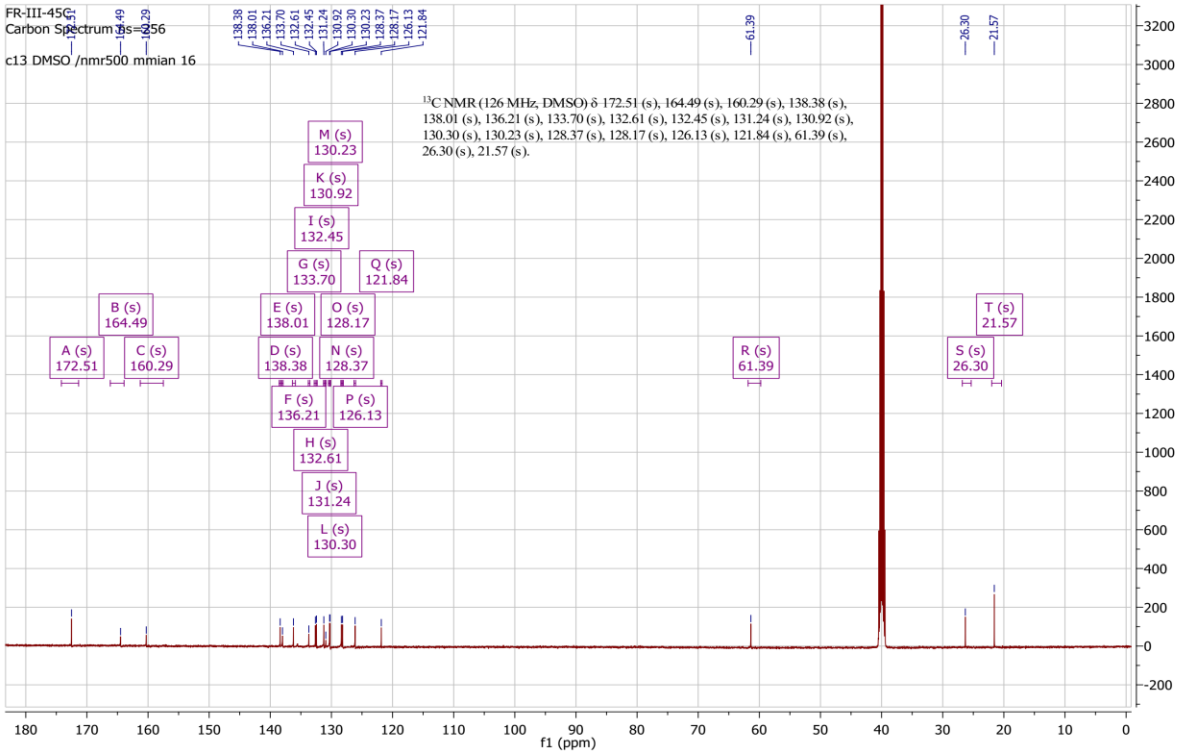

HRMS data

Data File: C:\LabSolutions\Data\Vilashini Rajaratnam\01272021 Analysis\FR-I-11_Farjana Analysis 01272021 Batch_8.lcd

Elmt	Val.	Min	Max	Elmt	Val.	Min	Max	Elmt	Val.	Min	Max	Use Adduct
H	1	5	9	O	2	0	2	S	2	0	0	H
2H	1	0	0	F	1	0	0	Cl	1	0	2	Na
C	4	10	15	Si	4	0	0	Br	1	0	2	K
N	3	0	2	P	3	0	0	I	3	0	0	NH4

Error Margin (ppm): 500
HC Ratio: unlimited
Max Isotopes: all
MSn Iso RI (%): 75.00

DBE Range: -100.0 - 2000.0
Apply N Rule: no
Isotope RI (%): 1.00
MSn Logic Mode: AND

Electron Ions: both
Use MSn Info: yes
Isotope Res: 10000
Max Results: 10

Event#: 1 MS(E+) Ret. Time : 0.600 -> 1.067 - 0.053 -> 0.193 Scan# : 91 -> 161 - 9 -> 29

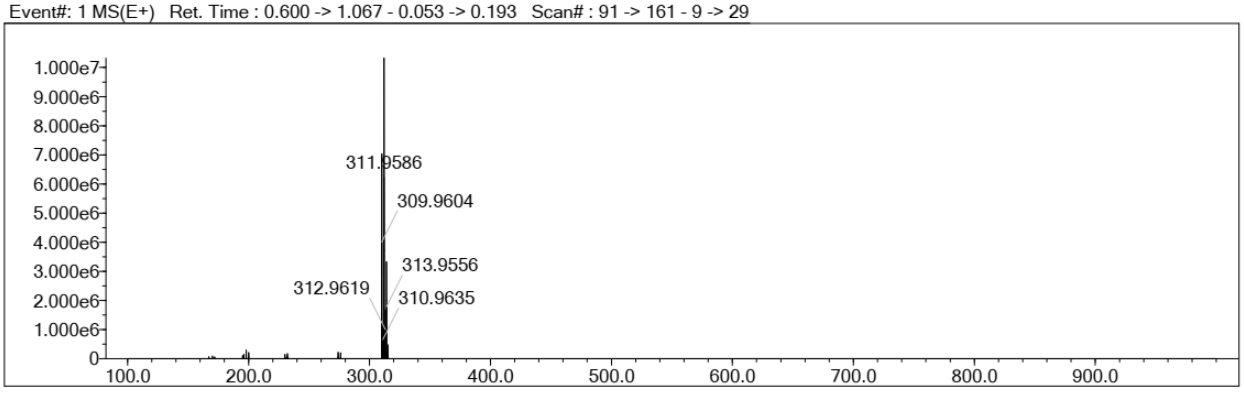

Measured region for 309.9604 m/z

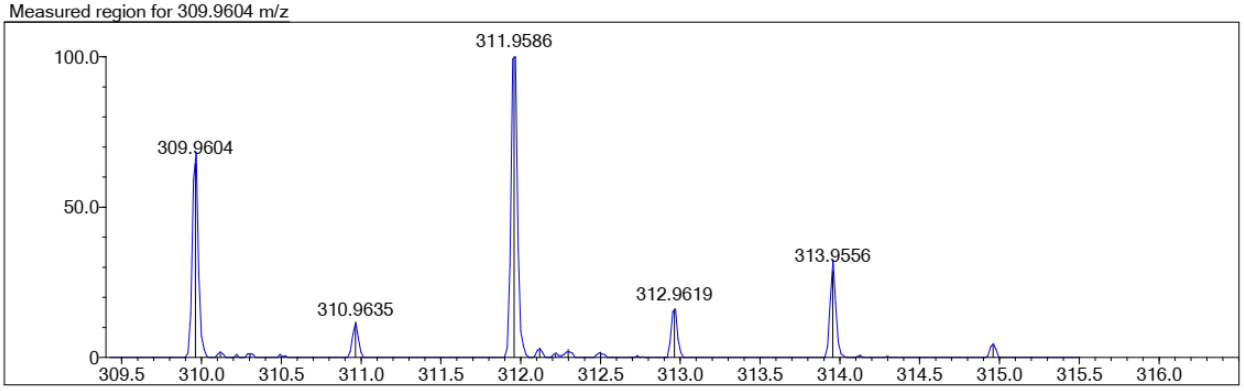

C13 H9 N O Cl Br [M+H]+ : Predicted region for 309.9629 m/z

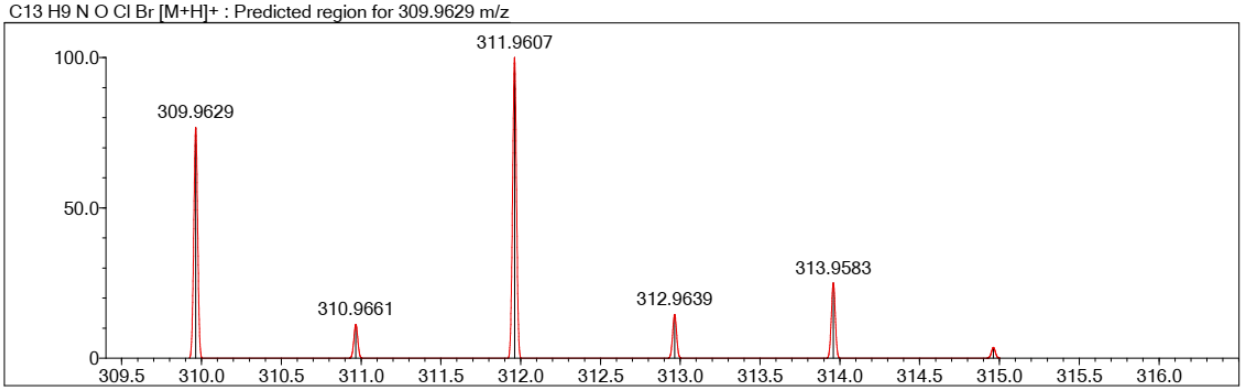

Rank	Score	Formula (M)	Ion	Meas. m/z	Pred. m/z	Df. (mDa)	Df. (ppm)	Iso	DBE
1	49.65	C13 H9 N O Cl Br	[M+H]+	309.9604	309.9629	-2.5	-8.07	83.73	9.0

Data File: C:\LabSolutions\Data\Vilashini Rajaratnam\01272021 Analysis\FR-I-20_Farjana Analysis 01272021 Batch_16.lcd

Elmt	Val.	Min	Max	Elmt	Val.	Min	Max	Elmt	Val.	Min	Max	Use Adduct
H	1	10	40	O	2	0	2	S	2	0	0	H
2H	1	0	0	F	1	0	0	Cl	1	0	2	Na
C	4	10	35	Si	4	0	0	Br	1	0	2	K
N	3	0	3	P	3	0	0	I	3	0	0	NH4

Error Margin (ppm): 500
HC Ratio: unlimited
Max Isotopes: all
MSn Iso RI (%): 75.00

DBE Range: -100.0 - 2000.0
Apply N Rule: no
Isotope RI (%): 1.00
MSn Logic Mode: AND

Electron Ions: both
Use MSn Info: yes
Isotope Res: 10000
Max Results: 10

Event#: 1 MS(E+) Ret. Time : 0.293 -> 0.573 - 1.427 -> 1.720 Scan# : 45 -> 87 - 215 -> 259

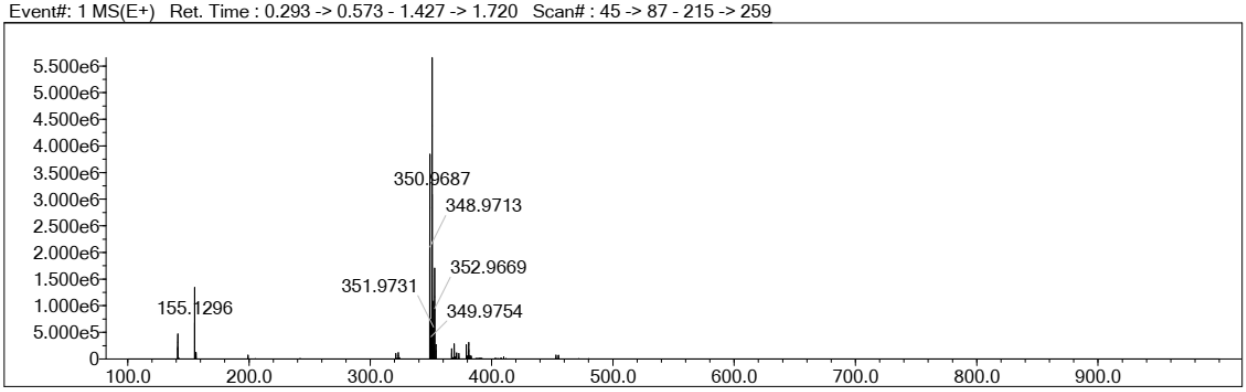

Measured region for 348.9713 m/z

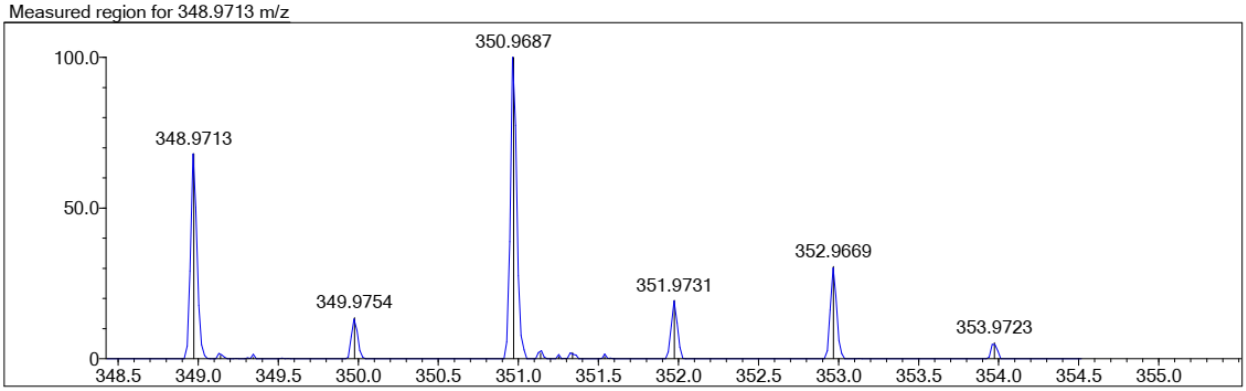

C15 H10 N2 O Cl Br [M+H]+ : Predicted region for 348.9738 m/z

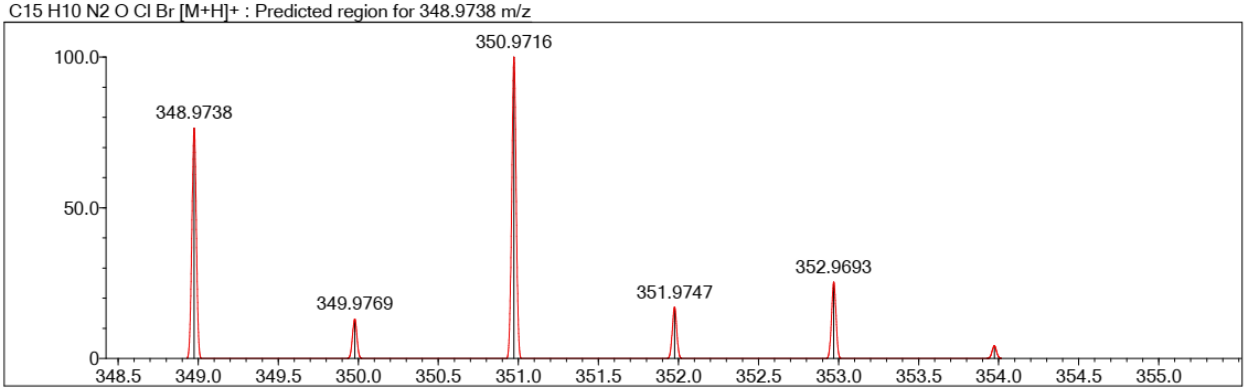

Rank	Score	Formula (M)	Ion	Meas. m/z	Pred. m/z	Df. (mDa)	Df. (ppm)	Iso	DBE
5	47.53	C15 H10 N2 O Cl Br	[M+H]+	348.9713	348.9738	-2.5	-7.16	69.49	11.0

Data File: C:\LabSolutions\Data\Vilashini Rajaratnam\01272021 Analysis\FR-I-44_Farjana Analysis 01272021 Batch_22.lcd

Elmt	Val.	Min	Max	Elmt	Val.	Min	Max	Elmt	Val.	Min	Max	Use Adduct
H	1	10	40	O	2	0	2	S	2	0	0	H
2H	1	0	0	F	1	0	0	Cl	1	0	2	Na
C	4	10	35	Si	4	0	1	Br	1	0	2	K
N	3	0	3	P	3	0	0	I	3	0	0	NH4

Error Margin (ppm): 500
HC Ratio: unlimited
Max Isotopes: all
MSn Iso RI (%): 75.00

DBE Range: -100.0 - 2000.0
Apply N Rule: no
Isotope RI (%): 1.00
MSn Logic Mode: AND

Electron Ions: both
Use MSn Info: yes
Isotope Res: 10000
Max Results: 10

Event#: 1 MS(E+) Ret. Time : 0.520 -> 0.653 - 0.040 -> 0.059 Scan# : 79 -> 99 - 7 -> 9

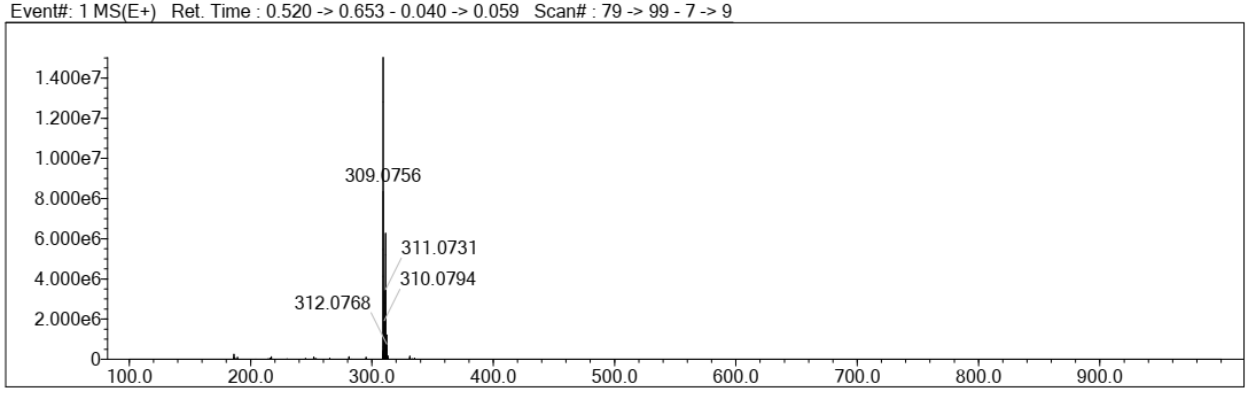

Measured region for 309.0756 m/z

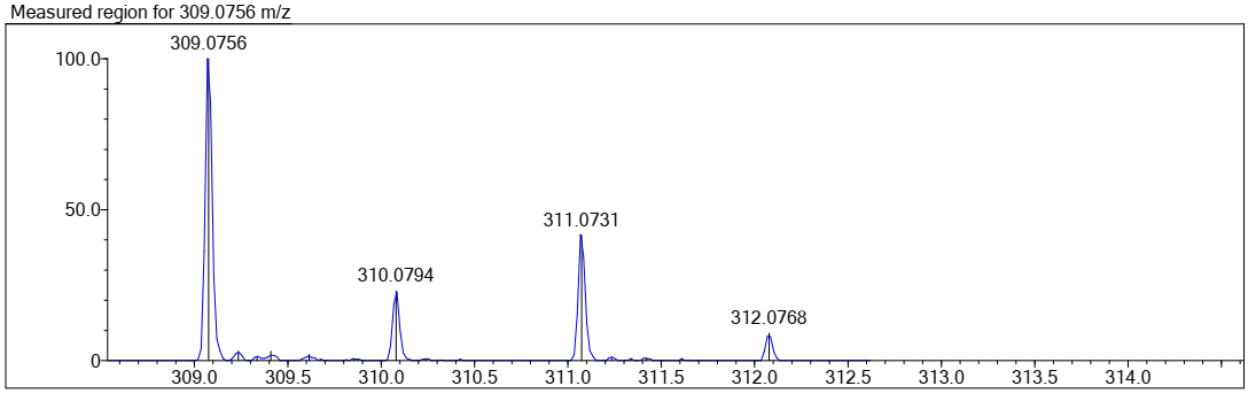

C18 H13 N2 O Cl [M+H]+ : Predicted region for 309.0789 m/z

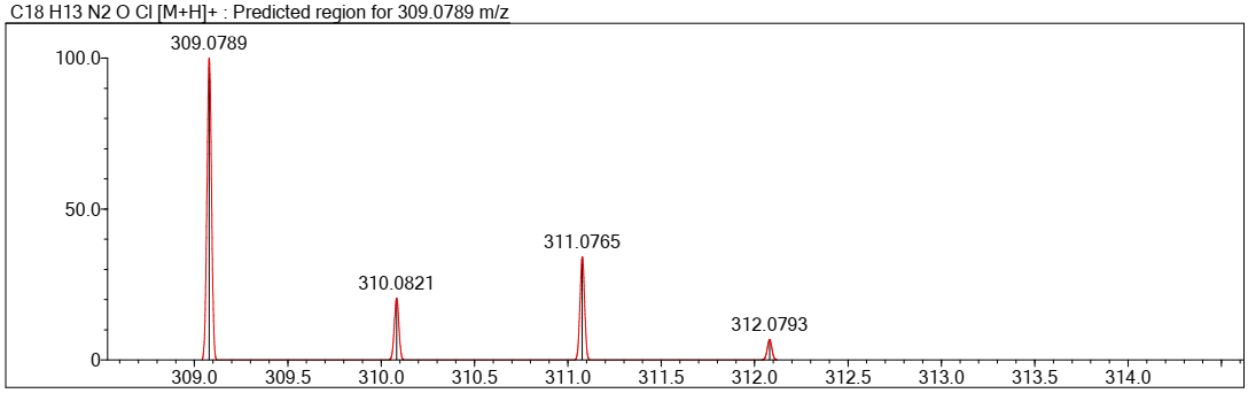

Rank	Score	Formula (M)	Ion	Meas. m/z	Pred. m/z	Df. (mDa)	Df. (ppm)	Iso	DBE
9	25.03	C18 H13 N2 O Cl	[M+H]+	309.0756	309.0789	-3.3	-10.68	65.54	13.0

Data File: C:\LabSolutions\Data\Vilashini Rajaratnam\01272021 Analysis\FR-I-45_Farjana Analysis 01272021 Batch_12.lcd

Elmt	Val.	Min	Max	Elmt	Val.	Min	Max	Elmt	Val.	Min	Max	Use Adduct
H	1	10	40	O	2	0	3	S	2	0	0	H
2H	1	0	0	F	1	0	0	Cl	1	0	2	Na
C	4	10	35	Si	4	0	0	Br	1	0	2	K
N	3	0	3	P	3	0	0	I	3	0	0	NH4

Error Margin (ppm): 500
HC Ratio: unlimited
Max Isotopes: all
MSn Iso RI (%): 75.00

DBE Range: -100.0 - 2000.0
Apply N Rule: no
Isotope RI (%): 1.00
MSn Logic Mode: AND

Electron Ions: both
Use MSn Info: yes
Isotope Res: 10000
Max Results: 10

Event#: 1 MS(E+) Ret. Time : 0.280 -> 0.307 - 1.253 -> 1.579 Scan# : 43 -> 47 - 189 -> 237

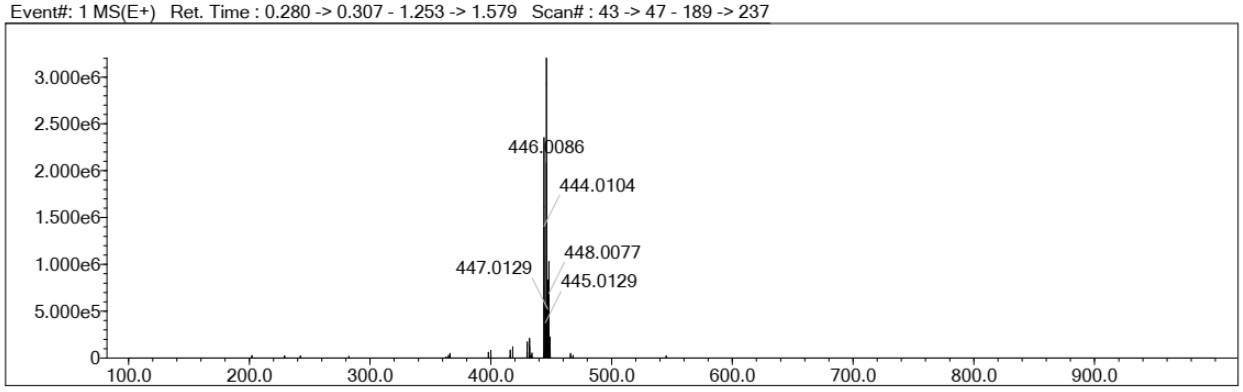

Measured region for 444.0104 m/z

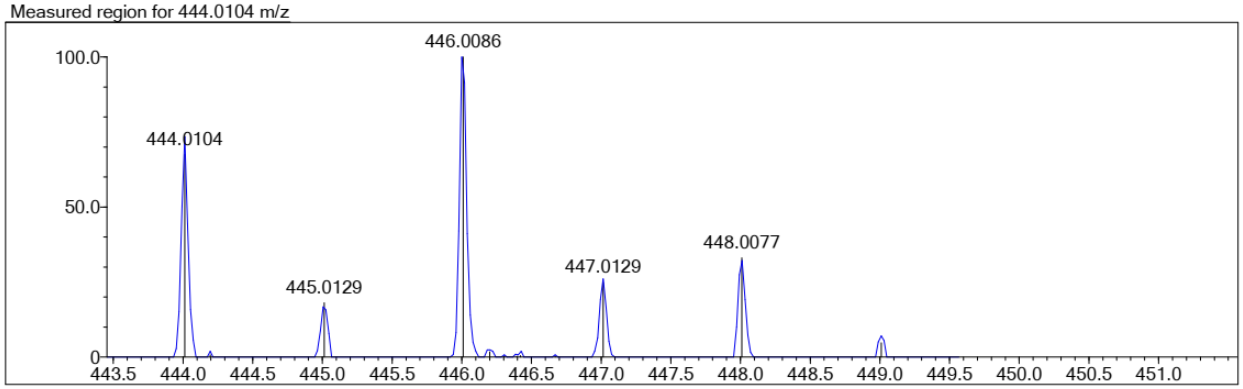

C20 H15 N3 O2 Cl Br [M+H]+ : Predicted region for 444.0109 m/z

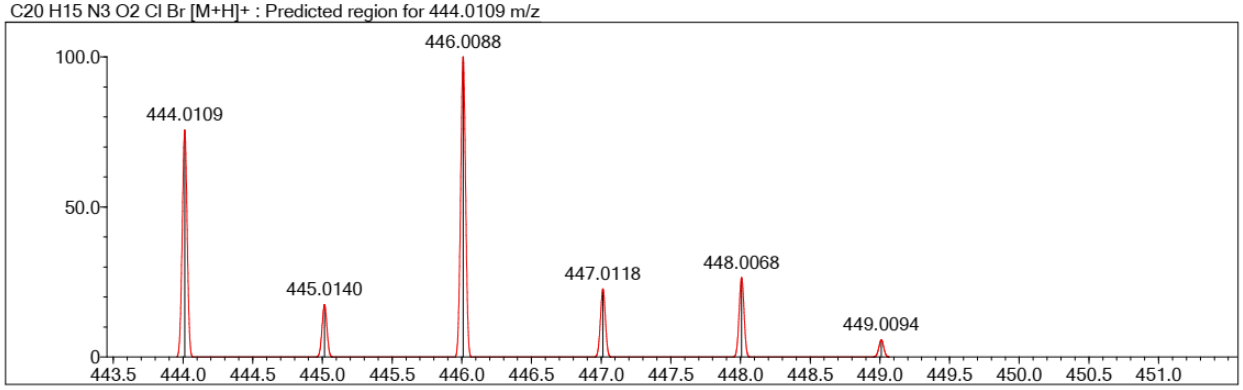

Rank	Score	Formula (M)	Ion	Meas. m/z	Pred. m/z	Df. (mDa)	Df. (ppm)	Iso	DBE
1	97.89	C20 H15 N3 O2 Cl Br	[M+H]+	444.0104	444.0109	-0.5	-1.13	98.21	14.0

Data File: C:\LabSolutions\Data\Vilashini Rajaratnam\01272021 Analysis\FR-I-59_Farjana Analysis 01272021 Batch_26.lcd

Elmt	Val.	Min	Max	Elmt	Val.	Min	Max	Elmt	Val.	Min	Max	Use Adduct
H	1	10	40	O	2	0	2	S	2	0	0	H
2H	1	0	0	F	1	0	0	Cl	1	0	2	Na
C	4	10	35	Si	4	0	1	Br	1	0	2	K
N	3	0	3	P	3	0	0	I	3	0	0	NH4

Error Margin (ppm): 500
HC Ratio: unlimited
Max Isotopes: all
MSn Iso RI (%): 75.00

DBE Range: -100.0 - 2000.0
Apply N Rule: no
Isotope RI (%): 1.00
MSn Logic Mode: AND

Electron Ions: both
Use MSn Info: yes
Isotope Res: 10000
Max Results: 10

Event#: 1 MS(E+) Ret. Time : 0.333 -> 0.493 - 1.347 -> 1.623 Scan# : 51 -> 75 - 203 -> 245

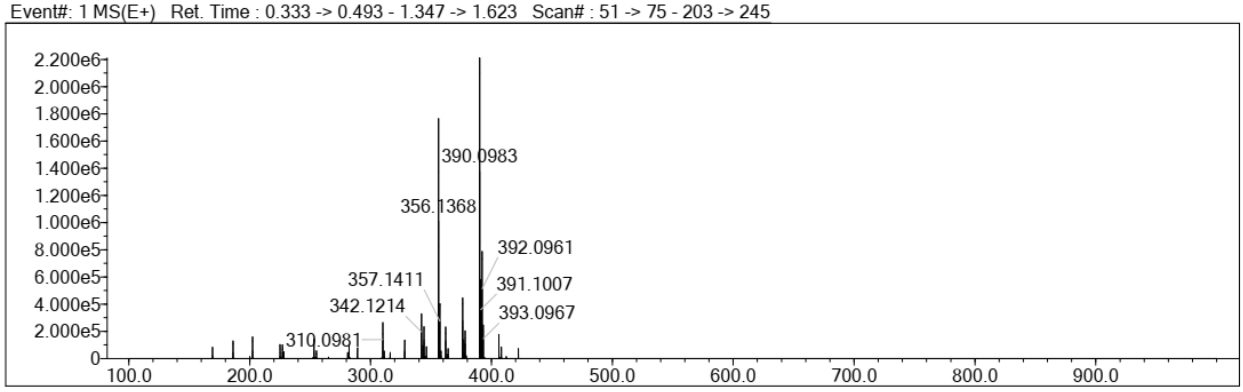

Measured region for 390.0983 m/z

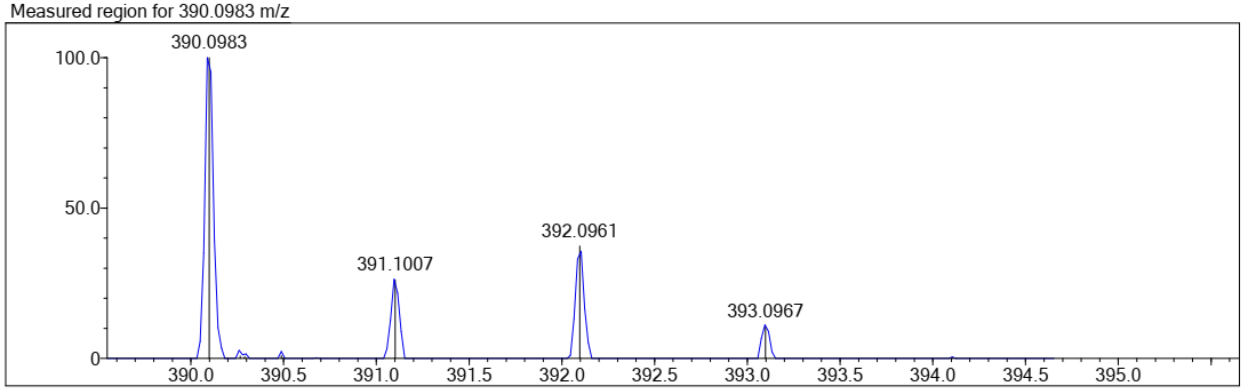

C22 H16 N3 O2 Cl [M+H]+ : Predicted region for 390.1004 m/z

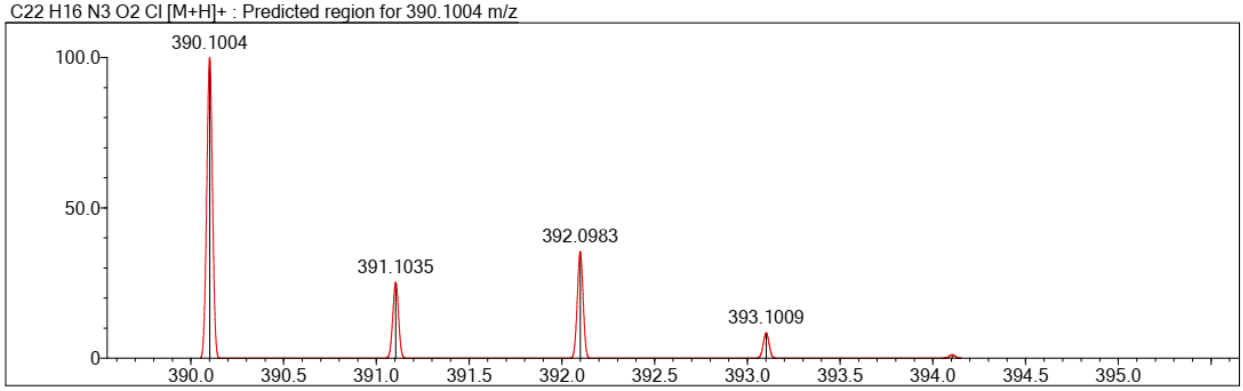

Rank	Score	Formula (M)	Ion	Meas. m/z	Pred. m/z	Df. (mDa)	Df. (ppm)	Iso	DBE
2	84.66	C22 H16 N3 O2 Cl	[M+H]+	390.0983	390.1004	-2.1	-5.38	98.21	16.0

Data File: C:\LabSolutions\Data\Vilashini Rajaratnam\01272021 Analysis\FR-I-74_Farjana Analysis 01272021 Batch_20.lcd

Elmt	Val.	Min	Max	Elmt	Val.	Min	Max	Elmt	Val.	Min	Max	Use Adduct
H	1	10	40	O	2	0	2	S	2	0	0	H
2H	1	0	0	F	1	0	0	Cl	1	0	2	Na
C	4	10	35	Si	4	0	1	Br	1	0	2	K
N	3	0	3	P	3	0	0	I	3	0	0	NH4

Error Margin (ppm): 500
HC Ratio: unlimited
Max Isotopes: all
MSn Iso RI (%): 75.00

DBE Range: -100.0 - 2000.0
Apply N Rule: no
Isotope RI (%): 1.00
MSn Logic Mode: AND

Electron Ions: both
Use MSn Info: yes
Isotope Res: 10000
Max Results: 10

Event#: 1 MS(E+) Ret. Time : 0.293 -> 0.560 - 1.213 -> 1.323 Scan# : 45 -> 85 - 183 -> 199

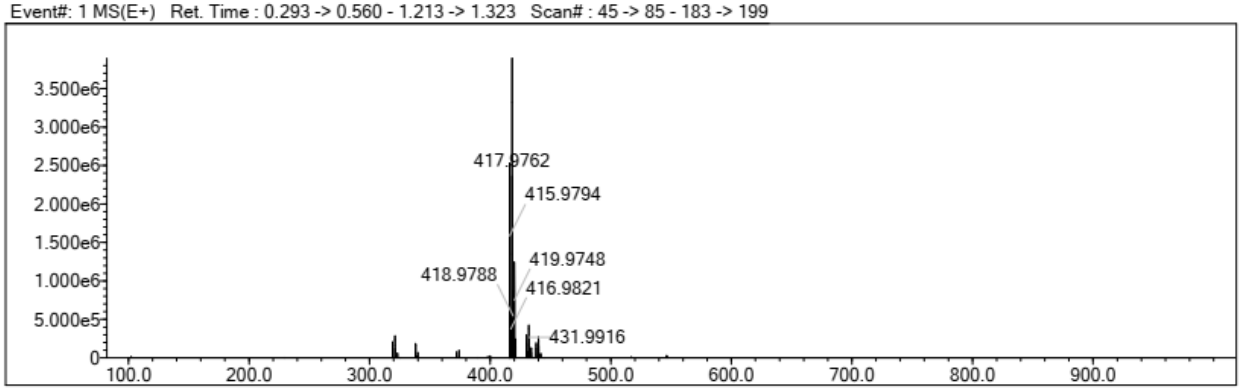

Measured region for 415.9794 m/z

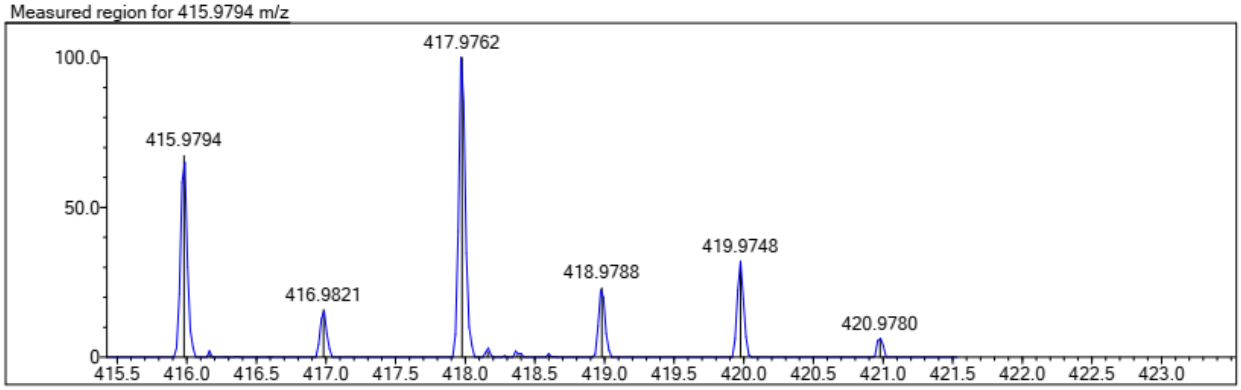

C18 H11 N3 O2 Cl Br [M+H]+ : Predicted region for 415.9796 m/z

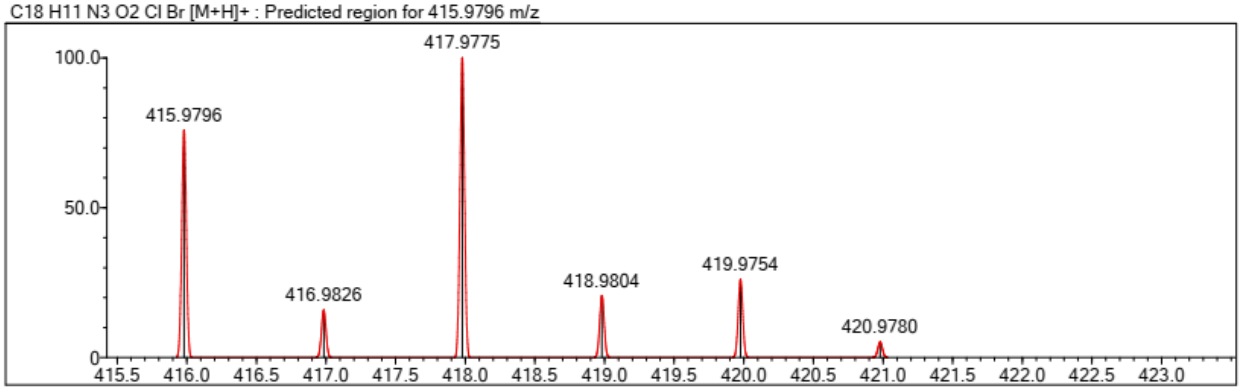

Rank	Score	Formula (M)	Ion	Meas. m/z	Pred. m/z	Df. (mDa)	Df. (ppm)	Iso	DBE
1	75.31	C18 H11 N3 O2 Cl Br	[M+H]+	415.9794	415.9796	-0.2	-0.48	75.31	14.0

Data File: C:\LabSolutions\Data\Vilashini Rajaratnam\01272021 Analysis\FR-I-93_Farjana Analysis 01272021 Batch_6.lcd

Elmt	Val.	Min	Max	Elmt	Val.	Min	Max	Elmt	Val.	Min	Max	Use Adduct
H	1	10	40	O	2	0	5	S	2	0	0	H
2H	1	0	0	F	1	0	0	Cl	1	0	2	Na
C	4	10	35	Si	4	0	0	Br	1	0	2	K
N	3	0	5	P	3	0	0	I	3	0	0	NH4

Error Margin (ppm): 500
HC Ratio: unlimited
Max Isotopes: all
MSn Iso RI (%): 75.00

DBE Range: -100.0 - 2000.0
Apply N Rule: no
Isotope RI (%): 1.00
MSn Logic Mode: AND

Electron Ions: both
Use MSn Info: yes
Isotope Res: 10000
Max Results: 10

Event#: 1 MS(E+) Ret. Time : 0.600 -> 0.693 - 1.360 -> 1.919 Scan# : 91 -> 105 - 205 -> 289

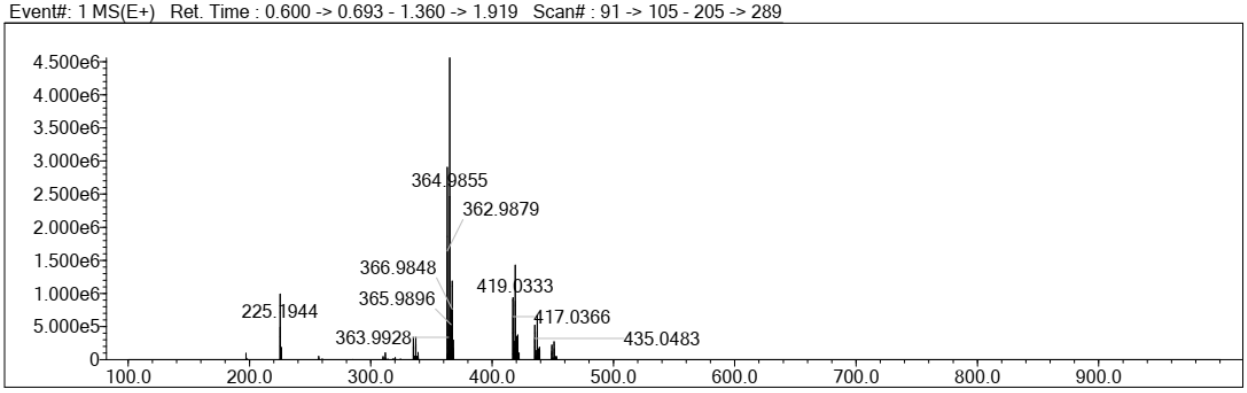

Measured region for 362.9879 m/z

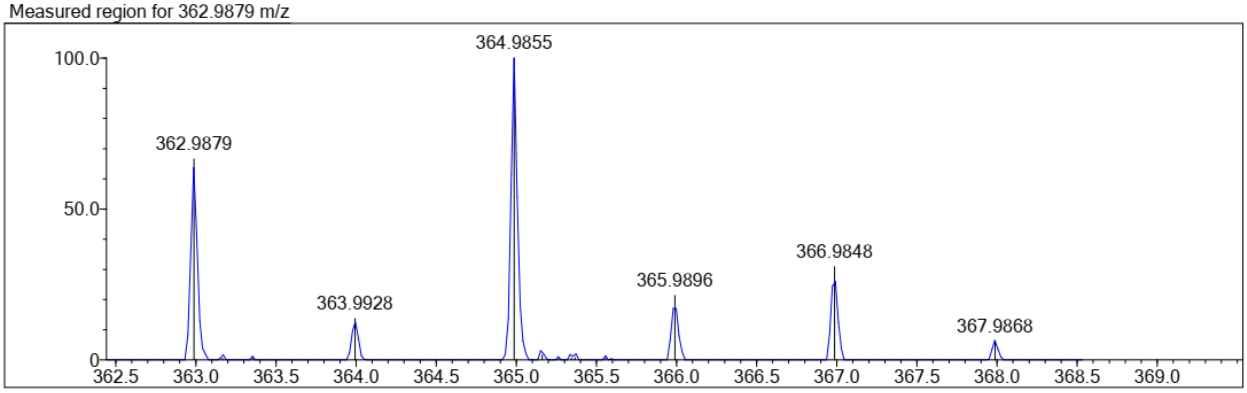

C16 H12 N2 O Cl Br [M+H]+ : Predicted region for 362.9894 m/z

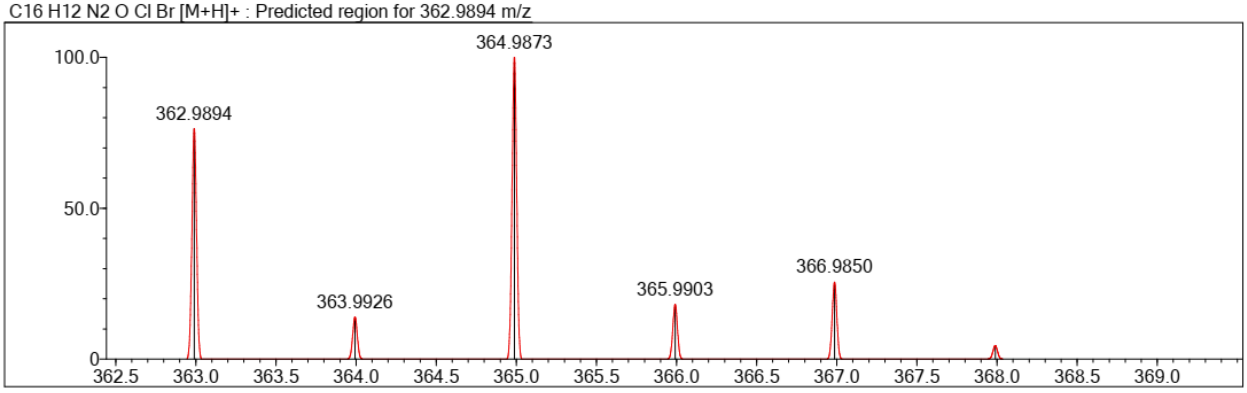

Rank	Score	Formula (M)	Ion	Meas. m/z	Pred. m/z	Df. (mDa)	Df. (ppm)	Iso	DBE
8	67.49	C16 H12 N2 O Cl Br	[M+H]+	362.9879	362.9894	-1.5	-4.13	73.22	11.0

Data File: C:\LabSolutions\Data\Vilashini Rajaratnam\01272021 Analysis\FR-II-29_Farjana Analysis 01272021 Batch_18.lcd

Elmt	Val.	Min	Max	Elmt	Val.	Min	Max	Elmt	Val.	Min	Max	Use Adduct
H	1	10	40	O	2	0	2	S	2	0	0	H
2H	1	0	0	F	1	0	0	Cl	1	0	2	Na
C	4	10	35	Si	4	0	1	Br	1	0	2	K
N	3	0	3	P	3	0	0	I	3	0	0	NH4

Error Margin (ppm): 500
HC Ratio: unlimited
Max Isotopes: all
MSn Iso RI (%): 75.00

DBE Range: -100.0 - 2000.0
Apply N Rule: no
Isotope RI (%): 1.00
MSn Logic Mode: AND

Electron Ions: both
Use MSn Info: yes
Isotope Res: 10000
Max Results: 10

Event#: 1 MS(E+) Ret. Time : 0.267 -> 0.360 - 1.640 -> 1.869 Scan# : 41 -> 55 - 247 -> 281

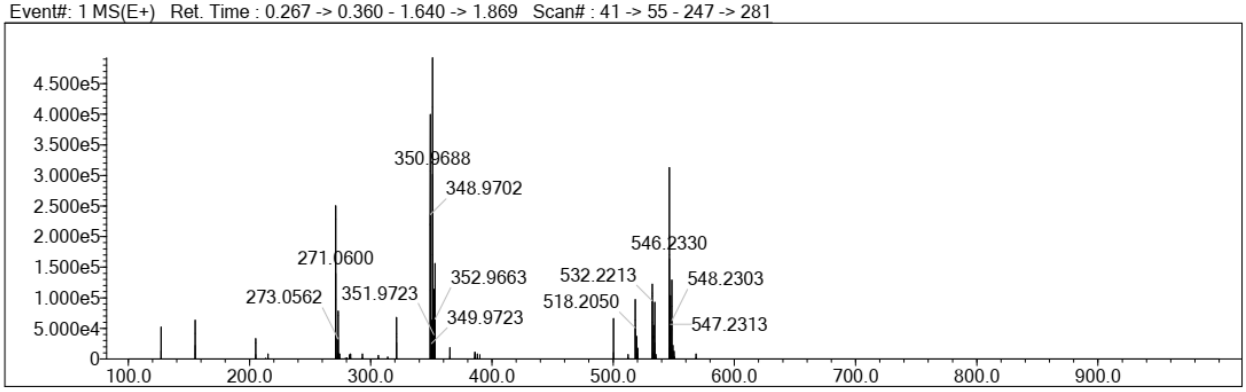

Measured region for 546.2330 m/z

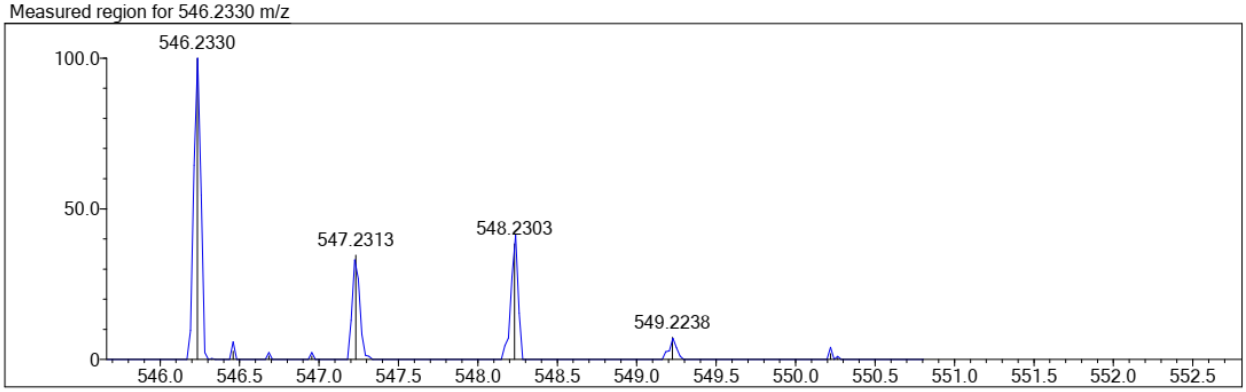

C31 H36 N3 O2 Si Cl [M+H]+ : Predicted region for 546.2338 m/z

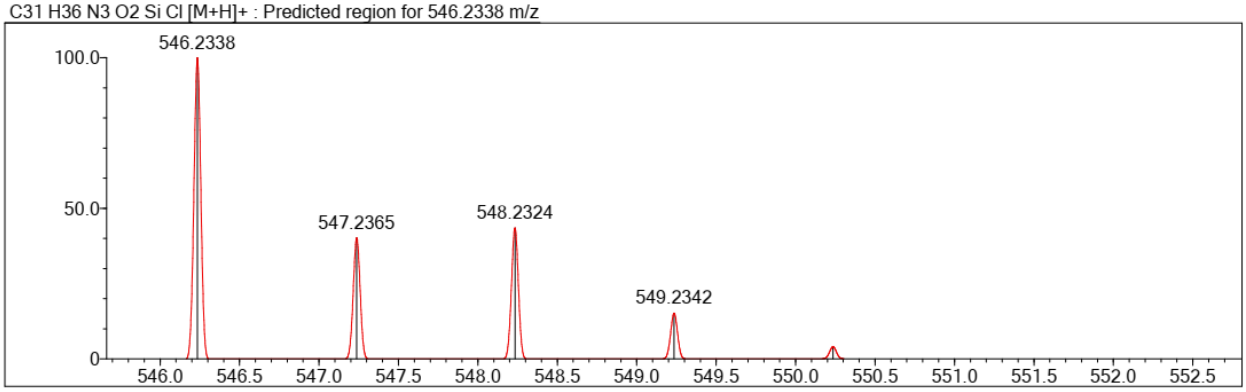

Rank	Score	Formula (M)	Ion	Meas. m/z	Pred. m/z	Df. (mDa)	Df. (ppm)	Iso	DBE
5	46.88	C31 H36 N3 O2 Si Cl	[M+H]+	546.2330	546.2338	-0.8	-1.46	47.42	16.0

Data File: C:\LabSolutions\Data\Vilashini Rajaratnam\01272021 Analysis\FR-III-04_Farjana Analysis 01272021 Batch_34.lcd

Elmt	Val.	Min	Max	Elmt	Val.	Min	Max	Elmt	Val.	Min	Max	Use Adduct
H	1	30	40	O	2	1	2	S	2	0	0	H
2H	1	0	0	F	1	0	0	Cl	1	0	1	Na
C	4	30	35	Si	4	0	1	Br	1	0	0	K
N	3	1	3	P	3	0	0	I	3	0	0	NH4

Error Margin (ppm): 500
HC Ratio: unlimited
Max Isotopes: all
MSn Iso RI (%): 75.00

DBE Range: -100.0 - 2000.0
Apply N Rule: no
Isotope RI (%): 1.00
MSn Logic Mode: AND

Electron Ions: both
Use MSn Info: yes
Isotope Res: 10000
Max Results: 10

Event#: 1 MS(E+) Ret. Time : 0.347 -> 0.467 - 1.440 -> 1.542 Scan# : 53 -> 71 - 217 -> 233

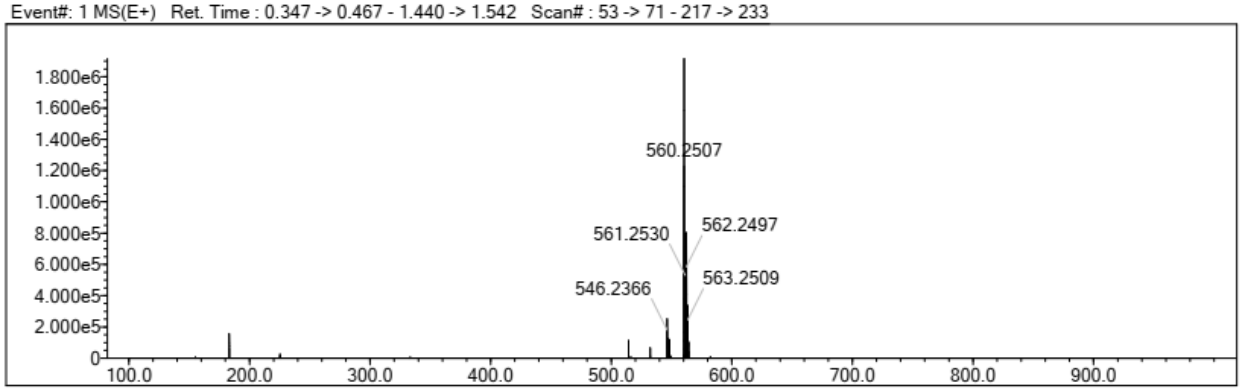

Measured region for 560.2507 m/z

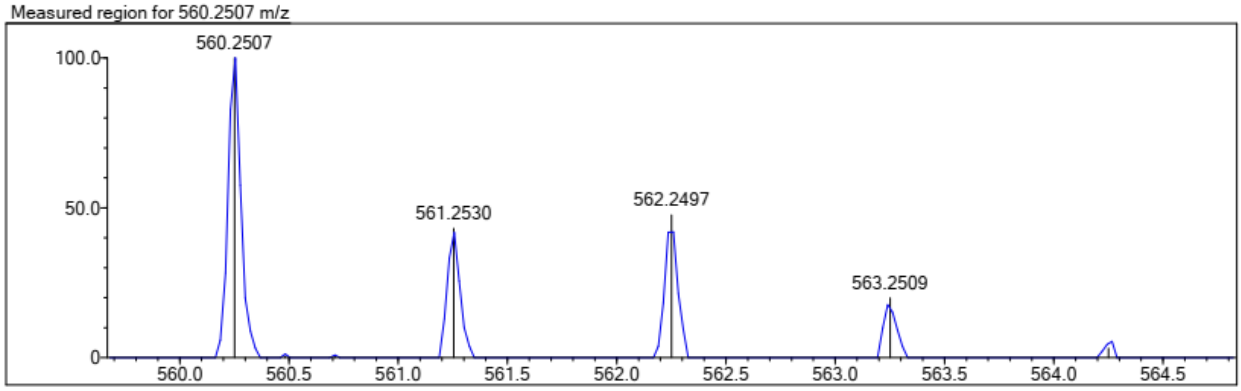

C32 H38 N3 O2 Si Cl [M+H]+ : Predicted region for 560.2495 m/z

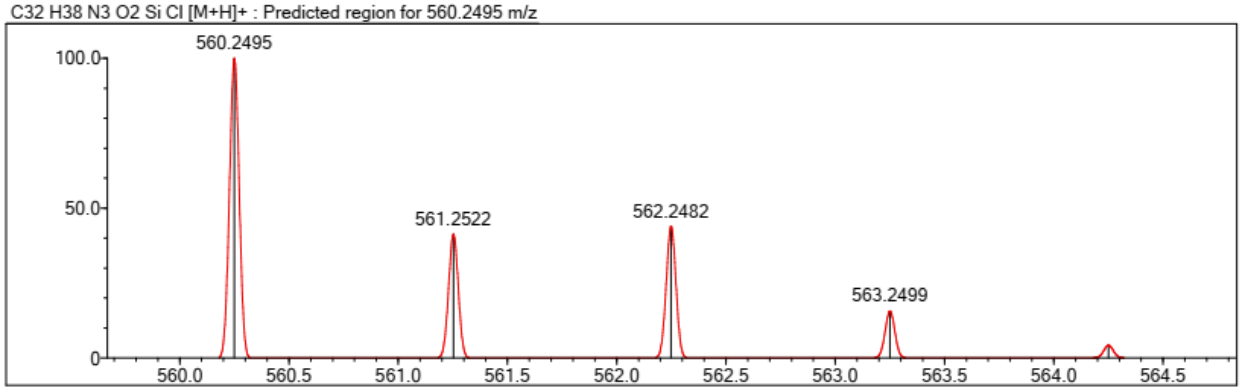

Rank	Score	Formula (M)	Ion	Meas. m/z	Pred. m/z	Df. (mDa)	Df. (ppm)	Iso	DBE
2	86.91	C32 H35 N2 O2 Si Cl	[M+NH4]+	560.2507	560.2495	1.2	2.14	89.46	17.0

Data File: C:\LabSolutions\Data\Vilashini Rajaratnam\01272021 Analysis\FR-III-05_Farjana Analysis 01272021 Batch_24.lcd

Elmt	Val.	Min	Max	Elmt	Val.	Min	Max	Elmt	Val.	Min	Max	Use Adduct
H	1	10	40	O	2	0	2	S	2	0	0	H
2H	1	0	0	F	1	0	0	Cl	1	0	2	Na
C	4	10	35	Si	4	0	1	Br	1	0	2	K
N	3	0	3	P	3	0	0	I	3	0	0	NH4

Error Margin (ppm): 500
HC Ratio: unlimited
Max Isotopes: all
MSn Iso RI (%): 75.00

DBE Range: -100.0 - 2000.0
Apply N Rule: no
Isotope RI (%): 1.00
MSn Logic Mode: AND

Electron Ions: both
Use MSn Info: yes
Isotope Res: 10000
Max Results: 10

Event#: 1 MS(E+) Ret. Time : 0.293 -> 0.320 - 0.040 -> 0.081 Scan# : 45 -> 49 - 7 -> 13

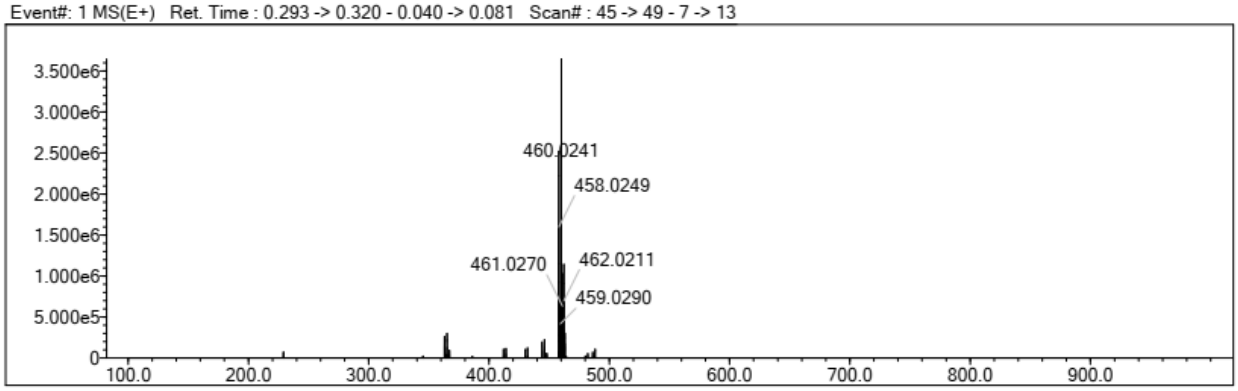

Measured region for 458.0249 m/z

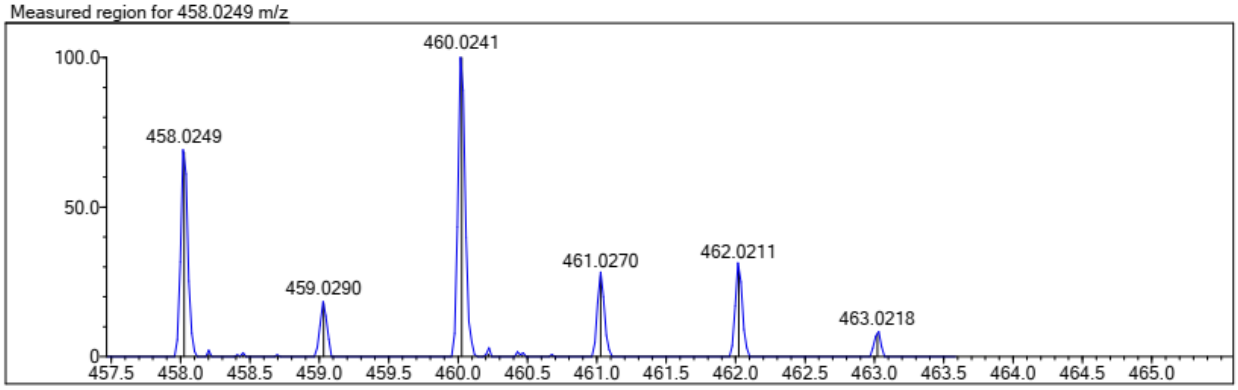

C21 H17 N3 O2 Cl Br [M+H]+ : Predicted region for 458.0265 m/z

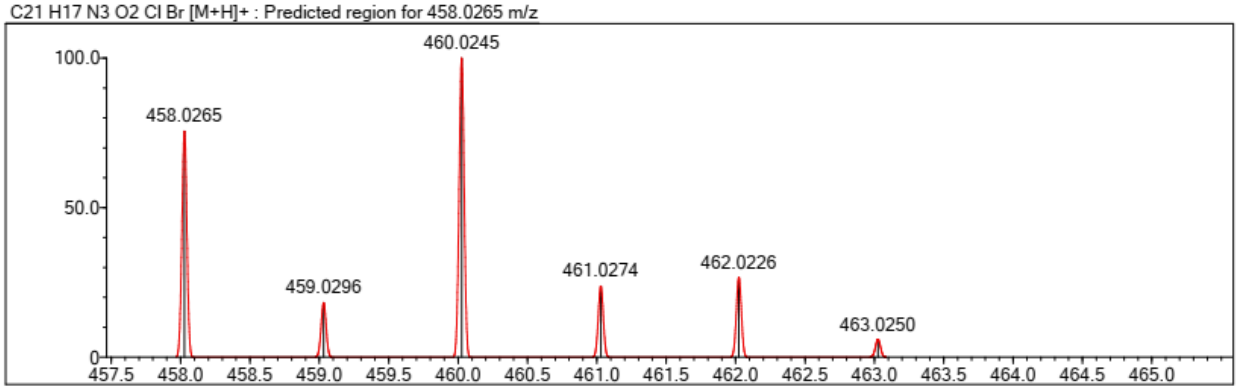

Rank	Score	Formula (M)	Ion	Meas. m/z	Pred. m/z	Df. (mDa)	Df. (ppm)	Iso	DBE
3	75.49	C21 H17 N3 O2 Cl Br	[M+H]+	458.0249	458.0265	-1.6	-3.49	80.50	14.0

Data File: C:\LabSolutions\Data\Vilashini Rajaratnam\01272021 Analysis\FR-I-19_Farjana Analysis 01272021 Batch_30.lcd

Elmt	Val.	Min	Max	Elmt	Val.	Min	Max	Elmt	Val.	Min	Max	Use Adduct
H	1	10	40	O	2	0	3	S	2	0	0	H
2H	1	0	0	F	1	0	0	Cl	1	0	2	Na
C	4	10	35	Si	4	0	1	Br	1	0	2	K
N	3	0	5	P	3	0	0	I	3	0	0	NH4

Error Margin (ppm): 500
HC Ratio: unlimited
Max Isotopes: all
MSn Iso RI (%): 75.00

DBE Range: -100.0 - 2000.0
Apply N Rule: no
Isotope RI (%): 1.00
MSn Logic Mode: AND

Electron Ions: both
Use MSn Info: yes
Isotope Res: 10000
Max Results: 10

Event#: 1 MS(E+) Ret. Time : 0.293 -> 0.320 - 1.453 -> 1.523 Scan# : 45 -> 49 - 219 -> 229

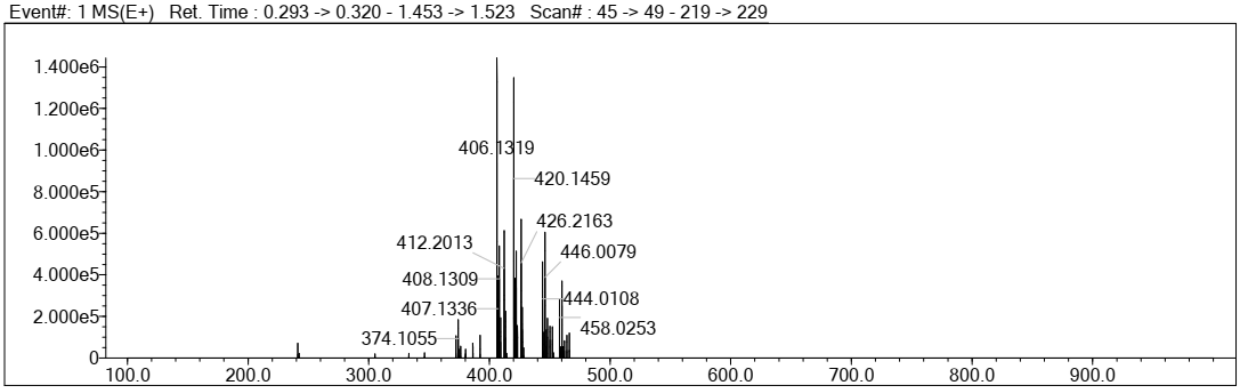

Measured region for 406.1319 m/z

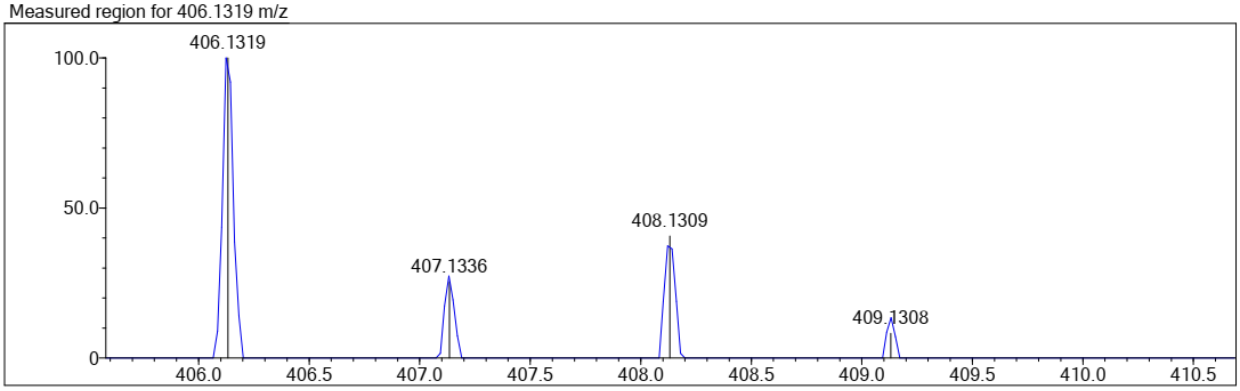

C23 H20 N3 O2 Cl [M+H]+ : Predicted region for 406.1317 m/z

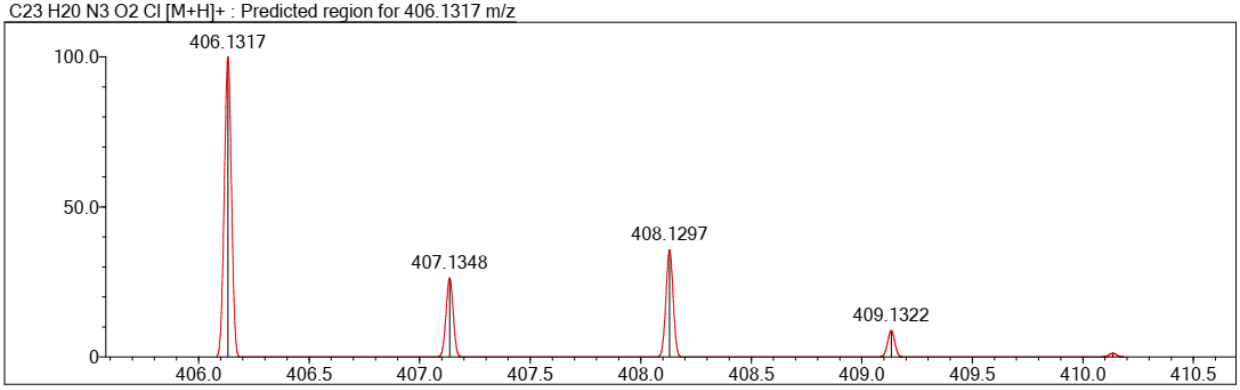

Rank	Score	Formula (M)	Ion	Meas. m/z	Pred. m/z	Df. (mDa)	Df. (ppm)	Iso	DBE
1	86.66	C23 H20 N3 O2 Cl	[M+H]+	406.1319	406.1317	0.2	0.49	86.66	15.0

Data File: C:\LabSolutions\Data\Vilashini Rajaratnam\06042021 Analysis\FR-03-39_06042021 Analysis HRMS_18.lcd

Elmt	Val.	Min	Max	Elmt	Val.	Min	Max	Elmt	Val.	Min	Max	Elmt	Val.	Min	Max	Use Adduct
H	1	10	40	O	2	0	2	P	3	0	0	I	3	0	0	H
2H	1	0	0	F	1	0	0	S	2	0	0					Na
C	4	15	35	Na	1	0	0	Cl	1	0	1					K
N	3	2	6	Si	4	0	1	Br	1	0	1					NH4

Error Margin (ppm): 500
HC Ratio: unlimited
Max Isotopes: all
MSn Iso RI (%): 75.00

DBE Range: -100.0 - 2000.0
Apply N Rule: yes
Isotope RI (%): 1.00
MSn Logic Mode: AND

Electron Ions: both
Use MSn Info: yes
Isotope Res: 10000
Max Results: 10

Event#: 1 MS(E+) Ret. Time : 0.413 -> 0.880 - 1.613 -> 1.726 Scan# : 63 -> 133 - 243 -> 259

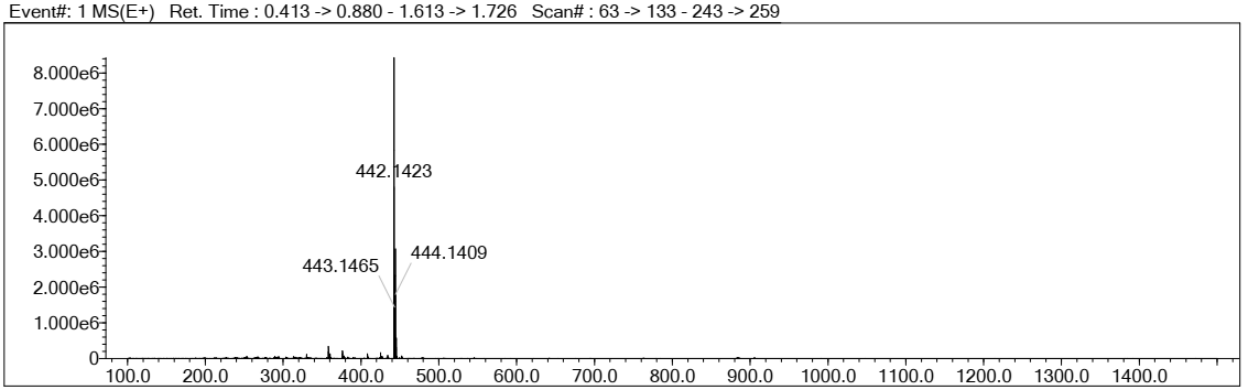

Measured region for 442.1423 m/z

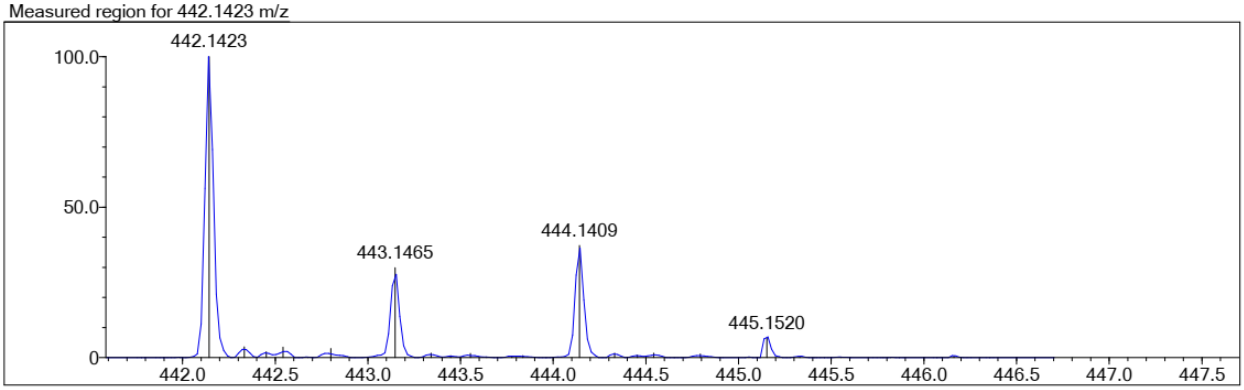

C25 H20 N5 O Cl [M+H]+ : Predicted region for 442.1429 m/z

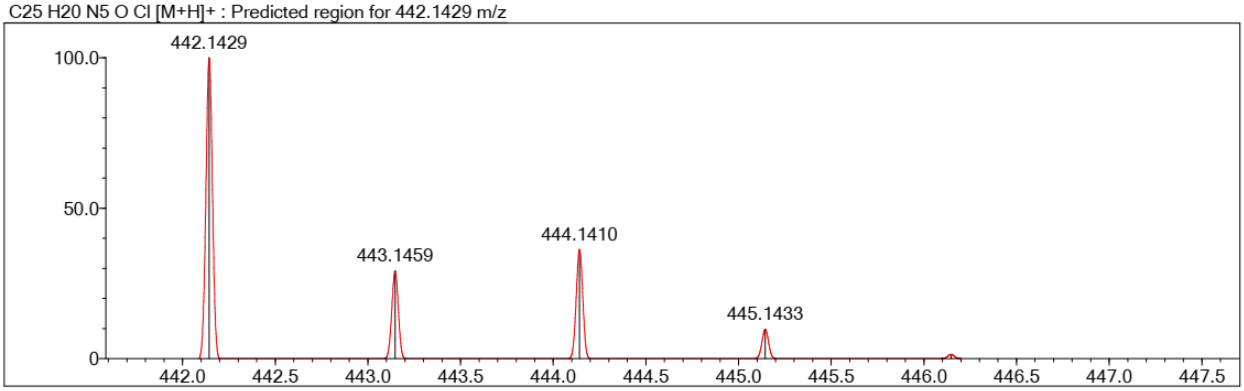

Rank	Score	Formula (M)	Ion	Meas. m/z	Pred. m/z	Df. (mDa)	Df. (ppm)	Iso	DBE
1	61.86	C25 H20 N5 O Cl	[M+H]+	442.1423	442.1429	-0.6	-1.36	62.43	18.0

Data File: C:\LabSolutions\Data\Vilashini Rajaratnam\06042021 Analysis\FR-03-51_06042021 Analysis HRMS_12.lcd

Elmt	Val.	Min	Max	Elmt	Val.	Min	Max	Elmt	Val.	Min	Max	Elmt	Val.	Min	Max	Use Adduct
H	1	10	40	O	2	0	2	P	3	0	0	I	3	0	0	H
2H	1	0	0	F	1	0	0	S	2	0	0					Na
C	4	15	35	Na	1	0	0	Cl	1	0	1					K
N	3	2	6	Si	4	0	1	Br	1	0	1					NH4

Error Margin (ppm): 500
HC Ratio: unlimited
Max Isotopes: all
MSn Iso RI (%): 75.00

DBE Range: -100.0 - 2000.0
Apply N Rule: yes
Isotope RI (%): 1.00
MSn Logic Mode: AND

Electron Ions: both
Use MSn Info: yes
Isotope Res: 10000
Max Results: 10

Event#: 1 MS(E+) Ret. Time : 0.400 -> 0.853 - 1.320 -> 1.507 Scan# : 61 -> 129 - 199 -> 227

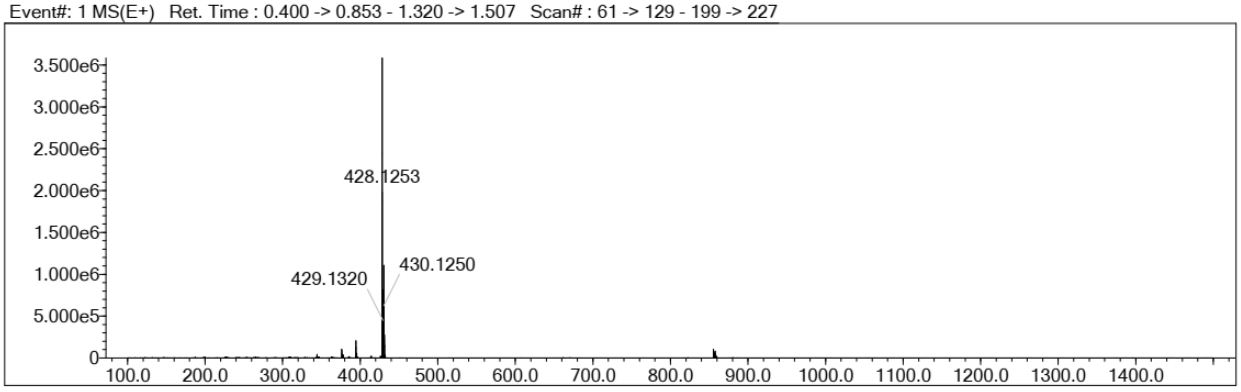

Measured region for 428.1253 m/z

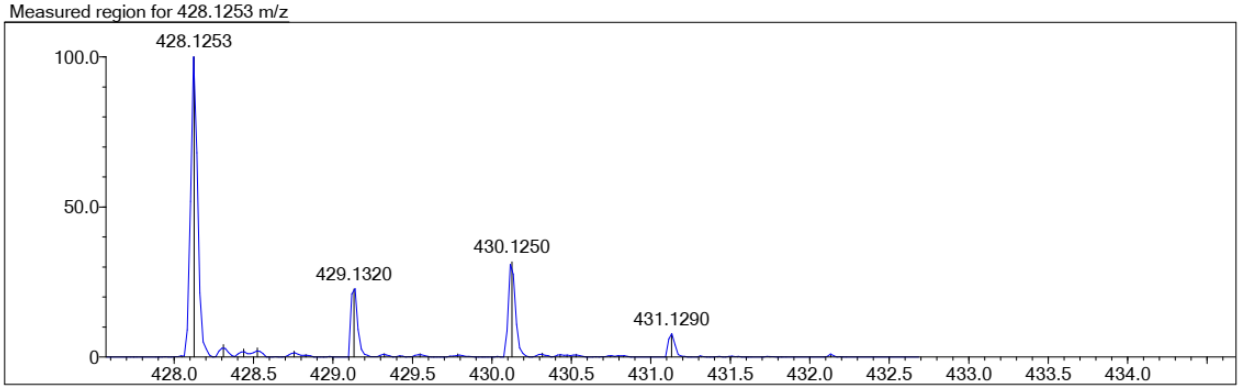

C24 H18 N5 O Cl [M+H]+ : Predicted region for 428.1273 m/z

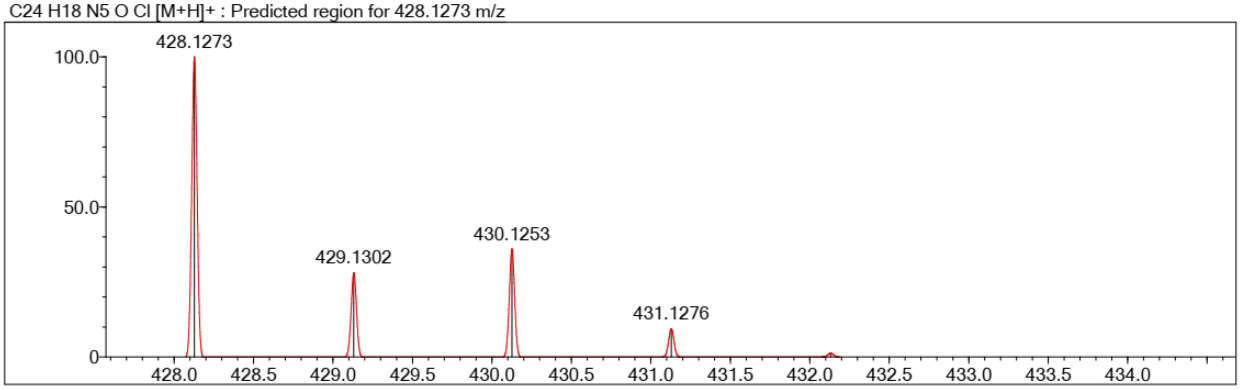

Rank	Score	Formula (M)	Ion	Meas. m/z	Pred. m/z	Df. (mDa)	Df. (ppm)	Iso	DBE
2	64.81	C24 H18 N5 O Cl	[M+H]+	428.1253	428.1273	-2.0	-4.67	71.35	18.0

Data File: C:\LabSolutions\Data\Vilashini Rajaratnam\06042021 Analysis\FR-01-70_06042021 Analysis HRMS_26.lcd

Elmt	Val.	Min	Max	Elmt	Val.	Min	Max	Elmt	Val.	Min	Max	Elmt	Val.	Min	Max	Use Adduct
H	1	10	20	O	2	0	2	P	3	0	0	I	3	0	0	H
2H	1	0	0	F	1	0	0	S	2	0	0					Na
C	4	15	25	Na	1	0	0	Cl	1	0	1					K
N	3	2	6	Si	4	0	0	Br	1	0	1					NH4

Error Margin (ppm):	500	DBE Range:	-100.0 - 2000.0	Electron Ions:	both
HC Ratio:	unlimited	Apply N Rule:	yes	Use MSn Info:	yes
Max Isotopes:	all	Isotope RI (%):	1.00	Isotope Res:	10000
MSn Iso RI (%):	75.00	MSn Logic Mode:	AND	Max Results:	10

Event#: 1 MS(E+) Ret. Time : 0.413 -> 0.907 - 1.493 -> 1.666 Scan# : 63 -> 137 - 225 -> 251

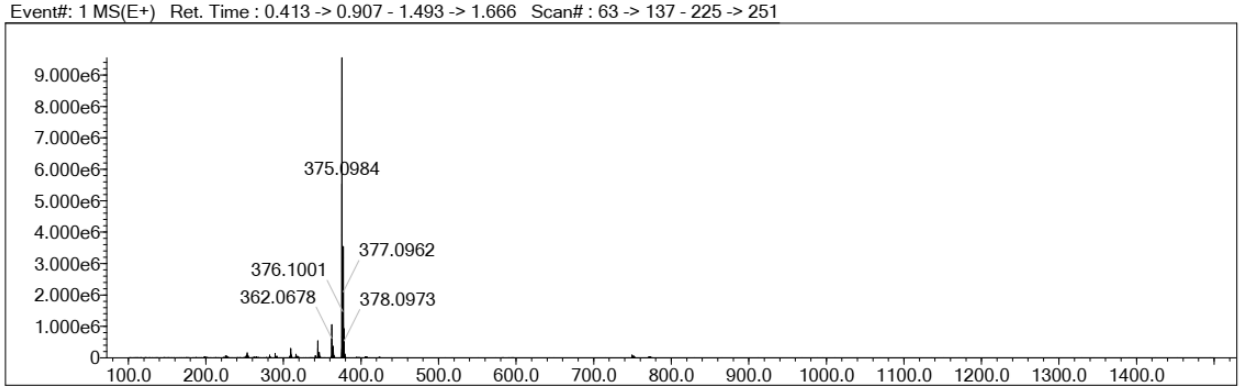

Measured region for 375.0984 m/z

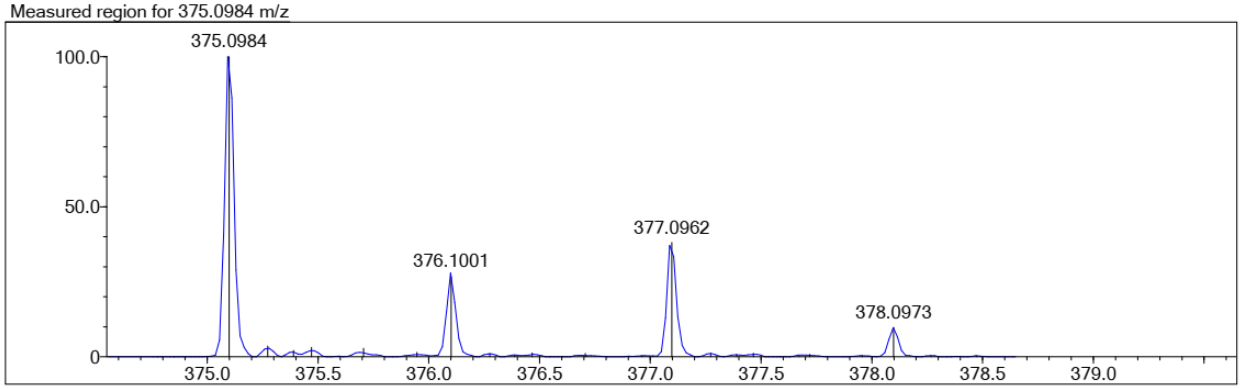

C21 H15 N4 O Cl [M+H]+ : Predicted region for 375.1007 m/z

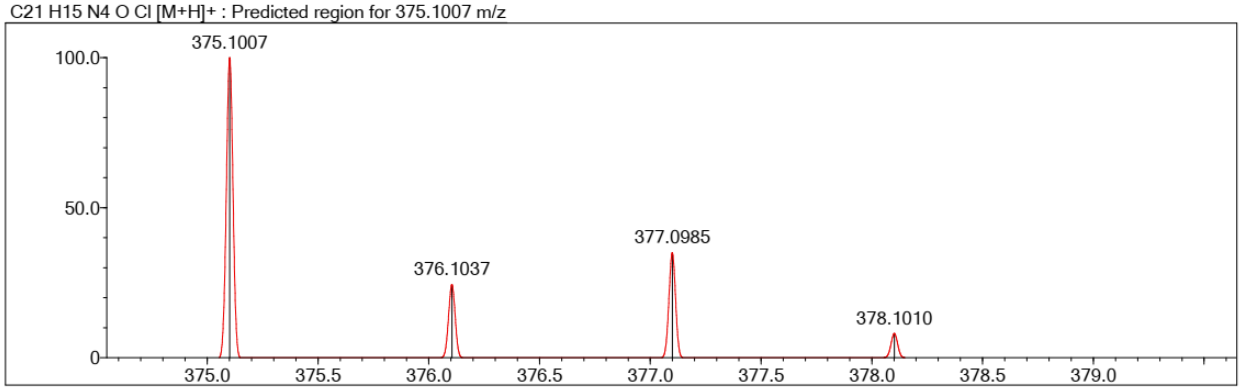

Rank	Score	Formula (M)	Ion	Meas. m/z	Pred. m/z	Df. (mDa)	Df. (ppm)	Iso	DBE
2	63.65	C21 H15 N4 O Cl	[M+H]+	375.0984	375.1007	-2.3	-6.13	80.88	16.0

Data File: C:\LabSolutions\Data\Vilashini Rajaratnam\06042021 Analysis\FR-01-72_06042021 Analysis HRMS_10.lcd

Elmt	Val.	Min	Max	Elmt	Val.	Min	Max	Elmt	Val.	Min	Max	Elmt	Val.	Min	Max	Use Adduct
H	1	10	20	O	2	0	2	P	3	0	0	I	3	0	0	H
2H	1	0	0	F	1	0	0	S	2	0	0					Na
C	4	15	25	Na	1	0	0	Cl	1	0	1					K
N	3	2	6	Si	4	0	0	Br	1	0	1					NH4

Error Margin (ppm): 500
HC Ratio: unlimited
Max Isotopes: all
MSn Iso RI (%): 75.00

DBE Range: -100.0 - 2000.0
Apply N Rule: yes
Isotope RI (%): 1.00
MSn Logic Mode: AND

Electron Ions: both
Use MSn Info: yes
Isotope Res: 10000
Max Results: 10

Event#: 1 MS(E+) Ret. Time : 0.360 -> 1.000 - 1.573 -> 1.678 Scan# : 55 -> 151 - 237 -> 253

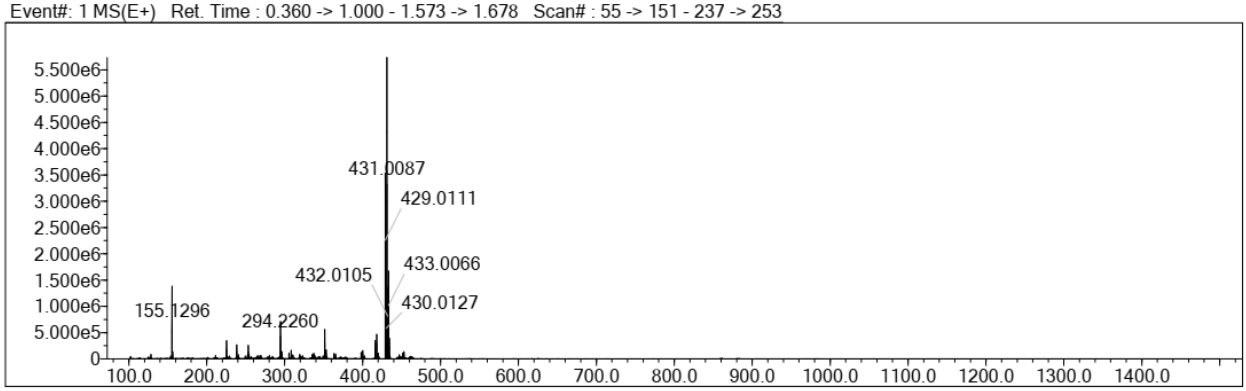

Measured region for 429.0111 m/z

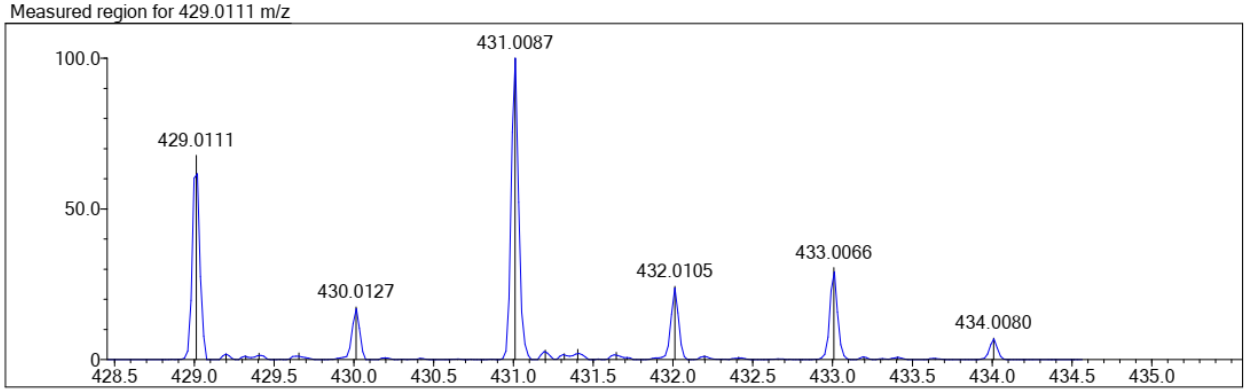

C19 H14 N4 O Cl Br [M+H]+ : Predicted region for 429.0112 m/z

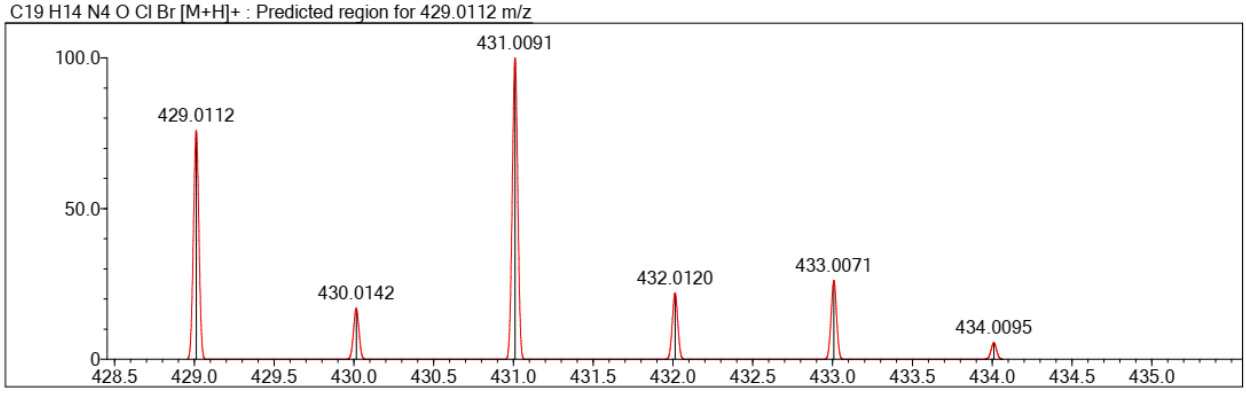

Rank	Score	Formula (M)	Ion	Meas. m/z	Pred. m/z	Df. (mDa)	Df. (ppm)	Iso	DBE
2	74.91	C19 H14 N4 O Cl Br	[M+H]+	429.0111	429.0112	-0.1	-0.23	74.91	14.0

Data File: C:\LabSolutions\Data\Vilashini Rajaratnam\06042021 Analysis\FR-01-75_06042021 Analysis HRMS_16.lcd

Elmt	Val.	Min	Max	Elmt	Val.	Min	Max	Elmt	Val.	Min	Max	Elmt	Val.	Min	Max	Use Adduct
H	1	10	20	O	2	0	2	P	3	0	0	I	3	0	0	H
2H	1	0	0	F	1	0	0	S	2	0	0					Na
C	4	15	25	Na	1	0	0	Cl	1	0	1					K
N	3	2	6	Si	4	0	0	Br	1	0	1					NH4

Error Margin (ppm): 500
HC Ratio: unlimited
Max Isotopes: all
MSn Iso RI (%): 75.00

DBE Range: -100.0 - 2000.0
Apply N Rule: yes
Isotope RI (%): 1.00
MSn Logic Mode: AND

Electron Ions: both
Use MSn Info: yes
Isotope Res: 10000
Max Results: 10

Event#: 1 MS(E+) Ret. Time : 0.413 -> 0.867 - 0.187 -> 0.238 Scan# : 63 -> 131 - 29 -> 37

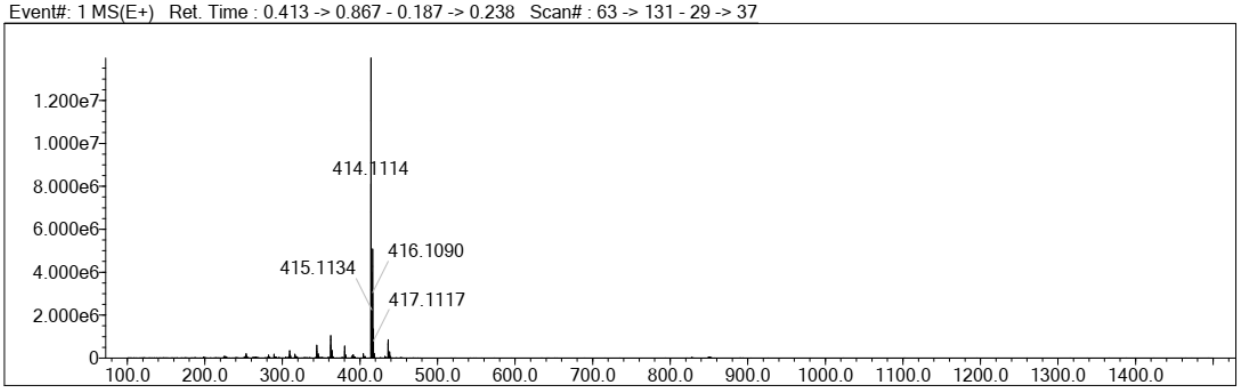

Measured region for 414.1114 m/z

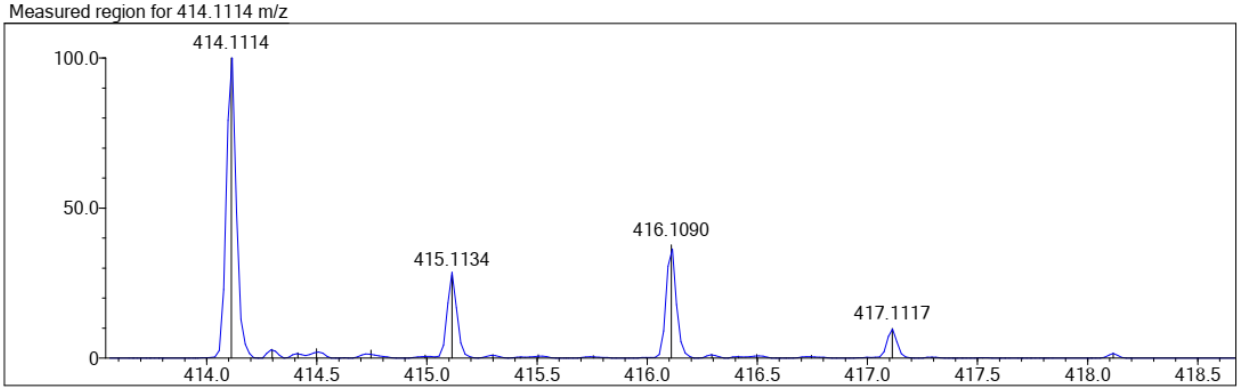

C23 H16 N5 O Cl [M+H]+ : Predicted region for 414.1116 m/z

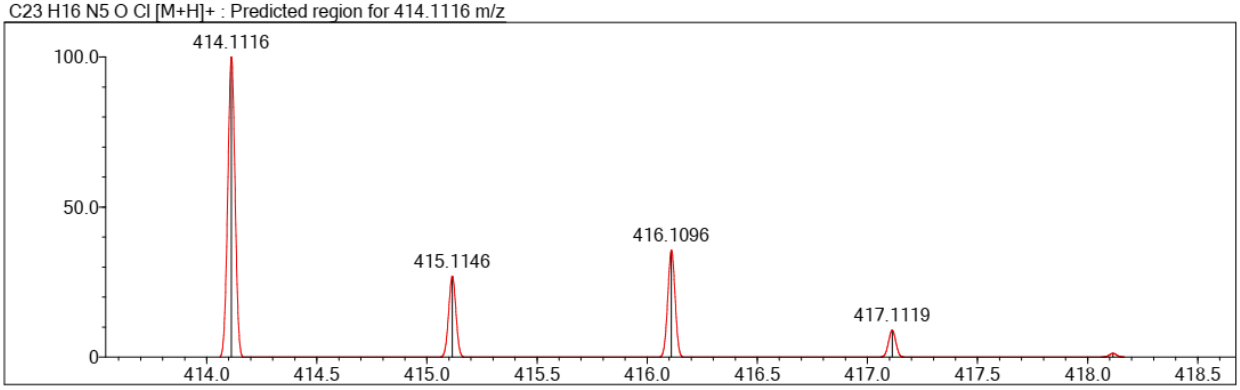

Rank	Score	Formula (M)	Ion	Meas. m/z	Pred. m/z	Df. (mDa)	Df. (ppm)	Iso	DBE
1	100.00	C23 H16 N5 O Cl	[M+H]+	414.1114	414.1116	-0.2	-0.48	100.00	18.0

Data File: C:\LabSolutions\Data\Vilashini Rajaratnam\06042021 Analysis\FR-01-98_06042021 Analysis HRMS_14.lcd

Elmt	Val.	Min	Max	Elmt	Val.	Min	Max	Elmt	Val.	Min	Max	Elmt	Val.	Min	Max	Use Adduct
H	1	10	20	O	2	0	2	P	3	0	0	I	3	0	0	H
2H	1	0	0	F	1	0	0	S	2	0	0					Na
C	4	15	25	Na	1	0	0	Cl	1	0	1					K
N	3	2	6	Si	4	0	0	Br	1	0	1					NH4

Error Margin (ppm): 500
HC Ratio: unlimited
Max Isotopes: all
MSn Iso RI (%): 75.00

DBE Range: -100.0 - 2000.0
Apply N Rule: yes
Isotope RI (%): 1.00
MSn Logic Mode: AND

Electron Ions: both
Use MSn Info: yes
Isotope Res: 10000
Max Results: 10

Event#: 1 MS(E+) Ret. Time : 0.400 -> 0.840 Scan# : 61 -> 127

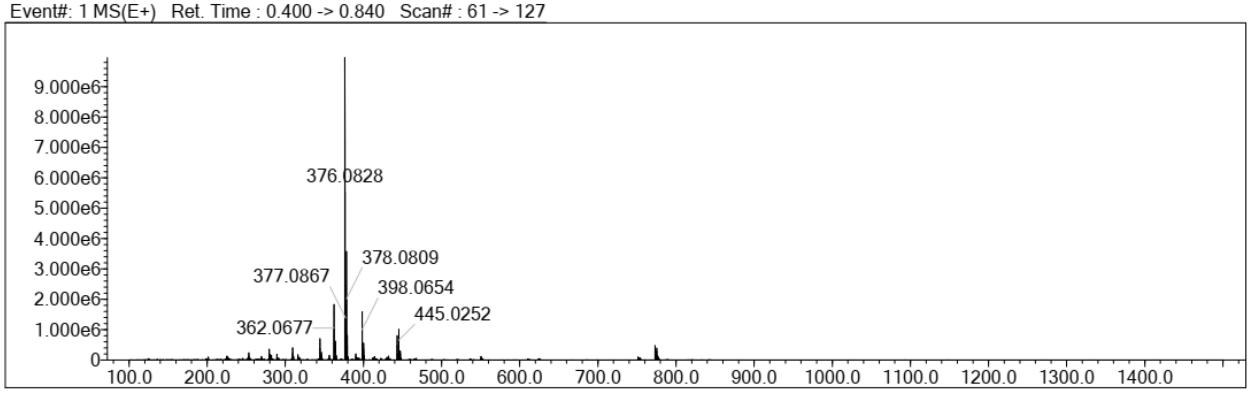

Measured region for 376.0828 m/z

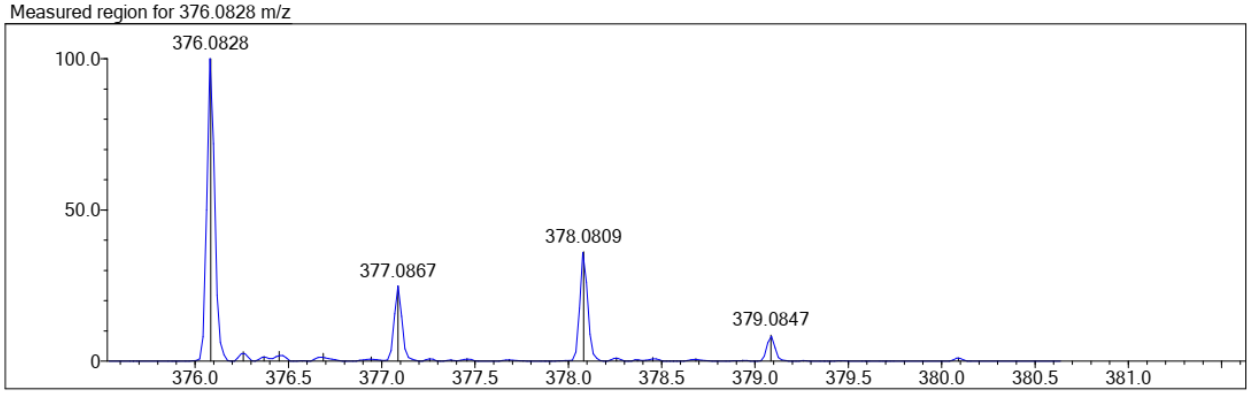

C21 H14 N3 O2 Cl [M+H]+ : Predicted region for 376.0847 m/z

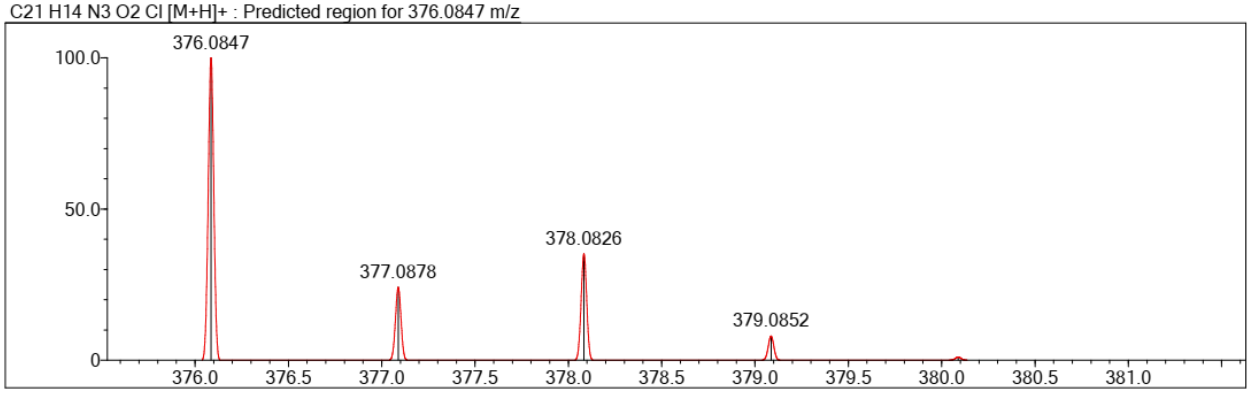

Rank	Score	Formula (M)	Ion	Meas. m/z	Pred. m/z	Df. (mDa)	Df. (ppm)	Iso	DBE
3	77.44	C21 H14 N3 O2 Cl	[M+H]+	376.0828	376.0847	-1.9	-5.05	86.53	16.0

Data File: C:\LabSolutions\Data\Vilashini Rajaratnam\06042021 Analysis\FR-II-60_06042021 Analysis HRMS_22.lcd

Elmt	Val.	Min	Max	Elmt	Val.	Min	Max	Elmt	Val.	Min	Max	Elmt	Val.	Min	Max	Use Adduct
H	1	10	20	O	2	0	2	P	3	0	0	I	3	0	0	H
2H	1	0	0	F	1	0	0	S	2	0	0					Na
C	4	15	25	Na	1	0	0	Cl	1	0	1					K
N	3	2	6	Si	4	0	0	Br	1	0	1					NH4

Error Margin (ppm): 500
HC Ratio: unlimited
Max Isotopes: all
MSn Iso RI (%): 75.00

DBE Range: -100.0 - 2000.0
Apply N Rule: yes
Isotope RI (%): 1.00
MSn Logic Mode: AND

Electron Ions: both
Use MSn Info: yes
Isotope Res: 10000
Max Results: 10

Event#: 1 MS(E+) Ret. Time : 0.413 -> 0.867 - 1.640 -> 1.862 Scan# : 63 -> 131 - 247 -> 281

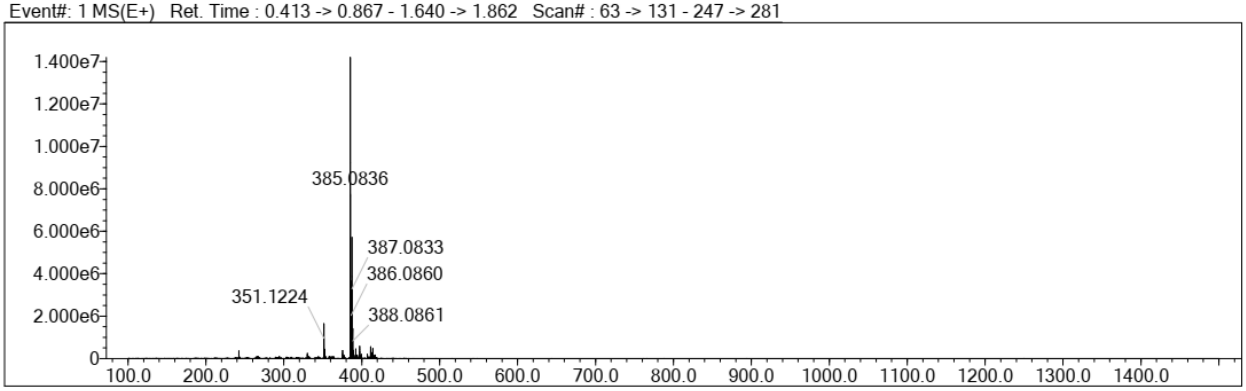

Measured region for 385.0836 m/z

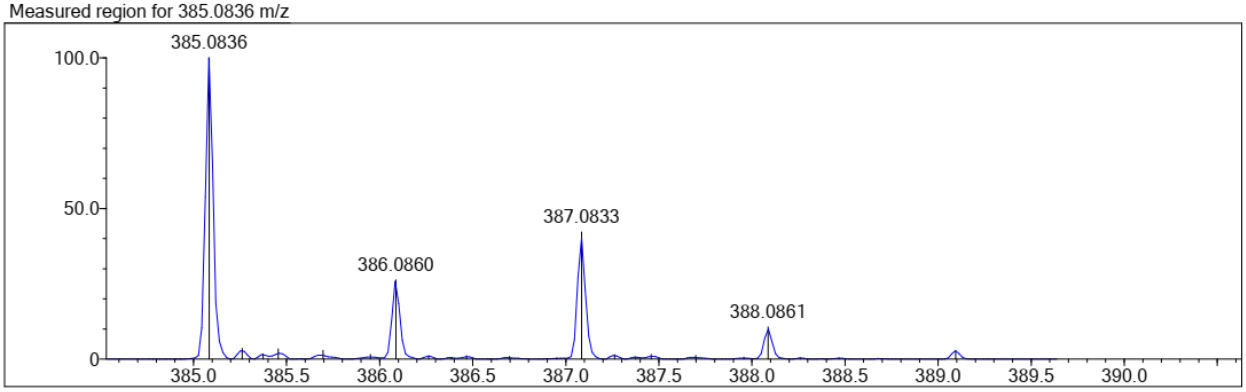

C22 H13 N4 O Cl [M+H]+ : Predicted region for 385.0851 m/z

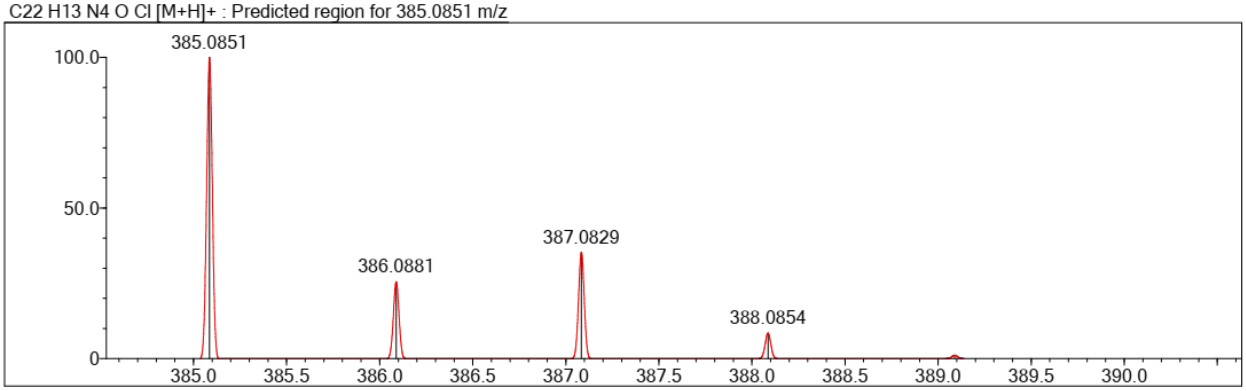

Rank	Score	Formula (M)	Ion	Meas. m/z	Pred. m/z	Df. (mDa)	Df. (ppm)	Iso	DBE
2	80.06	C22 H13 N4 O Cl	[M+H]+	385.0836	385.0851	-1.5	-3.90	86.32	18.0

Data File: C:\LabSolutions\Data\Vilashini Rajaratnam\06042021 Analysis\FR-0B-45_06042021 Analysis HRMS_28.lcd

Elmt	Val.	Min	Max	Elmt	Val.	Min	Max	Elmt	Val.	Min	Max	Elmt	Val.	Min	Max	Use Adduct
H	1	10	40	O	2	0	2	P	3	0	0	I	3	0	0	H
2H	1	0	0	F	1	0	0	S	2	0	0					Na
C	4	15	35	Na	1	0	0	Cl	1	0	1					K
N	3	2	6	Si	4	0	1	Br	1	0	1					NH4

Error Margin (ppm):	500	DBE Range:	-100.0 - 2000.0	Electron Ions:	both
HC Ratio:	unlimited	Apply N Rule:	yes	Use MSn Info:	yes
Max Isotopes:	all	Isotope RI (%):	1.00	Isotope Res:	10000
MSn Iso RI (%):	75.00	MSn Logic Mode:	AND	Max Results:	10

Event#: 1 MS(E+) Ret. Time : 0.413 -> 0.787 - 1.560 -> 1.774 Scan# : 63 -> 119 - 235 -> 267

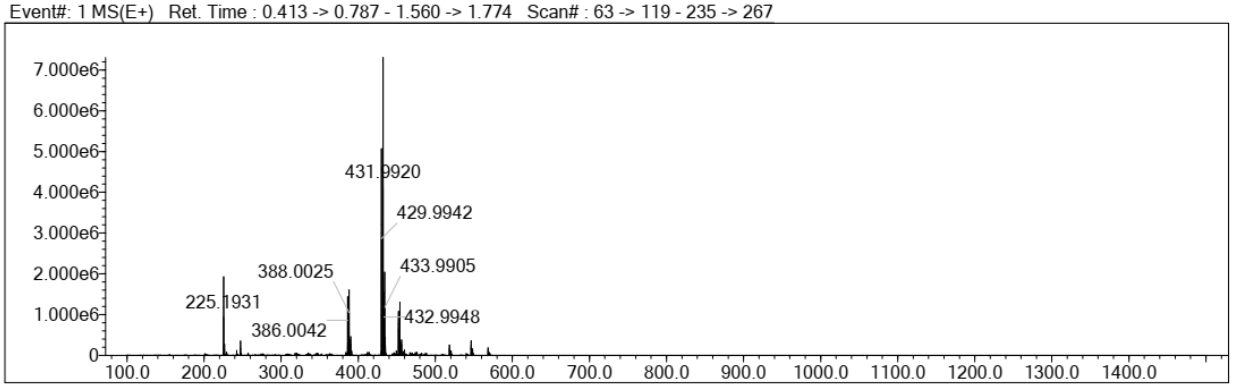

Measured region for 546.2370 m/z

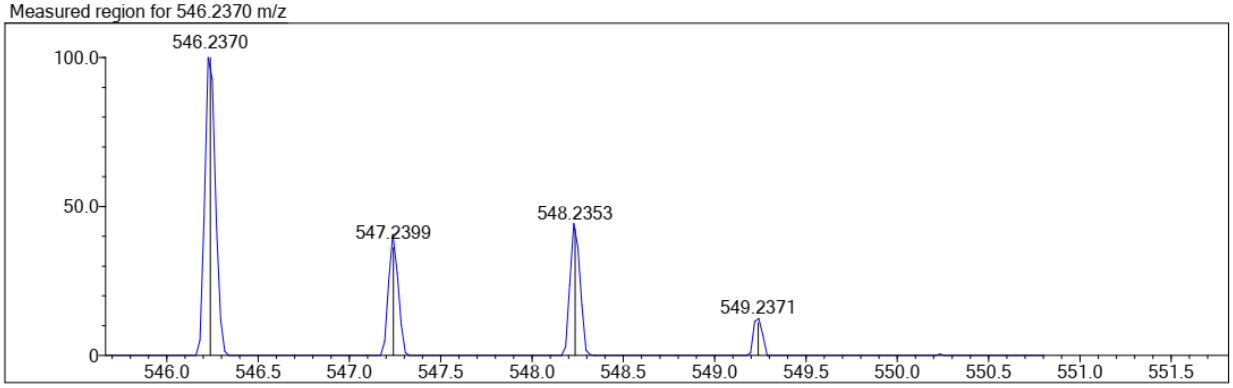

C31 H36 N3 O2 Si Cl [M+H]+ : Predicted region for 546.2338 m/z

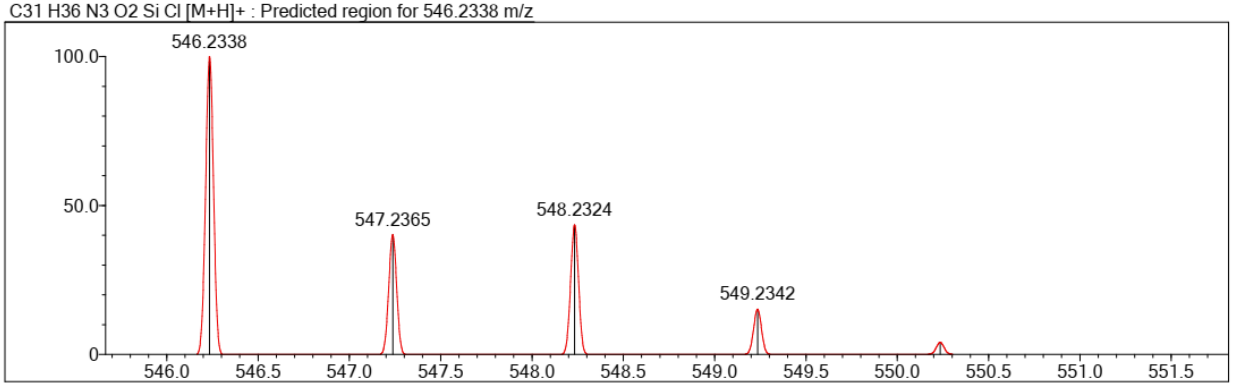

Rank	Score	Formula (M)	Ion	Meas. m/z	Pred. m/z	Df. (mDa)	Df. (ppm)	Iso	DBE
4	68.40	C31 H36 N3 O2 Si Cl	[M+H]+	546.2370	546.2338	3.2	5.86	84.03	16.0

Data File: C:\LabSolutions\Data\Vilashini Rajaratnam\06042021 Analysis\FR-03-47_06042021 Analysis HRMS_4.lcd

Elmt	Val.	Min	Max	Elmt	Val.	Min	Max	Elmt	Val.	Min	Max	Elmt	Val.	Min	Max	Use Adduct
H	1	10	20	O	2	0	2	P	3	0	0	I	3	0	0	H
2H	1	0	0	F	1	0	0	S	2	0	0					Na
C	4	20	25	Na	1	0	0	Cl	1	0	1					K
N	3	2	6	Si	4	0	0	Br	1	0	0					NH4

Error Margin (ppm): 500
HC Ratio: unlimited
Max Isotopes: all
MSn Iso RI (%): 75.00

DBE Range: -100.0 - 2000.0
Apply N Rule: yes
Isotope RI (%): 1.00
MSn Logic Mode: AND

Electron Ions: both
Use MSn Info: yes
Isotope Res: 10000
Max Results: 10

Event#: 1 MS(E+) Ret. Time : 0.453 -> 0.760 - 0.093 -> 0.337 Scan# : 69 -> 115 - 15 -> 51

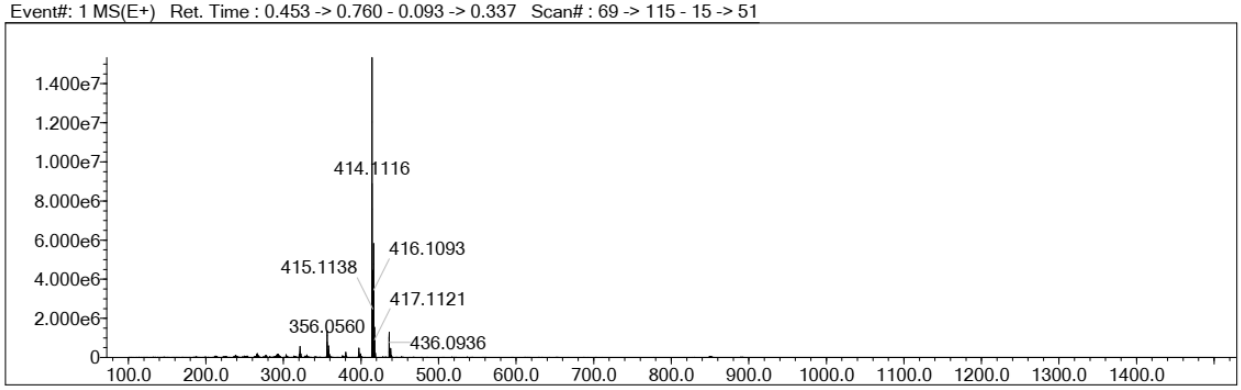

Measured region for 414.1116 m/z

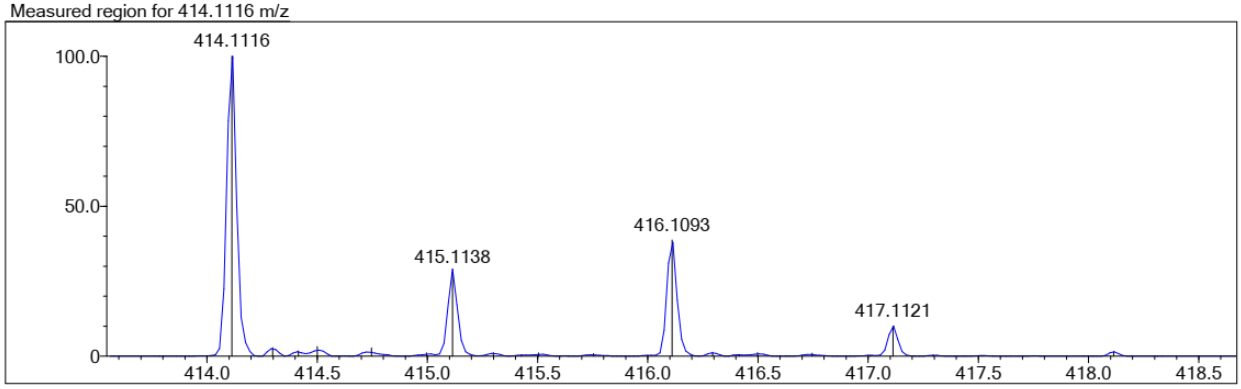

C23 H16 N5 O Cl [M+H]+ : Predicted region for 414.1116 m/z

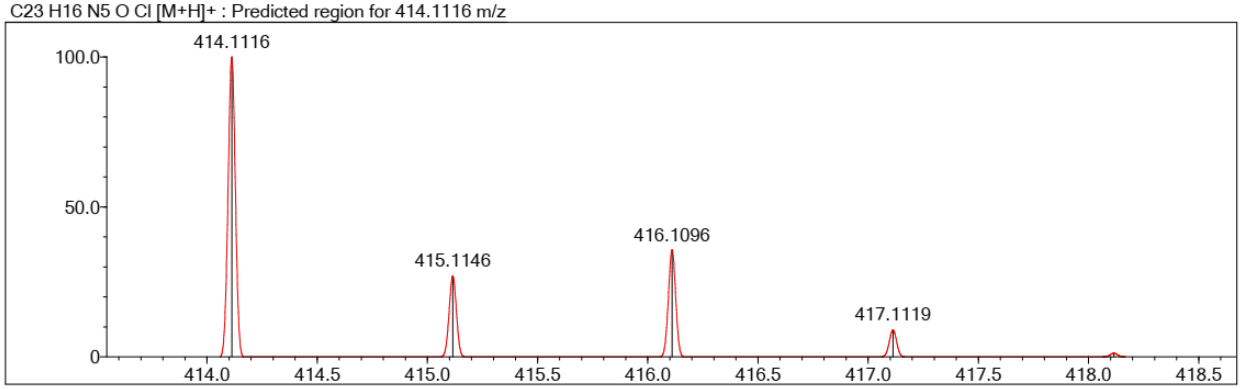

Rank	Score	Formula (M)	Ion	Meas. m/z	Pred. m/z	Df. (mDa)	Df. (ppm)	Iso	DBE
1	99.03	C23 H16 N5 O Cl	[M+H]+	414.1116	414.1116	-0.0	0.00	99.03	18.0

Chromatogram
fr2_grad2 ABBA_02072020_841_003.lcd

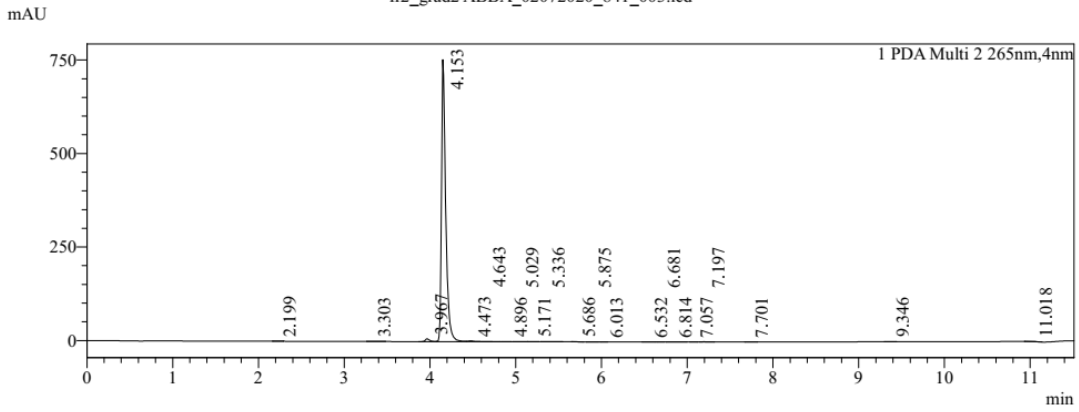

Chromatogram
fr2_grad2 ABBA_02072020_841_003.lcd

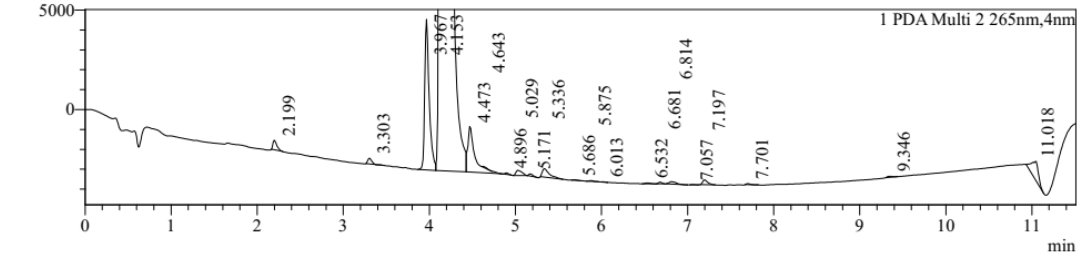

Peak Table fr2_grad2 ABBA_02072020_841_003.lcd

PDA Ch2 265nm

Peak#	Ret. Time	Area	Area%
1	2.199	1478	0.056
2	3.303	832	0.031
3	3.967	27211	1.029
4	4.153	2590578	97.955
5	4.473	13013	0.492
6	4.643	85	0.003
7	4.896	202	0.008
8	5.029	1252	0.047
9	5.171	302	0.011
10	5.336	2261	0.085
11	5.686	64	0.002
12	5.875	158	0.006
13	6.013	24	0.001
14	6.532	204	0.008
15	6.681	217	0.008
16	6.814	733	0.028
17	7.057	36	0.001
18	7.197	929	0.035
19	7.701	163	0.006
20	9.346	218	0.008
21	11.018	4702	0.178
Total		2644663	100.000

Appendix B

Posters

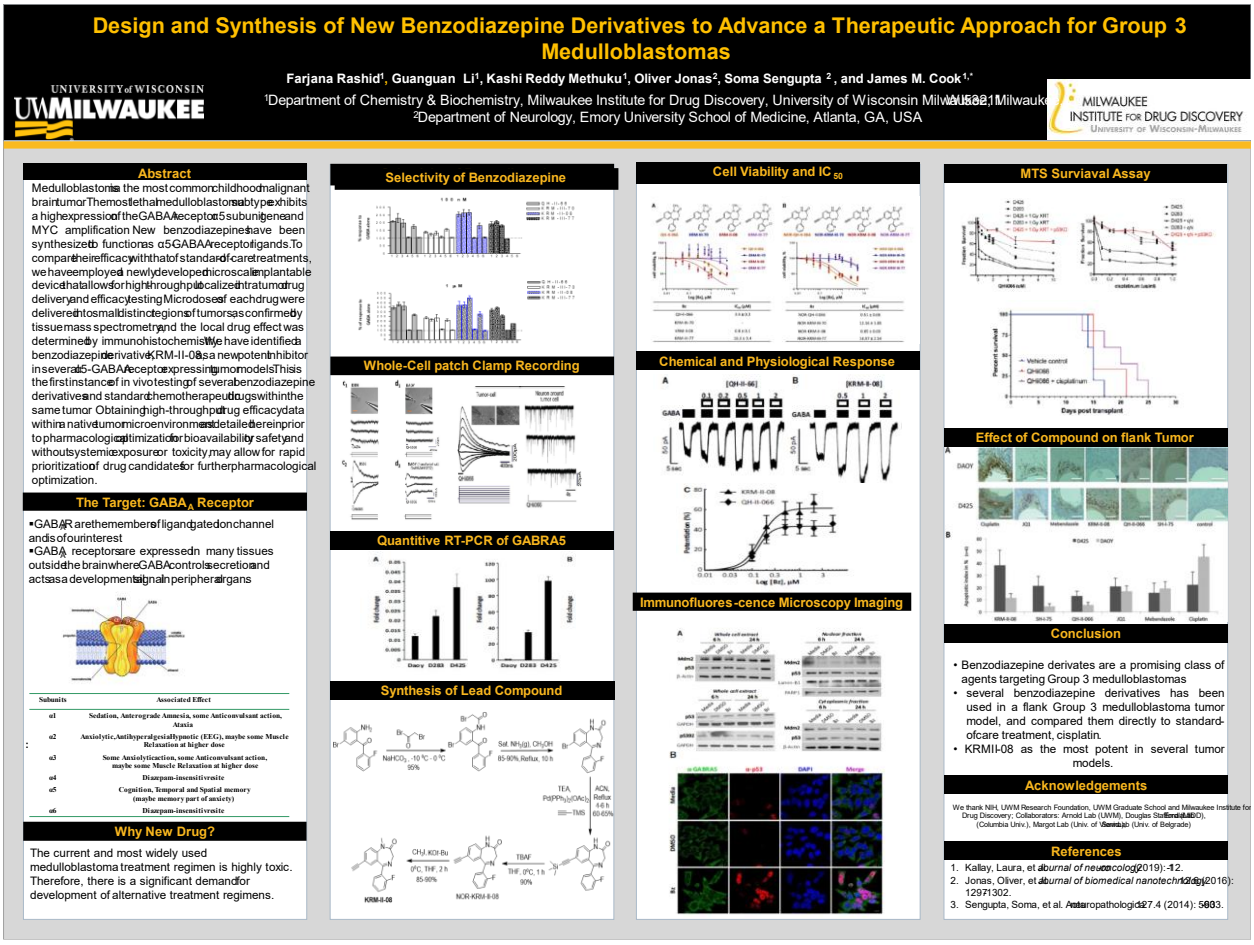

Design and Synthesis of New Benzodiazepine Derivatives to Advance a Therapeutic Approach for Group 3 Medulloblastomas

Farjana Rashid[1], Guanguan Li[1], Kashi Reddy Methuku[1], Oliver Jonas[2], Soma Sengupta [2] , and James M. Cook[1,*]

[1]Department of Chemistry & Biochemistry, Milwaukee Institute for Drug Discovery, University of Wisconsin Milwaukee, WI 53211, Milwaukee

[2]Department of Neurology, Emory University School of Medicine, Atlanta, GA, USA

Abstract

Medulloblastoma is the most common childhood malignant brain tumor. The most lethal medulloblastoma subtype exhibits a high expression of the GABA$_A$ receptor α5 subunit gene and MYC amplification. New benzodiazepines have been synthesized to function as α5 GABA$_A$ receptor ligands. To compare their efficacy with that of standard-of-care treatments, we have employed a newly developed microscale implantable device that allows for high-throughput localized intratumoral drug delivery and efficacy testing. Microdoses of each drug were delivered into small distinct regions of tumors as confirmed by tissue mass spectrometry, and the local drug effect was determined by immunohistochemistry. We have identified a benzodiazepine derivative, KRM-II-08, as a new potent inhibitor in several α5-GABA$_A$ receptor expressing tumor models. This is the first instance of in vivo testing of several benzodiazepine derivatives and standard chemotherapeutic drugs within the same tumor. Obtaining high-throughput drug efficacy data within a native tumor microenvironment as detailed herein prior to pharmacological optimization for bioavailability, safety, and without systemic exposure or toxicity, may allow for rapid prioritization of drug candidates for further pharmacological optimization.

The Target: GABA$_A$ Receptor

- GABA$_A$R are the members of ligand gated ion channel and is of our interest
- GABA$_A$ receptors are expressed in many tissues outside the brain where GABA controls secretion and acts as a development signal in peripheral organs

Subunits	Associated Effect
α1	Sedation, Anterograde Amnesia, some Anticonvulsant action, Ataxia
α2	Anxiolytic, Antihyperalgesia Hypnotic (EEG), maybe some Muscle Relaxation at higher dose
α3	Some Anxiolytic action, some Anticonvulsant action, maybe some Muscle Relaxation at higher dose
α4	Diazepam-insensitive site
α5	Cognition, Temporal and Spatial memory (maybe memory part of anxiety)
α6	Diazepam-insensitive site

Why New Drug?

The current and most widely used medulloblastoma treatment regimen is highly toxic. Therefore, there is a significant demand for development of alternative treatment regimens.

Selectivity of Benzodiazepine

Whole-Cell patch Clamp Recording

Quantitive RT-PCR of GABRA5

Synthesis of Lead Compound

Cell Viability and IC$_{50}$

Chemical and Physiological Response

Immunofluores-cence Microscopy Imaging

MTS Surviaval Assay

Effect of Compound on flank Tumor

Conclusion

- Benzodiazepine derivates are a promising class of agents targeting Group 3 medulloblastomas
- several benzodiazepine derivatives has been used in a flank Group 3 medulloblastoma tumor model, and compared them directly to standard-ofcare treatment, cisplatin.
- KRMII-08 as the most potent in several tumor models.

Acknowledgements

We thank NIH, UWM Research Foundation, UWM Graduate School and Milwaukee Institute for Drug Discovery; Collaborators: Arnold Lab (UWM), Douglas Stafford (UMDD), (Columbia Univ.), Margot Lab (Univ. of Vienna), Lab (Univ. of Belgrade)

References

1. Kallay, Laura, et al. *Journal of neuro-oncology* (2019): 1-12.
2. Jonas, Oliver, et al. *Journal of biomedical nanotechnology* 12.12 (2016): 12971302.
3. Sengupta, Soma, et al. *Neuropathology* 27.4 (2014): 503.

Modulating $GABA_A$ receptors in medulloblastoma with benzodiazepine-derivatives induces cell death

Laura Kallay[1], Havva Keskin[1], Alexandra Ross[1], Manali Rupji[2], Olivia A. Moody[3], Xin Wang[4,5], Guanguan Li[6], Taukir Ahmed[6], Farjana Rashid[6], Michael Rajesh Stephen6, Kirsten A. Cottrill[7], T. Austin Nuckols[7], Maxwell Xu[8], Deborah E. Martinson[2], Frank Tranghese[9], Yanxin Pei[10], James M. Cook[6], Jeanne Kowalski[2,11], Michael D. Taylor[4,5,12], Andrew Jenkins[13], Daniel A. Pomeranz Krummel[1,2], Soma Sengupta[1,2,14,15]

[1]Dept. Neurology, Emory Univ. School of Medicine, Atlanta; [2]Winship Cancer Inst., Emory Univ. School of Medicine, Atlanta; [3]Dept. Cell Biology, Emory Univ. School of Medicine, Atlanta; [4]The Arthur and Sonia Labatt Brain Tumour Research Centre, The Hospital for Sick Children, Toronto, Canada; [5]Developmental & Stem Cell Biology Program, The Hospital for Sick Children, Toronto, Canada; [6]Dept. Chemistry & Biochemistry, Univ. of Wisconsin-Milwaukee, Milwaukee; [7]Molecular & Systems Pharmacology Graduate Training Program, Emory Univ., Atlanta; [8]Dept. Biomedical Engineering, Johns Hopkins Univ., Baltimore; [9]Electrical and Computer Engineering Dept., Boston Univ., Boston; [10]Center for Cancer and Immunology Research, Brain Tumor Inst., Children's National Medical Center, Washington DC; [11]Department of Biostatistics & Bioinformatics, Rollins School of Public Health, Emory Univ., Atlanta; [12]Division of Neurosurgery, The Hospital for Sick Children, Toronto, Canada; [13]Dept. Anesthesiology & Pharmacology, Emory Univ. School of Medicine, Atlanta; [14]Dept. of Hematology & Medical Oncology, Emory Univ. School of Medicine, Atlanta; [15]Dept. Neurosurgery, Emory Univ. School of Medicine, Atlanta

Introduction

Medulloblastoma, a pediatric malignant primary brain tumor, is classified into four molecular subgroups: wingless, WNT; Sonic Hedgehog, SHH; Group 3; Group 4 [1]. Group 3 patients have a survival rate of ~20% and associated with higher rates of relapse and metastasis. Group 3 exhibits high expression of *GABRA5*, which codes for the α5 subunit of the ligand-gated ionotropic γ-aminobutyric acid type A receptor ($GABA_AR$). $GABA_ARs$ are fundamental in determining an excitation/inhibition balance in the CNS and consist of 2α, 2β, and 1γ subunits arranged as α-β-γ-α-β to create a Cl^- conduction pore (**Fig. 1**). Benzodiazepines bind at the $GABA_AR$ γ-α interface and are positive allosteric modulators, acting to increase effectiveness of GABA, which binds at α-β interfaces.

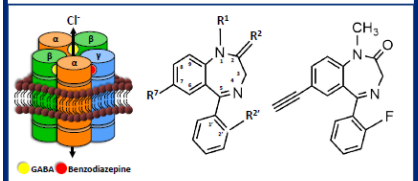

Fig. 1. $GABA_AR$ and benzodiazepine structures. Cartoon of a $GABA_AR$ (left). Shown are GABA and benzodiazepine binding sites. Core structure of a benzodiazepine (middle). Introduction of an ethinyl bond at R^7 imparts the drug with a α5-$GABA_AR$ preference (right).

Methods

Benzodiazepines were synthesized as described [2]. Medulloblastoma cell lines were obtained from ATCC. Effect of benzodiazepines on cell growth was assessed using an MTS assay, performed as described [3, 4]. Confocal microscopy was performed to examine p53 and cellular apoptosis in combination with DAPI staining, as previously described [3]. Whole-cell patch clamp electrophysiology techniques were standard. Normalized gene expression data for sixteen *GABR* genes and *MYC* from 763 primary resected medulloblastoma specimens was used [5]. Samples were classified into four medulloblastoma subgroups and further into twelve subtypes: two WNT subgroup [α (*n=49*), β (*n= 21*)], four SHH subgroup [α (*n= 65*), β (*n= 35*), γ (*n= 47*), δ (*n= 76*)], three group 3 subgroup (α (*n= 67*), β (*n= 37*), γ (*n= 40*)] and three group 4 subgroups [α (*n=98*), β (*n = 109*), γ (*n = 119*)]. Heatmaps were generated using Morpheus.

Results

Gene expression analysis of medulloblastoma tumors shows high expression of *GABR* genes (**Fig. 2**). There is observed *GABR* subgroup-specific expression. Group 3 has high *GABRA5*, *GABRB3*, *GABRG2/3* expression which code for α5, β3, and γ2 and 3 subunits of $GABA_AR$, respectively.

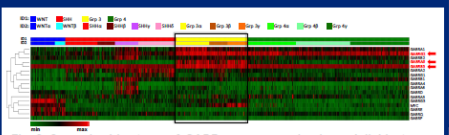

Fig. 2. Supervised heatmap of *GABR* gene expression in medulloblastoma. We analyzed normalized gene expression data for sixteen *GABR* genes from a 763 medulloblastoma tumor dataset [5].

Group 3 cells stain for α5-$GABA_AR$ subunit and have ~1000 $GABA_AR$/cell mediating a basal chloride-anion efflux of $2x10^9$ ions/sec (**Fig. 3**).

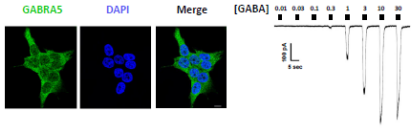

Fig. 3. $GABA_AR$ receptor is functional in medulloblastoma cells. Left, Localization of GABRA5 in Group 3 cells shows diffuse staining at the cell membrane. Right, Whole-cell patch clamp recording of Group 3 cells shows an active $\alpha_5\beta_3\gamma_{2/3}$-like receptor with increasing GABA (calibration bar: 100 pA, 5 sec).

$GABA_AR$ in Group 3 cells can be modulated by benzodiazepines, most effectively those which were designed to have an α5-preference. Treating Group 3 cells with the benzodiazepines impairs the cell viability. We find that the benzodiazepine causes within 10 minutes, depolarization of mitochondria and following an upregulation in *TP53* expression, p53 localization to the cytoplasm, and increased staining for the Bcl-2-associated death promoter protein BAD (**Fig. 4**).

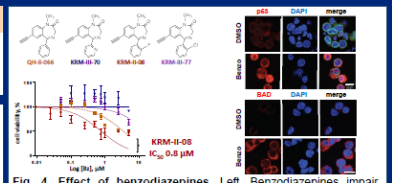

Fig. 4. Effect of benzodiazepines. Left, Benzodiazepines impair Group 3 cell viability. (IC_{50} 0.8 μM). Right, Benzodiazepine treatment results in p53 and BAD cytoplasmic localization.

Summary

- Analysis of gene expression of medulloblastoma tumors shows high expression of *GABR* genes, which code for subunits of the $GABA_AR$.
- Group 3 cells have functional $\alpha_5\beta_3\gamma_{2/3}$-like $GABA_AR$ that mediates $2x10^9$ ions/sec efflux.
- Benzodiazepines, positive allosteric modulators that enhance the effect of GABA, can impair Group 3 cell viability.
- Benzodiazepines may work by depolarizing the mitochondria and eliciting a stress response pathway that includes role for p53 signaling (**Summary Model below**).

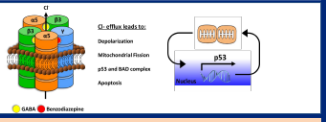

References

1. Cho YJ, *et al.* (2011) Integrative genomic analysis of medulloblastoma identifies a molecular subgroup that drives poor clinical outcome. J. Clin. Onc. 29: 1424-1430.
2. Huang Q, et al. (1996) Benzo-fused benzodiazepines employed as topological probes for the study of benzodiazepine receptor subtypes. Medicinal Chem. Res. 6(3): 384–391.
3. Sengupta S, *et al.* (2014) alpha5-GABAA receptors negatively regulate MYC-amplified medulloblastoma growth. Acta Neuropath. 127: 593-603.
4. Jonas O, *et al.* (2016) First in vivo testing of compounds targeting Group 3 medulloblastoma using an implantable microdevice as a new paradigm for drug development. J. Biomed. Nanotech. 12(6): 1297-1302.
5. Cavalli FMG, et al (2017) Intertumoral heterogeneity within medulloblastoma subgroups. Cancer Cell 31:737-754.

Acknowledgements

Financial support: NIH-NINDS under award K08 NS083626, American Cancer Society Institutional Research grant (IRG-14-188-01), and B*CURED Brain Cancer Research Investigator Award to S.S.; NIH under award NS076517, MH096463, and HL118561 to J.M.C. and use by J.M.C. of the Shimadzu Analytical Laboratory of Southeastern Wisconsin for mass spectroscopy; Biostatistics & Bioinformatics Shared Resource of the Winship Cancer Inst. of Emory Univ. and NIH-NCI under award number P30CA138292. The content is solely the responsibility of the authors and does not necessarily represent the official views of the National Institutes of Health.

Defense Slides

1. Design and Synthesis of Achiral α2/3Imidazodiazepines for the Treatment of Epilepsy and Pain

2. Design and Synthesis of Chiral α5 Ligands for the Treatment of Schizophrenia and Depression as well as Asthma

3. Development of Achiral α5 Benzodiazepines for the Treatment of Cancer

Farjana Rashid
Dr. James Cook Research Group
Final Defense
6-17-2021

UNIVERSITY of WISCONSIN UWMILWAUKEE

Outline

- Introduction
- Project Background
- Biological Data
- Synthetic Scheme
- Conclusion

2

GABAA R : Introduction

Human full-length
α1β3γ2 $GABA_AR$
in complex with
Alprazolam (ALP, Xanax)
and GABA

Masiulis, S.; Desai, R.; Uchanski, T.; Serna Martin, I.; Laverty, D.; Karia, D.; Malinauskas, T.; Zivanov, J.; Pardon, E.; Kotecha, A.; Steyaert, J.; Miller, K. W.; Aricescu, A. R., $GABA_A$ receptor signalling mechanisms revealed by structural pharmacology. *Nature* **2019,** *565* (7740), 454-459

Classical GABAergic Drugs Lack Subtype Selectivity

- Benzodiazepines (BZP's) like Diazepam can exhibit multiple, undesired effects
- BZP's act at α1–3 & α5 subtypes: diazepam-sensitive (DS) sites at α+γ– interface
- α4 & α6 subtypes: diazepam-insensitive (DI) sites at α+γ– interface
  - Binding pocket too small for pendant ring of DZP.
  - H102 residue (α1–3 & α5). R102 residue (α4 & α6).
- $GABA_AR$ subtype functionally selective ligands are ideal drug candidates

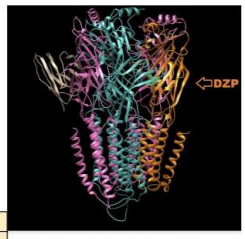

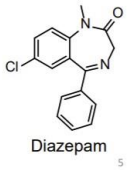

Diazepam

Subtype	Associated Effect
α1	DS site: Sedation, ataxia, anterograde amnesia, anticonvulsant action (some), and addiction
α2	DS site: Anxiolytic, antihyperalgesic effects, anticonvulsant action
α3	DS site: Some anxiolytic, some antinociceptive effects, anticonvulsant action at higher doses, some muscle relaxation at much higher doses
α4	DI site: lung disorders in the periphery
α5	DS site: Cognition, learning, temporal and spatial memory (maybe memory component of anxiety); schizophrenia, depression and in the periphery-asthma
α6	DI site: Tic disorders, Tourette's syndrome, migraine, trigeminal or orofacial pain and perhaps schizophrenia

5

Scenario of Epilepsy and Current Drugs

- Epilepsy: 2.3 million (U.S. adults), cost $12.5 billion a year[1]
- Pain disorders
  - Types: Chronic pain, complex regional pain syndrome, back pain, cancer pain, neuropathic pain, inflammatory pain, etc.
  - Cost $261-300 billion a year
  - 100 million (U.S. adults)[2]
- Problems
  - Classical BDZ have major side effects (tolerance, addiction, sedation, adverse psychological and physical effects)
  - SSRI's: Takes 3 weeks to have effect and causes sexual dysfunction.
  - Opioids agonists: Very effective for severe pain; however, for every opioid on the market addiction, tolerance and constipation are serious problems (opioid epidemic)
  - NSAIDS: Causes severe stomach pains, bleeding and can lead to death.
  - Patient compliance is a problem with all these treatments.
- Solution: novel imidazodiazepine (IMDZ) allosteric modulators targeting at α2, α3 or α2/α3 subunit of the $GABA_AR$

[1] https://www.nimh.nih.gov/health/statistics
[2] Hill, et al.; Cannabis and Cannabinoid Research, 2017, 2.1, 96

5

Project Background

Hz-166 active as an:
- Anticonvulsant[3]
- Non-sedating anxiolytic[1]
- Antihyperalgesic (neuropathic and inflammatory pain)[4]

Hz-166 and its bioisosteres

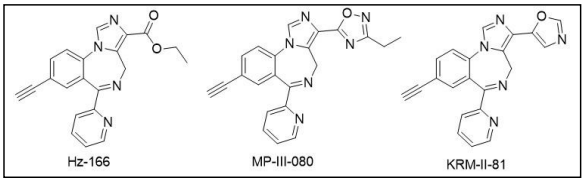

[1] Fischer, et al. *Neuropharmacol* **2010**, *59*, 612
[2] Namjoshi et al. *Bioorg. Med. Chem.* **2013**, *21*, 93
[3] Rivas, et al. *J. Med. Chem.* **2009**, *52*, 1795
[4] DiLio, et al. *Neuropharmacol.* **2011**, *60*, 626
[5] CRO
[6] Li, et al. *Synthesis* **2018**, *50* (20), 4124

6

KRM-II-81 : A Clinical Candidate

- An epileptic drug and novel therapy for post traumatic epilepsy
- A potential agent for pharmaco-resistant epilepsies
- Posses anxiolytic activity
- Antinociceptive activity
- Anti-seizure effects

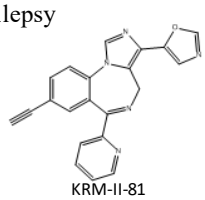

KRM-II-81

1. *Neuropharmacology*, 2018, 137:332-343
2. *J. med. Chem.*,2016, 59(23),10800-10806
3. *ACS Chem Neurosci*, 2017, 8(6), 1305-1312
4. *ACS Chem. Neurosci.* 2020, 11, 17, 2624-2637
5. *Pharmacol Biochem Behav.*,2019,pii:S0091-3057(18)
6. *Pharmacology, Biochemistry and Behavior* .2020, 196, 172996

UWMILWAUKEE

Analogue Design

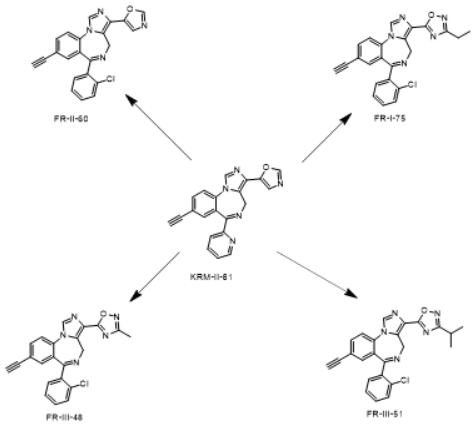

8

Rationalization of Ligand Design :Alprazolam vs KRM-II-81

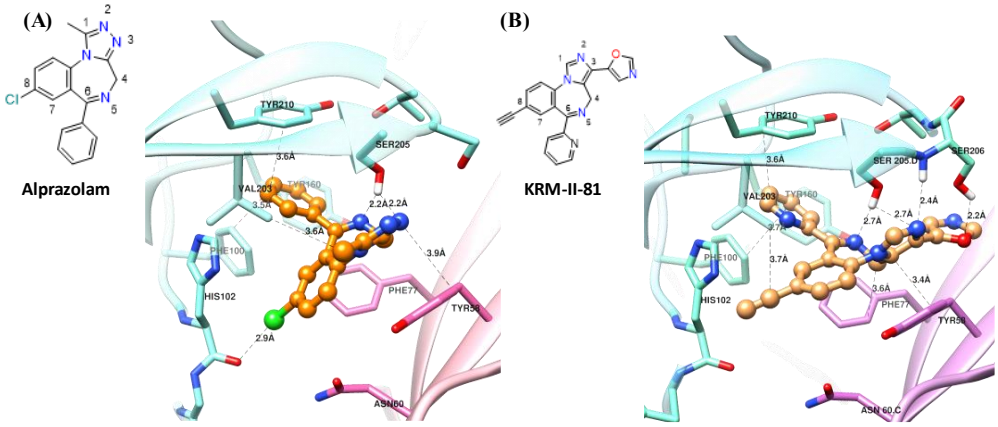

Masiulis, S.; Desai, R.; Uchanski, T.; Serna Martin, I.; Laverty, D.; Karia, D.; Malinauskas, T.; Zivanov, J.; Pardon, E.; Kotecha, A.; Steyaert, J.; Miller, K. W.; Aricescu, A. R., $GABA_A$ receptor signalling mechanisms revealed by structural pharmacology. *Nature* **2019,** *565* (7740), 454-459

Rationalization of Ligand Design :Alprazolam vs FR-II-60

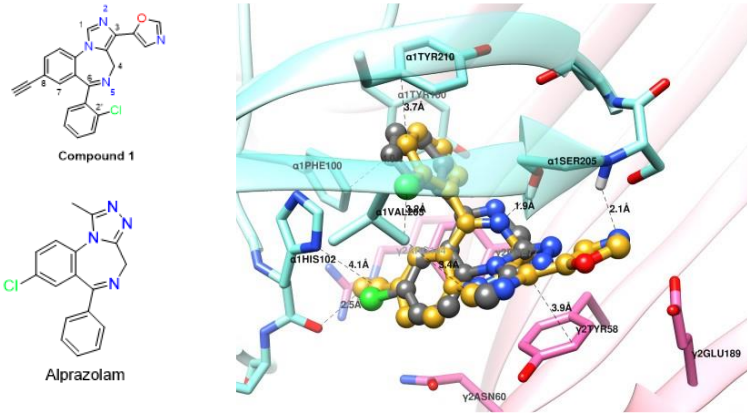

Rotarod and Cytotoxicity of FR-II-60

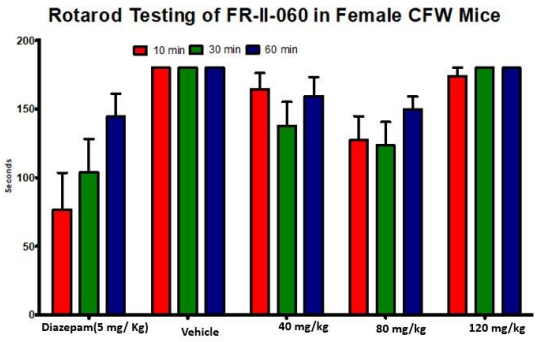

No sedation at 120mg/kg

Cytotoxicity: It is not cytotoxic at higher concentration until 300 µM

Selectivity of FR -II-60 and FR-I-75

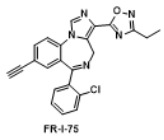

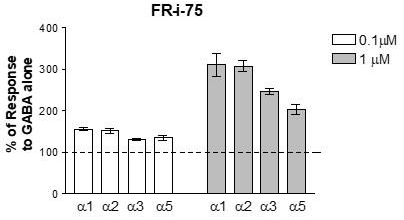

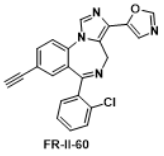

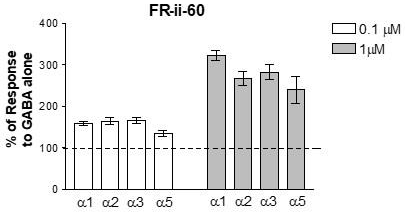

Anticonvulsant Effects of FR -II-60

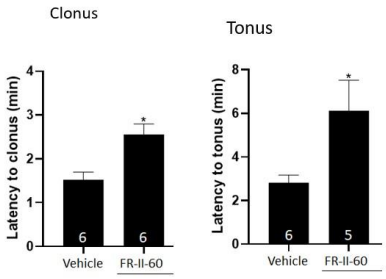

10 mg/kg

Group	Mortality (within 1 h)	Latency to death (min)
Vehicle	3/6 (50%)	32.3 ± 10.1
FR-II-60	0/6 (0%)	-

Figure : PTZ-induced seizures in C57BL/6 mice

Anticonvulsant Activity of FR-II-60 : ETSP

Time(Hours)		0.25		0.5		2.0	
Test	Dose (mg/kg)	N / F	Comment Code	N / F	Comment Code	N / F	Comment Code
6HZ	30			3 / 4		1 / 4	
	100			3 / 4		3 / 4	
	300			3 / 4		4 / 4	
MES	30			2 / 4		1 / 4	
	100			4 / 4		4 / 4	
	300			4 / 4		4 / 4	
Rotarod	30			4 / 8		0 / 8	
	100			6 / 8		5 / 8	
	300			8 / 8		7 / 8	
72 hour mortality	30	0 / 16					
	100	0 / 16					
	300	0 / 16					

The data for each condition is presented as N/F, where N = number of animals protected and F = number of animals tested. For rotarod test, N = number of animals displaying adverse motor effects and F = number of animals tested. Any adverse effects, including deaths, are noted. An observer blinded to treatment confirms behavioral observations.
Mild writhing after dosing mice. All time points were affected.

14

Metabolic Study of FR-II-60

KIDNEY	Mean (nmol/kg)	SEM
FR-II-60 15 min	191.11	27.36
FR-II-60 30 min	165.08	44.43
FR-II-60 1 h	110.20	13.43
FR-II-60 2 h	431.42	67.89
FR-II-60 4 h	113.16	11.02
FR-II-60 8 h	576.57	9.18
FR-II-60 24 h	569.30	400.01

KIDNEY	Mean	SEM
Cmax (ng/ml)	322.52	98.65
tmax (h)	13.33	5.33
AUC0_24 (ng*h/ml)	4424.84	1177.88
AUC0 -∞ (ng*h/ml)	5575.96	2245.95
t1/2 (h)	4.94	1.52
β (1/h)	0.15	0.05

BRAIN	Mean (nmol/kg)	SEM
FR-II-60 15 min	26.09	0.55
FR-II-60 30 min	28.19	4.69
FR-II-60 1 h	27.60	1.88
FR-II-60 2 h	40.11	5.51
FR-II-60 4 h	143.80	112.18
FR-II-60 8 h	30.45	4.15
FR-II-60 24 h	28.26	3.07

BRAIN	Mean	SEM
Cmax (ng/ml)	58.55	41.58
tmax (h)	4.67	1.76
AUC0_24 (ng*h/ml)	407.87	112.44
AUC0 -∞ (ng*h/ml)	548.37	165.89
t1/2 (h)	6.89	0.20
β (1/h)	0.10	0.00

PLASMA	Mean (nmol/L)	SEM
FR-II-60 15 min	7.17	0.18
FR-II-60 30 min	10.50	1.66
FR-II-60 1 h	18.14	5.19
FR-II-60 2 h	9.47	1.14
FR-II-60 4 h	10.12	1.11
FR-II-60 8 h	217.46	114.77
FR-II-60 24 h	127.65	32.83

PLASMA	Mean	SEM
Cmax (ng/ml)	124.86	47.55
tmax (h)	9.00	7.51
AUC0_24 (ng*h/ml)	1153.73	489.79
AUC0 -∞ (ng*h/ml)	1183.04	478.76
t1/2 (h)	2.07	1.11
β (1/h)	0.58	0.25

Behavioral observations in Female Rhesus Monkeys after Administration of FR-II-60 (mg/kg, iv)

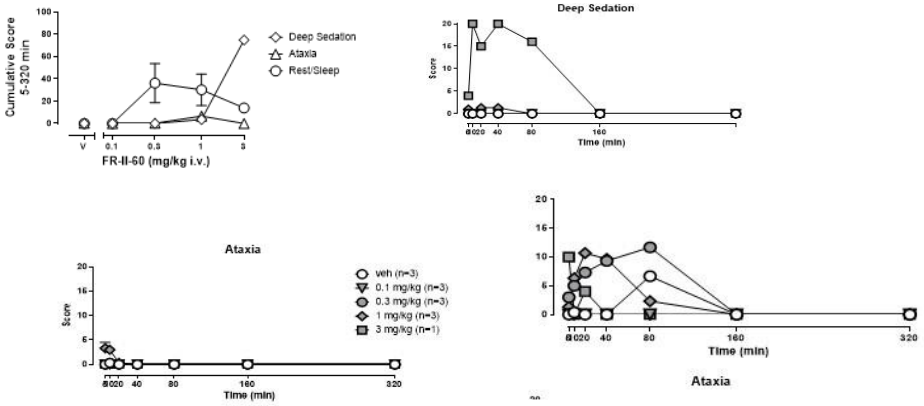

Synthesis of FR-II-60
Overall Yield-26%

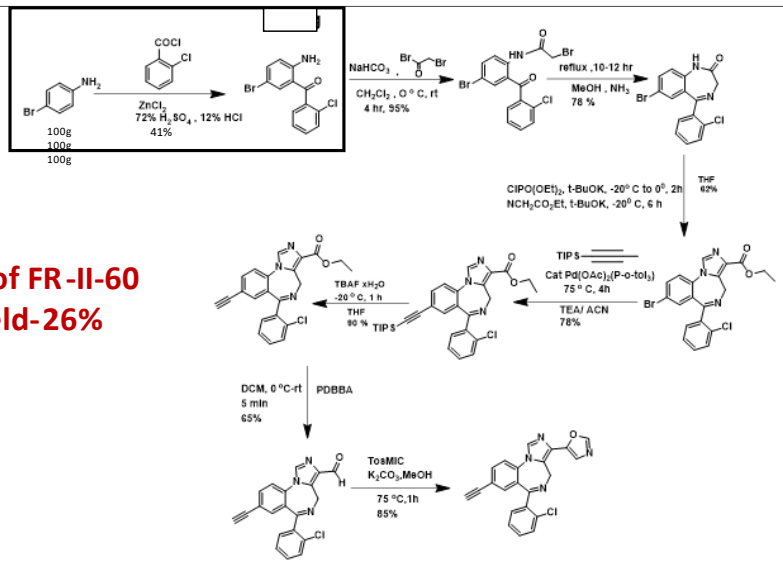

UNIVERSITY of WISCONSIN UWMILWAUKEE

Optimization of Large Scale Starting Material

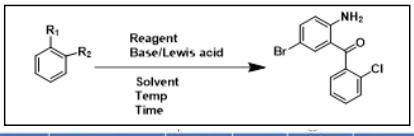

Entry	R1	R2	Reagent	Lewis Acid	Base	Solvent	Temp (0 C)	Time	% yield
1.	Br	Cl		–	n-BuLi	THF	70	24 hr	–
2.	I	Cl		–	n-BuLi	THF	70	24 hr	–
3.	COCl	Cl		Silver Triflate	–	neat	120-230	42hr	–
4.	COCl	Cl		Cu(II) triflate	–	neat	120-230	42hr	–
5.	COCl	Cl		ZnCl2	–	neat	120-230	42hr	41%

18

Synthesis of Large Scale Starting Material

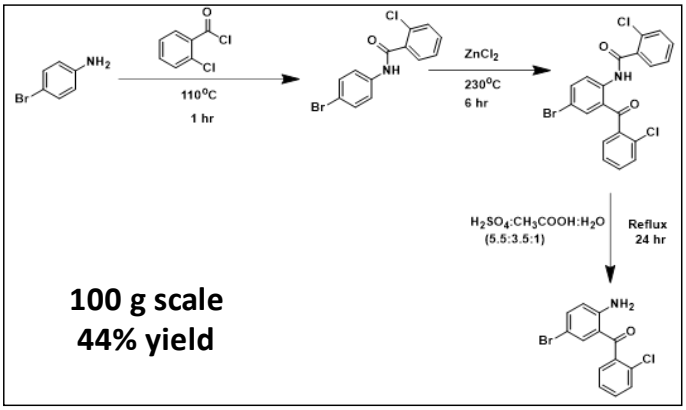

100 g scale
44% yield

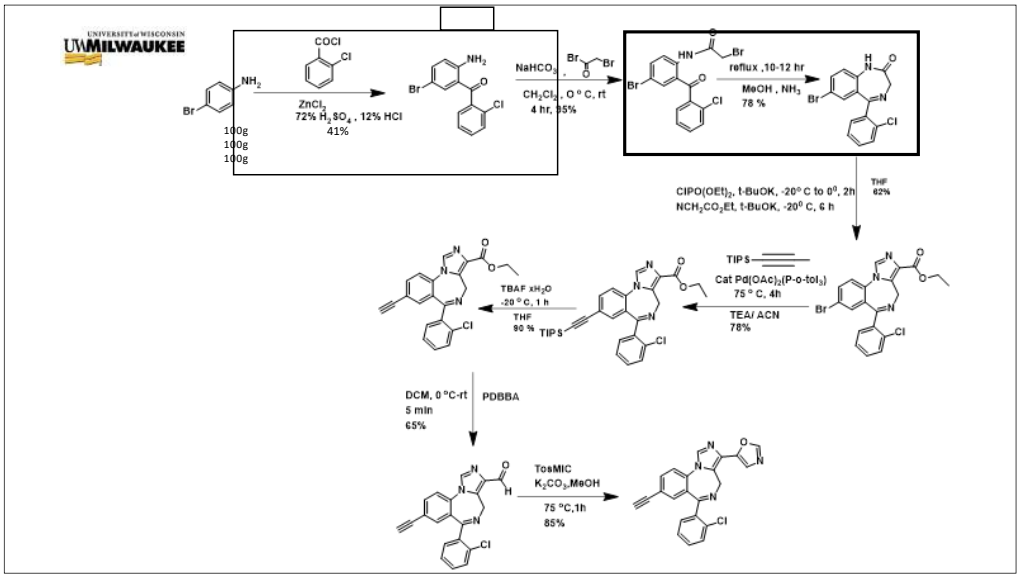

UWMILWAUKEE

Hexamethylenetetramine-Based Cyclization Reaction

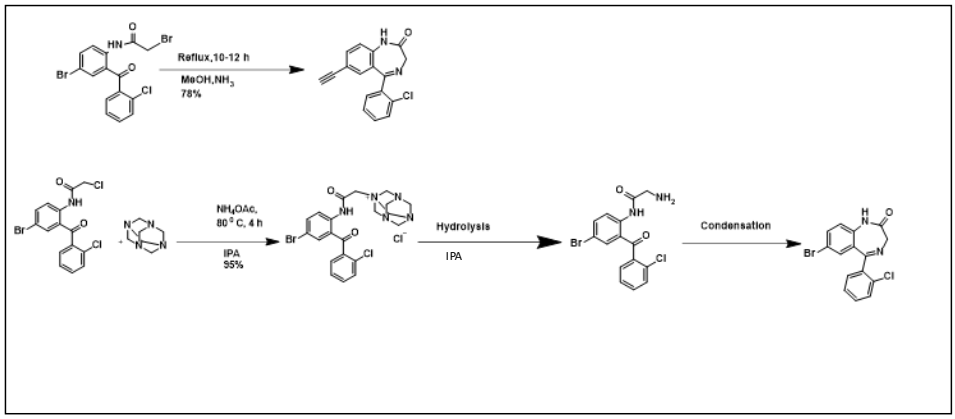

21

UWMILWAUKEE

Synthesis of FR-II-60

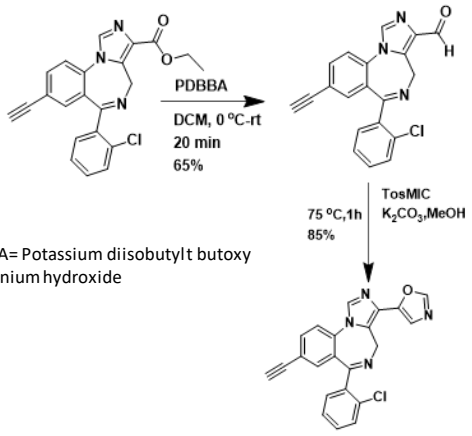

PDBBA= Potassium diisobutylt butoxy aluminium hydroxide

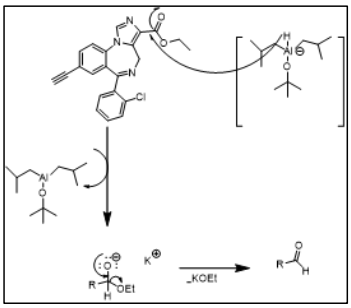

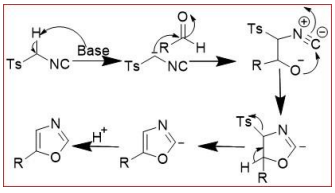

Synthesis of FR-I-75

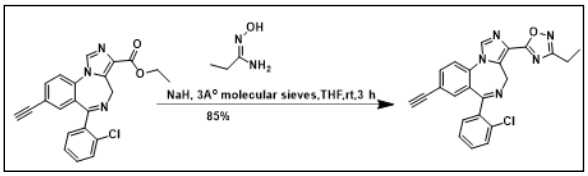

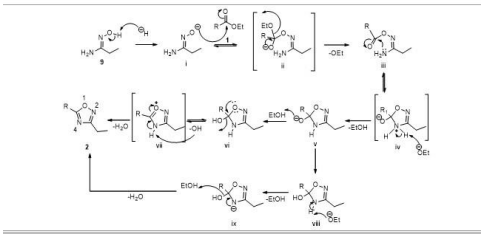

Cook, J.; Li, G.; **Rashid, F.,** *Synthesis* **2018,** *50* (20), 4124-4132.

Analogues of FR-II-60

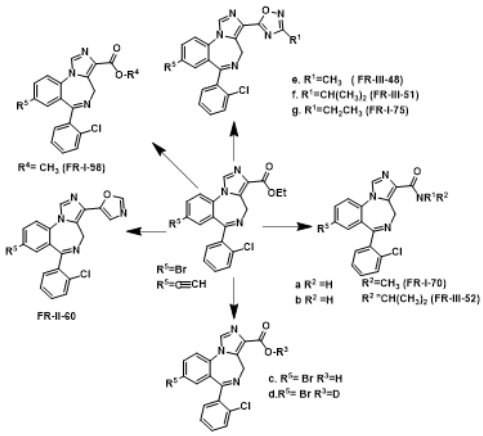

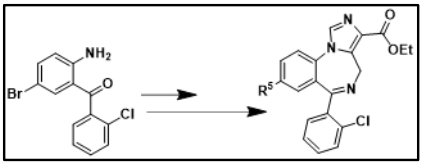

Synthesis of Hz-166

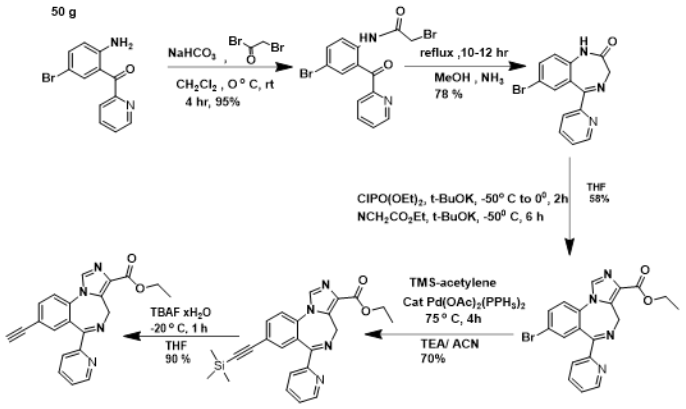

UNIVERSITY of WISCONSIN
UWMILWAUKEE

PATENT (CONFIDENTIAL)

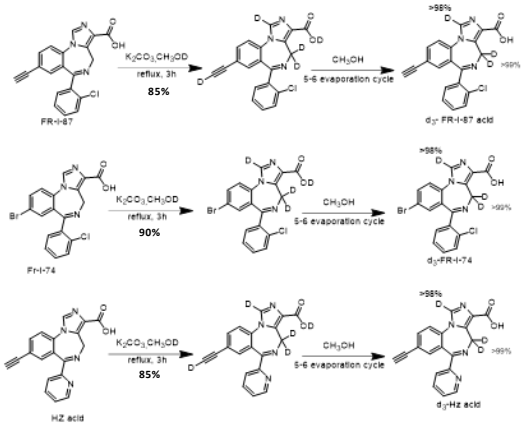

Conclusion

- FR-II-60 is little less potent than KRM -II-81 but still promising.
- The yield was increased from 19% to 26% in case of FR -II-60 synthesis.
- The yield of 2 amino 5 bromo 2'Cl benzophenone was increased

UNIVERSITY of WISCONSIN UWMILWAUKEE

Part 2: Chiral α5 Ligands for Schizophrenia, Depression and Asthma

α5-PAM(Positive allosteric Modulators) Summary

Properties	Parent compounds		Intermediate compounds	Generation 1–2 compounds		
	SH-053-2F-R-CH3	MP-III-022	n ~15–20	GL-II-73	GL-11-74	GL-11-75
Brain penetrant	Yes	Yes	Various intermediate values	Yes	Yes	Yes
Stable	Yes	Yes		Yes	Yes	Yes
Toxic	No	No		No	No	No
Activity at α5	++	++		+	++	++
Anxiolytic	Mild	Yes		Yes	Yes	Yes
Antidepressive	Mild	Yes		Yes	Yes	Yes
Sedative	No	No		No	Yes	Yes
Procognitive	No	Mild		Yes	No	Yes

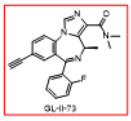

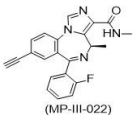

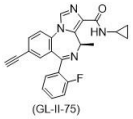

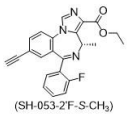

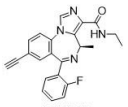

Prevot, et al *Molecular Neuropsychiatry***2019**

Synthesis of FR-III-10

5 Steps
Scale 100 g
28% Overall Yield

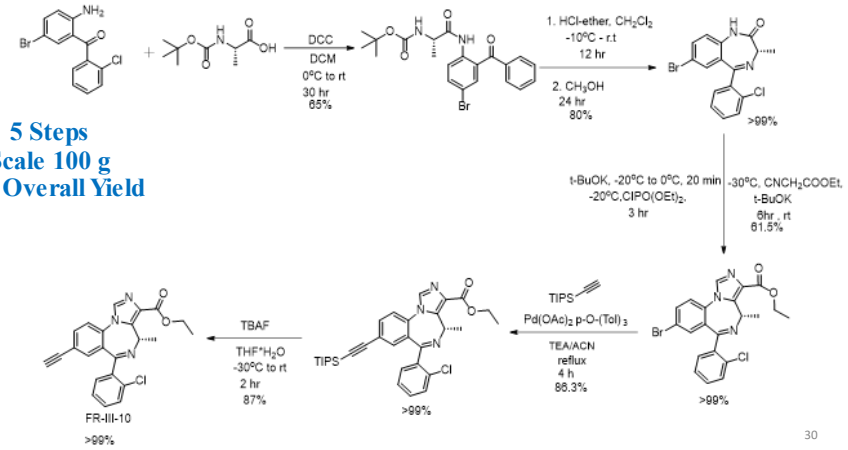

Synthetic Route to Benzodiazepine With NCA Reagent

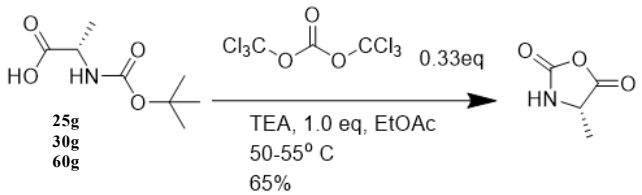

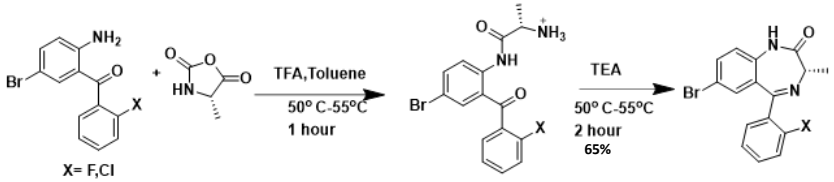

Analogs search of GL-II-73

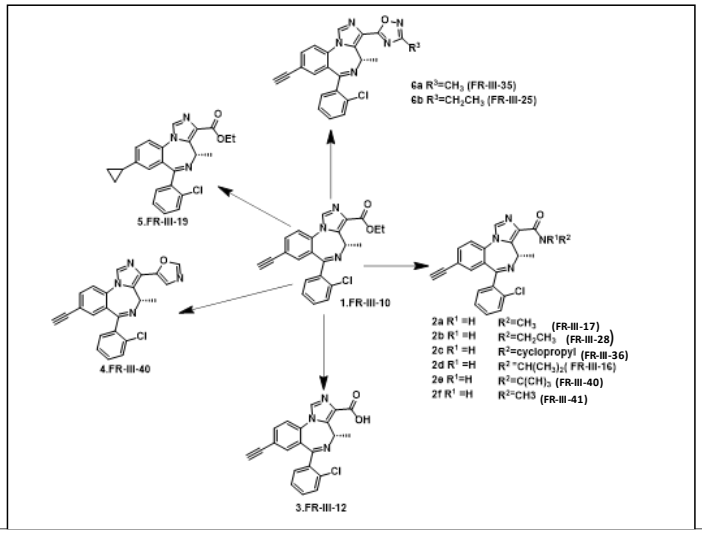

Cytotoxicity assay data

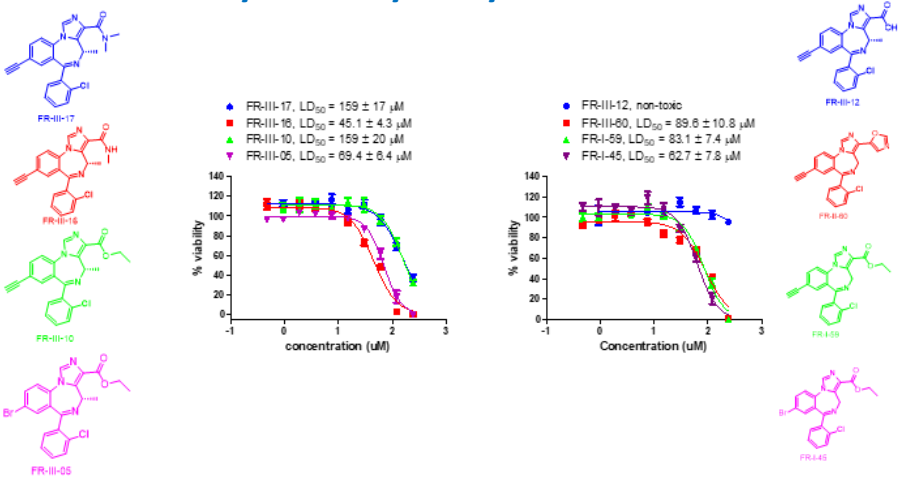

Synthesis of GL-I-54

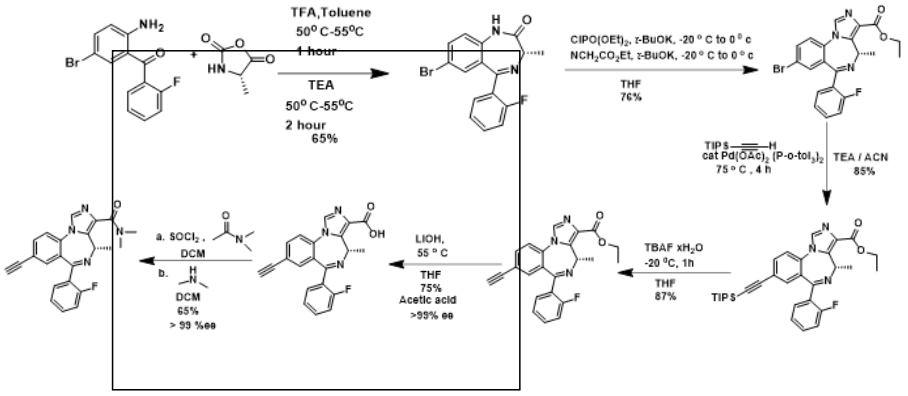

Asthma Project

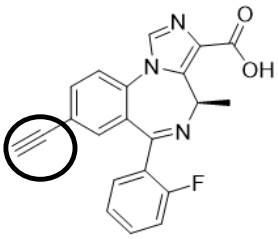

SH-2'F-R-CH_3 acid

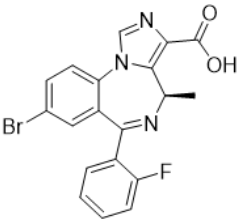

MIDD0301

Current Lead compound

- Good PK
- Non-toxic
- Significant effect In ASM assay
- Without any CNS side effect

Analogs of MIDD 0301

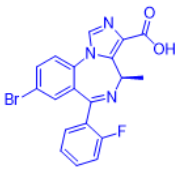

MIDD 0301

MYM-FR-II-88

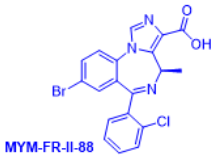

MYM-FR-II-88

Smooth Muscle Relaxation of MYM-FR-II-88

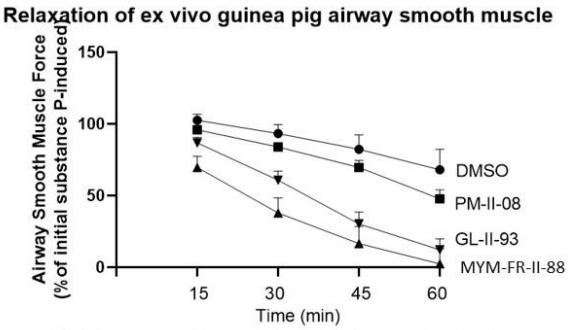

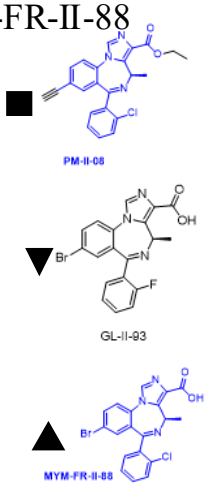

Fig. Ex vivo smooth muscle force in guinea pig tracheal rings. Rings were pre-contracted with 1uM substance P and then treated with vehicle (0.1% DMSO) or 100uM of indicated compounds. Data is expressed as the amount of muscle force remaining at indicated time points. n=4

Confidential

Smooth Muscle Relaxation of MYM-FR-II-88

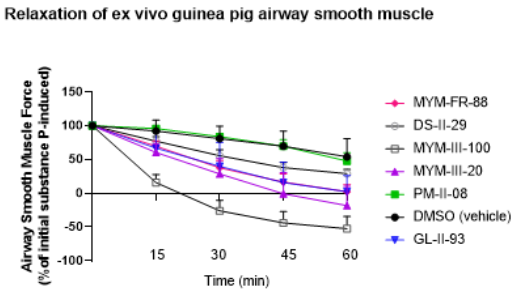

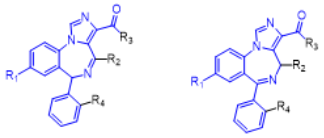

Fig. Ex vivo smooth muscle force in guinea pig tracheal rings. Rings were pre-contracted with 1uM substance P and then treated with vehicle (0.1% DMSO) or 100uM of indicated compounds and resulting relaxation was measured at 15,30,45 and 60min. Data is expressed as the amount of muscle force remaining at indicated time points. n=4-7.

Confidential

Smooth Muscle Relaxation of FR-III-45

Relaxation of ex vivo guinea pig airway smooth muscle

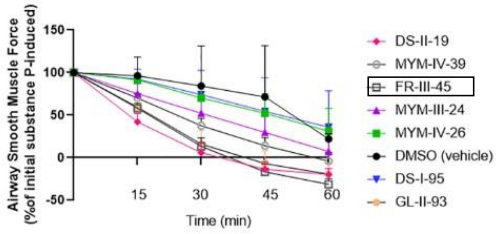

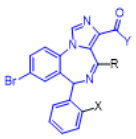

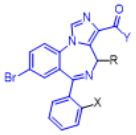

Fig. Ex vivo smooth muscle force in guinea pig tracheal rings. Rings were pre-contracted with 1uM substance P and then treated with vehicle (0.1% DMSO) or 100uM of indicated compounds and resulting relaxation was measured at 15,30,45 and 60min. Data is expressed as the amount of muscle force remaining at indicated time points. n=3.

Confidential

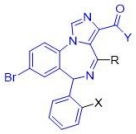

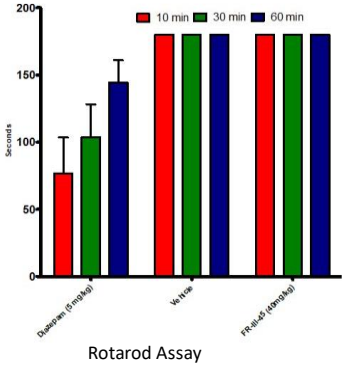

Rotarod Assay

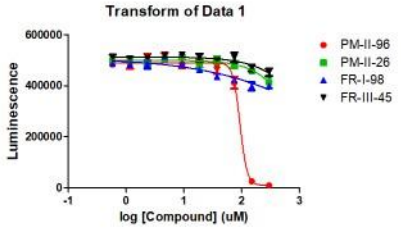

Cytotoxicity Assay

Conclusion

To investigate the role of chirality in the structure of drug's therapeutic properties in the treatment of asthma, schizophrenia and depression, many S analoge of 2'Cl had been synthesized.

FR-III-45, MYM-FR-88 showed better promising result than lead compound GL-II-93 in ASM assays with no toxicity and sedation.

UNIVERSITY of WISCONSIN UWMILWAUKEE

Part 3: Achiral α5 Benzodiazepines for Treatment of Cancer

42

What is Medulloblastoma?

- Is a common pediatric malignant primary brain tumor
- Classified into four subgroup: WNT, sonic hedgehog, SHIH, Group 4(1,2) and Group 3
- Group 3 patients are refractory to treatment, have a survival rate of 20%

Group 3 Medulloblastoma exhibits a molecular signature that include High Expression of GABRA5, isoform of $GABA_A$ receptor.

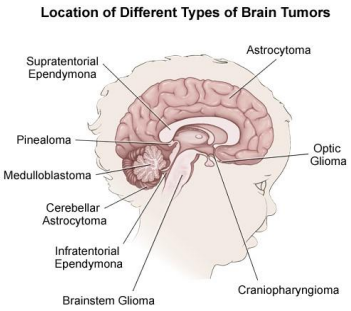

43

Comparison Between Related Benzodiazepine and Standard Treatment

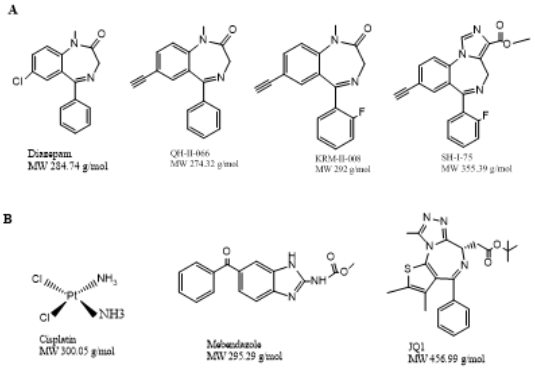

Chemical structures of compounds. (A) Structurally related benzodiazepines used in the study. The compounds consist of the core benzodiazepine chemical structure, fusion of benzene and diazepam rings. (B) Chemical structures of the standard-of-case treatment compounds used in the study. JQ1 shares a similar structural format as the benzodiazepine SH-I-75

Oliver.; *Journal of Biomedical Nanotechnology*, **12**,1297-1302

UNIVERSITY of WISCONSIN UWMILWAUKEE

Effect of compounds on flank tumors

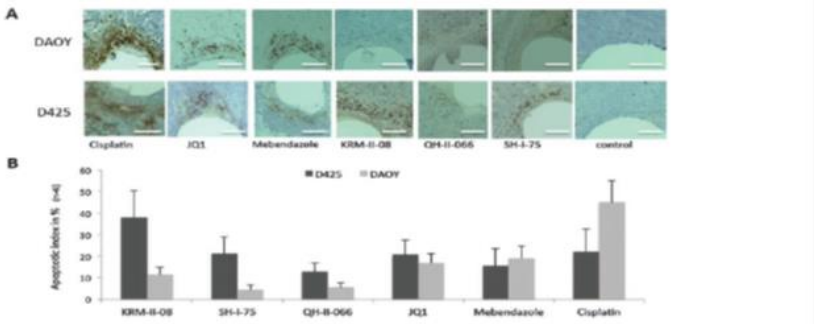

(A) Representative images of D425 and DAOY tumor sections removed 24 hours after exposure to microdose of each drug from the device, showing distinct regions of apoptosis assessed by cleaved caspase-3 expression (brown) after 24 hours. Scale bars, 250μm. (B) Apoptotic index (%apoptotic cells/all cells in drug affected tissue region) for human D425 and DAOY tumors exposed to KRM-II-08, SH-I-75, QH-II-066, JQ1, mebendazole and cisplatin (all 35% drug in PEG1450). Averages are taken from 6 spatially distinct reservoirs from at least 3 tumors please give ($p < 0.01$).

Oliver.; *Journal of Biomedical Nanotechnology* , **12**,1297-1302

45

UNIVERSITY of WISCONSIN UWMILWAUKEE

QH-II-066 vs Diazepam at $\alpha^{+}\gamma^{-}$ Interface of $GABA_A$ Receptor

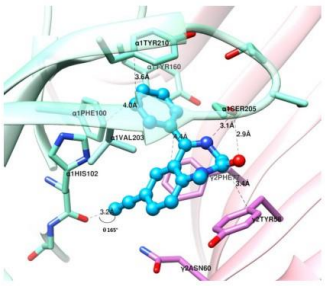

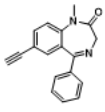

QH-II-66

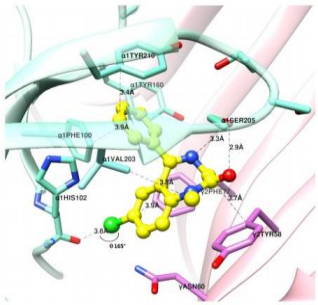

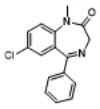

Diazepam

46

KRM-II-08 vs Diazepam at $\alpha^{+}\gamma^{-}$ Interface of $GABA_A$ Receptor

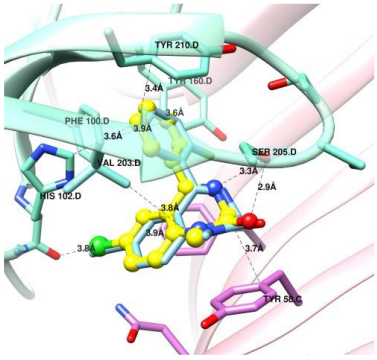

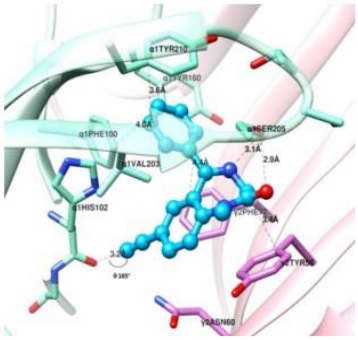

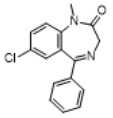

Diazepam

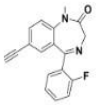

KRM-II-08

FR-I-44 vs Diazepam at $\alpha^{+}\gamma^{-}$ Interface of $GABA_A$ Receptor

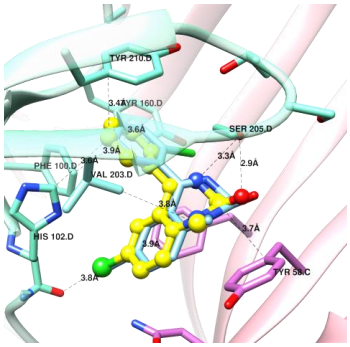

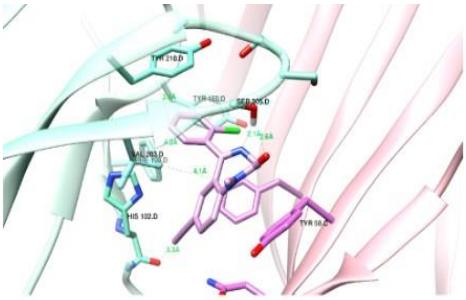

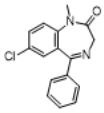

Diazepam

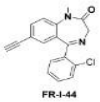

FR-I-44

Rotarod data of FR-I 44 and Others

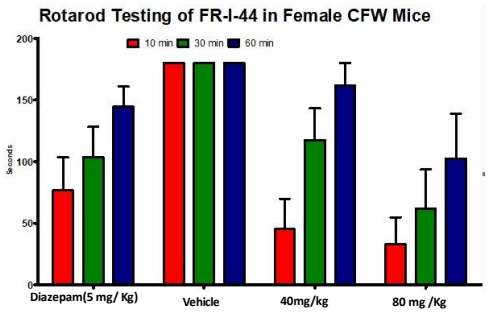

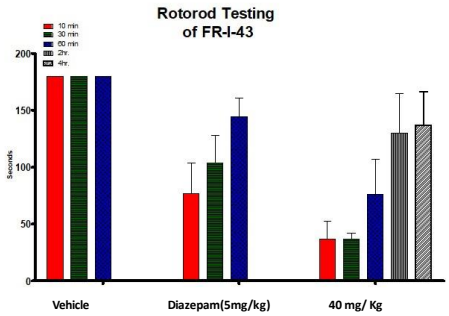

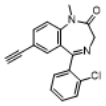

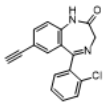

49

Selectivity of FR-I-44 and analogues

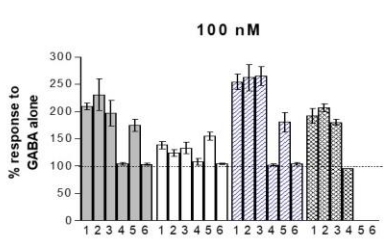

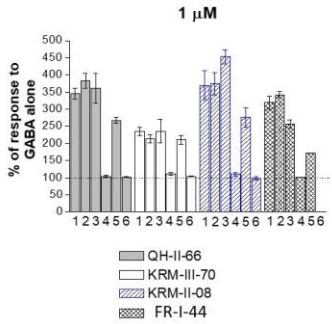

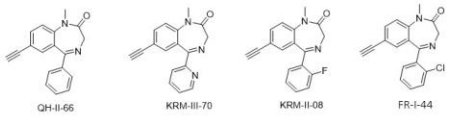

50

Synthesis Route of KRM-III-77 and FR-I-43

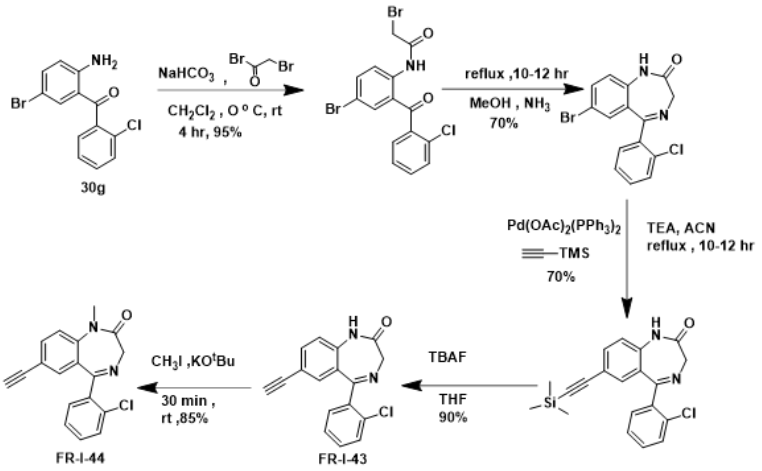

51

Cytotoxicity Data of Cancer Analogs

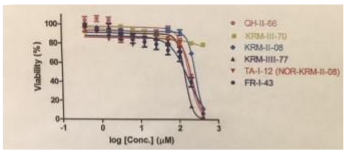

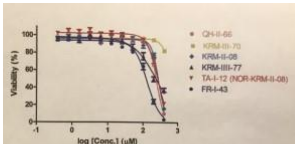

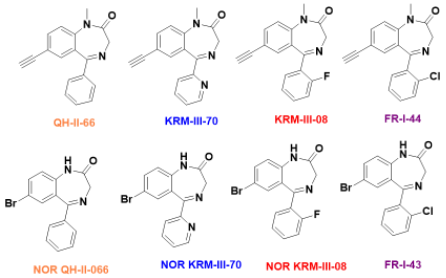

S. NO.	Code	HEK293 LD 50	HEPG2 LD 50
1	QH-II-66	174.6 ± 13	242.7 ± 10
2	KRM-III-70	>400	>400
3	KRM-II-08	257.5 ± 12.9	277.4 ± 15.5
4	FR-I-44(KRM-III-77)	138.5 ± 8.7	248.4 ± 32.5
5	NOR-KRM-II-08	210.1 ± 11.6	260.8 ± 13.5
6	FR-I-43	165.1 ± 22.9	130.9 ± 6.7
7	NOR-KRM-III-70	NA	NA
8	NOR-QH-II-66	NA	NA

Anti-cancer activity of FR-I-44 and others

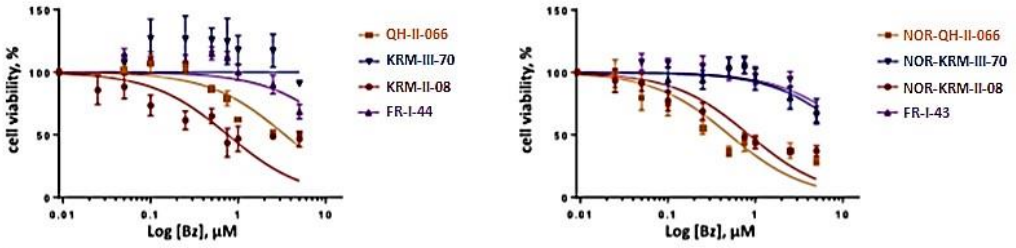

Bz	IC_{50} (µM)
QH-II-066	3.4 ± 0.3
KRM-II-70	-
KRM-II-08	0.8 ± 0.1
FR-I-44	16.3 ± 3.4

Bz	IC_{50} (µM)
NOR-QH-II-066	0.51 ± 0.06
NOR-KRM-III-70	12.16 ± 1.85
NOR-KRM-II-08	0.85 ± 0.09
FR-I-43	14.97 ± 2.54

Conclusion

FR-I-44 not promising as KRM -II-008.

The replacement of 2'Cl group with 2'F group of active KRM -II-008 greatly decrease the efficacy at the particular cancer cell line.

It might be active any other cancer cell line.

CURRICULUM VITAE

FARJANA **RASHID**

2480 N Oakland Ave, Apt 206, Milwauke, WI-53211 · (414) 690-2124
farjanarashid18@gmail.com · linkedin.com/in/farjana-rashid-03220a102/

Goal-oriented professional and an expert in Medicinal Chemistry and Organic Synthesis, Structure-Activity Relationship (SAR) Analysis, Plant Extraction, Pharmacological evaluation of biologically active compounds, Mass spectrometry, Chromatographic separation technique (HPLC), Nuclear Magnetic Resonance Spectroscopy. Seeking the position of organic chemist at a vibrant, professional and state-of-the-art industrial environment.

CHIEF ACHIEVEMENTS

Synthesized achiral α5 benzodiazepines for the treatment of cancer.

Designed and synthesized chiral α5 or α2/3/5 ligands for the treatment of schizophrenia and depression.

Synthesized achiral α2/3 imidazodiazepines for the treatment of epilepsy and pain.

EDUCATION

2.1. August, 2013 - present

Ph.D. in Chemistry, University of Wisconsin-Milwaukee

Working towards a doctorate degree in chemistry, specializing in organic chemistry. Expected graduation date is in August, 2021.

2.2. APRIL, 2010 – APRIL, 2011

M.S. in Organic Chemistry, University of Dhaka

Obtained master's degree in organic chemistry (1st class) with thesis titled "Separation and Characterization of Starch from Waste Potato Peels".

2.3. APRIL, 2005 – FEBRUARY, 2010

B.Sc. in Chemistry, University of Dhaka

Obtained bachelor's degree in chemistry (2nd class, with honors).

RESEARCH EXPERIENCES

PhD research at University of Wisconsin-Milwaukee (2013-Present)

- Synthesis of achiral α5 Benzodiazepines for the Treatment of Cancer
  - Designing of new α5 Benzodiazepines ligands targeting GABA A receptor based on molecular modeling.
  - Synthesis of new designed ligands and monitoring of the reaction by thin layer chromatography.
  - Purification of the synthesized ligands using recrystallization and column chromatography.
  - Characterization of the ligands by mass spectrometry and NMR.
  - Biological evaluation of the synthesized ligands.
- Design and synthesis Chiral α5 or α2/3/5 Ligands for the Treatment of Schizophrenia and Depression
  - Synthesis of GABA A receptor alpha-5 subtype selective ligands.
  - Separation, purification and characterization of the ligands by chromatography, mass spectrometry and NMR.
  - Chiral separation by HPLC.
  - % purity by HPLC.
- Synthesis of Achiral α2/3 Imidazodiazepines for the Treatment of Epilepsy and Pain
  - Design alpha 2,3 subtype selective GABA receptor ligand according to molecular modeling.
  - Synthesis large scale reaction, optimization new route reaction (temperature, time), skilled in modern new organic synthesis technique.
  - Purification by crystallization and column chromatography.
  - Characterized compounds by using mass spectrometry, NMR and HPLC.

Masters research at University of Dhaka (2010-2011)

- Separation and characterization of starch from waste potato peels
  - Delignification of potato peels.
  - Liquid-liquid extraction, separation, purification.
  - Characterization the starch using NMR, IR, Mass spectroscopy.

LIST OF PUBLICATIONS

Li, Guanguan, Lalit K. Golani, Rajwana Jahan, Farjana Rashid, and James M. Cook. "Improved synthesis of anxiolytic, anticonvulsant and antinociceptive α2/α3-GABA (A) ergic receptor subtype selective ligands as promising agents to treat anxiety, epilepsy, as well as neuropathic Pain." *Synthesis* 50, no. 20 (2018): 4124.

Kallay, Laura, Havva Keskin, Alexandra Ross, Manali Rupji, Olivia A. Moody, Xin Wang, Guanguan Li et al. "Modulating native GABA A receptors in medulloblastoma with positive allosteric benzodiazepine-derivatives induces cell death." *Journal of neuro-oncology* 142, no. 3 (2019): 411-422.

Witkin, Jeffrey M., Guanguan Li, Lalit K. Golani, Wenhui Xiong, Jodi L. Smith, Xingjie Ping, Farjana Rashid, Rajwana Jahan, James M. Cook, and Xiaoming Jin. "The positive allosteric modulator of α2/3-containing GABAA receptors, KRM-II-81, is active in pharmaco-resistant models of epilepsy and reduces hyperexcitability after traumatic brain injury." *Journal of Pharmacology and Experimental Therapeutics* 372, no. 1 (2020): 83-94.

Berro, Lais F., Daniela Rüedi-Bettschen, Jemma E. Cook, Lalit K. Golani, Guanguan Li, Rajwana Jahan, Farjana Rashid, James M. Cook, James K. Rowlett, and Donna M. Platt. "GABAA receptor subtypes and the abuse-related effects of ethanol in rhesus monkeys: experiments with selective positive allosteric modulators." *Alcoholism: Clinical and Experimental Research* 43, no. 5 (2019): 791-802.

Witkin, Jeffrey M., Xingjie Ping, Claire Mouser, Xiaoming Jin, Jon Hobbs, Veera Venkata Naga Phani Babu Tiruveedhula, Guanguan Li et al. "The value of human epileptic tissue in the characterization and development of novel antiepileptic drugs: The example of CERC-611 and KRM-II-81." *Brain research* 1722 (2019): 146356.

Biggerstaff, A., B. Kivell, J. L. Smith, Md Y. Mian, L. K. Golani, F. Rashid, D. Sharmin et al. "The α2, 3-selective potentiators of GABAA receptors, KRM-II-81 and MP-III-80, produce anxiolytic-like effects and block chemotherapy-induced hyperalgesia in mice without tolerance development." *Pharmacology Biochemistry and Behavior* 196 (2020): 172996.

Knutson, Daniel E., Jodi L. Smith, Xingjie Ping, Xiaoming Jin, Lalit K. Golani, Guanguan Li, VVN Phani Babu Tiruveedhula et al. "Imidazodiazepine Anticonvulsant, KRM-II-81, Produces Novel, Non-diazepam-like Antiseizure Effects." *ACS Chemical Neuroscience* 11, no. 17 (2020): 2624-2637.

Pandey, Kamal P., Md Zubair Ahmed Khan, Lalit K. Golani, Prithu Mondal, Md Yeunus Mian, Farjana Rashid, VVN Phani Babu Tiruveedhula et al. "Design, synthesis and characterization of novel gamma-aminobutyric acid type A receptor ligands." *Organic Chemistry* part vii (2020): 242-256.

McCusker, Paul, Md Yeunus Mian, Guanguan Li, Michael D. Olp, VVN Phani Babu Tiruveedhula, Farjana Rashid, Lalit Kumar Golani et al. "Non-sedating benzodiazepines cause paralysis and tissue damage in the parasitic blood fluke Schistosoma mansoni." *PLoS neglected tropical diseases* 13, no. 11 (2019): e0007826.

Kallay, Laura, Havva Keskin, Alexandra Ross, Olivia Moody, Kirsten Cottrill, Austin Nuckols, Guanguan Li et al. "PDTM-45. POSITIVE MODULATION OF NATIVE GABAA RECEPTORS IN MEDULLOBLASTOMA CANCER CELLS WITH BENZODIAZEPINES INDUCES RAPID MITOCHONDRIAL FRAGMENTATION AND TP53-DEPENDENT, CELL CYCLE-INDEPENDENT APOPTOSIS." *Neuro-Oncology* 20, no. suppl_6 (2018): vi213-vi213.

Rashid, Farjana, Guanguan Li, Taukir Ahmed, Oliver Jonas, Soma Sengupta, and James Cook. "Synthesis of new benzodiazepines that function as alpha 5-GABAA receptor ligands to target group 3 medulloblastomas." In *ABSTRACTS OF PAPERS OF THE AMERICAN CHEMICAL SOCIETY*, vol. 256. 1155 16TH ST, NW, WASHINGTON, DC 20036 USA: AMER CHEMICAL SOC, 2018.

Li, Guanguan, Lalit K. Golani, Rajwana Jahan, Farjana Rashid, and James M. Cook. "Improved Synthesis of Anxiolytic, Anticonvulsant and Antinociceptive 伪 2/伪 3 GABA (A) ergic Receptor Subtype Selective Ligands as Promising Agents to Treat Anxiety, Epilepsy, as well as Neuropathic Pain."